Aristotle University of Thessaloniki
Department of Physics
Sector of Astrophysics, Astronomy and Mechanics
Astronomy Lab

Single pulse statistical analysis of magnetar AXP J1809-194

Xylaki Theodora

Supervisor:
J. H. Seiradakis
Co-supervisor:
Kosmas Lazaridis
Committee members:
E. Plionis and N. Stergioulas

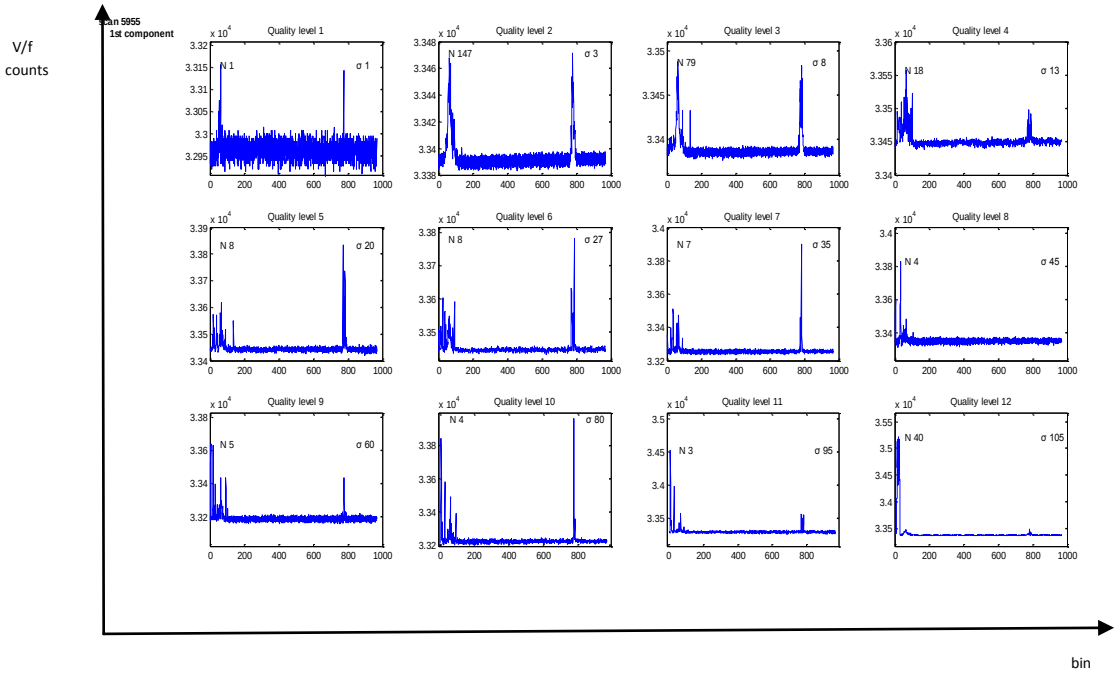

Thessaloniki, January 2014

Abstract

Neutron stars are one of the possible final stages in the life of massive stars and their existence was confirmed through the discovery of the first pulsar in 1967. Pulsars are rapidly rotating neutron stars with large magnetic fields and they emit highly periodic signals that allow us to observe them.

Conditions in the interior of neutron stars are extreme and so far no complete theory exists that can describe matter in these conditions. If an equation of state was to be found for the description of matter in such states, neutron stars would be physicists' laboratories for the study of matter in these extreme conditions. Also pulsars are a very good probe of the interstellar medium. These are some of the reasons pulsars were and are studied thoroughly.

Magnetars are also neutron stars that have extremely strong magnetic fields ~10^{15} G, which are several orders of magnitude greater than the magnetic field of a typical pulsar. They were proposed to explain Soft Gamma Repeaters (SGRs) and Anomalous X-ray Pulsars (AXPs) and observations have shown that magnetars are probably a particular stage in the lifespan of neutron stars.

Using appropriate algorithms as well as coding a part of the "jhspuls" program in "matlab", single pulses from the magnetar AXP J1809-194 and the pulsars PSR 1133+16 and PSR 0329+54 have been statistically investigated. The results were then compared.

Περίληψη

Οι αστέρες νετρονίων είναι μια από τις πιθανές τελικές καταστάσεις των αστέρων μεγάλης μάζας και η ύπαρξή τους επιβεβαιώθηκε από την ανακάλυψη του πρώτου pulsar το 1967. Τα pulsar είναι ταχέως περιστρεφόμενοι αστέρες νετρονίων που διαθέτουν ισχυρά μαγνητικά πεδία, η παρουσία των οποίων γίνεται αισθητή λόγω των εξαιρετικά περιοδικών σημάτων που εκπέμπουν.

Οι συνθήκες που επικρατούν στο εσωτερικό των αστέρων νετρονίων είναι ακραίες και μέχρι σήμερα δεν υπάρχει μια πλήρης θεωρία που να περιγράφει τη συμπεριφορά της ύλης σε αυτές τις καταστάσεις. Η πιθανή εύρεση μιας καταστατικής εξίσωσης που θα περιγράφει την ύλη σε αυτές τις καταστάσεις, θα καταστήσει τους αστέρες νετρονίων ως τα πλέον κατάλληλα μέσα για την μελέτη της ύλης σε ακραίες και μη επιτεύξιμες από τον άνθρωπο συνθήκες. Επίσης αποτελούν πολύ σημαντικά εργαλεία στην μελέτη του μεσοατρικού χώρου. Αυτοί είναι κάποιοι από τους λόγους που τα pulsar έχουν και συνεχίζουν να μελετώνται διεξοδικά.

Τα magnetar είναι επίσης αστέρες νετρονίων οι οποίοι έχουν πολύ ισχυρά μαγνητικά πεδία ~10^{15} G, αρκετές τάξεις μεγέθους πιο ισχυρά από τα pulsar, και προτάθηκαν για να εξηγήσουν τα Soft Gamma Repeaters (SGRs) και τα Anomalous X-ray Pulsars (AXPs). Διάφορες παρατηρήσεις έχουν δείξει ότι ίσως τα magnetar αποτελούν ένα στάδιο στη ζωή των pulsar.

Με χρήση ήδη υπαρχόντων κατάλληλων αλγόριθμων αλλά και προγραμματισμού ενός τμήματος του προγράμματος “jhspuls” σε περιβάλλον “matlab” έγινε στατιστική ανάλυση δεδομένων του magnetar AXP J1810-197 και των pulsars PSR 1133+16 και PSR 0329+54 και μετέπειτα η σύγκριση των αποτελεσμάτων.

CONTENTS

Appendix B

B.1 Quality plots: distribution of single pulses in each quality class.

Bibliography

1. Discovery

The discovery of pulsars was made by Jocelyn Bell, a PhD student, and her thesis advisor Antony Hewish in 1967 at Cambridge university. It was discovered by chance, since Hewish and Bell weren't looking for pulsars, but they were studying at the frequency of 85.5 MHz the scintillation that radio waves from distant sources (quasars) show as they pass through the solar wind. Bell noticed on her recordings that a certain signal reappeared every 23 h and 56 minutes, in other words once a sidereal day. At the beginning they made also the assumption that the signal came from an extraterrestrial civilization but when they found another perfectly periodic signal from another part of the sky they knew that it had to be something else. The conclusion was that these periodic signals came from a new category of stars called pulsars (pulsating stars) but soon it became clear that pulsars were rapidly rotating neutron stars. The existence of neutron stars was proposed in 1934 - after the discovery of the neutron by Chadwick in 1932 - by Walter Baade and Fritz Zwicky in an attempt to explain the explosion of a supernova.

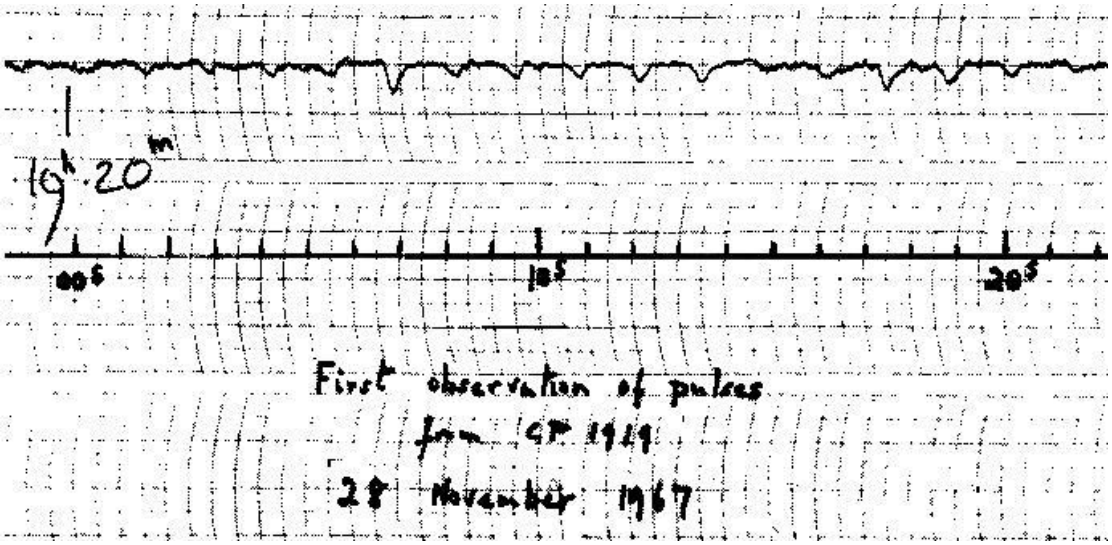

2. Structure of the Neutron Star

Neutron stars are the collapsed cores of type II supernovae remnants and they exhibit the highest stable densities and pressures known in the universe. They squeeze 0,5 - 2,5 Solar masses into a city-size volume (typical density of 10^{15} gr/cm^3) with a radius of 9 - 14 km and are very strongly magnetized (B = 10^{12} - 10^{15} G). The nature of the matter under these conditions, where the four fundamental forces of Nature are simultaneously important, is still an unsolved problem.

A neutron star consists of its atmosphere, the crust (inner and outer) and core region (inner and outer). The atmosphere contains mainly ^{56}Fe nuclei. The outer crust consists mainly of ions and electrons whereas the inner crust of electrons, neutrons and various types of nuclei. As we get to the core of the neutron star, our knowledge is limited: the outer core consists of a proton and neutron Fermi plasma as for the inner core little do we know, but many assumptions are being made. Some of the assumptions are that the inner core consists of

i. neutrons,
ii. strange quark matter,
iii. neutrons and high energy pions and kaons ,
iv. hyper dense degenerate matter of quarks.

The equation of state P = P(ρ) which describes the matter at the interior of neutron stars is known only with some certainty for low densities which we find in the outer crust of the star whereas for high densities in the core of the star uncertainty reigns. Today several equations of state exist, all of them different versions of high energy theoretical physics. Every equation grants a different relation between mass and radius for the neutron stars, but because we know with accuracy that the mass of pulsar J1614-2230 is 1.97 Solar masses, any equation of state that grants a maximum mass less than 1.97 Solar masses have already been rejected.

The majority of neutron stars that have been observed belong to the category of pulsars.

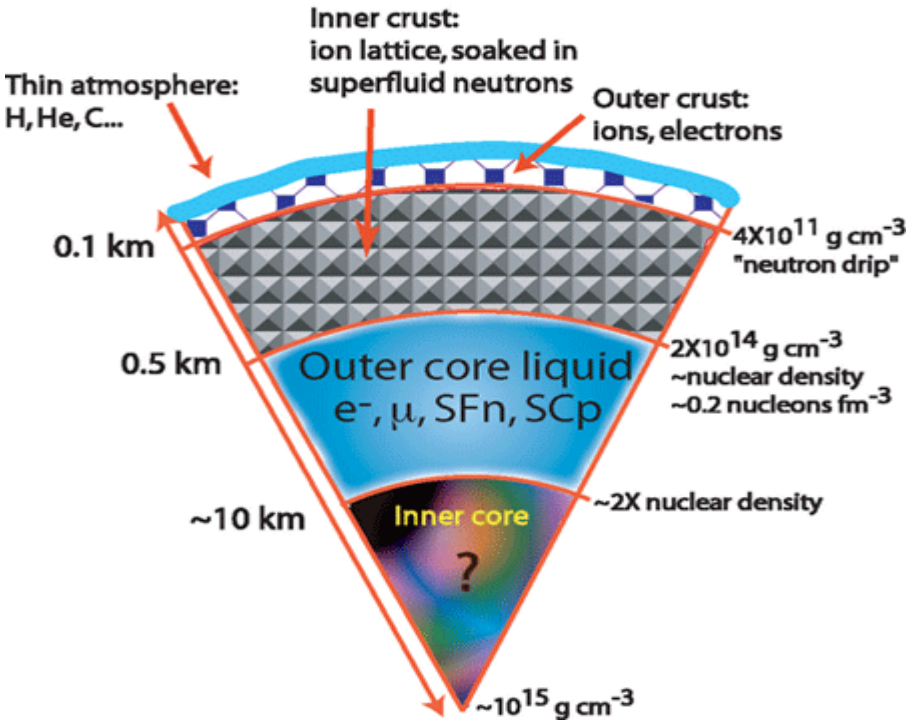

Structure of a neutron star.

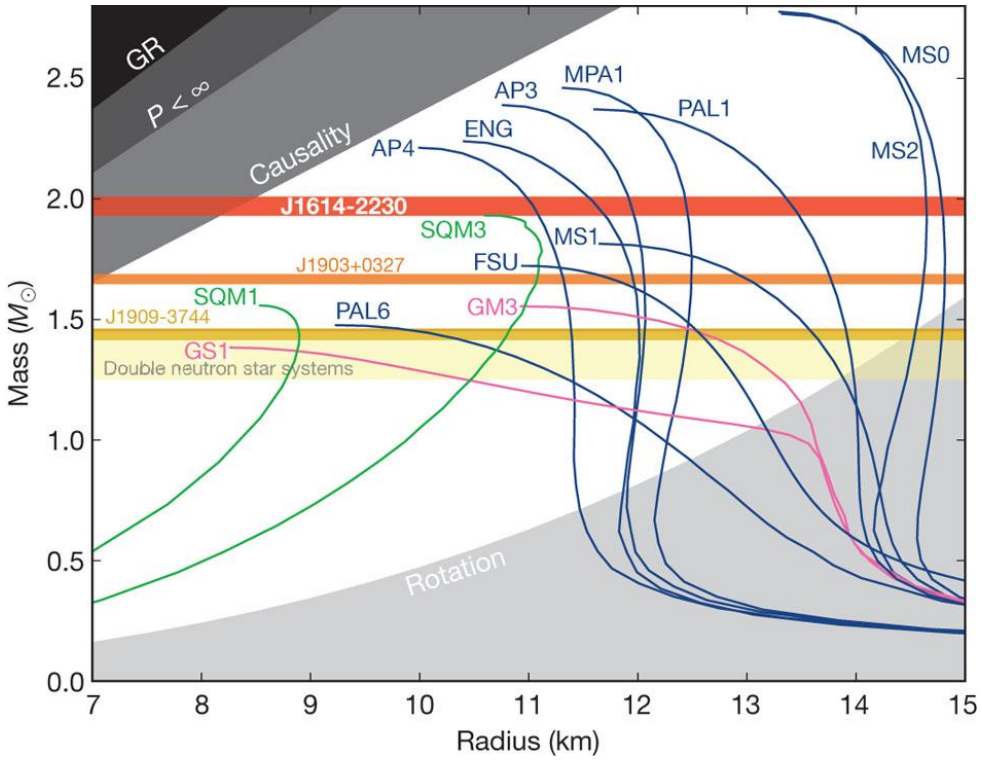

The Equations Of State are the snake-like curves. Each snake represents the predictions of a different theory of what is inside a superdense object.

3. Pulsars

Pulsars are rapidly rotating neutron stars which have strong magnetic fields and emit a beam of electromagnetic radiation. This radiation can only be observed on earth if the beam of emission is pointing towards it. If we consider how someone sees the beam of a lighthouse, we can understand why the emission of a pulsar has a pulsed appearance. But how is a pulsar able to emit such an electromagnetic radiation?

3.1 Classes of Pulsars

According to the source of the power of the electromagnetic radiation that the pulsars emit, astronomers divide them into categories:

i. accretion powered pulsars: pulsars that are found in binary systems and whose pulses are generated by the accretion flow striking the neutron star. (NASA)

ii. rotation powered pulsars: pulsars - in general isolated radio pulsars - with strong magnetic fields that cause accelerated charged particles to radiate. (NASA)

iii. nuclear-powered millisecond pulsars: millisecond pulsars whose X-ray pulses are generated by burst oscillations lasting only a few seconds during type I X-ray bursts. (NASA)

iv. magnetars: the decay of an extremely strong magnetic field provides the electromagnetic power.

From what has been stated above, pulsars can be found isolated and in binary systems. Most of the pulsars found till this day were discovered through their radio emission. Some of them go beyond radio; they also emit pulses of visible light, X-rays, gamma-rays. In 2008 Fermi made a very different discovery: they found a purely gamma-ray pulsar which lies within a supernova remnant known as CTA 1 in the constellation Cepheus (Discovered: A New Kind Of Pulsar, 2008).

3.2 Pulsar Magnetosphere

Because of the stars' extremely high density, its gravitational fields at the surface are enormously strong; consequently if the star had an atmosphere its height would be very low, ~1cm. That is why it can be assumed that the star is in vacuum.

3.2.1 *The orthogonal rotator model*

When the rotating dipole magnetic field forms an angle θ with the rotational axis, electromagnetic radiation is emitted with a rate of:

$$\dot{E} = -\frac{1}{6c^3} B^2 R^6 \left(\frac{2\pi}{P}\right)^4 \sin^2\theta \quad .$$

If we assume that the emission of electromagnetic energy is generated completely from the loss of rotational kinetic energy, then

$$\dot{E} = \dot{E_{kin}} => -\frac{1}{6c^3} B^2 R^6 \left(\frac{2\pi}{P}\right)^4 \sin^2\theta = \mathrm{I}\Omega\dot{\Omega}$$

where I is the moment of inertia and $\Omega = \frac{2\pi}{P}$, thus

$$B = \frac{\sqrt{I6c^3}}{2\pi R^3 \sin\theta} \sqrt{P\dot{P}}.$$

Angle θ is considered to be 90^0 in this model and that is why it is called orthogonal.

The complex pulse shapes and their polarization properties make this mechanism an unlikely source of the coherent radio emission.

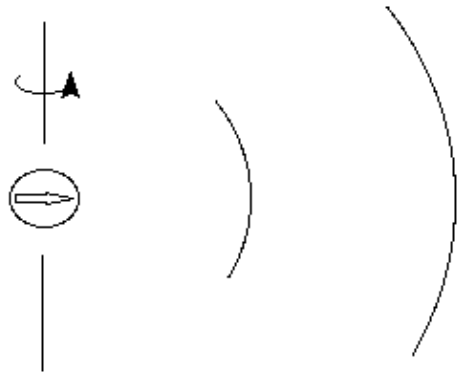

The orthogonal rotator model

But since pulsars are highly magnetized, their rotation generates electric fields in the surrounding space. Goldreich and Julian (1969) suggested that the space surrounding the star could not be vacuum, but must contain charge. That space is called the magnetosphere of the pulsar and because the observed radio pulses originate somewhere in the space surrounding the star, the understanding of the properties of this region (magnetosphere) is very important.

3.2.2 *Goldreich - Julian model*

In this model the rotation axis is parallel to the magnetic field axis and thus the magnetic field is static. Goldreich and Julian argued that the conductivity of the material of the neutron star is very high and can be assumed infinite. Also the inertia of the electric charges has a negligible effect on their kinetic state, therefore

$$\vec{E} + \frac{1}{c}\left[\left(\vec{\Omega} \times \vec{r}\right) \times \vec{B}\right] = 0$$

where **E** and **B** are the electric and magnetic fields respectively and **Ω** is the vector angular velocity of the star. Due to the relationship above, it is valid that

$$\vec{E} \cdot \vec{B} = 0$$

which means that the conductivity is nonzero only along the magnetic field lines. The solution of Laplace's equation taken into consideration appropriate boundary conditions at the surface of the star, which gives the electrostatic potential

$$\Phi = -\frac{B\Omega R^5}{6cr^3}\left(3\cos^2\theta - 1\right) \ (r \geq R)$$

where θ is the polar angle from the rotation axis. The electric field that corresponds to this potential is

$$\left(\overrightarrow{E} \cdot \vec{B}\right)_{r=R} = -\frac{\Omega R}{c} B^2 \cos^3\theta$$

For B~10^{12} G the magnitude of electric field that is parallel to the magnetic field on the surface of the star is

$E \sim \frac{\Omega R}{c} B \sim 6 \times 10^{10} P^{-1}$ $(V\ cm^{-1})$, P in seconds.

Electrons and ions that are found in fields of such magnitude are given an acceleration that is far greater in magnitude than the acceleration of gravity and therefore the normal factors determining the scale height are completely dominated by electromagnetic effects. The magnetosphere is co-rotating with the star as a solid body, yet the co-rotation cannot persist beyond the surface where the tangential velocity equals the velocity of light. This surface is

called the light cylinder and the cylinders' radius is $R_c = \frac{c}{\Omega}$. On the light cylinder and beyond him, the magnetosphere and the neutron star do not co-rotate. On the magnetosphere we can find open and closed field lines: open field lines begin from a small polar region and permeate the light cylinder $(r > R_c)$ whereas closed field lines do not permeate the light cylinder $(r \leq R_c)$ (see illustration below). Since $\sin^2 \frac{\theta}{r}$ is constant for dipole field lines, the radius of the region which contains the open field lines (polar cap region) is

$$R_p \sim \mathrm{R}\sin\theta_p \sim (R^3 R_c)^{1/2}$$

The only way charged particles can escape the neutron star is if they are moving along open field lines and because near the rotation axis $\frac{d\Phi}{dr} > 0$ (which means that the potential increases as the distance r from the center of the star increases), electrons will move along these open field lines away from the stellar surface to form an increasing external potential. At some critical field line the two potentials are equal so that at the annular region (the region between the critical field line and the last open field line) the potential will be positive and so positively charged ions will flow from that region of the star surface to the magnetosphere. The critical field lines' position is determined by the condition that there be no net charge flow from the star:

$$\Phi = 0\,, \cos^2\theta_0 = \frac{1}{3}$$

which determines the regions of positive $(\theta < \theta_0)$ and negative $(\theta > \theta_0)$ charges. The magnetosphere is divided into regions of positive and negative charges.

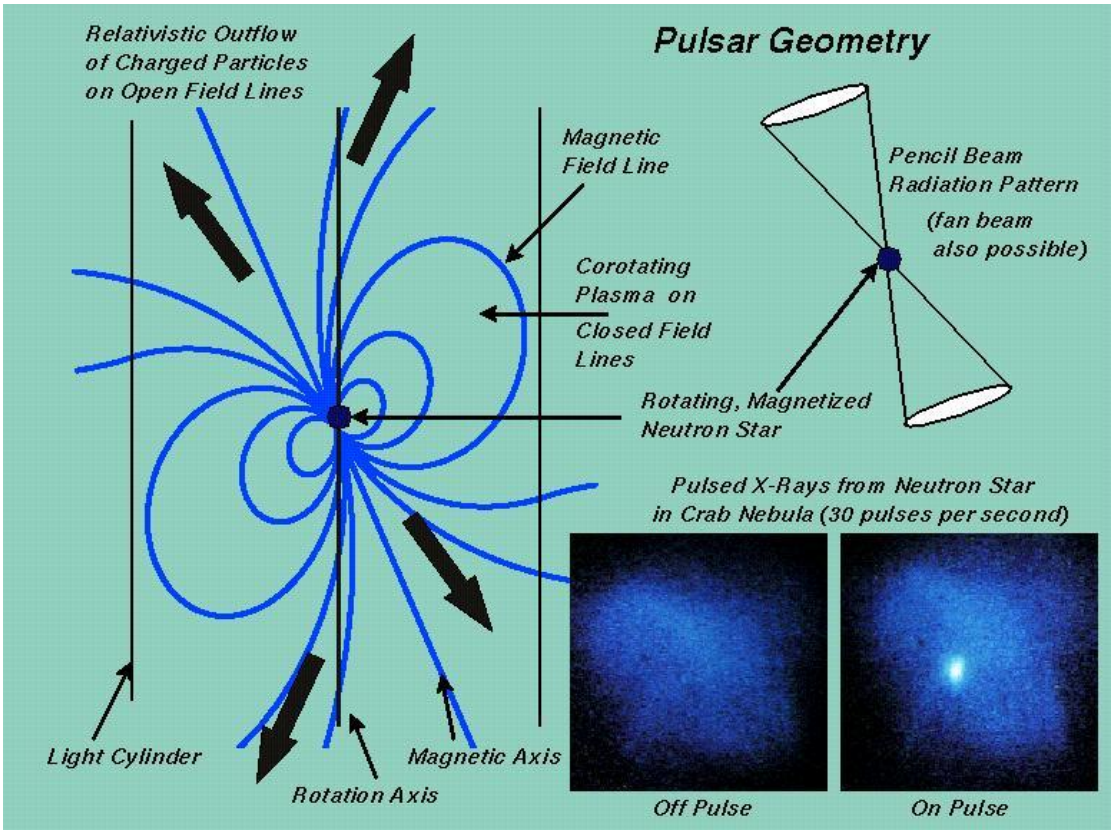

The Goldreich and Julian model overcame the vacuum assumption but had simplifications such as the flow of charge of one sign through space containing charge of the opposite sign, an event that is very unlikely to occur in real pulsars.

Many scientists have worked on the Goldreich-Julian model in order to improve it and make it more realistic e.g. Mestel (1971) ,Cohen and Toton (1971) showed that the Goldreich-Julian model remained valid for a perpendicular rotator.

4. General Characteristics of Pulsars

At this time about 1800 pulsars have been observed and each one of them is designated by a "PSR" prefix followed by its right ascension (α) and declination (δ). For example PSR 0531+21 stands for a pulsar with coordinates $\alpha = 5^h31^m$ and $\delta = +21^o$.

All the pulsars share a number of basic characteristics of which the most important are:

- emission of broadband radio noise in the form of a periodic sequence of pulses (Manchester & Taylor, 1977) . Most pulsars have periods between 0.25 s and 2 s and they are so well-defined they would make exceptionally accurate clocks.
- periods of all pulsars increase gradually as the pulses slow down, the rate of increase being given by the period derivative $\dot{P} = \frac{dP}{dt}$. Typically $\dot{P} \approx 10^{-15}$ and $T = \frac{P}{\dot{P}} \approx 10^7$ years, where T the characteristic time of the pulsar (the time it would take the pulses to cease if $\dot{P}$ were constant) (Carroll & Ostlie, 2006).
- a stable integrated profile that characterizes each pulsar.

If the observations of a pulsar are being made at a higher resolution (instrumental time constant ~ 1ms), more complex structures of the pulses become visible: often an individual pulse consists of two or more subpulses. Subpulses vary in the aspect of longitude or phase within the integrated profile. An even higher resolution (~10 μs) might reveal that some pulsars within subpulses show microstructure.

There are pulsars having a single component (peak) in their profile and there are others that have several components, sometimes partially overlapping.

4.1 Characteristics of integrated profiles

An integrated profile is the superposition of some hundreds of successive pulses. In general the shape of a pulsars integrated profile may be slightly frequency depended, but the ground character of the shape is stable. So, as mentioned above, the integrated profile of a pulsar is his trade mark.

A pulsars integrated profile may exhibit differences, such as:

- mode changing: the mean profile of a pulsar abruptly changes between two or more quasi stable states.
- pulse nulling: a phenomenon in which the pulse energy suddenly drops to zero or near zero and then just suddenly returns to its normal state (Backer, 1970).
- drifting subpulses: the emission of a pulsar is observed in an interval lasting ~1/30 of a period (pulse window). If the width of the window remains stable, the subpulses may drift across it.
- polarization: the radiation that pulsars emit is highly polarized. Individual pulses may present 100% elliptical polarization, even full linear or circular polarization can be seen. The polarization of the integrated profile is lower (Spyrou, 2008) . High polarization indicates the presence of a strong magnetic field.

Manchester and Taylor classify the pulsars into two broad groupings, according to whether they have "single" or "double" profiles. *Type S* (simple) pulsars have single profiles, usually short periods and weak polarization whereas *Type C* (complex) pulsars have double profiles, usually long periods (> 1s) and strong linear polarization. If pulsars exhibit drifting subpulses they are called *Type D* and if more detail is needed *Type SD* or *CD* indicating a simple or complex profile.

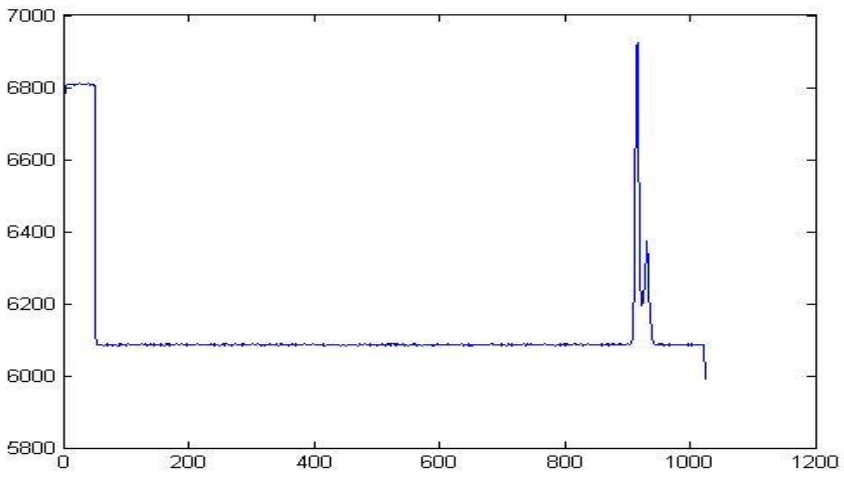

Integrated profile of PSR 1133+16

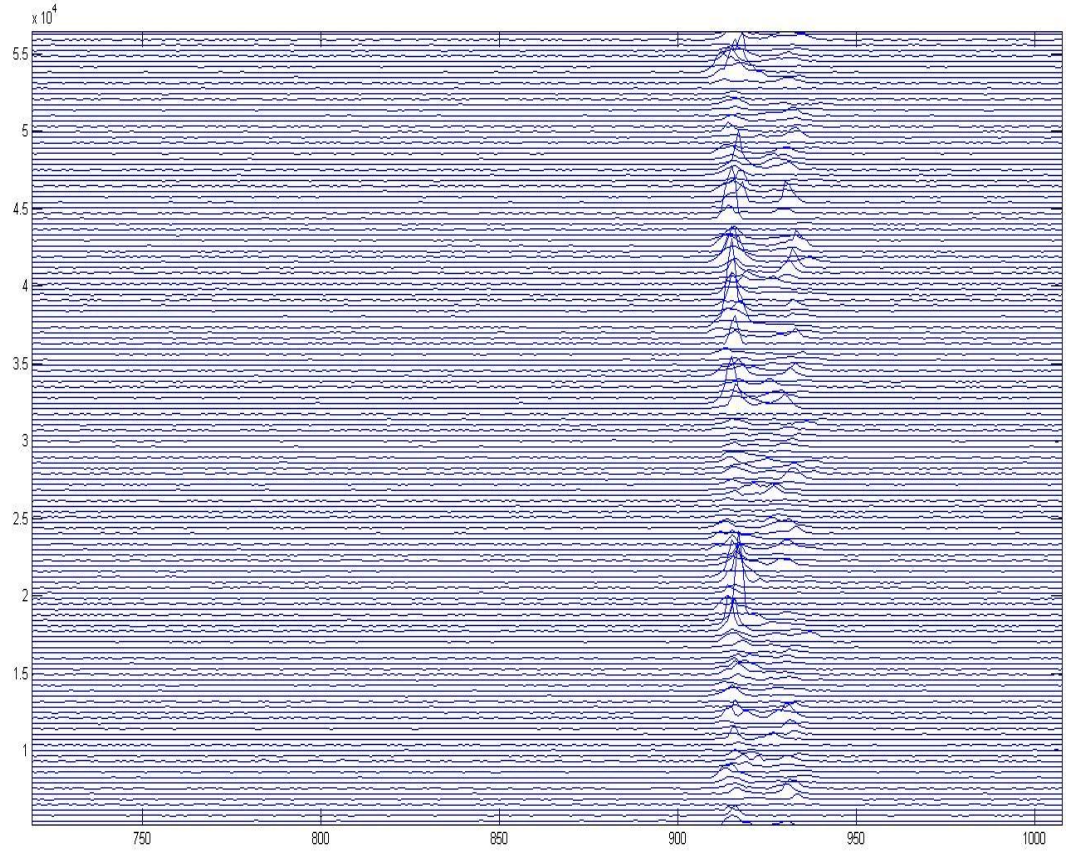

Individual pulses of PSR 1133+16

4.2 Characteristics of individual pulses

Because the integrated profile for a given pulsar is stable, one might be expecting that its individual pulses won't vary greatly. But the fact is that individual pulses of a pulsar vary greatly and chaotically - from one period to the next - in shape, intensity and polarization. Therefore the components of an integrated profile are formed when subpulses are stronger and/or occur more frequently at a given longitude.

There are different types of intensity fluctuation. Pulse nulling is one of them and it is very characteristic. Pulsar nulling can occur for a few up to hundreds of pulses. (Ritchings, 1976) states that an estimate was made of the fraction of time spent by each of 32 observed pulsars in the nulled state, and it is found that pulse nulling is a characteristic of pulsar old

age: it is suggested that pulse nulls correspond to the time intervals between bursts and that the bursts occur less frequently as a pulsar grows older. The pulsar will effectively die when the separation of the bursts becomes much larger than their duration.

Drifting subpulses is another characteristic of individual pulses. In their case we can define a new period P_2 which is the time needed so that the pulse profile repeats itself exactly and it is far greater that the neutron stars axial rotation period P. Except for P_2, another period P_3 can be defined which designates the distance between the subpulses and during P_3 the energy distribution of the pulse repeats itself.

When high resolution is applied to pulsars with short periods, subpulses show significant variations in intensity on time scales of ~10-100μs . These variations are called micropulses and their time scales are smaller than those characterizing subpulses. The relationship of micropulses to subpulses is very similar to the one between subpulses and integrated profiles.

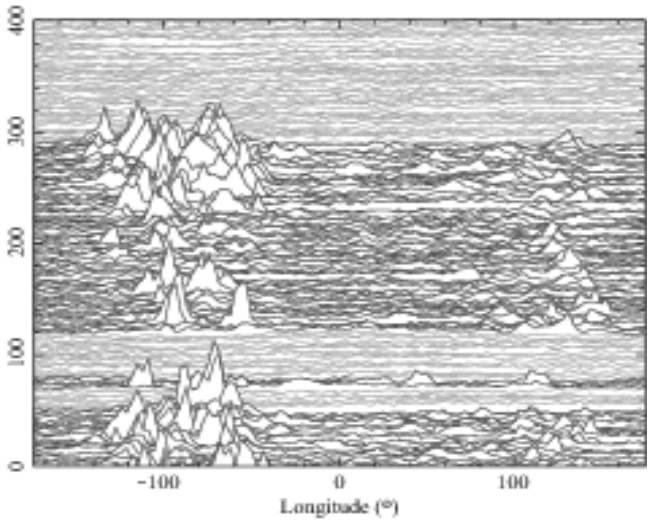

This illustration shows several nulls in light gray and a transition to a weak mode interval lasting several thousand pulses, starting at pulse number 300.

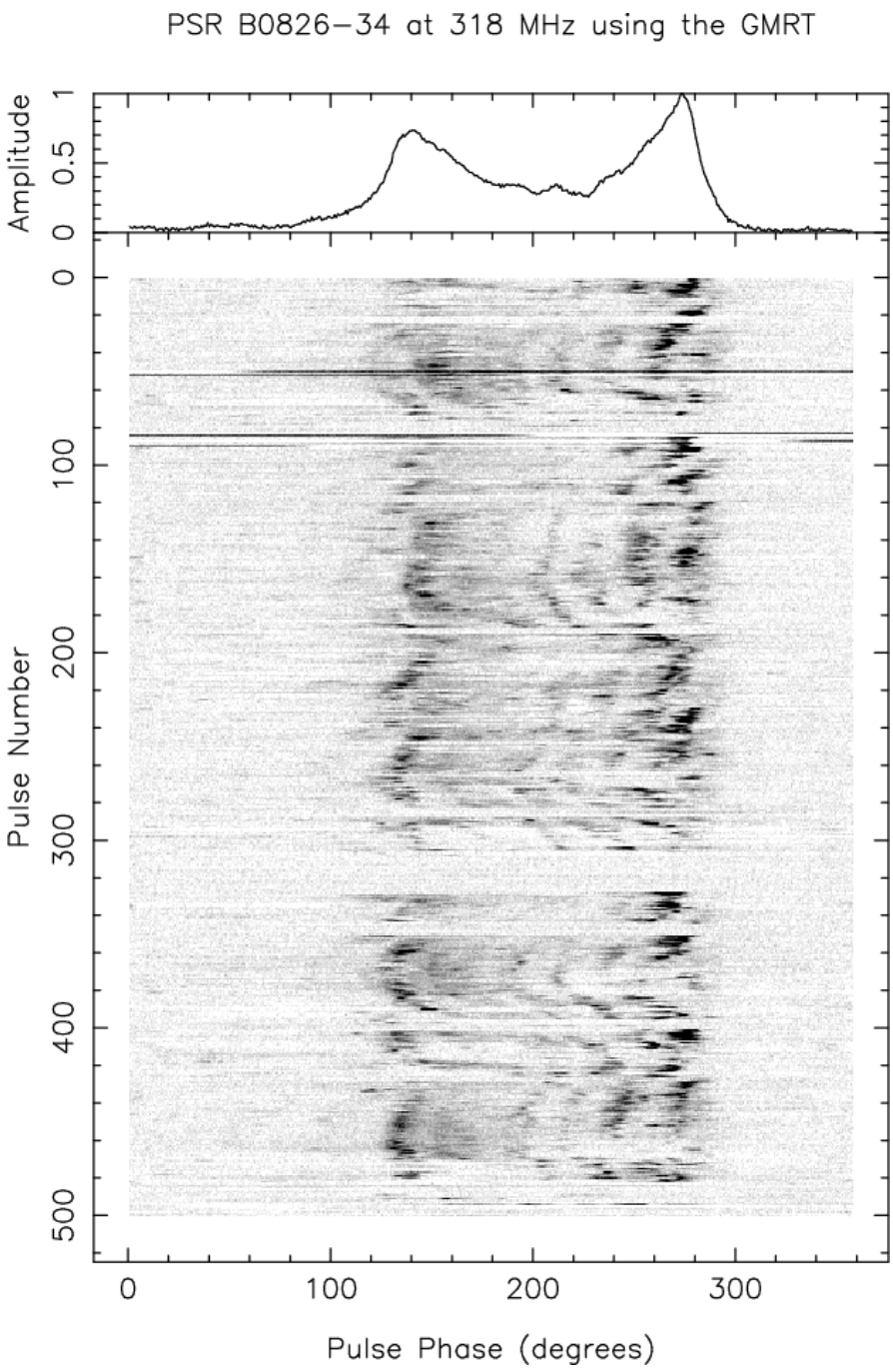

Illustration of how individual pulses, who normally consist of one or more subpulses, form the components of the pulsars integrated profile.

5. Emission Mechanisms

The main characteristic of pulsars is that they emit electromagnetic radiation, hence the name. So it is very important to understand the emission mechanisms of pulsars in order to understand the true nature of these objects. Till this day though not only no emission mechanism has been proposed that can fully explain our observations but some propose that different pulsars can possibly have different emission mechanisms.

A valid emission mechanism should interpret the following basic observational characteristics:

i. the generation of a beam of radiation that is orientation wise fixed with respect to the rotating star, and has a width ~ 10^{o} in the longitude direction that is constant to an outside observer.
ii. the polarization of pulses
iii. the shape and intensity of pulses exhibit fluctuations mainly in radio frequencies
iv. the production of observed luminosities and brightness temperatures of different regions of the spectrum (e.g. radio, optical)
v. the pulses are double with many interpulses.

Observations at radio frequencies show brightness temperatures higher than 10^{30} K. Taking into account that for incoherent emission there is the fundamental thermodynamic limitation that the brightness temperature $T_b \leq \varepsilon/k$ ($\varepsilon \rightarrow$particle energy, $k \rightarrow$ Boltzmann's constant), particle energies of 10^{26} eV or more would be required in order to observe $T_b \sim 10^{30}$ K. But such particle energies are far greater than any known mechanism can produce and if these particles existed they would radiate in high frequencies, thus it is almost certain that only a highly coherent emission mechanism with many particles radiating in phase can produce such radio pulse intensities. On the other hand optical and X-ray observations show brightness temperatures $T_b \leq 10^{11}$ K which are many orders of magnitude lower than the T_b at radio frequencies. In this case an incoherent emission mechanism accounts for such T_b since the particle energies required are $\sim 10^{7}$ eV and such energies are similar to those expected in pulsar magnetospheres. A piece of evidence that reinforces the incoherence of optical pulses is the observed lack of intensity fluctuations in them. Since the plasma is probably turbulent, the absence of intensity fluctuations suggests that optical pulses originate from a region that is large relative to the scale of the turbulence. Though radio and optical emission processes are different, the time of their peaks coincide and that is a fact that gives us good reason to suspect a close relationship between these different emission processes.

5.1 Coherent radio emission

When particles radiate in phase, the emission is referred as coherent. There are three general forms of coherent mechanisms:

a. The presence of particle bunches of dimensions less than a wavelength, separated by distances greater than a wavelength is required. In this case fields are added rather than intensities so that if N is the number of particles per bunch, the resulting intensity is $I_\nu \approx N^2 I_{\nu,i}$. The wavelength being the wavelength of the coherent radiation.
b. Maser amplification is required, i.e. stimulated emission of radiation. In the case of maser radiation, the specific intensity of the source is $I_\nu = \frac{j}{\kappa}\left(1 - e^{-\kappa l}\right)$, where l is the size of the source and j, κ are the coefficients of spontaneous emission and absorption respectively. If κ<0 and κl<-1, then I_ν increases exponentially with the size of the source.
c. A reactive instability corresponds to an intrinsically growing wave in which growth occurs due to phase bunching. (Melrose, Oct.15,1992)

From these general forms a maser type emission is intrinsically the most plausible for any coherent emission from an astrophysical source.

But emission processes in plasmas are also categorized according to the way the waves escape the plasma to infinity: some wave modes are unable to escape the plasma due to encounters with stop bands which reflect them or regions that absorb them. So the emission processes are classified as follows:

a. Direct emission: the waves' mode allows it to escape the astrophysical plasma e.g. curvature, cyclotron and linear acceleration emissions.
b. Indirect emission: the waves' mode hinders its escape and thus it has to be transformed into a mode that can escape.

Where a pulsars' emission originates is also debatable. According to the emission mechanisms proposed, the emission can originate from: outside the light cylinder, the closed field-line region and the open field-line region.

5.1.1 *The Hollow Cone model*

It is a model proposed by Radhakrishnan & Cooke in 1969 and it is a polar cap model which means that the emission (usually curvature radiation) originates near the polar regions of the pulsar. The main assumption being made is that the cone is centered on the magnetic field axis which is pointing at latitude μ according to a reference frame designated by the rotational axis of the neutron star. In this polar cap model electrons move along the open field lines and radiate because of the field lines' curvature. The average pulse profile is determined by the average intensity distribution along the cut of the line of sight through part of the hollow cone. (Sieber, 1996)

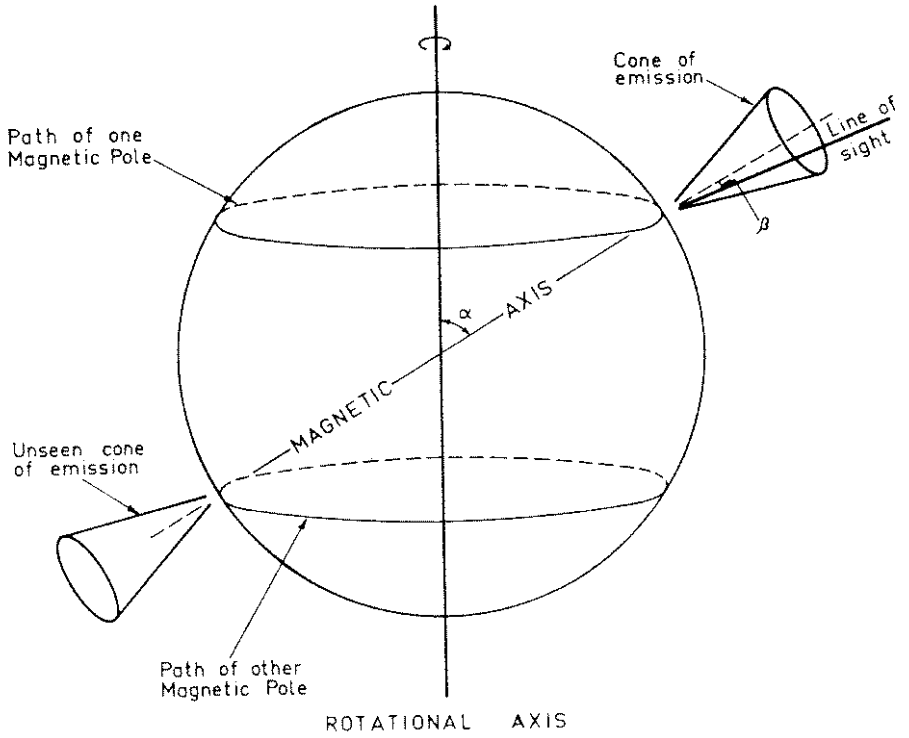

The Hollow Cone model.

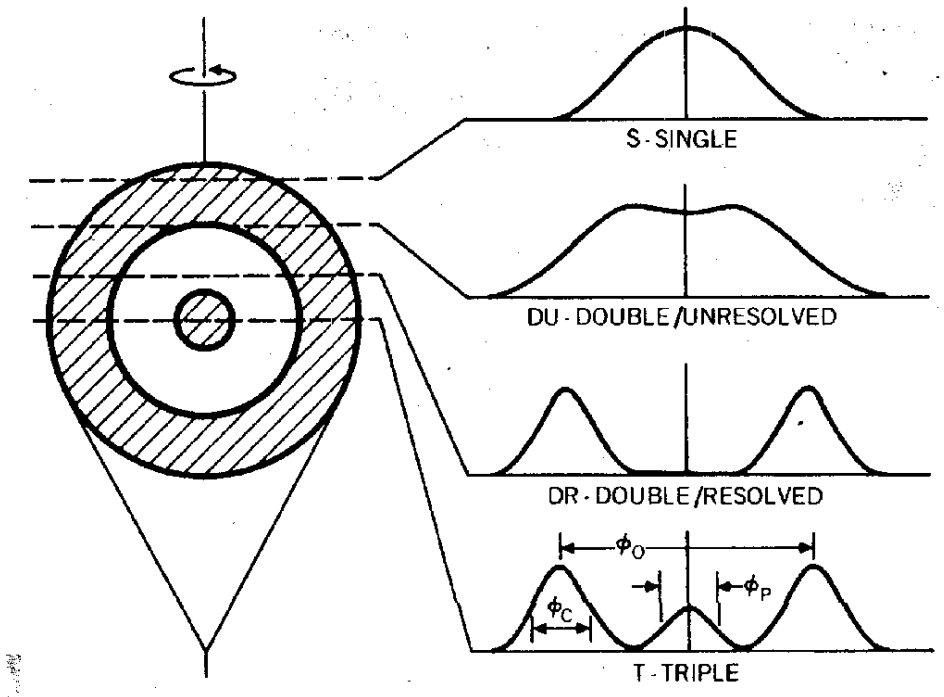

As shown in the above figure a decrease in secondary plasma density occurs in the central regions of the open magnetic field lines. Making the assumption that the radio emission is connected with the outflowing plasma density we can easily conclude that the radio emission decreases as we go to the center of the directivity pattern and so we should expect a single profile in pulsars where the line of sight is far from the center of the directivity pattern and a double in those whose line of sight is near the center. (Beskin, 2010)

5.1.2 *Pair Creation Cascades*

It is a model that was proposed by Sturrock in 1970 and refined by Ruderman & Sutherland in 1975. In this model the magnetic dipole axis is not aligned with the spin axis and the pulsar is rotating in a vacuum. Electrons are accelerated by the electric field to high energies causing them to emit hard gamma rays due to their curvature radiation in following the dipolar magnetic field lines (Michel, 1991). The charged particles (*e*+*e*−) are produced by $\gamma + B \rightarrow e+ + e-$ in the polar caps and so the open field lines sustain a wind made of particles of both signs.

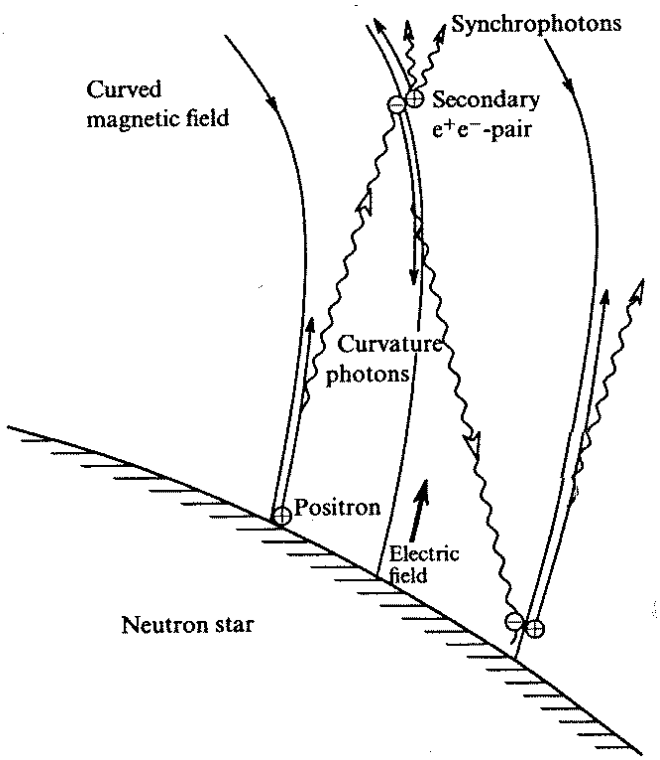

Pair Creation Cascade model.

6. Pulsars' radio emission interaction with the interstellar medium

6.1 Interstellar dispersion

The interstellar medium is considered as an isotropic and homogenous plasma whose electrons cause the dispersion of the electromagnetic waves emit by pulsars. The presence of electrons in the plasma has an effect on the propagation velocity of different wavelengths which results in a different arrival time for these wavelengths even if the difference between the propagation velocities is minimum: this effect is known as dispersion of the electromagnetic waves. Dispersion is greater for low frequency waves and thus if a

wave consists of several wavelengths, waves of high frequency arrive at the observer before waves of low frequency do.

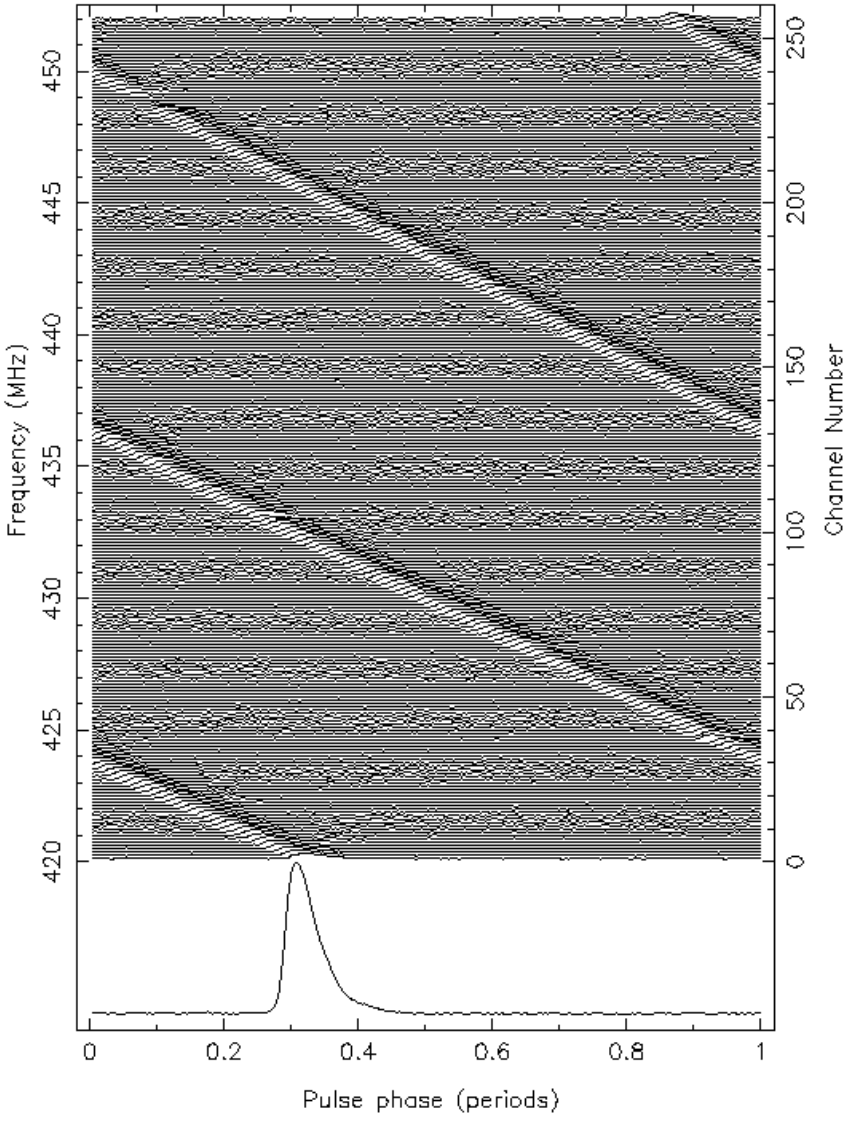

Dispersed pulses of the Vela Pulsar: arrival time depends on frequency.

The time t the waves need to travel a distance d is given by:

$$t_1 = \frac{d}{u_g},$$

where u_g is the group velocity of radio waves and it depends on the wavelength λ. It is evident that the time of propagation is different in vacuum since there electromagnetic waves travel with the speed of light t_2=d/c. Thus the wave will have a delay in propagation in the interstellar medium comparing to vacuum:

$$t = t_2 - t_1 \approx \frac{e^2}{2\pi m_e c}\frac{DM}{f^2},$$

where e is the electron charge, m_e the electron mass, f the wave frequency and

$$DM = \int_0^d n_e dl = n_e d$$

where n_e is the electron density of the interstellar medium and DM is called the dispersion measure and it represents the number of free electrons contained in a cylinder of the medium with a one unit base area and height d. If we know the electron density of the interstellar medium we can compute the dispersion measure and thus the distance of the pulsar using the above relations.

6.2 Faraday rotation

The interstellar medium is magnetized due to the presence of free electrons. So when the polarized radio waves of a pulsar propagate through the medium, the B_0 component of the magnetic field which is parallel to the line of propagation of radio waves causes the polarization plane to rotate, a process which is called Faraday Rotation.

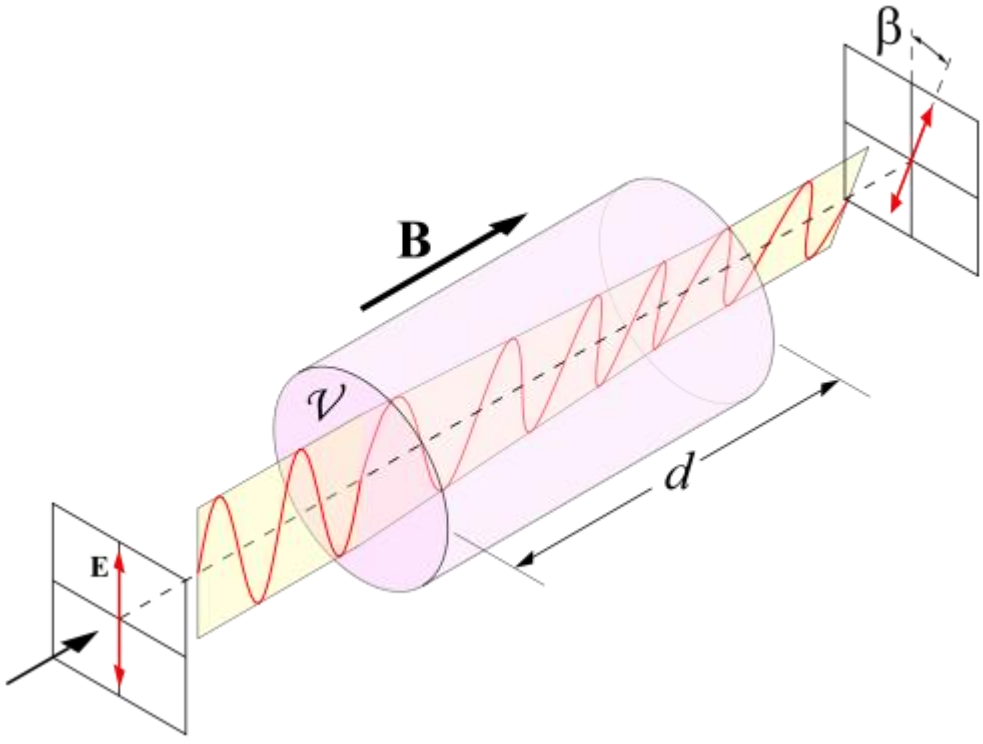

Faraday Rotation

For a linearly polarized radiation, the Faraday rotation angle is

$$\varphi = \lambda^2 (RM),$$

λ being the radiations' wavelength and RM the rotation measure

$$RM = \frac{e^3}{2\pi m_e c^4} \int_0^d n\, B \cos\theta \, dl \,,$$

where θ is the angle between the line of sight and the vector $\vec{B}$, d the distance and dl the elementary distance travelled by the radiation. The rotation measure RM is positive when the magnetic field is directed towards the observer and negative on opposite circumstances. When the measure of dispersion and rotation are known, we can compute the average value of the interstellar magnetic field along the line of sight

$$< B \cos\theta >= \frac{\int_0^d n_e B \cos\theta \, dl}{\int_0^d n_e \, dl} = \frac{1.232\, RM}{DM}$$

Pulsars are a useful tool in the study of the interstellar magnetic field because we know the distances of pulsars and therefore we can calculate the interstellar magnetic field of several areas of the galaxy using pulsars of different distances.

7. Magnetars

Magnetars are neutron stars that have a very strong magnetic field ~10^{11} T which is several orders of magnitude greater than the magnetic field of a typical pulsar and they also have relatively slow rotation periods . They were proposed to explain Soft Gamma Repeaters (SGRs) -which are objects that emit bursts of hard x-rays and soft gamma-rays - and Anomalous X-ray Pulsars (AXPs).

Some general properties of Magnetars are:

a. strong soft and hard x-ray emission
b. short x/gamma-ray flares and long outbursts
c. periods of ~0.3-12 s
d. magnetic fields ~10^{13} - 10^{15} Gauss
e. period derivatives of ~10^{-14} - 10^{-11} s/s

Magnetars are essentially a class of pulsars and the main characteristic that distinguishes them from ordinary pulsars is that they are powered by their own magnetic energy. But what led scientists in the search of a different energy source?

Rotation as source of energy: pulsars that are powered by the loss of rotational energy. These pulsars are mainly observed in radio frequencies but their energy output in this band is only a very small fraction of $\dot{E}_{rot}$.The efficiency is much higher in x-ray and gamma-ray energies. But AXPs/SGRs have $\dot{P}$ larger than radio pulsars do and that entails them to values of $\dot{E}_{rot}$~10^{32} - 10^{34} erg/s which are too small to power their luminosities.

Accretion as source of energy: x-ray pulsars are members of binary systems in which the x-ray emission is powered by the release of gravitational potential energy as matter is accreted from a massive star companion. AXPs were thought to be also powered by a binary

companion, but the lack of optical/NIR (near infrared) luminous counterparts expected if these pulsars were in high-mass binaries pointed to a different theory. Low-mass binaries were also ruled out due to the lack of orbital Doppler shifts for binary motion. Now optical and NIR counterparts have been solidly either identified or proposed and many objections have been risen. The main objection to an accretion powered model of AXPs is that it cannot account for the bursts and flares in AXPs/SGRs.

Residual Heat as source of energy: When neutron stars are born they have very high internal temperatures of ~10^{11}K and the main cooling mechanism for the upcoming 10^5 - 10^6 years is neutrino emission from the star's isothermal core. Such thermal x-ray emission can be generated by isolated neutron stars, but they have to be close enough and with little interstellar absorption of the x-rays in order to be observed. But two observational properties of AXPs/SGRs cannot be interpreted solely with the residual heat as source: (i) 'the production of a variety of strongly variable and energetic events, ranging from short bursts to giant flares, and (ii) the presence of hard tails in the spectra of the persistent emission' (Mereghetti, 2012).

Magnetic energy as power source seemed to be the last resort: a NS with a magnetic field of B=10^{15} G has enough energy to power a luminosity of ~10^{35} erg/s for ~ 10^5 years which is a probable age for AXPs/SGRs since they are often associated with supernova remnants or young massive star clusters. Also SGRs' s giant flares properties reinforces the existence of strong magnetic fields as do short bursts in both AXPs/SGRs.

8. Analysis

8.1 Data and analysis method

The objective of this thesis was the analysis and comparison of single pulses of a magnetar and two pulsars. The data that were analyzed were taken 100-m telescope at Effelsberg and they are shown in the Tables below.

Magnetar Data

Date	*Scan*	*#Single Pulses*	*Observation frequency (GHz)*	*σ*	*Quality*
10.07.06	5954	323	8.35	0,0026	10
	5955	324	8.35	0,0022	11
	5956	644	8.35	0,0009	12
17.07.06	7202	324	8.35	0,0012	11
	7203	324	8.35	0,0015	10
	7204	322	8.35	0,0014	11
	7205	324	8.35	0,001	10
	7206	323	8.35	0,0019	9
	7207	323	8.35	0,0029	5
	7209	323	8.35	0,0009	12
22.07.06	8093	322	8.35	0,0009	9
	8095	319	8.35	0,002	5
26.07.06	8512	324	4.85	0,0008	5
	8510	324	8.35	0,0006	9
28.07.06	8700	323	8.35	0,0024	6
	8701	324	8.35	0,0007	7
05.08.06	9671	282	2.64	0,002	10
	9672	308	2.64	0,0026	10
	9673	319	2.64	0,0021	9

Pulsar Data

Pulsar	*Scan*	*#Single Pulses*	*Observation frequency (GHz)*	*σ*	*Quality*
psr 1133+16	2691	378	8.35	0,0007	12
		378	8.35		
		375	8.35		
psr 0329+54	2709	373	8.35	0,001	12
		373	8.35		
		373	8.35		

I used the "jhspuls" program in its matlab "version" in order to do the data analysis. The matlab "jhspuls" program consists of several subroutines and each one of them carries out a different part of the analysis process.

The analysis process always begins with the command set_defaults that sets parameters which are necessary for the next steps of the process. Afterwards we need to call the data file that we want to analyze and with the subroutine get_data we load the file's data.

>> set_defaults

G2 =

1.5000

>> filename='pul5956.dat'

filename =

pul5956.dat

>> get_data

id1 =

PSR 1809-194 8.3505 GHz Scan 5956 mjd 53927.4814

>>

A significant part of my work on my thesis was the coding of a script called quality which exists in the program's prototype that is coded in fortran, but not in its matlab version. The task of the subroutine quality is to classify the single pulses into 12 classes according to their quality, where quality is defined as the ratio of the pulse's intensity to the standard deviation of the baseline. The quality classification can be done either based on the energy of the pulse, or based on the maximum of the pulse. Standard deviation will be from now on referred to as sigma.

So after the course of action described above I call the subroutine quality. This subroutine carries out the following: it adds up channels 1 and 2 which contain the single pulses data and plots the integrated profile. From the figure we can manually select the beginning and the end of the calibration signal which is needed for further calculations. Subsequently we select again from the figure manually two "windows" on either sides of the pulse, in order to calculate the sigma of every single pulse. Lastly we select manually the beginning and the end of the pulse we want to analyze. In the analysis that I did, I first selected the whole pulse and then it's components.

After everything described above the single pulses can be finally classified according to their quality in classes that are defined by the user. I used different classes for the two different classifications ($\frac{pulse\ energy}{sigma}$ and $\frac{pulse\ maximum}{sigma}$) that I kept the same for all data analyzed.

>> pul_quality

Please select beginning & end of calibration signal

Please select sigma boundaries
Please magnify the plot
Please enter the number of components (peaks only): 2

ATTENTION: Select first begining and end of the whole pulse.
Please enter the rx_type wavelength of the signal
Please call subroutine convertsigK>> rx36mm
K>> convertsig

ans =

<Tsys1>= 32.0 error 1.8 K <Tsys2>= 31.4 error 1.8 K

eta_p =

0.7624

meanS =

0.0071

dS =

6.6001e-004

K>> return
K>> return

Do you want to set new qlimitsE ? [y/n] n

Do you want to set new qlimitsM ? [y/n] n

Quality ends with the pop up of a number of figures (plots) that is equal to the number of components of the pulsar. Every figure contains 12 plots and each of them belongs to one of the 12 quality classes. Every plot shows the sum of the single pulses that belong to the same quality class as the plot.

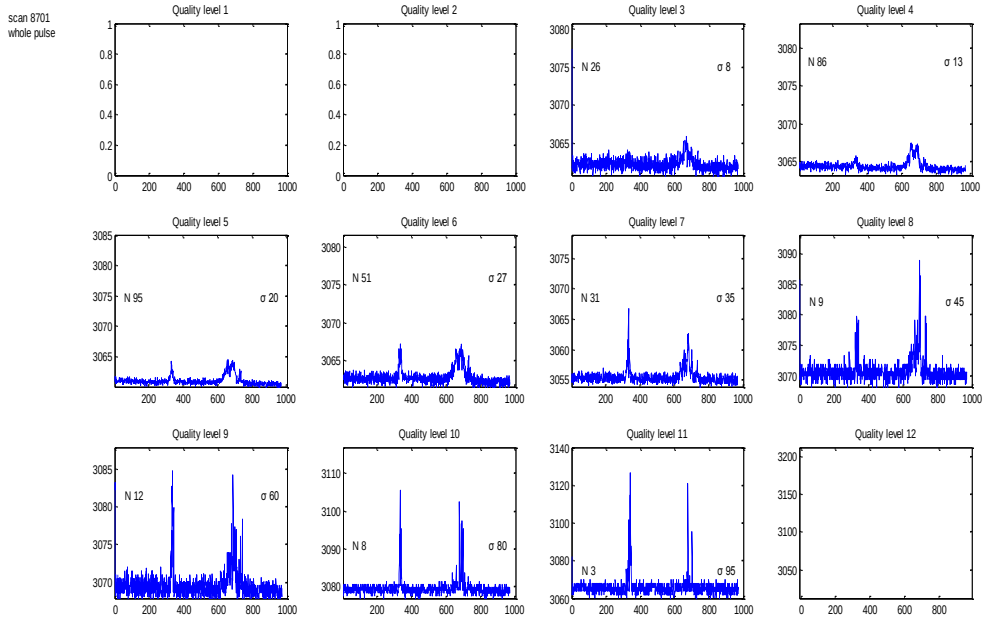

8.1.1 Main characteristics of AXP 1809-194, PSR B0329+54 and PSR B1133+16

As already mentioned, the data that were analyzed come from the magnetar AXP J1809-194 and the pulsars PSR B0329+54 and PSR B1133+16. The main characteristics of these NS as well as an integrated profile, are shown below.

Name	***RA***	***Dec.***	***Period P(s)***	$\dot{P}$ $(10^{-15}ss^{-1})$	***DM*** $(cm^{-3}pc)$	***Age*** $(10^6\ yr)$
AXP J1809-194	18 06 53.4	-19 44 27.8	5.54	11500	178	
PSR B0329+54	03 29 11	+54 24 37	0.7145	2.05	26.7	5.5
PSR B1133+16	11 33 27	+16 07 35	1.1879	3.73	4.8	5.0

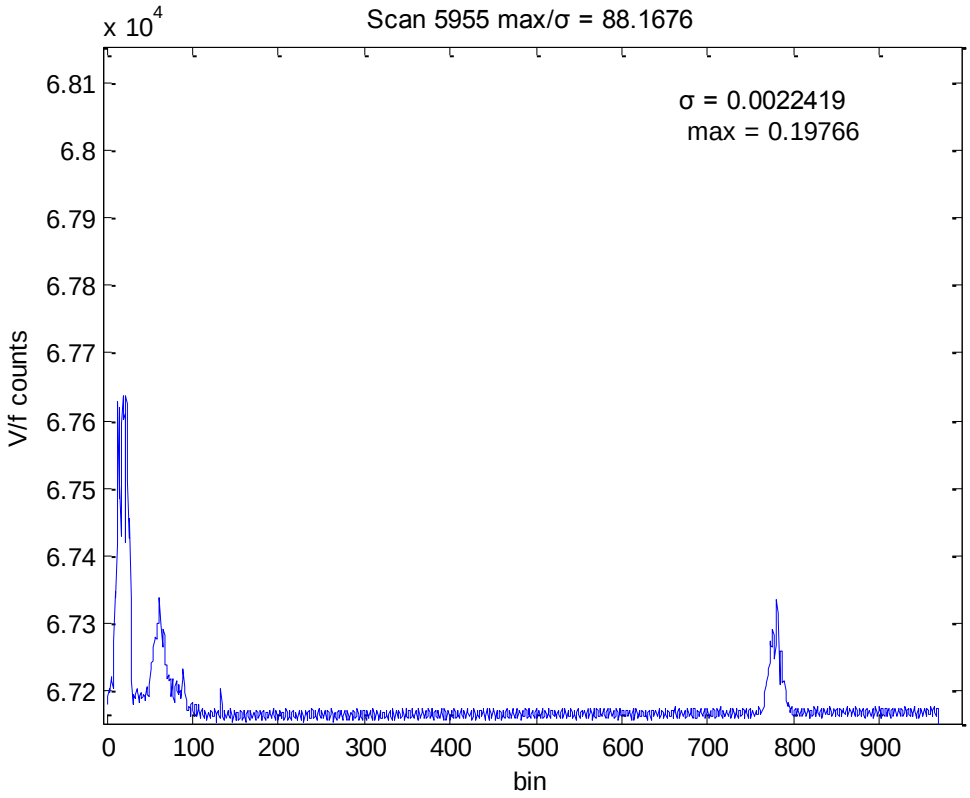

Integrated profile of AXP 1809-194 (The ATNF Pulsar Database).

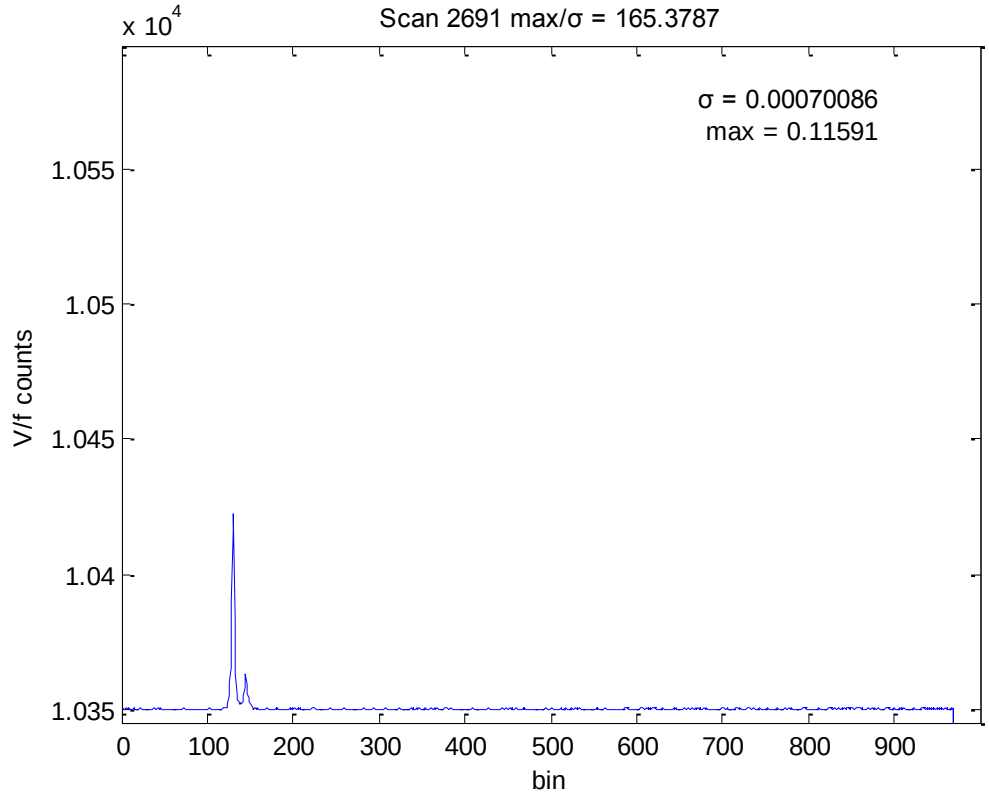

Integrated profile of PSR B1133+16.

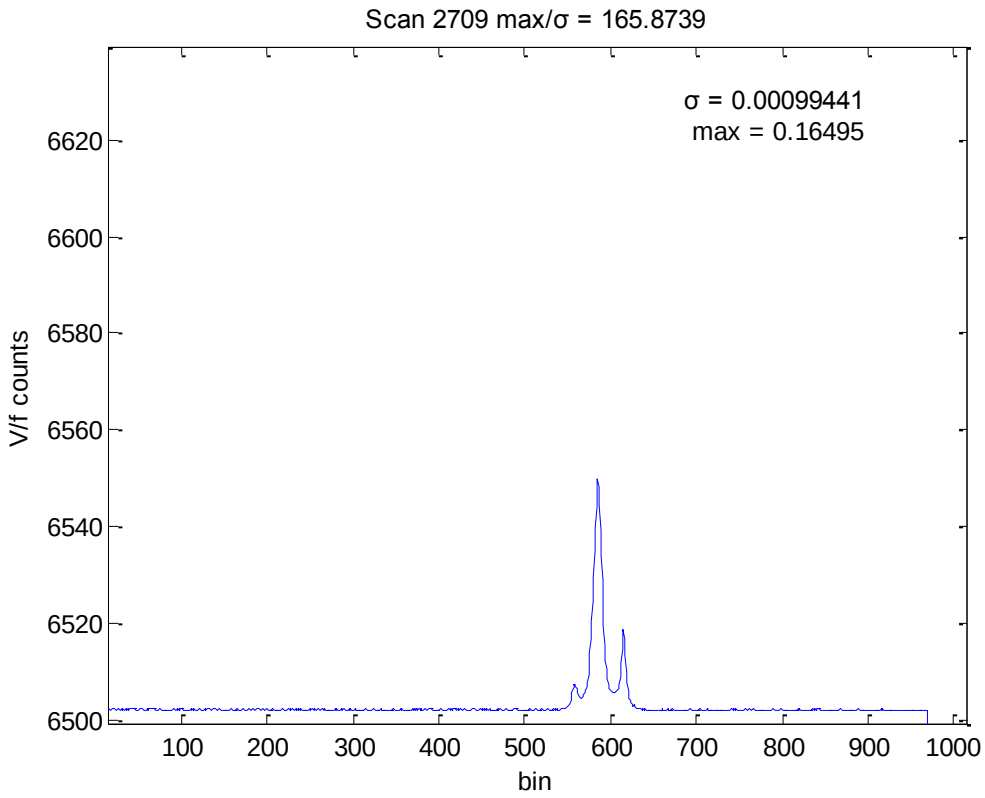

Integrated profile of PSR B0329+54.

8.2 Statistics

The single pulses of each scan were analyzed and classified according to their quality with respect to both energy and maximum of the pulse. The results for each scan were then summarized in a Table. That Table contains for each component of the pulse the number of single pulses in each quality class. The Tables are shown below.

AXP 1809-194, Scan 5954max

Quality (σ)	***Whole pulse***	***Main Pulse***	***1st Component***	***2nd Component***	***3rd Component***	***Interpulse***
0-1	0	0	0	0	2	0
1-3	0	1	163	2	293	168
3-8	39	49	75	60	12	36
8-13	41	71	21	86	5	12
13-20	54	60	8	76	5	25
20-27	39	42	4	43	2	15
27-35	32	25	1	31	0	14
35-45	13	12	3	11	0	4
45-60	23	10	1	10	2	15
60-80	23	11	8	3	0	16
80-95	9	5	4	1	0	4
>95	50	37	35	0	2	14

AXP 1809-194, Scan 5954 energy

Quality (σ)	*Whole pulse*	*Main Pulse*	*1st Component*	*2nd Component*	*3rd Component*	*Interpulse*
0-1	301	255	257	172	316	235
1-1.5	13	25	9	104	2	23
1.5-3	8	14	10	46	3	32
3-5	1	6	7	1	2	20
5-7	0	8	6	0	0	12
7-9	0	10	5	0	0	1
9-11	0	2	2	0	0	0
11-13	0	2	1	0	0	0
13-16	0	0	2	0	0	0
16-19	0	0	3	0	0	0
19-25	0	1	5	0	0	0
>25	0	0	16	0	0	0

AXP 1809-194, Scan 5955 max

Quality (σ)	*Whole pulse*	*Main Pulse*	*1st Component*	*2nd Component*	*3rd Component*	*Interpulse*
0-1	0	0	1	0	1	1
1-3	0	0	147	0	309	175
3-8	22	26	79	35	7	26
8-13	44	56	18	68	1	15
13-20	45	60	8	80	1	25
20-27	46	57	8	61	2	9
27-35	26	29	7	29	0	11
35-45	29	26	4	28	-	10
45-60	24	19	5	18	-	9
60-80	16	7	4	5	0	12
80-95	9	3	3	0	0	7
>95	63	41	40	0	-	24

AXP 1809-194, Scan 5955 energy

Quality (σ)	*Whole pulse*	*Main Pulse*	*1st Component*	*2nd Component*	*3rd Component*	*Interpulse*
0-1	292	228	247	141	320	235
1-1.5	7	43	12	99	0	11
1.5-3	21	16	16	79	3	34
3-5	4	8	5	5	0	26
5-7	0	3	7	0	1	12
7-9	0	7	0	0	0	5
9-11	0	6	0	0	0	1
11-13	0	6	2	0	0	0
13-16	0	3	5	0	0	0
16-19	0	3	2	0	0	0
19-25	0	1	3	0	0	0
>25	0	0	25	0	0	0

AXP 1809-194, Scan 5956 max

Quality (σ)	***Whole pulse***	***Main Pulse***	***1st Component***	***2nd Component***	***3rd Component***	***Interpulse***
0-1	0	0	0	0	4	0
1-3	1	1	234	4	606	343
3-8	28	50	178	77	21	99
8-13	74	103	58	130	4	33
13-20	123	142	36	175	2	24
20-27	76	90	12	107	2	15
27-35	70	69	6	77	1	15
35-45	46	35	2	35	1	20
45-60	52	42	12	33	2	18
60-80	31	11	6	5	0	24
80-95	15	6	6	0	0	14
>95	128	95	94	1	1	39

AXP 1809-194, Scan 5956 energy

Quality (σ)	***Whole pulse***	***Main Pulse***	***1st Component***	***2nd Component***	***3rd Component***	***Interpulse***
0-1	587	409	468	256	636	497
1-1.5	17	113	37	203	2	24
1.5-3	39	45	22	181	3	56
3-5	1	23	15	4	2	36
5-7	0	12	14	0	1	18
7-9	0	15	10	0	0	8
9-11	0	16	6	0	0	5
11-13	0	6	9	0	0	0
13-16	0	5	6	0	0	0
16-19	0	0	3	0	0	0
19-25	0	0	13	0	0	0
>25	0	0	41	0	0	0

AXP 1809-194, Scan 7202 max

Quality (σ)	***Whole pulse***	***Main Pulse***	***1st Component***	***2nd Component***	***3rd Component***	***Interpulse***
0-1	0	0	1	0	11	0
1-3	0	1	99	1	293	145
3-8	29	48	120	71	7	46
8-13	64	105	47	114	3	10
13-20	70	92	37	81	2	16
20-27	36	35	9	31	2	13
27-35	16	14	2	12	0	8
35-45	26	14	4	8	2	14
45-60	21	10	4	4	2	14
60-80	16	2	0	2	0	14
80-95	8	1	1	0	0	8
>95	38	2	0	0	2	36

AXP 1809-194, Scan 7202 energy

Quality (σ)	***Whole pulse***	***Main Pulse***	***1st Component***	***2nd Component***	***3rd Component***	***Interpulse***
0-1	324	317	297	270	318	241
1-1.5	0	7	18	46	1	21
1.5-3	0	0	8	8	3	33
3-5	0	0	1	0	1	20
5-7	0	0	0	0	1	4
7-9	0	0	0	0	0	2
9-11	0	0	0	0	0	2
11-13	0	0	0	0	0	1
13-16	0	0	0	0	0	0
16-19	0	0	0	0	0	0
19-25	0	0	0	0	0	0
>25	0	0	0	0	0	0

AXP 1809-194, Scan 7203 max

Quality (σ)	***Whole pulse***	***Main Pulse***	***1st Component***	***2nd Component***	***3rd Component***	***Interpulse***
0-1	0	0	0	0	1	1
1-3	0	0	80	1	294	170
3-8	35	53	128	71	12	51
8-13	71	86	55	104	2	15
13-20	66	85	36	75	4	11
20-27	44	49	16	37	4	9
27-35	22	22	6	13	4	5
35-45	22	15	0	14	1	10
45-60	16	8	0	8	0	9
60-80	7	1	0	1	0	6
80-95	6	1	1	0	0	5
>95	35	4	2	0	2	32

AXP 1809-194, Scan 7203 energy

Quality (σ)	***Whole pulse***	***Main Pulse***	***1st Component***	***2nd Component***	***3rd Component***	***Interpulse***
0-1	322	299	280	213	320	261
1-1.5	2	18	26	74	2	17
1.5-3	0	5	14	37	0	17
3-5	0	2	1	0	1	17
5-7	0	0	1	0	1	6
7-9	0	0	1	0	0	4
9-11	0	0	1	0	0	1
11-13	0	0	0	0	0	0
13-16	0	0	0	0	0	1
16-19	0	0	0	0	0	0
19-25	0	0	0	0	0	0
>25	0	0	0	0	0	0

AXP 1809-194, Scan 7204 max

Quality (σ)	*Whole pulse*	*Main Pulse*	*1st Component*	*2nd Component*	*3rd Component*	*Interpulse*
0-1	0	0	5	0	7	0
1-3	0	0	83	1	286	114
3-8	20	25	108	35	16	51
8-13	46	78	61	89	4	15
13-20	61	84	35	86	2	16
20-27	39	60	15	48	3	7
27-35	24	35	10	30	1	8
35-45	31	19	0	18	1	20
45-60	18	14	2	11	1	13
60-80	17	4	1	3	1	15
80-95	9	1	1	0	0	8
>95	57	2	1	1	0	55

AXP 1809-194, Scan 7204 energy

Quality (σ)	*Whole pulse*	*Main Pulse*	*1st Component*	*2nd Component*	*3rd Component*	*Interpulse*
0-1	312	271	263	178	315	217
1-1.5	8	37	39	98	4	18
1.5-3	2	14	16	44	3	43
3-5	0	0	3	2	0	29
5-7	0	0	1	0	0	9
7-9	0	0	0	0	0	3
9-11	0	0	0	0	0	0
11-13	0	0	0	0	0	1
13-16	0	0	0	0	0	2
16-19	0	0	0	0	0	0
19-25	0	0	0	0	0	0
>25	0	0	0	0	0	0

AXP 1809-194, Scan 7205 max

Quality (σ)	*Whole pulse*	*Main Pulse*	*1st Component*	*2nd Component*	*3rd Component*	*Interpulse*
0-1	0	0	6	0	11	0
1-3	1	1	130	1	292	131
3-8	63	88	104	115	13	73
8-13	86	108	50	100	3	28
13-20	61	77	21	72	1	11
20-27	18	18	4	14	2	8
27-35	20	15	3	13	0	8
35-45	12	7	1	5	1	9
45-60	13	5	2	2	1	9
60-80	16	3	1	2	0	14
80-95	6	0	0	0	0	6
>95	28	2	2	0	0	27

AXP 1809-194, Scan 7205 energy

Quality (σ)	*Whole pulse*	*Main Pulse*	*1st Component*	*2nd Component*	*3rd Component*	*Interpulse*
0-1	320	295	266	246	317	247
1-1.5	2	20	29	62	5	24
1.5-3	2	9	23	16	2	26
3-5	0	0	3	0	0	19
5-7	0	0	2	0	0	3
7-9	0	0	1	0	0	4
9-11	0	0	0	0	0	0
11-13	0	0	0	0	0	1
13-16	0	0	0	0	0	0
16-19	0	0	0	0	0	0
19-25	0	0	0	0	0	0
>25	0	0	0	0	0	0

AXP 1809-194, Scan 7206 max

Quality (σ)	*Whole pulse*	*Main Pulse*	*1st Component*	*2nd Component*	*3rd Component*	*Interpulse*
0-1	0	0	0	0	5	0
1-3	0	0	98	1	297	92
3-8	21	39	137	50	9	84
8-13	56	98	50	99	2	14
13-20	58	73	22	75	2	17
20-27	44	57	10	53	0	8
27-35	33	26	2	26	1	15
35-45	19	16	2	12	2	7
45-60	11	6	0	5	1	9
60-80	19	6	2	2	2	17
80-95	9	0	0	0	0	9
>95	53	2	0	0	2	51

AXP 1809-194, Scan 7206 energy

Quality (σ)	*Whole pulse*	*Main Pulse*	*1st Component*	*2nd Component*	*3rd Component*	*Interpulse*
0-1	323	288	287	178	315	211
1-1.5	0	32	22	93	2	22
1.5-3	0	3	13	52	5	39
3-5	0	0	1	0	1	27
5-7	0	0	0	0	0	13
7-9	0	0	0	0	0	8
9-11	0	0	0	0	0	3
11-13	0	0	0	0	0	0
13-16	0	0	0	0	0	0
16-19	0	0	0	0	0	0
19-25	0	0	0	0	0	0
>25	0	0	0	0	0	0

AXP 1809-194, Scan 7207 max

Quality (σ)	*Whole pulse*	*Main Pulse*	*1st Component*	*2nd Component*	*3rd Component*	*Interpulse*
0-1	0	0	1	0	2	0
1-3	0	0	125	1	293	221
3-8	34	47	123	58	5	35
8-13	86	99	40	105	6	14
13-20	81	81	20	85	6	11
20-27	40	42	10	35	0	7
27-35	25	24	1	22	2	6
35-45	20	14	2	9	2	8
45-60	15	11	1	5	5	4
60-80	11	2	0	1	1	9
80-95	5	1	0	0	1	4
>95	6	2	0	2	0	4

AXP 1809-194, Scan 7207 energy

Quality (σ)	*Whole pulse*	*Main Pulse*	*1st Component*	*2nd Component*	*3rd Component*	*Interpulse*
0-1	323	265	288	151	309	280
1-1.5	0	44	18	104	3	15
1.5-3	0	14	15	67	9	20
3-5	0	0	2	1	2	7
5-7	0	0	0	0	0	1
7-9	0	0	0	0	0	0
9-11	0	0	0	0	0	0
11-13	0	0	0	0	0	0
13-16	0	0	0	0	0	0
16-19	0	0	0	0	0	0
19-25	0	0	0	0	0	0
>25	0	0	0	0	0	0

AXP 1809-194, Scan 7209 max

Quality (σ)	*Whole pulse*	*Main Pulse*	*1st Component*	*2nd Component*	*3rd Component*	*Interpulse*
0-1	0	0	0	0	1	0
1-3	0	0	131	0	258	206
3-8	30	37	122	50	34	20
8-13	80	101	51	111	7	18
13-20	75	92	12	81	9	12
20-27	31	41	3	39	6	4
27-35	27	23	1	22	2	9
35-45	17	15	2	11	2	4
45-60	12	6	0	6	0	7
60-80	14	3	0	2	1	11
80-95	9	2	1	0	1	7
>95	28	3	0	1	2	25

AXP 1809-194, Scan 7209 energy

Quality (σ)	*Whole pulse*	*Main Pulse*	*1st Component*	*2nd Component*	*3rd Component*	*Interpulse*
0-1	322	272	292	125	309	262
1-1.5	1	45	23	132	7	5
1.5-3	0	5	7	63	3	24
3-5	0	0	0	2	2	22
5-7	0	1	0	0	2	8
7-9	0	0	1	1	0	2
9-11	0	0	0	0	0	0
11-13	0	0	0	0	0	0
13-16	0	0	0	0	0	0
16-19	0	0	0	0	0	0
19-25	0	0	0	0	0	0
>25	0	0	0	0	0	0

AXP 1809-194, Scan 8093 max

Quality (σ)	*Whole pulse*	*Main Pulse*	*1st Component*	*2nd Component*	*3rd Component*	*Interpulse*
0-1	0	0	0	4	7	5
1-3	4	4	5	273	273	256
3-8	54	60	67	36	10	36
8-13	79	83	88	6	3	8
13-20	94	96	95	3	11	2
20-27	43	42	44	0	4	3
27-35	21	17	15	0	2	5
35-45	11	11	6	0	5	0
45-60	6	4	2	0	2	2
60-80	4	3	0	0	3	1
80-95	3	1	0	0	1	2
>95	3	1	0	0	1	2

AXP 1809-194, Scan 8093 energy

Quality (σ)	*Whole pulse*	*Main Pulse*	*1st Component*	*2nd Component*	*3rd Component*	*Interpulse*
0-1	322	317	304	320	305	308
1-1.5	0	5	14	2	5	6
1.5-3	0	0	4	0	9	3
3-5	0	0	0	0	2	3
5-7	0	0	0	0	1	2
7-9	0	0	0	0	0	0
9-11	0	0	0	0	0	0
11-13	0	0	0	0	0	0
13-16	0	0	0	0	0	0
16-19	0	0	0	0	0	0
19-25	0	0	0	0	0	0
>25	0	0	0	0	0	0

AXP 1809-194, Scan 8095 max

Quality (σ)	*Whole pulse*	*Main Pulse*	*1st Component*	*2nd Component*	*3rd Component*	*Interpulse*
0-1	0	0	0	1	1	0
1-3	4	6	9	260	277	167
3-8	51	70	81	45	7	60
8-13	88	109	114	9	9	24
13-20	73	69	60	3	12	20
20-27	42	40	39	-	3	9
27-35	23	15	12	0	4	11
35-45	11	4	3	0	1	7
45-60	10	2	-	0	1	8
60-80	8	0	0	0	0	8
80-95	0	0	0	0	0	0
>95	9	4	0	0	4	5

AXP 1809-194, Scan 8095 energy

Quality (σ)	*Whole pulse*	*Main Pulse*	*1st Component*	*2nd Component*	*3rd Component*	*Interpulse*
0-1	319	315	294	315	308	283
1-1.5	0	3	24	4	5	17
1.5-3	0	1	1	0	2	11
3-5	0	0	0	0	3	8
5-7	0	0	0	0	1	0
7-9	0	0	0	0	0	0
9-11	0	0	0	0	0	0
11-13	0	0	0	0	0	0
13-16	0	0	0	0	0	0
16-19	0	0	0	0	0	0
19-25	0	0	0	0	0	0
>25	0	0	0	0	0	0

AXP 1809-194, Scan 8512 max

Quality (σ)	*Whole pulse*	*Main Pulse*	*Interpulse*
0-1	0	0	0
1-3	-	-	77
3-8	76	124	116
8-13	78	86	38
13-20	46	45	21
20-27	31	26	14
27-35	24	16	11
35-45	12	13	3
45-60	23	10	13
60-80	13	1	12
80-95	3	-	2
>95	17	0	17

AXP 1809-194, Scan 8512 energy

Quality (σ)	*Whole pulse*	*Main Pulse*	*Interpulse*
0-1	323	315	263
1-1.5	1	8	22
1.5-3	0	1	23
3-5	0	0	12
5-7	0	0	4
7-9	0	0	0
9-11	0	0	0
11-13	0	0	0
13-16	0	0	0
16-19	0	0	0
19-25	0	0	0
>25	0	0	0

AXP 1809-194, Scan 8510 max

Quality (σ)	*Whole pulse*	*Main Pulse*	*Interpulse*
0-1	0	0	33
1-3	38	57	174
3-8	158	189	49
8-13	47	48	11
13-20	25	17	13
20-27	15	9	7
27-35	15	2	13
35-45	9	2	7
45-60	7	0	7
60-80	4	0	4
80-95	4	0	4
>95	2	0	2

AXP 1809-194, Scan 8510 energy

Quality (σ)	*Whole pulse*	*Main Pulse*	*Interpulse*
0-1	324	324	310
1-1.5	0	0	6
1.5-3	0	0	7
3-5	0	0	1
5-7	0	0	0
7-9	0	0	0
9-11	0	0	0
11-13	0	0	0
13-16	0	0	0
16-19	0	0	0
19-25	0	0	0
>25	0	0	0

AXP 1809-194, Scan 8700 max

Quality (σ)	*Whole pulse*	*Main Pulse*	*1st Component*	*2nd Component*	*3rd Component*	*Interpulse*
0-1	0	0	0	0	1	0
1-3	0	2	12	54	192	57
3-8	42	94	155	170	67	73
8-13	97	130	107	65	31	62
13-20	83	64	44	23	14	51
20-27	38	16	3	6	8	31
27-35	34	8	1	2	5	28
35-45	13	5	0	1	4	9
45-60	14	3	1	2	0	11
60-80	2	1	0	0	1	1
80-95	0	0	0	0	0	0
>95	0	0	0	0	0	0

AXP 1809-194, Scan 8700 energy

Quality (σ)	*Whole pulse*	*Main Pulse*	*1st Component*	*2nd Component*	*3rd Component*	*Interpulse*
0-1	322	320	303	298	312	284
1-1.5	0	1	18	17	7	26
1.5-3	1	2	2	8	4	13
3-5	0	0	0	0	0	0
5-7	0	0	0	0	0	0
7-9	0	0	0	0	0	0
9-11	0	0	0	0	0	0
11-13	0	0	0	0	0	0
13-16	0	0	0	0	0	0
16-19	0	0	0	0	0	0
19-25	0	0	0	0	0	0
>25	0	0	0	0	0	0

AXP 1809-194, Scan 8701max

Quality (σ)	*Whole pulse*	*Main Pulse*	*Interpulse*
0-1	0	0	0
1-3	0	0	111
3-8	26	47	71
8-13	86	113	47
13-20	95	89	38
20-27	51	36	26
27-35	31	19	15
35-45	9	5	4
45-60	12	7	5
60-80	8	6	3
80-95	3	-	2
>95	3	-	-

AXP 1809-194, Scan 8701energy

Quality (σ)	*Whole pulse*	*Main Pulse*	*Interpulse*
0-1	323	302	281
1-1.5	1	19	26
1.5-3	0	3	12
3-5	0	0	3
5-7	0	0	2
7-9	0	0	0
9-11	0	0	0
11-13	0	0	0
13-16	0	0	0
16-19	0	0	0
19-25	0	0	0
>25	0	0	0

AXP 1809-194, Scan 9671 max

Quality (σ)	*Whole pulse*	*Main Pulse*	*1st Component*	*2nd Component*	*3rd Component*	*Interpulse*
0-1	0	0	0	14	0	0
1-3	0	33	138	250	83	2
3-8	20	178	132	16	140	27
8-13	30	47	10	1	38	28
13-20	61	16	2	1	13	57
20-27	50	4	0	0	4	49
27-35	45	2	0	0	2	44
35-45	35	0	0	0	0	35
45-60	25	2	0	0	2	24
60-80	10	0	0	0	0	10
80-95	2	0	0	0	0	2
>95	4	0	0	0	0	4

AXP 1809-194, Scan 9671 energy

Quality (σ)	*Whole pulse*	*Main Pulse*	*1st Component*	*2nd Component*	*3rd Component*	*Interpulse*
0-1	281	282	282	281	281	195
1-1.5	1	0	0	1	1	42
1.5-3	0	0	0	0	0	43
3-5	0	0	0	0	0	2
5-7	0	0	0	0	0	0
7-9	0	0	0	0	0	0
9-11	0	0	0	0	0	0
11-13	0	0	0	0	0	0
13-16	0	0	0	0	0	0
16-19	0	0	0	0	0	0
19-25	0	0	0	0	0	0
>25	0	0	0	0	0	0

AXP 1809-194, Scan 9672 max

Quality (σ)	*Whole pulse*	*Main Pulse*	*1st Component*	*2nd Component*	*3rd Component*	*Interpulse*
0-1	0	0	0	7	0	0
1-3	0	18	112	269	59	1
3-8	21	182	185	32	149	37
8-13	44	74	11	0	66	35
13-20	58	22	0	0	22	55
20-27	56	6	0	0	6	55
27-35	45	3	0	0	3	43
35-45	40	3	0	0	3	38
45-60	25	0	0	0	0	25
60-80	10	0	0	0	0	10
80-95	5	0	0	0	0	5
>95	4	0	0	0	0	4

AXP 1809-194, Scan 9672 energy

Quality (σ)	*Whole pulse*	*Main Pulse*	*1st Component*	*2nd Component*	*3rd Component*	*Interpulse*
0-1	308	307	306	306	296	198
1-1.5	0	1	2	2	11	74
1.5-3	0	0	0	0	1	36
3-5	0	0	0	0	0	0
5-7	0	0	0	0	0	0
7-9	0	0	0	0	0	0
9-11	0	0	0	0	0	0
11-13	0	0	0	0	0	0
13-16	0	0	0	0	0	0
16-19	0	0	0	0	0	0
19-25	0	0	0	0	0	0
>25	0	0	0	0	0	0

AXP 1809-194, Scan 9673 max

Quality (σ)	*Whole pulse*	*Main Pulse*	*1st Component*	*2nd Component*	*3rd Component*	*Interpulse*
0-1	0	0	1	24	0	0
1-3	0	22	89	275	81	10
3-8	22	187	201	20	151	30
8-13	38	66	22	0	49	32
13-20	66	37	5	0	32	56
20-27	59	7	1	0	6	57
27-35	48	0	0	0	0	48
35-45	32	0	0	0	0	32
45-60	36	0	0	0	0	36
60-80	13	0	0	0	0	13
80-95	2	0	0	0	0	2
>95	3	0	0	0	0	3

AXP 1809-194, Scan 9673 energy

Quality (σ)	*Whole pulse*	*Main Pulse*	*1st Component*	*2nd Component*	*3rd Component*	*Interpulse*
0-1	316	318	316	312	315	196
1-1.5	3	1	3	7	4	75
1.5-3	0	0	0	0	0	46
3-5	0	0	0	0	0	2
5-7	0	0	0	0	0	0
7-9	0	0	0	0	0	0
9-11	0	0	0	0	0	0
11-13	0	0	0	0	0	0
13-16	0	0	0	0	0	0
16-19	0	0	0	0	0	0
19-25	0	0	0	0	0	0
>25	0	0	0	0	0	0

PSR 1133 +16, Scan 2691a max

Quality (σ)	*Whole pulse*	*1st component*	*2nd component*
0-1	0	-	12
1-3	130	157	278
3-8	124	104	75
8-13	41	36	8
13-20	26	24	4
20-27	12	11	-
27-35	9	9	0
35-45	11	11	0
45-60	8	8	0
60-80	4	4	0
80-95	4	4	0
>95	-	-	0

PSR 1133 +16, Scan 2691a energy

Quality (σ)	*Whole pulse*	*1st component*	*2nd component*
0-1	267	231	338
1-1.5	39	43	28
1.5-3	43	50	9
3-5	15	24	3
5-7	4	12	0
7-9	6	2	0
9-11	1	6	0
11-13	1	0	0
13-16	1	4	0
16-19	0	2	0
19-25	1	2	0
>25	0	2	0

PSR 1133 +16, Scan 2691b max

Quality (σ)	*Whole pulse*	*1st component*	*2nd component*
0-1	0	4	11
1-3	114	151	247
3-8	139	115	94
8-13	38	27	16
13-20	32	29	6
20-27	14	11	3
27-35	11	11	0
35-45	8	8	1
45-60	2	2	0
60-80	7	7	0
80-95	0	0	0
>95	13	13	0

PSR 1133 +16, Scan 2691b energy

Quality (σ)	*Whole pulse*	*1st component*	*2nd component*
0-1	276	248	302
1-1.5	36	42	48
1.5-3	40	39	21
3-5	15	22	6
5-7	4	10	0
7-9	2	5	1
9-11	0	3	0
11-13	0	2	0
13-16	1	2	0
16-19	3	0	0
19-25	1	0	0
>25	0	5	0

PSR 1133 +16, Scan 2691c max

Quality (σ)	*Whole pulse*	*1st component*	*2nd component*
0-1	3	15	23
1-3	137	173	249
3-8	124	85	86
8-13	43	37	12
13-20	26	23	3
20-27	11	12	0
27-35	10	10	-
35-45	4	3	-
45-60	4	4	0
60-80	6	6	0
80-95	-	-	0
>95	-	-	0

PSR 1133 +16, Scan 2691c energy

Quality (σ)	*Whole pulse*	*1st component*	*2nd component*
0-1	243	223	298
1-1.5	52	43	48
1.5-3	57	54	23
3-5	10	28	4
5-7	4	11	1
7-9	4	3	1
9-11	2	3	0
11-13	1	1	0
13-16	1	4	0
16-19	0	2	0
19-25	1	1	0
>25	0	2	0

PSR 0329+54, Scan 2709a max

Quality (σ)	*Whole pulse*	*1st component*	*2nd component*	*3rd component*
0-1	0	5	0	0
1-3	30	313	57	219
3-8	150	52	139	123
8-13	76	=	68	18
13-20	59	0	55	9
20-27	23	0	20	3
27-35	20	0	19	1
35-45	-	0	-	0
45-60	-	0	-	0
60-80	-	0	-	0
80-95	0	0	0	0
>95	-	0	-	0

PSR 0329+54, Scan 2709a energy

Quality (σ)	*Whole pulse*	*1st component*	*2nd component*	*3rd component*
0-1	169	342	74	308
1-1.5	76	16	50	33
1.5-3	108	13	107	23
3-5	18	2	82	9
5-7	1	0	35	0
7-9	1	0	16	0
9-11	0	0	4	0
11-13	0	0	3	0
13-16	0	0	0	0
16-19	0	0	1	0
19-25	0	0	1	0
>25	0	0	0	0

PSR 0329+54, Scan 2709b max

Quality (σ)	*Whole pulse*	*1st component*	*2nd component*	*3rd component*
0-1	0	12	0	-
1-3	44	307	70	249
3-8	159	51	146	97
8-13	59	-	51	17
13-20	46	0	43	-
20-27	30	0	-	-
27-35	19	0	-	0
35-45	-	0	-	0
45-60	-	0	-	0
60-80	-	0	-	-
80-95	-	0	0	-
>95	0	0	0	0

PSR 0329+54, Scan 2709b energy

Quality (σ)	*Whole pulse*	*1st component*	*2nd component*	*3rd component*
0-1	198	337	82	300
1-1.5	72	26	61	32
1.5-3	83	9	121	32
3-5	17	1	52	6
5-7	2	0	34	0
7-9	1	0	13	2
9-11	0	0	6	0
11-13	0	0	1	1
13-16	0	0	3	0
16-19	0	0	0	0
19-25	0	0	0	0
>25	0	0	0	0

PSR 0329+54, Scan 2709c max

Quality (σ)	*Whole pulse*	*1st component*	*2nd component*	*3rd component*
0-1	0	-	0	-
1-3	42	311	83	236
3-8	151	56	122	103
8-13	68	-	61	22
13-20	49	0	47	-
20-27	27	0	26	-
27-35	10	0	10	0
35-45	17	0	16	-
45-60	-	0	-	-
60-80	-	0	-	0
80-95	-	0	-	0
>95	0	0	0	0

PSR 0329+54, Scan 2709c energy

Quality (σ)	*Whole pulse*	*1st component*	*2nd component*	*3rd component*
0-1	165	337	107	291
1-1.5	80	24	47	36
1.5-3	99	11	99	36
3-5	25	1	69	7
5-7	3	0	28	1
7-9	1	0	12	2
9-11	0	0	8	0
11-13	0	0	1	0
13-16	0	0	1	0
16-19	0	0	1	0
19-25	0	0	0	0
>25	0	0	0	0

8.3 Data processing and comparison

A

We processed the best (highest quality classification) scans of the magnetar and the pulsars in the aspect of pulse nulling. We found for every scan the percentage of single pulses that are null. The results are shown in the Tables below.

AXP 1809-194: Single pulses nulling.

Scan	*Frequency (GHz)*	*# Single Pulses*	*Whole Pulse*	*Main Pulse*	*1st Comp.*	*2nd Comp.*	*3rd Comp.*	*Interp.*
5954	8.35	323	0*%*	0.3*%*	50.5*%*	0.6*%*	91*%*	52*%*
5955	8.35	324	0*%*	0*%*	45.7*%*	0*%*	95.7*%*	54.3*%*
5956	8.35	644	0.15*%*	0.15*%*	36.3*%*	0.62*%*	94.7*%*	53.3*%*
7202	8.35	324	0*%*	0.3*%*	30.9*%*	0.3*%*	93.8*%*	44.75*%*
7203	8.35	324	0*%*	0*%*	24.7*%*	0.3*%*	91*%*	52.8*%*
7204	8.35	322	0*%*	0*%*	27.3*%*	0.3*%*	91*%*	35.4*%*
7205	8.35	324	0.3*%*	0.3*%*	42*%*	0.3*%*	93.5*%*	40.4*%*
7209	8.35	323	0*%*	0*%*	40.56*%*	0*%*	80.2*%*	63.8*%*
9671	2.64	282	0*%*	11.7*%*	48.9*%*	93.6*%*	29.4*%*	0.7*%*
9672	2.64	308	0*%*	5.8*%*	36.4*%*	89.6*%*	19.16*%*	0.33*%*
9673	2.64	319	0*%*	6.9*%*	28.2*%*	93.7*%*	25.4*%*	3.13*%*

PSR 1133+16, PSR 0329+54: Single pulses nulling.

Scan	*Frequency (GHz)*	*# Single Pulses*	*Whole Pulse*	*1st Comp.*	*2nd Comp.*	*3rd Comp.*
2691	8.35	378	34.4*%*	41.5*%*	76.7*%*	-
	8.35	378	30.2*%*	41*%*	68.3*%*	-
	8.35	375	37.3*%*	50.1*%*	72.5*%*	-
2709	8.35	373	8*%*	85.3*%*	15.3*%*	58.7*%*
	8.35	373	11.8*%*	85.5*%*	18.8*%*	67*%*
	8.35	373	11.26*%*	84.5*%*	22.3*%*	64.3*%*

Comparing the results concerning the nulling between magnetar and pulsars we can easily see that the nulling percentage of the pulsars is greater than the magnetars' is. Another information we obtain from the results is that there is a significant difference in the nulling of component 2, component 3 and the interpulse as we change frequencies from the 8.35 GHz to 2.6 GHz.

B

We calculated the interstellar broadening of the single pulses for the magnetar AXP J1809-194 and the two pulsars PSR B0329+54 and PSR B1133+16:

a) AXP J1809-194:

at the frequency of 8.35 GHz the bandwidth of the observations was 1Ghz so

$$\Delta t = 8.3 \times 10^3 \times 178 \times 8350^{-3} \times 1000 \rightarrow \Delta t = 2.54\, msec$$

at the frequency of 2.6 GHz the bandwidth of the observations was 0.1GHz so

$$\Delta t = 8.3 \times 10^3 \times 178 \times 2640^{-3} \times 100 \rightarrow \Delta t = 8.03\, msec$$

a) PSR B0329+54:

at the frequency of 8.35 GHz the bandwidth of the observations was 1Ghz so

$$\Delta t = 8.3 \times 10^3 \times 26.7 \times 8350^{-3} \times 1000 \rightarrow \Delta t = 0.38\, msec$$

b) PSR B1133+16:

at the frequency of 8.35 GHz the bandwidth of the observations was 1Ghz so

$$\Delta t = 8.3 \times 10^3 \times 4.8 \times 8350^{-3} \times 1000 \rightarrow \Delta t = 0.068\, msec$$

The resolution that was used to obtain the data we used in this paper was 5.3 msec. That means that it is enough for the 8.35 GHz observations that yielded the data for all three NS, but not for the 2.64 GHz observations of the magnetar since the dispersion broadening is greater than the resolution at this frequency.

C

In the graphs below the correlation between different components of the magnetar and pulsars in the aspect of the change of energy is shown. In each graph the mean of $\frac{pulse\ energy}{sigma}$ of each quality class of one component is plotted with respect to the mean of $\frac{pulse\ energy}{sigma}$ of the respective quality class of another component.

Figures of AXP J1809-194:

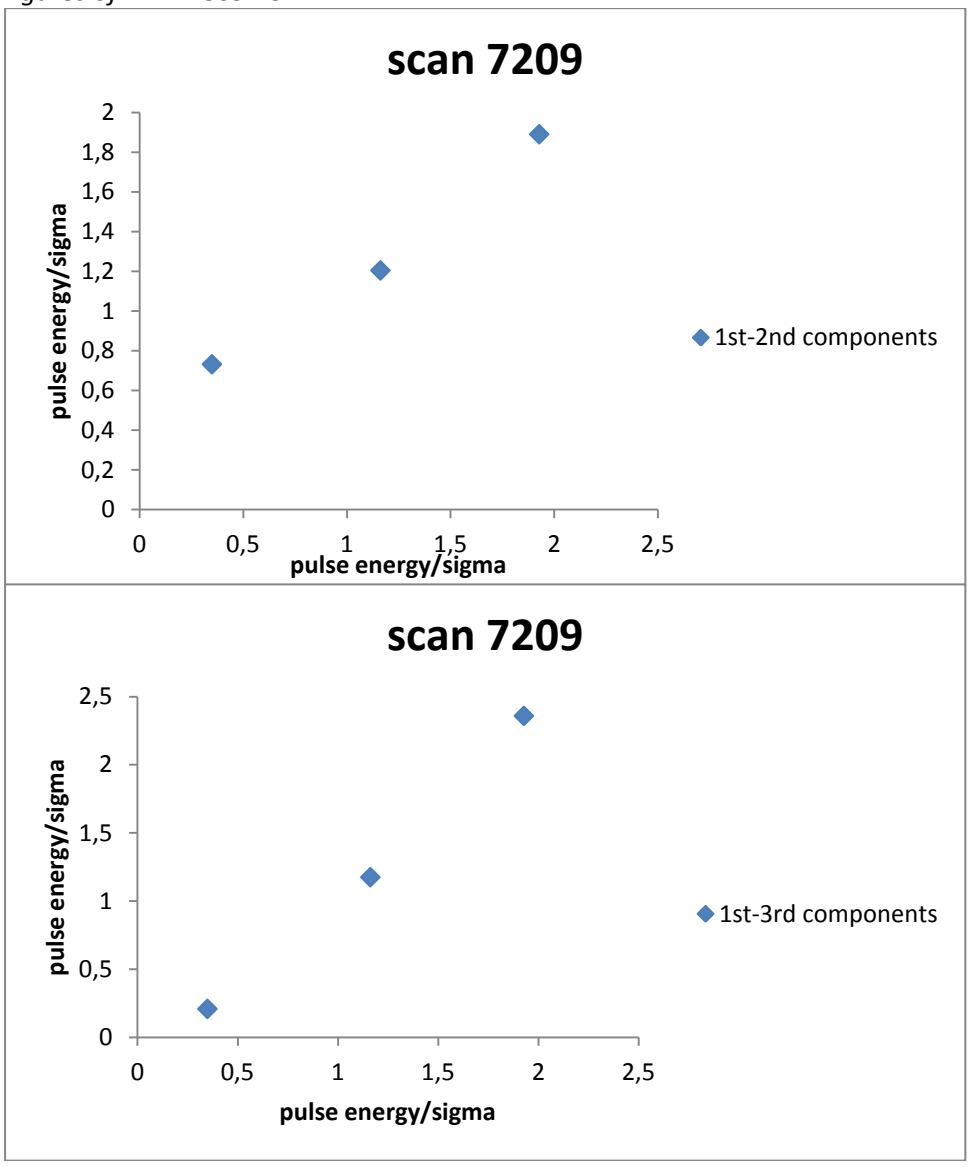

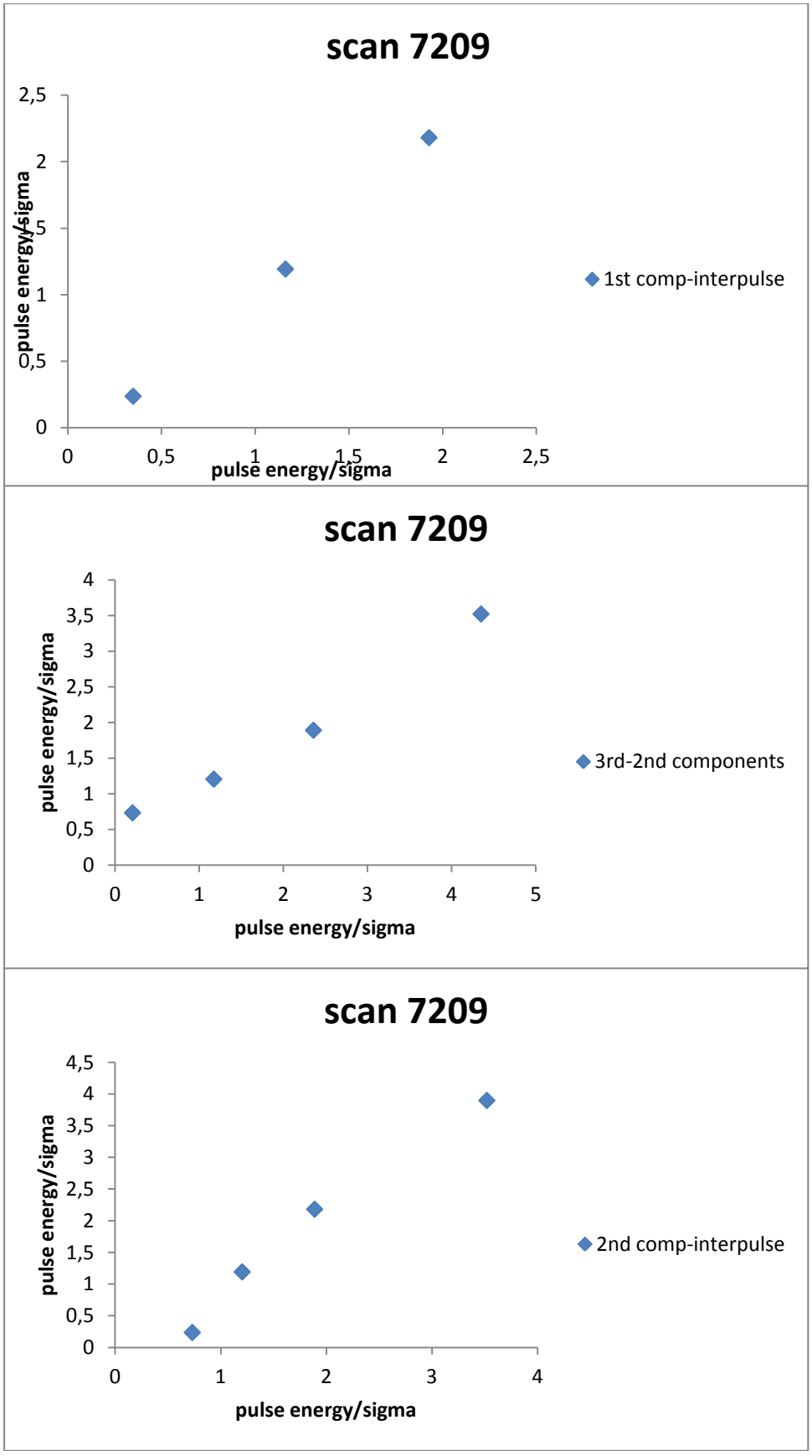
scan 7209
pulse energy/sigma
2,5
2
1,5
1
0,5
0
0
0,5
1
1,5
2
2,5
pulse energy/sigma
1st comp-interpulse
scan 7209
pulse energy/sigma
4
3,5
3
2,5
2
1,5
1
0,5
0
0
1
2
3
4
5
pulse energy/sigma
3rd-2nd components
scan 7209
pulse energy/sigma
4,5
4
3,5
3
2,5
2
1,5
1
0,5
0
0
1
2
3
4
pulse energy/sigma
2nd comp-interpulse

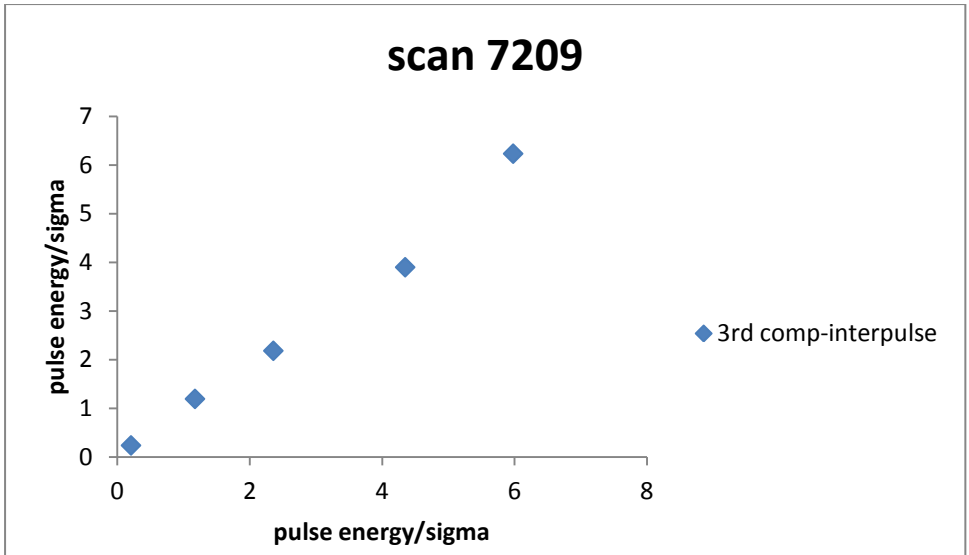
scan 7209
pulse energy/sigma
pulse energy/sigma
3rd comp-interpulse

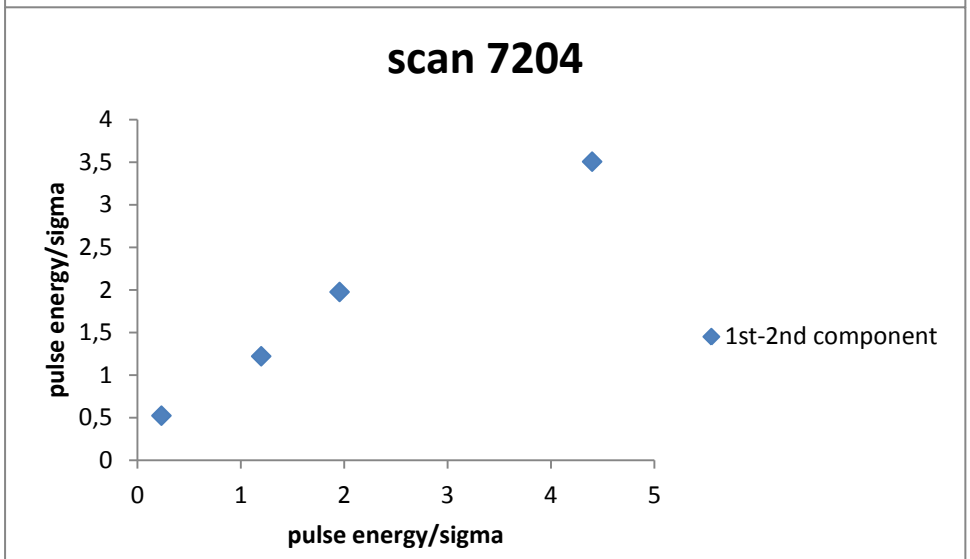
scan 7204
pulse energy/sigma
pulse energy/sigma
1st-2nd component

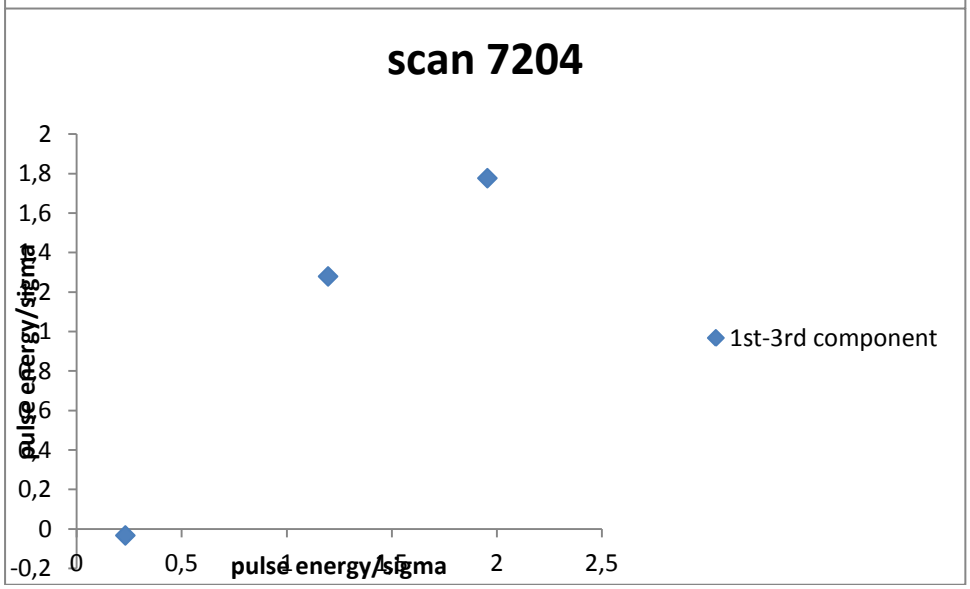
scan 7204
pulse energy/sigma
pulse energy/sigma
1st-3rd component

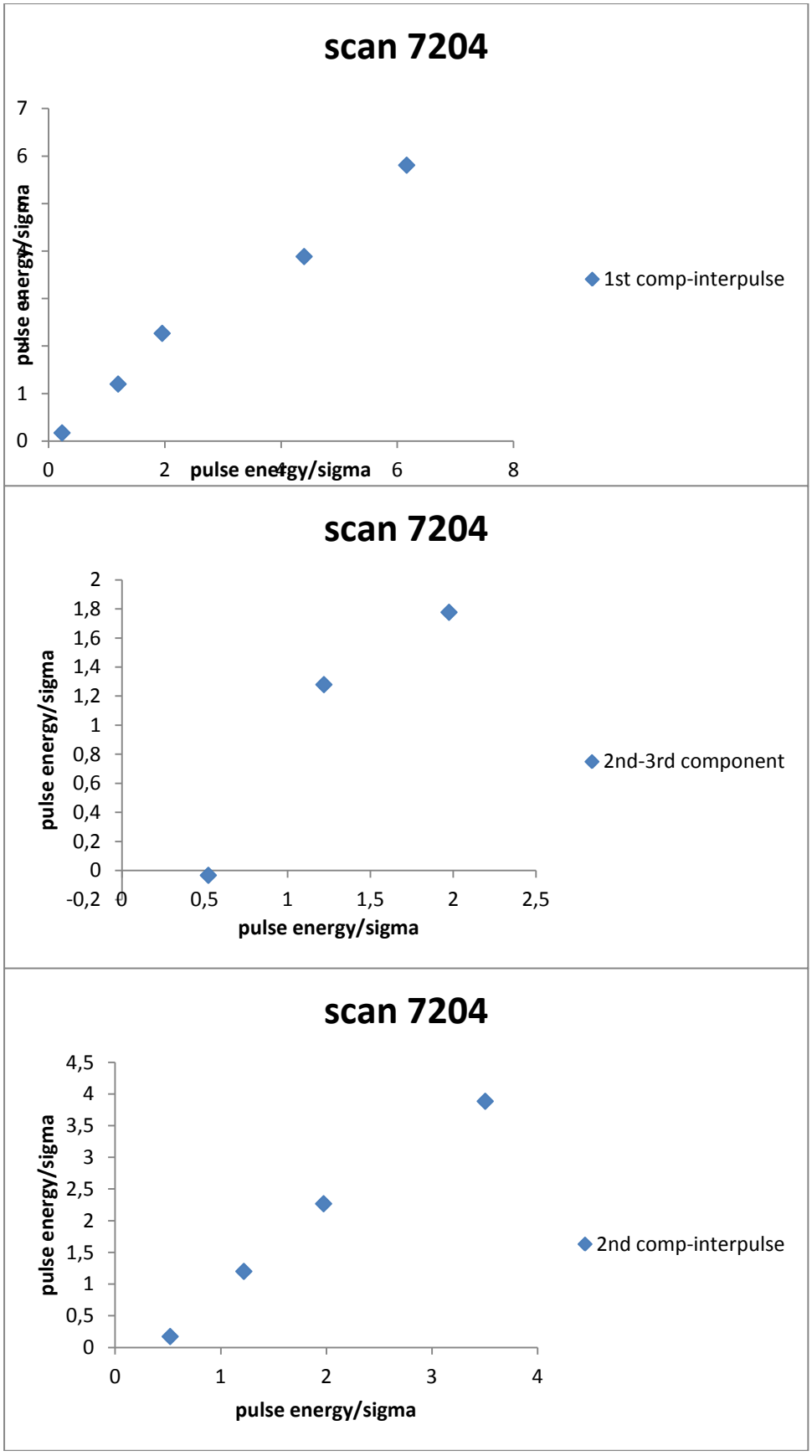
scan 7204
pulse energy/sigma
0
1
2
4
6
7
0
2
4
6
8
pulse energy/sigma
1st comp-interpulse
scan 7204
pulse energy/sigma
-0,2
0
0,2
0,4
0,6
0,8
1
1,2
1,4
1,6
1,8
2
0
0,5
1
1,5
2
2,5
pulse energy/sigma
2nd-3rd component
scan 7204
pulse energy/sigma
0
0,5
1
1,5
2
2,5
3
3,5
4
4,5
0
1
2
3
4
pulse energy/sigma
2nd comp-interpulse

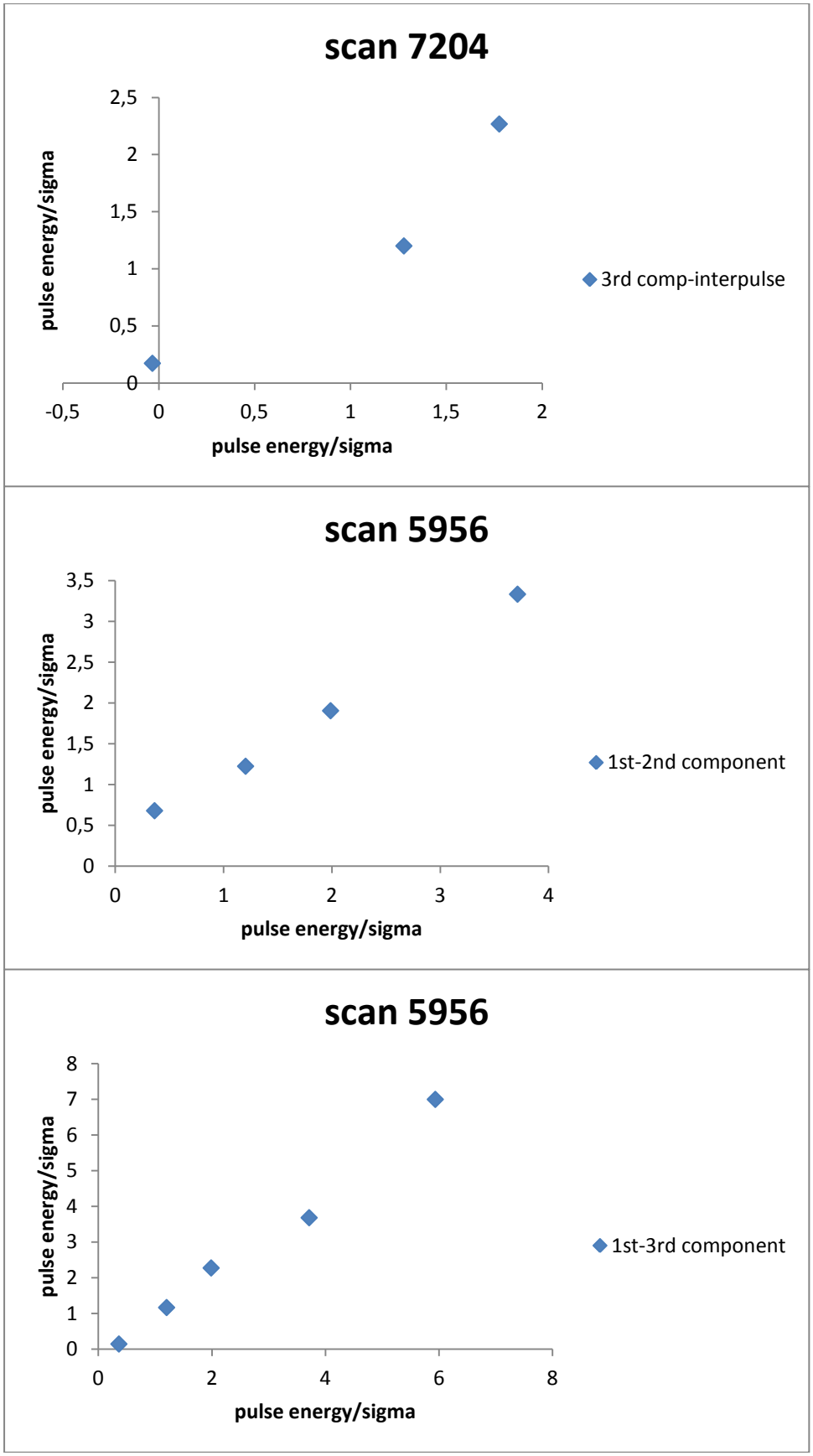
scan 7204
pulse energy/sigma
2,5
2
1,5
1
0,5
0
-0,5
0
0,5
1
1,5
2
pulse energy/sigma
3rd comp-interpulse
scan 5956
pulse energy/sigma
3,5
3
2,5
2
1,5
1
0,5
0
0
1
2
3
4
pulse energy/sigma
1st-2nd component
scan 5956
pulse energy/sigma
8
7
6
5
4
3
2
1
0
0
2
4
6
8
pulse energy/sigma
1st-3rd component

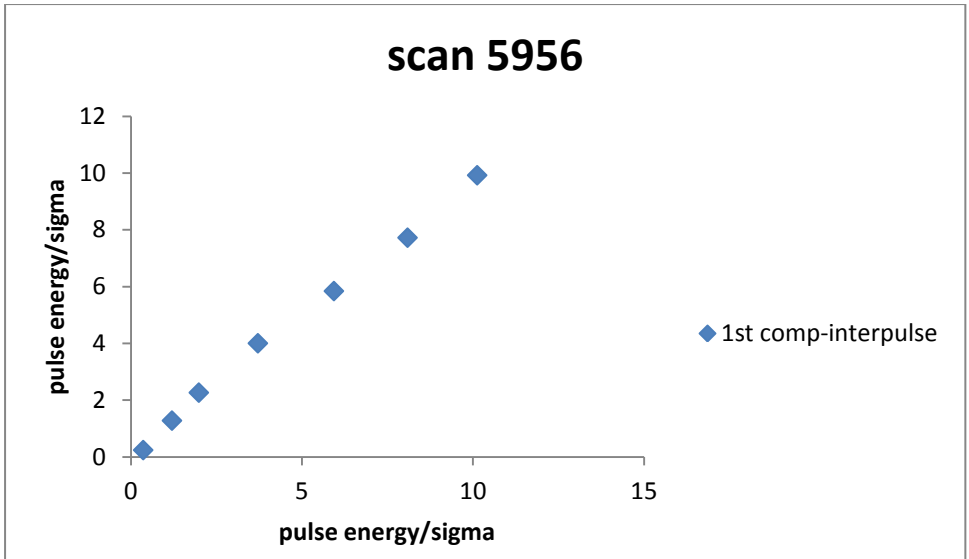
scan 5956
pulse energy/sigma
pulse energy/sigma
1st comp-interpulse

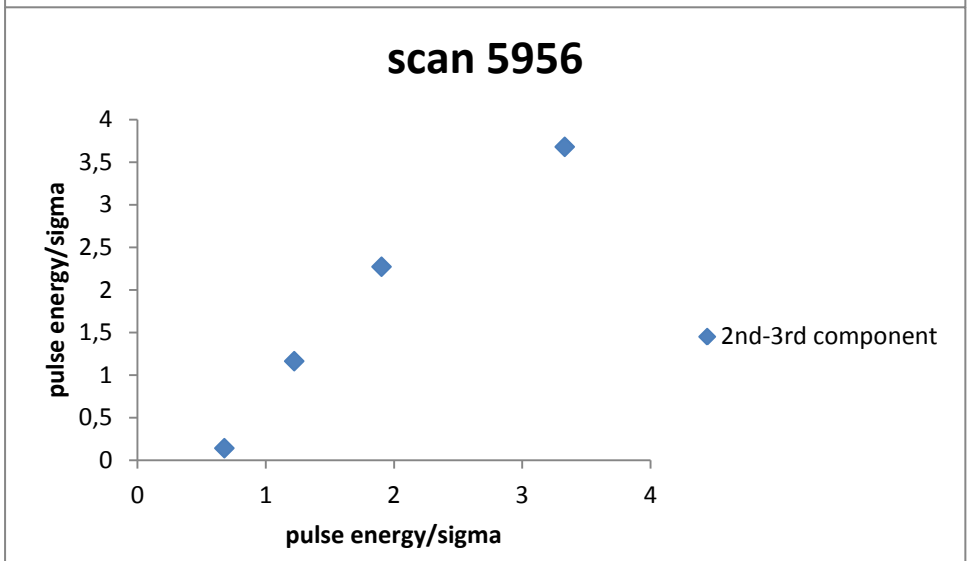
scan 5956
pulse energy/sigma
pulse energy/sigma
2nd-3rd component

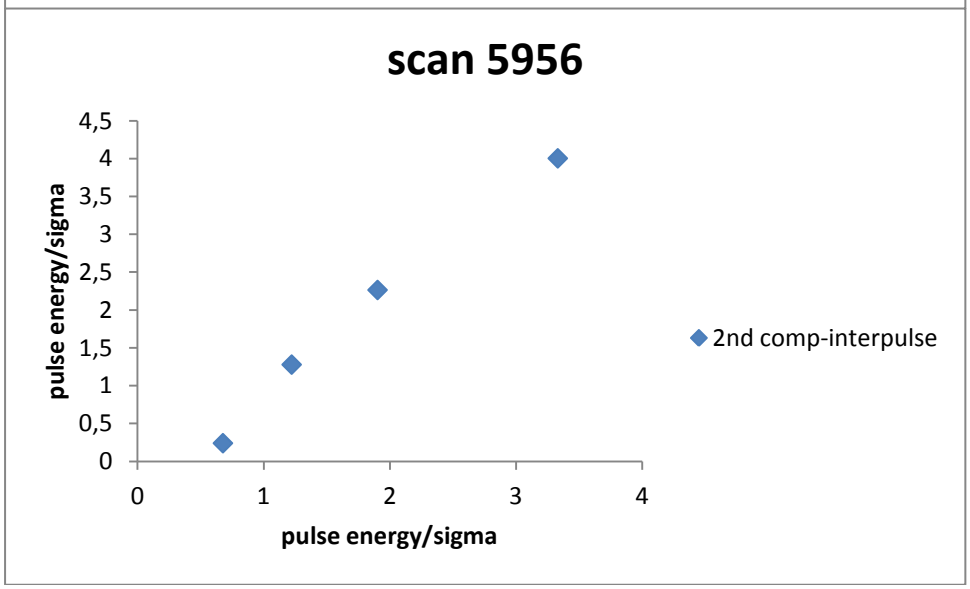
scan 5956
pulse energy/sigma
pulse energy/sigma
2nd comp-interpulse

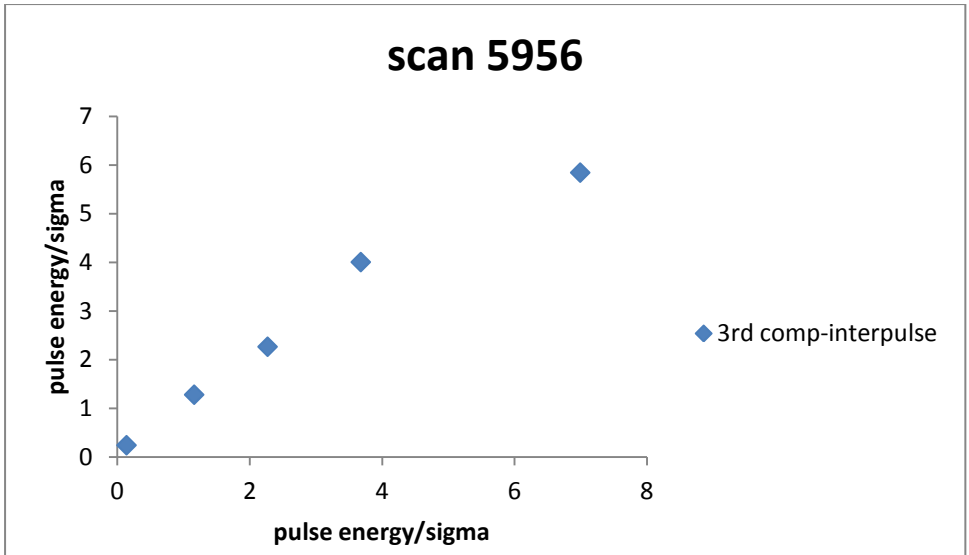
scan 5956
pulse energy/sigma
pulse energy/sigma
3rd comp-interpulse

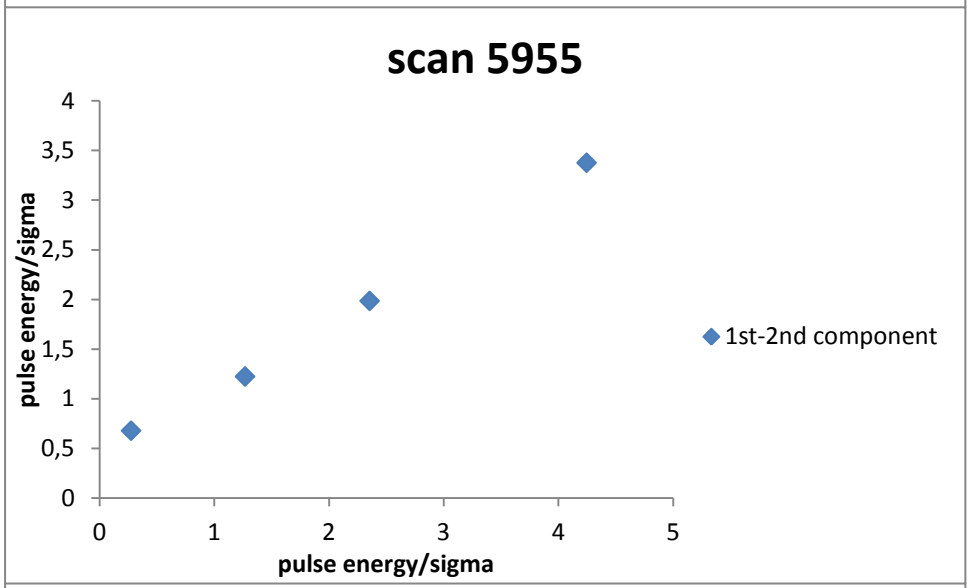
scan 5955
pulse energy/sigma
pulse energy/sigma
1st-2nd component

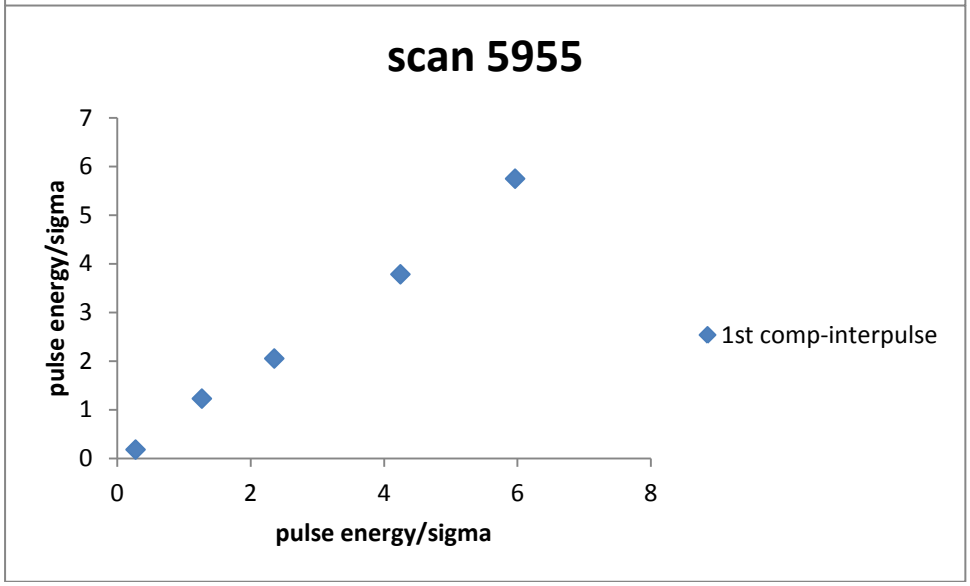
scan 5955
pulse energy/sigma
pulse energy/sigma
1st comp-interpulse

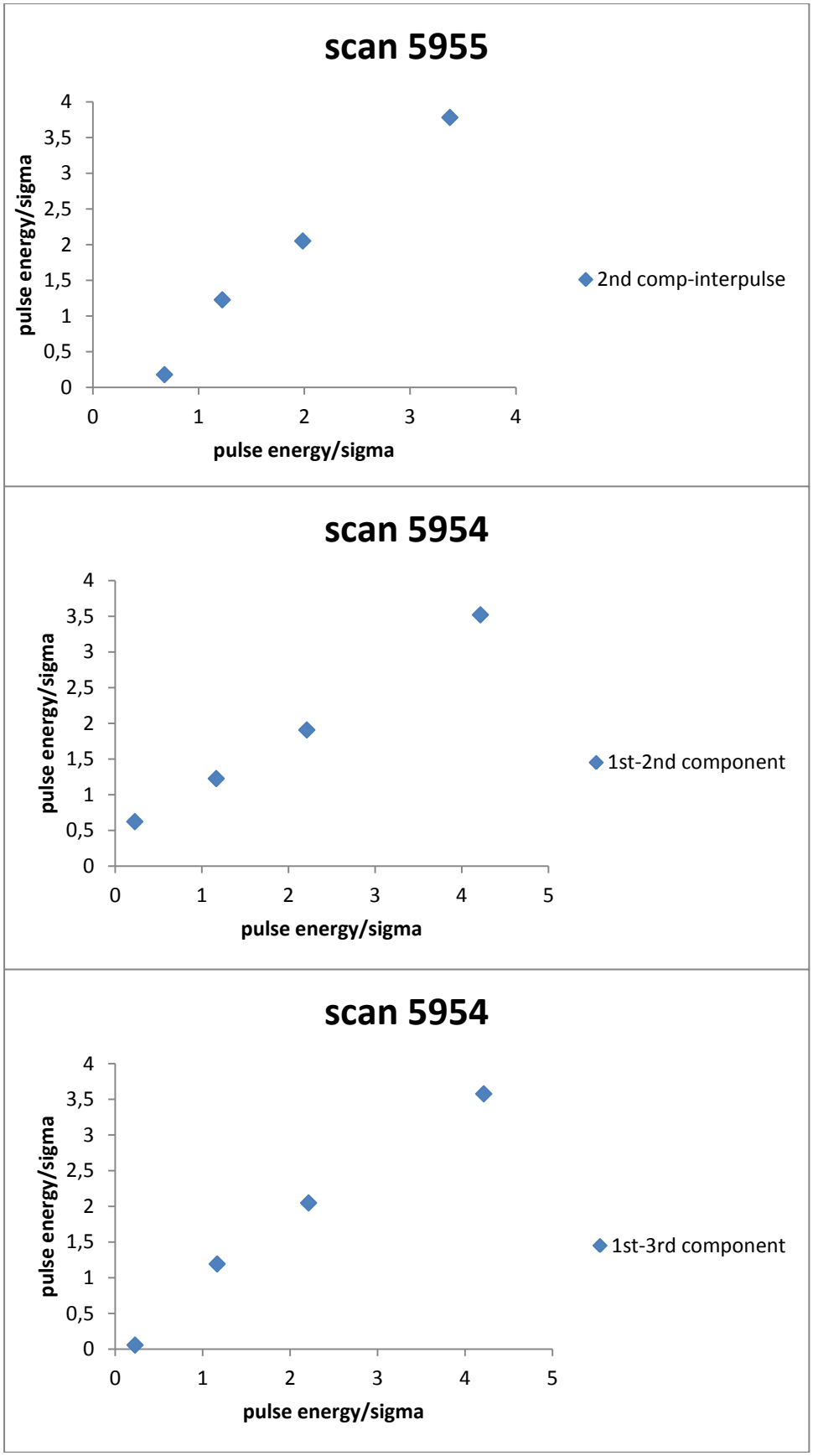
scan 5955
pulse energy/sigma
pulse energy/sigma
2nd comp-interpulse
scan 5954
pulse energy/sigma
pulse energy/sigma
1st-2nd component
scan 5954
pulse energy/sigma
pulse energy/sigma
1st-3rd component

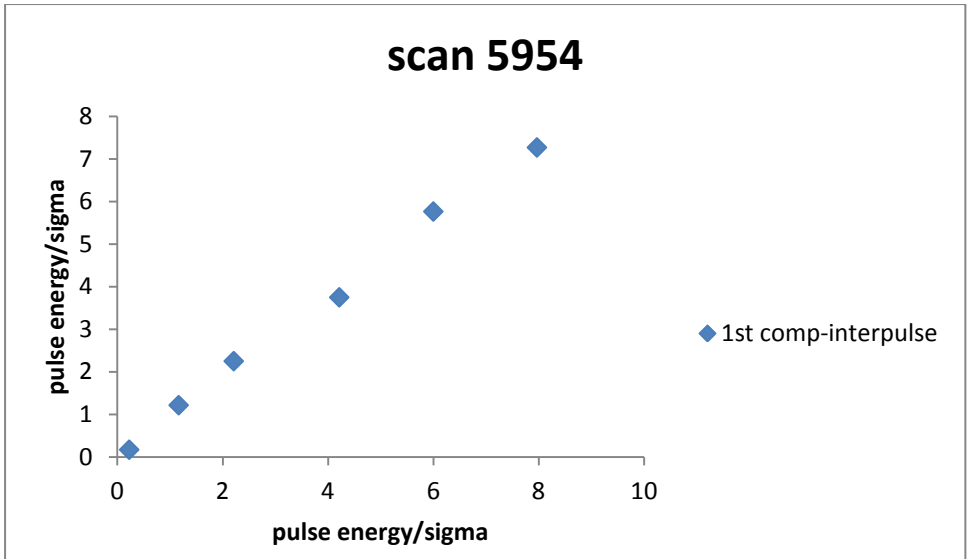
scan 5954
pulse energy/sigma
pulse energy/sigma
0
2
4
6
8
10
1
3
5
7
1st comp-interpulse

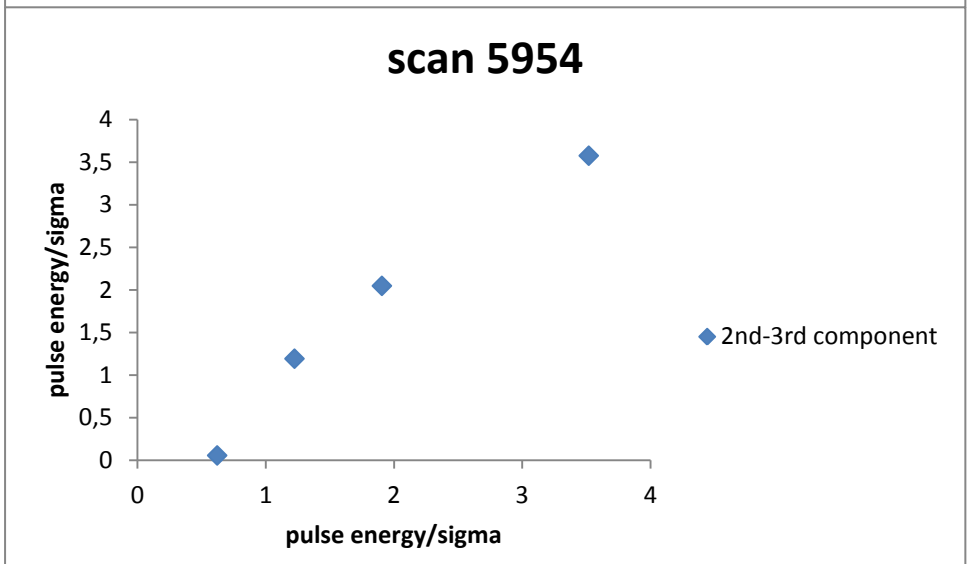
scan 5954
pulse energy/sigma
pulse energy/sigma
0
1
2
3
4
0,5
1,5
2,5
3,5
2nd-3rd component

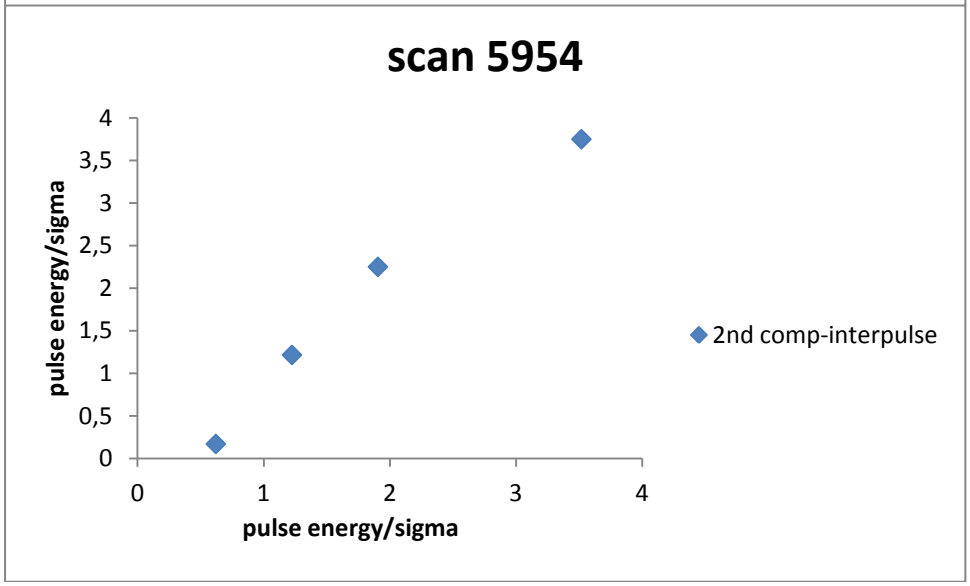
scan 5954
pulse energy/sigma
pulse energy/sigma
0
1
2
3
4
0,5
1,5
2,5
3,5
2nd comp-interpulse

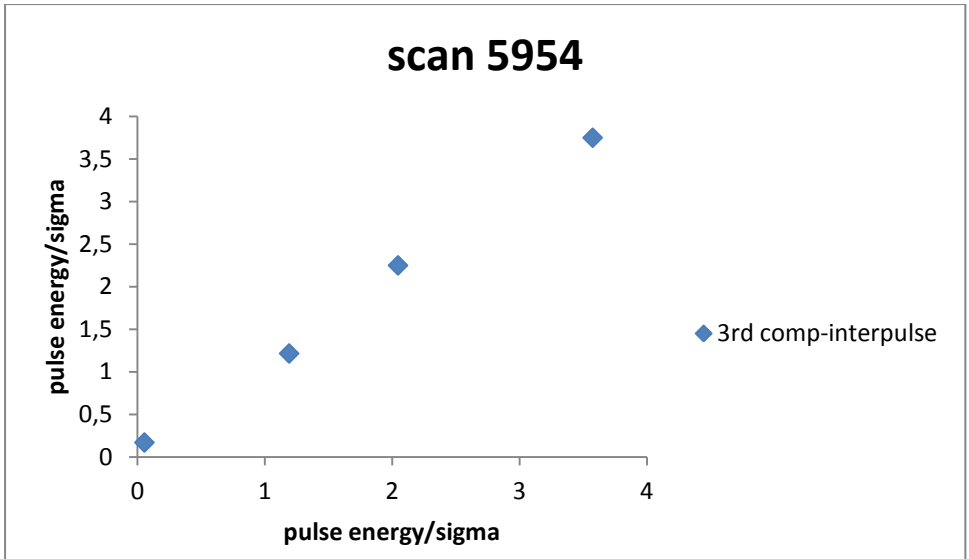
scan 5954
pulse energy/sigma
4
3,5
3
2,5
2
1,5
1
0,5
0
0
1
2
3
4
pulse energy/sigma
3rd comp-interpulse

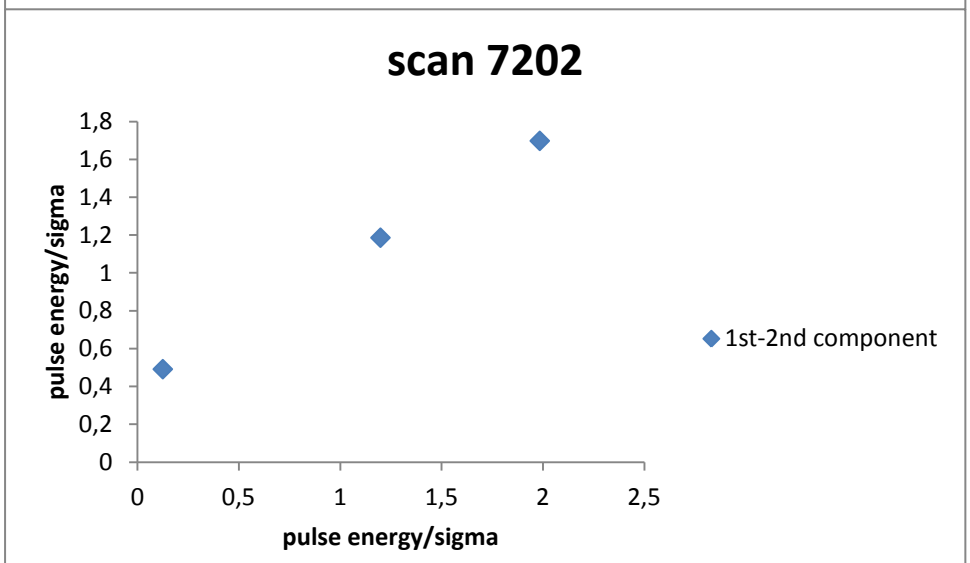
scan 7202
pulse energy/sigma
1,8
1,6
1,4
1,2
1
0,8
0,6
0,4
0,2
0
0
0,5
1
1,5
2
2,5
pulse energy/sigma
1st-2nd component

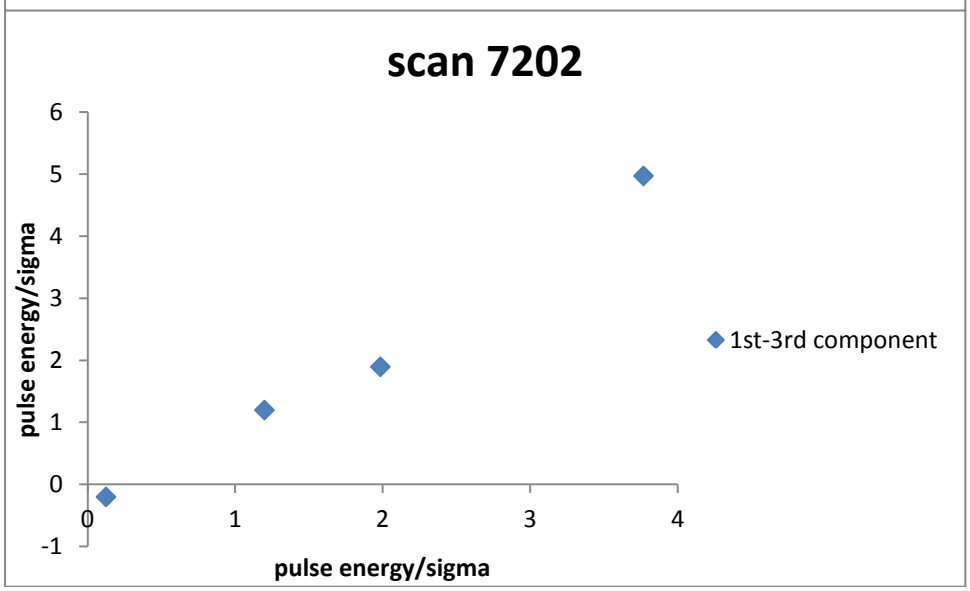
scan 7202
pulse energy/sigma
6
5
4
3
2
1
0
-1
0
1
2
3
4
pulse energy/sigma
1st-3rd component

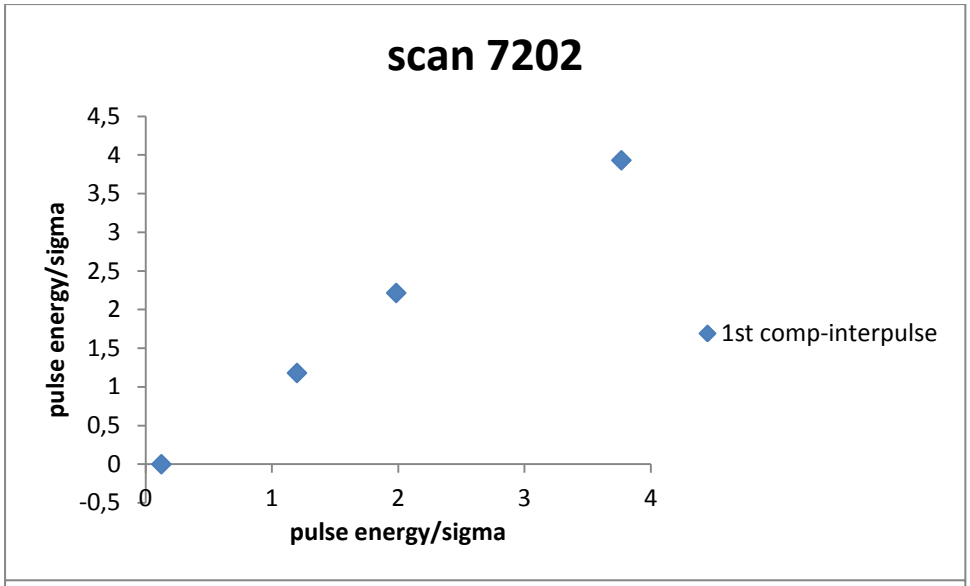
scan 7202
4,5
4
3,5
3
2,5
2
1,5
1
0,5
0
-0,5
0
1
2
3
4
pulse energy/sigma
pulse energy/sigma
1st comp-interpulse

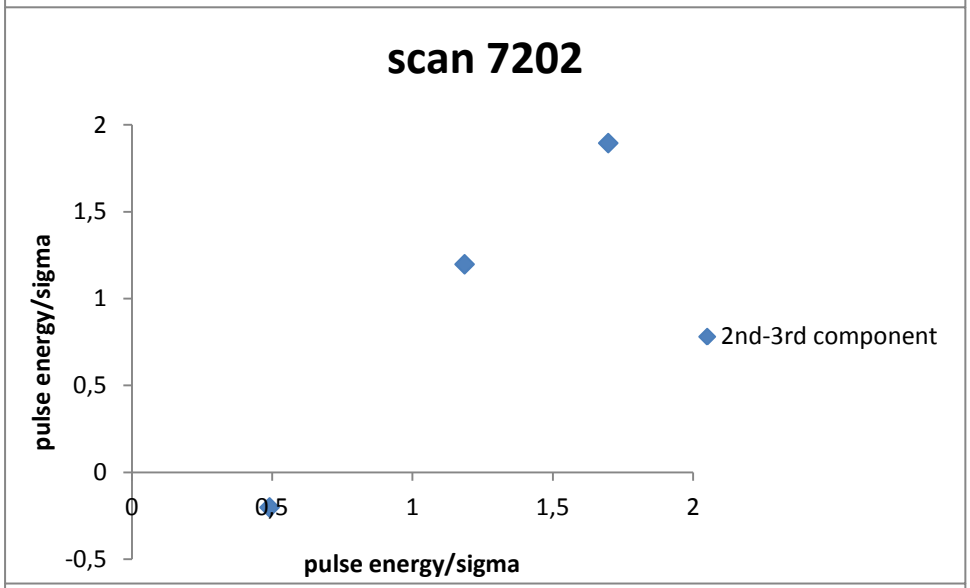
scan 7202
2
1,5
1
0,5
0
-0,5
0
0,5
1
1,5
2
pulse energy/sigma
pulse energy/sigma
2nd-3rd component

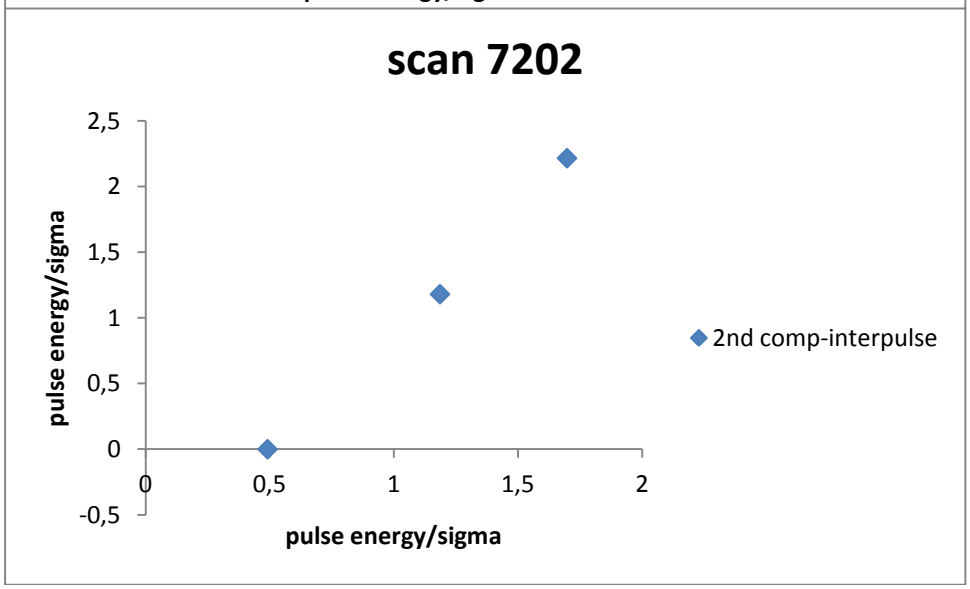
scan 7202
2,5
2
1,5
1
0,5
0
-0,5
0
0,5
1
1,5
2
pulse energy/sigma
pulse energy/sigma
2nd comp-interpulse

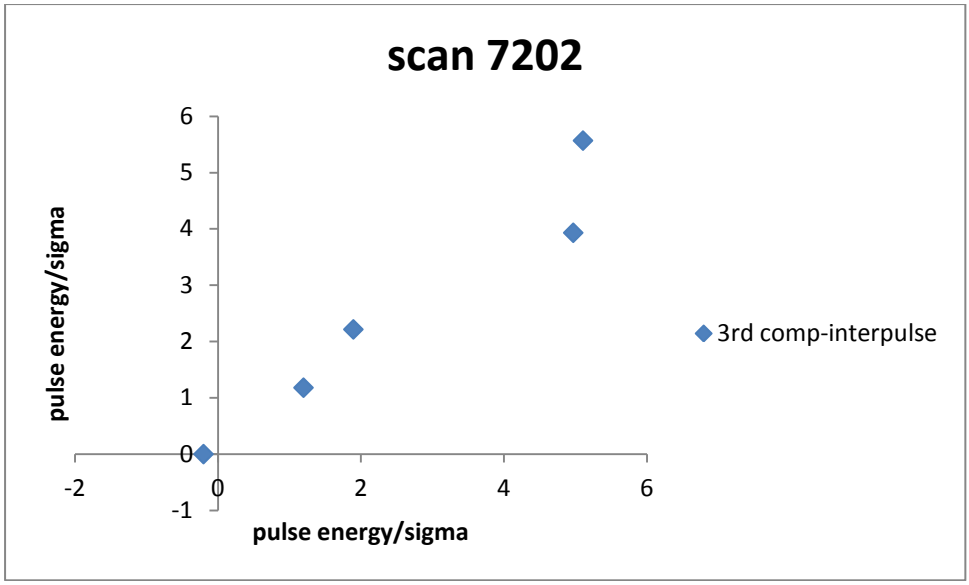

Figures of PSR B0329+54:

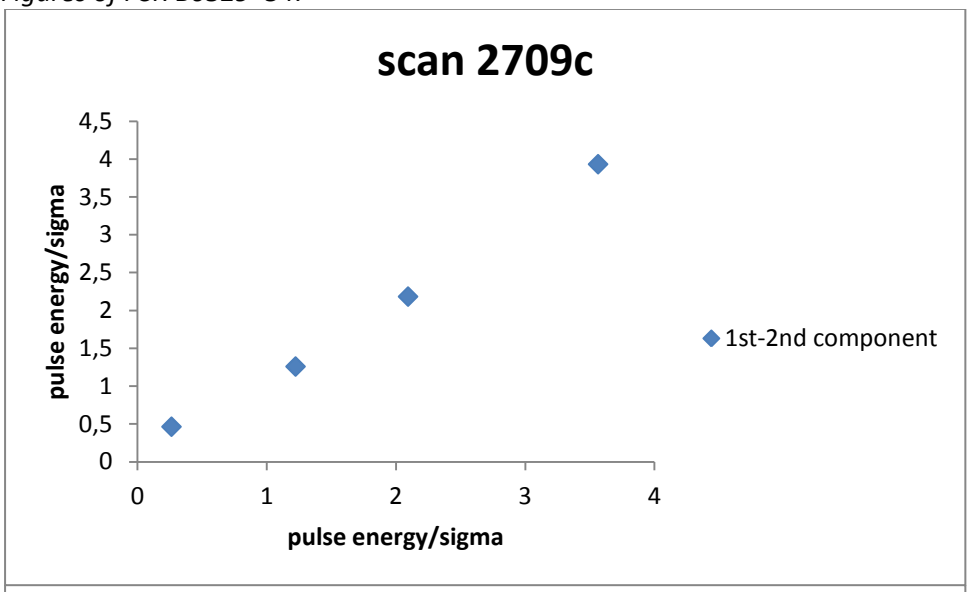

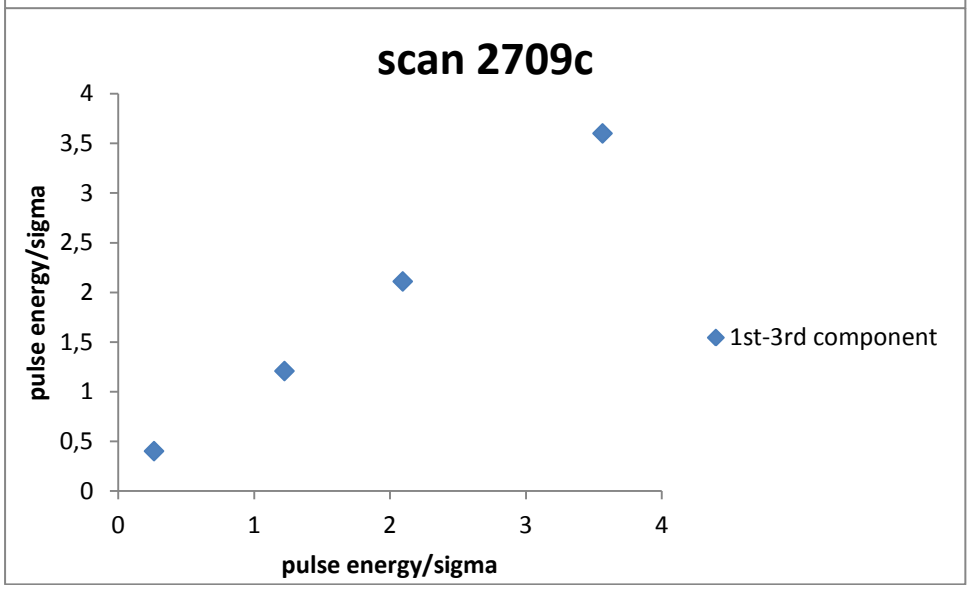

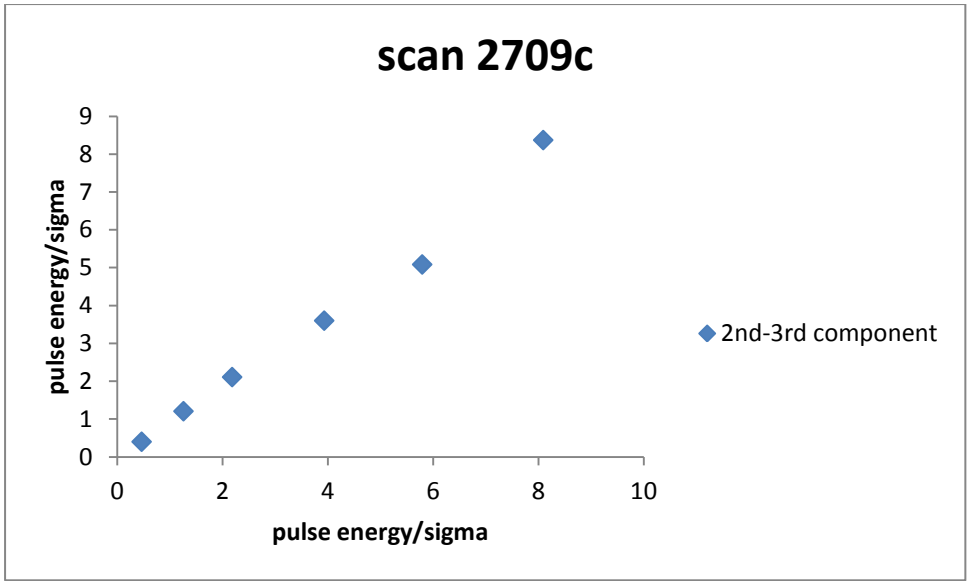

Figure of PSR B1133+16:

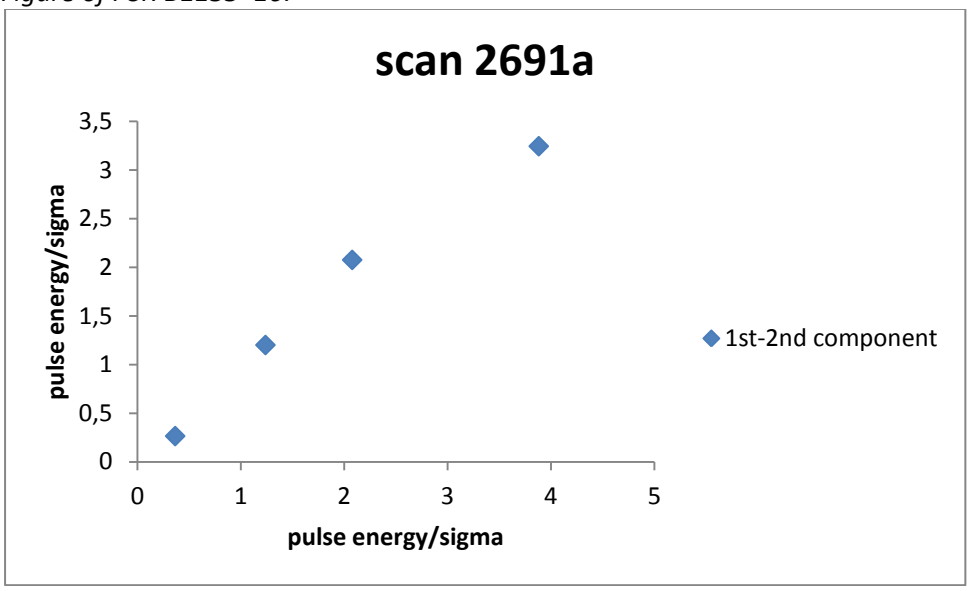

D

For the magnetar and pulsars the correlation between components of the pulse in the aspect of the number of single pulses that are in each quality class is shown in the figures below. For the magnetar we used some scans to show how the single pulses are distributed in the quality classes (with respect to both energy and maximum) concerning the main pulse and the interpulse. For the two pulsars we did the same by comparing 1st and 2nd component of the PSR 1133+16 and 2nd to 3rd component of the PSR 0329+54. The figures are shown below:

Figures of AXP J1809-194:

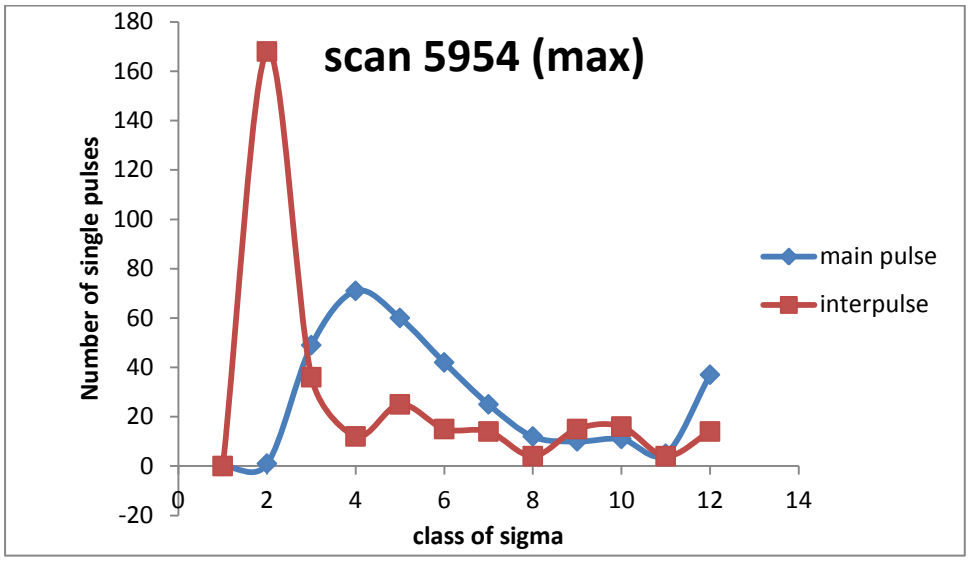

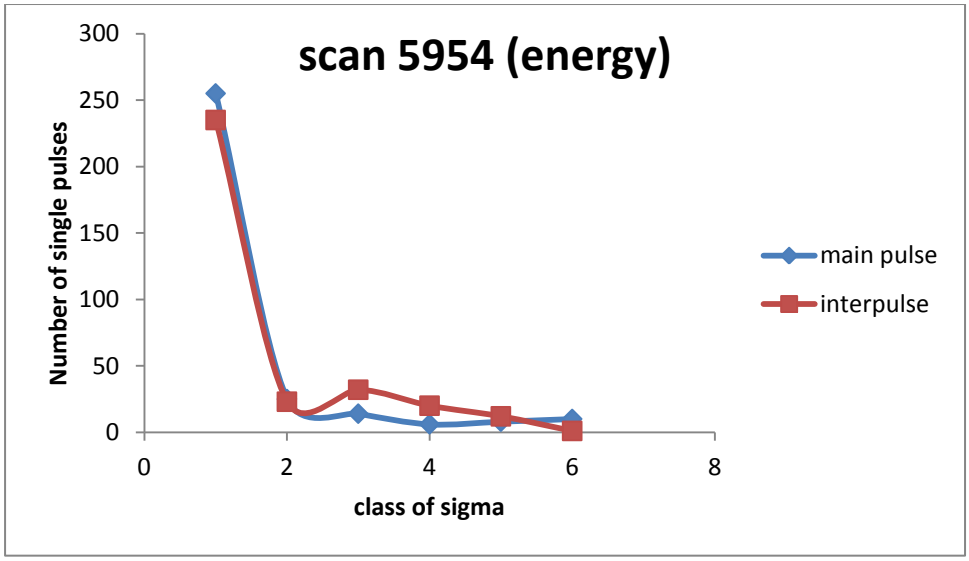

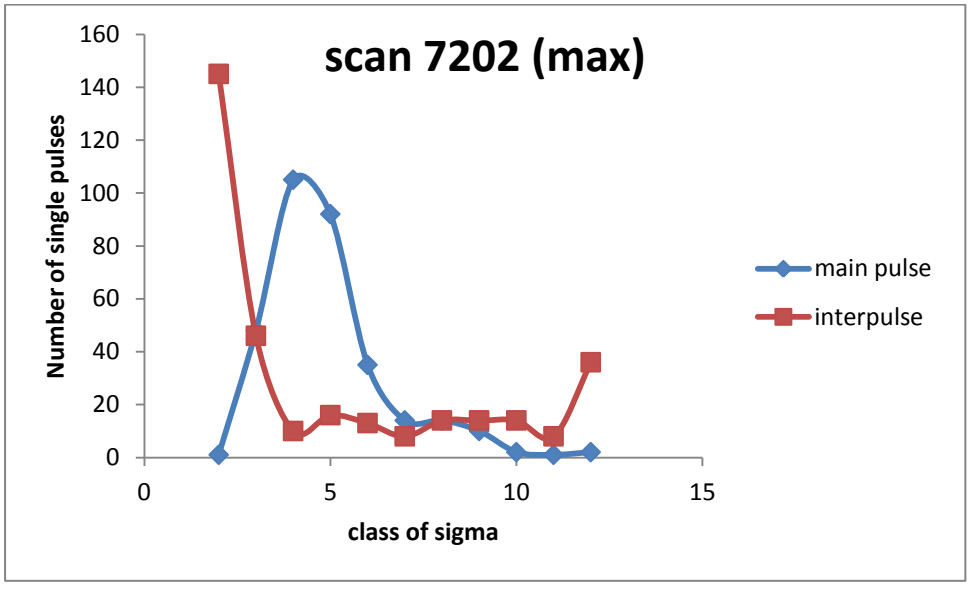

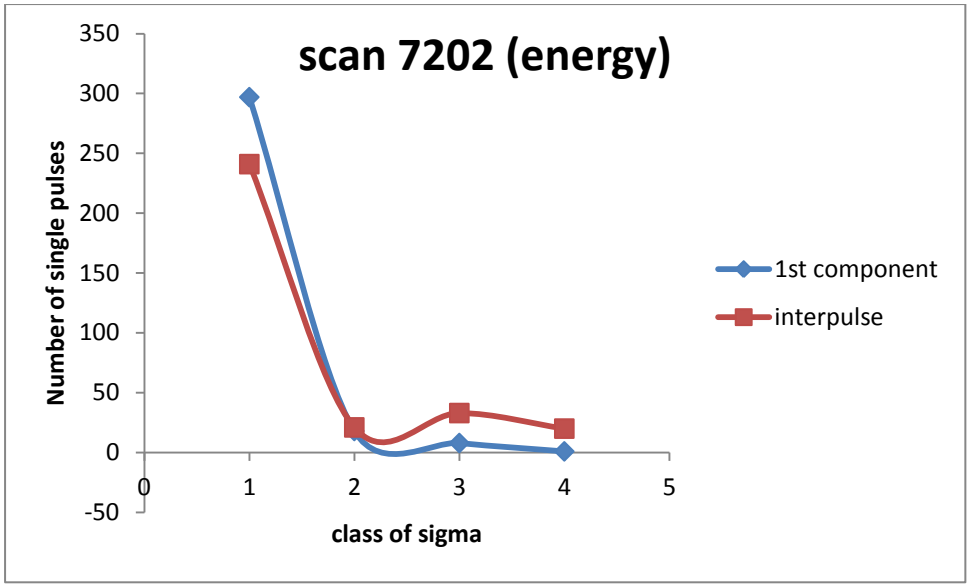
scan 7202 (energy)
Number of single pulses
class of sigma
1st component
interpulse

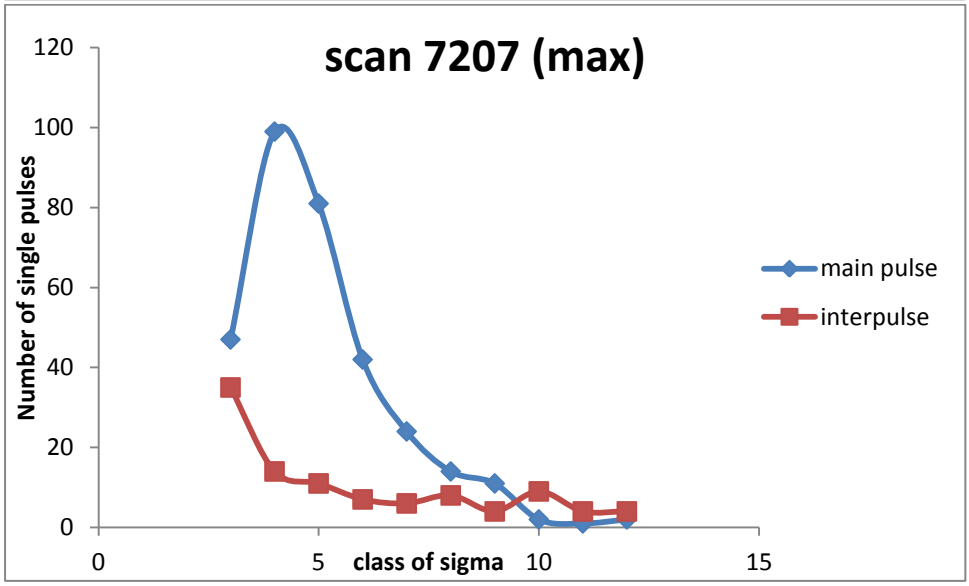
scan 7207 (max)
Number of single pulses
class of sigma
main pulse
interpulse

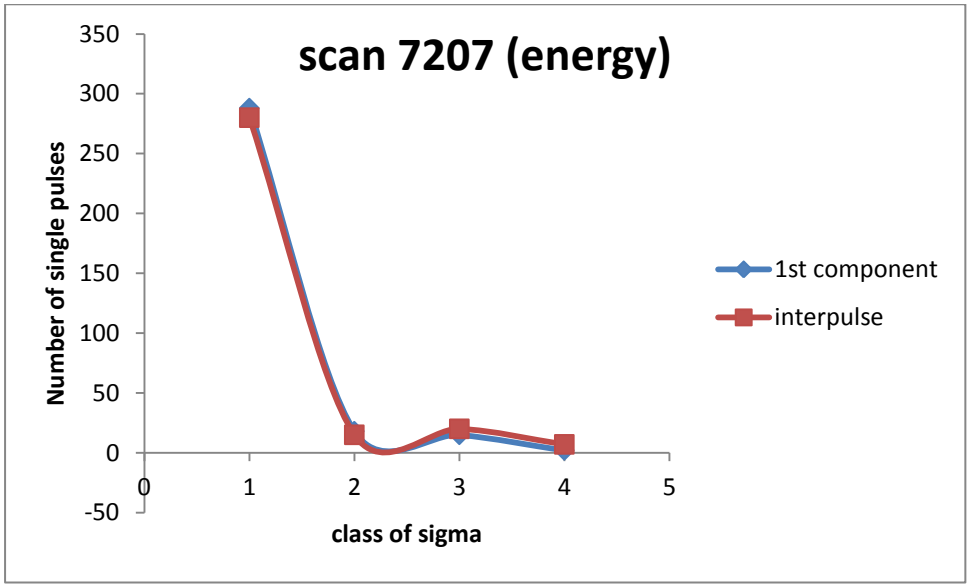
scan 7207 (energy)
Number of single pulses
class of sigma
1st component
interpulse

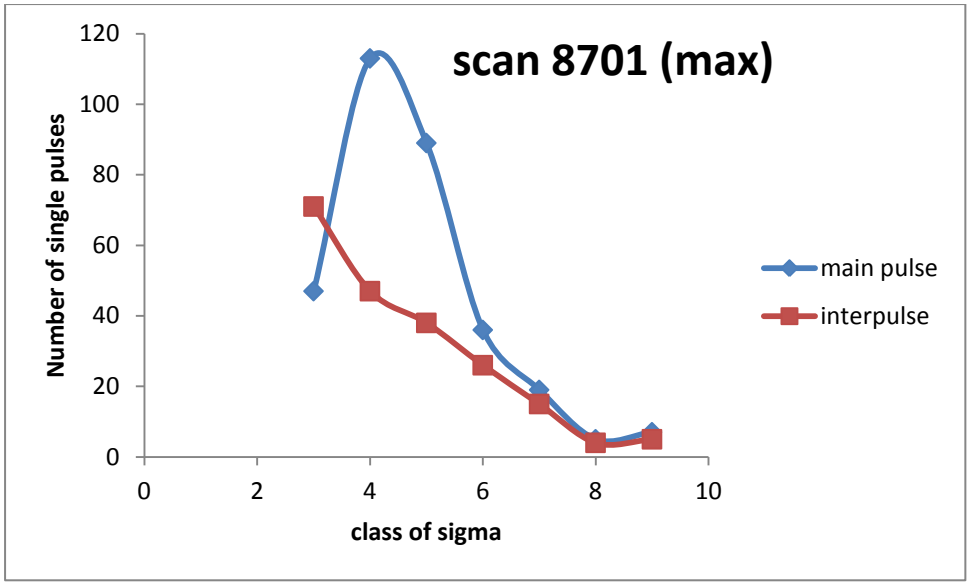
scan 8701 (max)
Number of single pulses
120
100
80
60
40
20
0
0
2
4
6
8
10
class of sigma
main pulse
interpulse

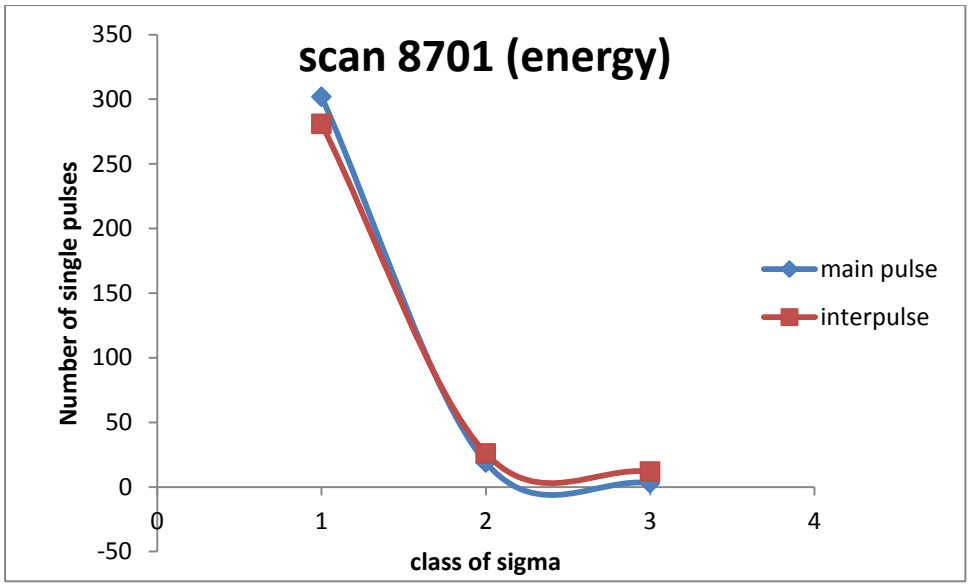
scan 8701 (energy)
Number of single pulses
350
300
250
200
150
100
50
0
-50
0
1
2
3
4
class of sigma
main pulse
interpulse

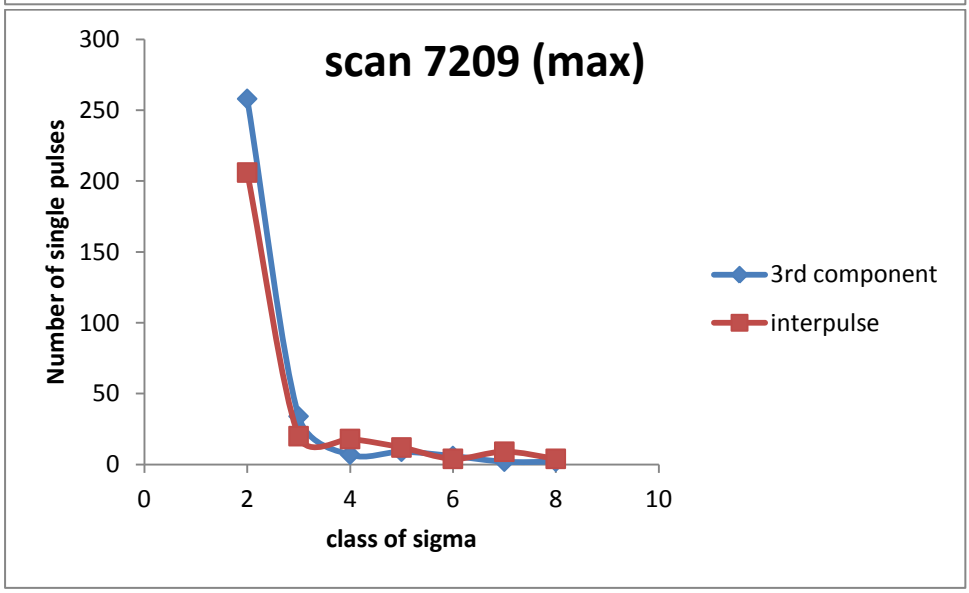
scan 7209 (max)
Number of single pulses
300
250
200
150
100
50
0
0
2
4
6
8
10
class of sigma
3rd component
interpulse

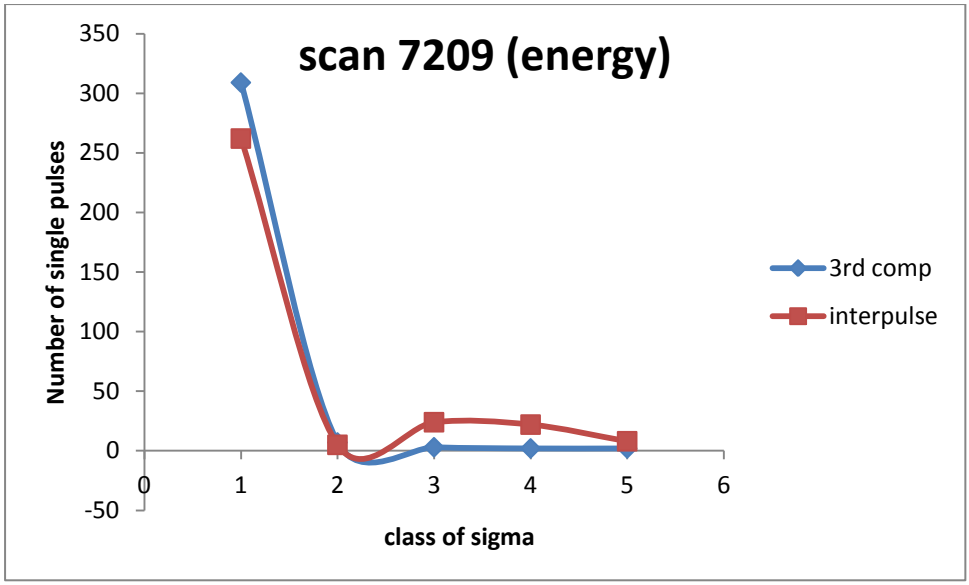
scan 7209 (energy)
Number of single pulses
350
300
250
200
150
100
50
0
-50
0
1
2
3
4
5
6
class of sigma
3rd comp
interpulse

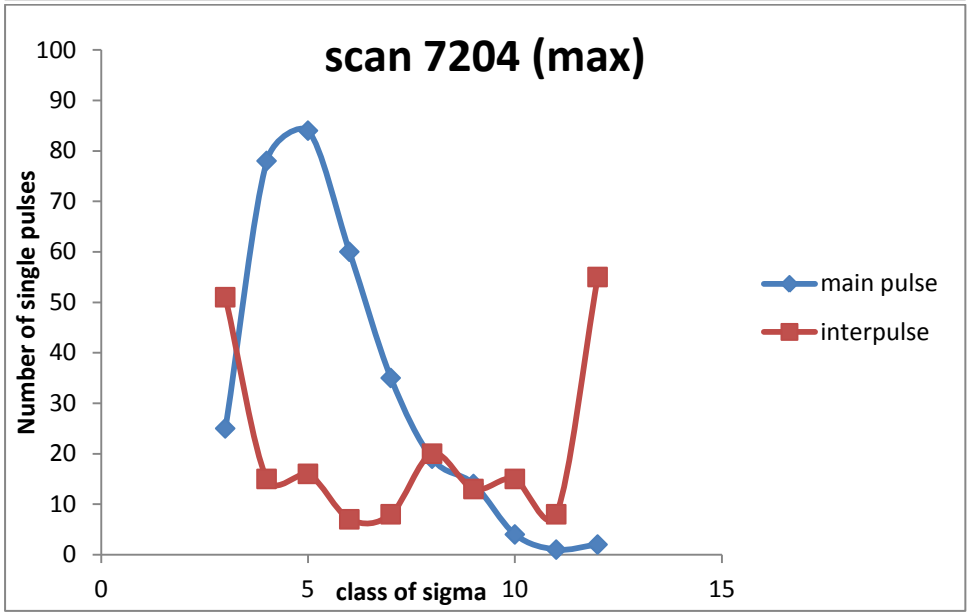
scan 7204 (max)
Number of single pulses
100
90
80
70
60
50
40
30
20
10
0
0
5
10
15
class of sigma
main pulse
interpulse

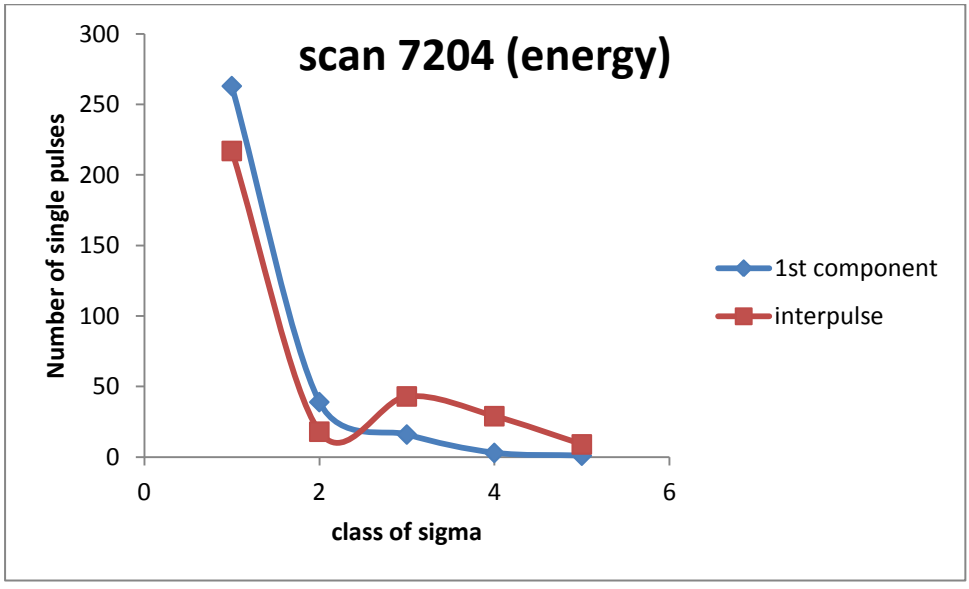
scan 7204 (energy)
Number of single pulses
300
250
200
150
100
50
0
0
2
4
6
class of sigma
1st component
interpulse

Figures of PSR B1133+16:

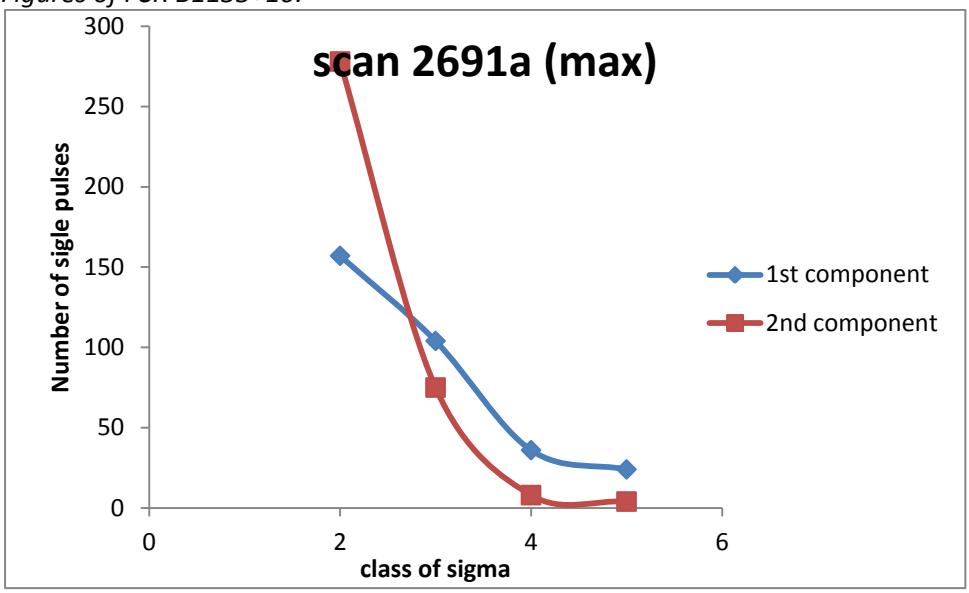

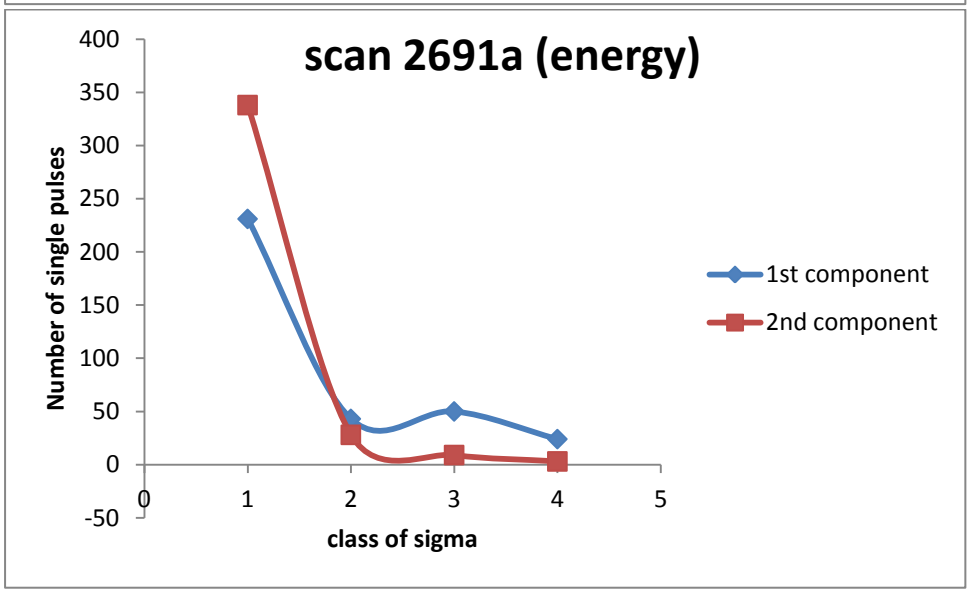

Figures of PSR B0329+54:

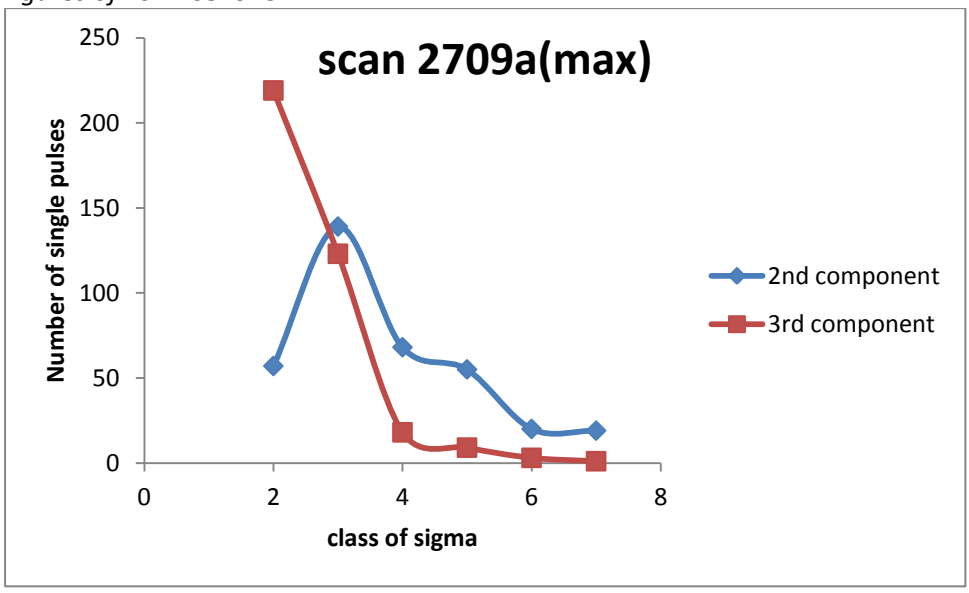

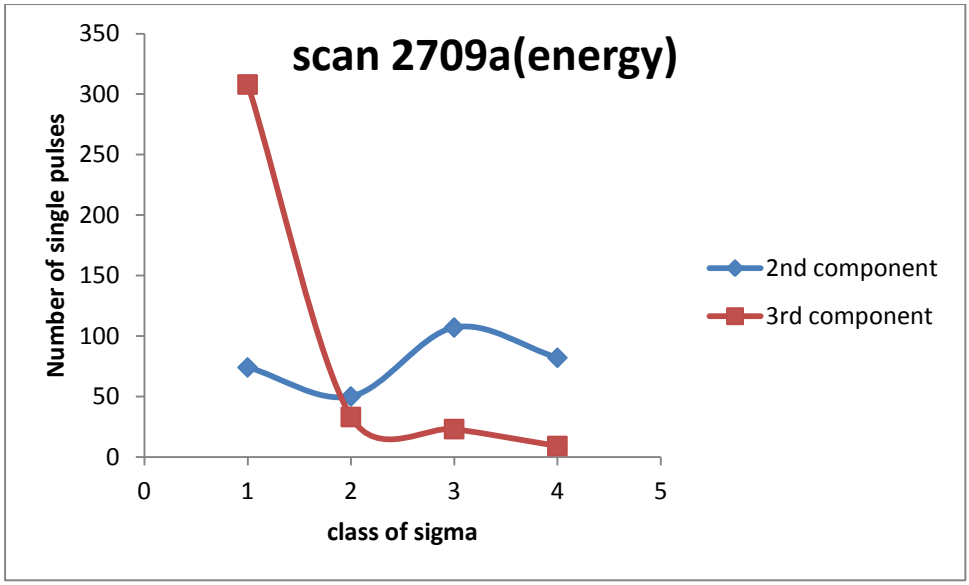

From the figures we can clearly see that for the two pulsars the components that appear to be dominant in the integrated profile have more single pulses in high quality classes than the weaker components do, whereas the number of single pulses for the weaker component is greater than those of the dominant in the low quality classes. But for the magnetar the pattern is not the same: the main pulse is dominant but the interpulse and main pulse have about the same number of single pulses in the highest quality classes and even sometimes the interpulse has more. Particularly for the classification with respect to energy, the main pulse and interpulse show the same behaviour.

8.4 Conclusions

- As already stated the percentage of single pulse nulling for the AXP J1809-194 is significantly lower than that of PSR B0329+54 and PSR B1133+16. That leads us to determine that the magnetar is a young object, younger than PSR B0329+54 and PSR B1133+16: it is in an early stage and thus has enough energy for continuous generation of radio emission. The single pulse nulling results are summarized in the Table below.

Pulsar	***Freq. (GHz)***	***Whole Pulse***	***1st Comp.***	***2nd Comp.***	***3rd Comp.***	***Interpul.***	***Age (10^6 yr)***
AXP J1809-194	8.35	0.06%	37.3%	0.3%	91.4%	49.6%	
AXP J1809-194	2.64	0%	37.8%	92.3%	24.65%	1.4%	
PSR B1133+16	8.35	34%	44.2%	72.5%	-	-	5.5
PSR B0329+54	8.35	10.35%	85.1%	18.8%	63.3%	-	5.0

- From the magnetars' integrated profile we can see that the distance between the main pulse and the interpulse is larger than half a period (it is approximately 75% of the period) which means that:
    i. they do not originate from the two different anti-diametrically located polar cap regions. Thus the magnetars' magnetic field axis is probably closely aligned with the rotation axis and the line of sight intersects the emission cone somewhere near the magnetic axis, so the main pulse and the interpulse originate from two different regions of the same magnetic pole. This, of course, is an assumption since polarization measurements are needed in order to verify this conclusion, or
    ii. they both originate from somewhere close to the light cylinder. The emission regions have a distance of about 75% of a period.

- Comparing the figures that show the correlation between the energy of the individual components of the integrated profile of the magnetar, we came to the conclusion that the energy of the single pulses remains roughly stable. This conclusion is corroborated by the investigation of the percentage of nulling of the individual components. Again the energy of the single pulses seems to be stable in all components, although the number of single pulses varies in each component.
- We calculated the characteristic age, $\tau = \frac{P}{2\dot{P}}$, of the magnetar AXP J1809-194:

  $\tau = \frac{P}{2\dot{P}} \rightarrow \tau = \frac{5.54}{1.15\times10^{-11}} \rightarrow \tau = 2.4 \times 10^{-11} sec \rightarrow \tau \approx 7600\ yrs$. This age, which is calculated assuming a dipolar magnetic field, indicates that the magnetar AXP J1809-194 is very young. This conclusion does not justify its very long period of rotation (5.4 s). Could it be that the magnetic field of this magnetar is not dipolar and therefore the calculated characteristic age does not apply to the magnetar AXP J1809-194?

Appendix A

A.1 Representative single pulses plots are for each of the three AXP J1809-194, PSR B0329+54and PSR B1133+16 are presented here.

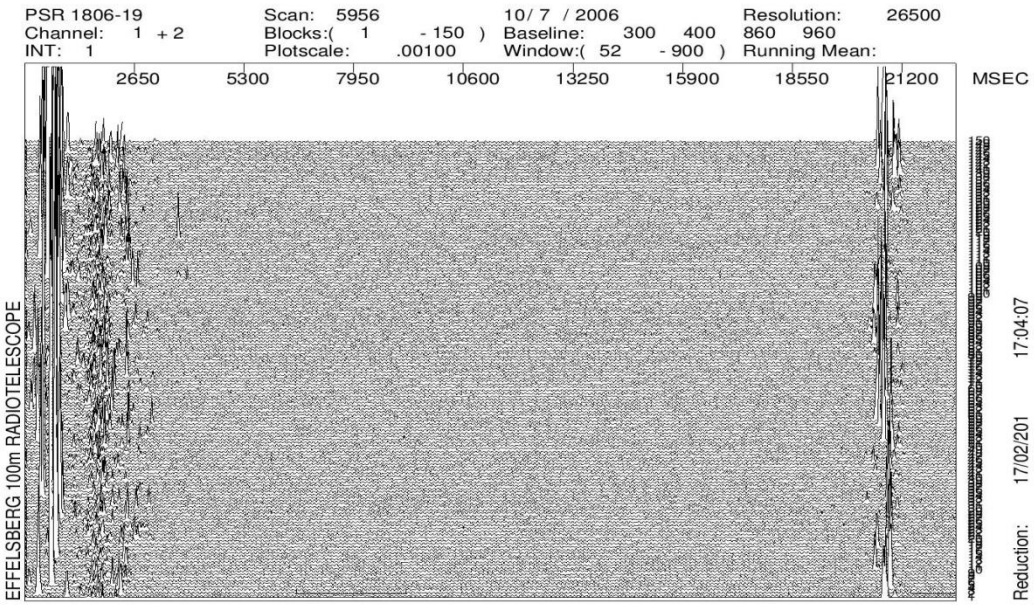

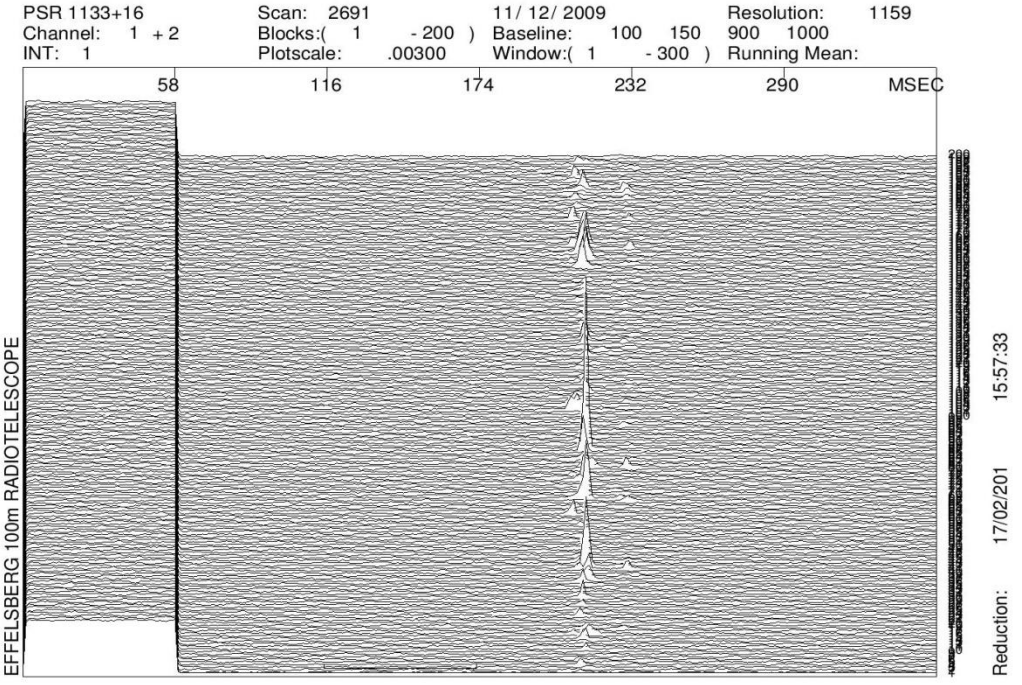

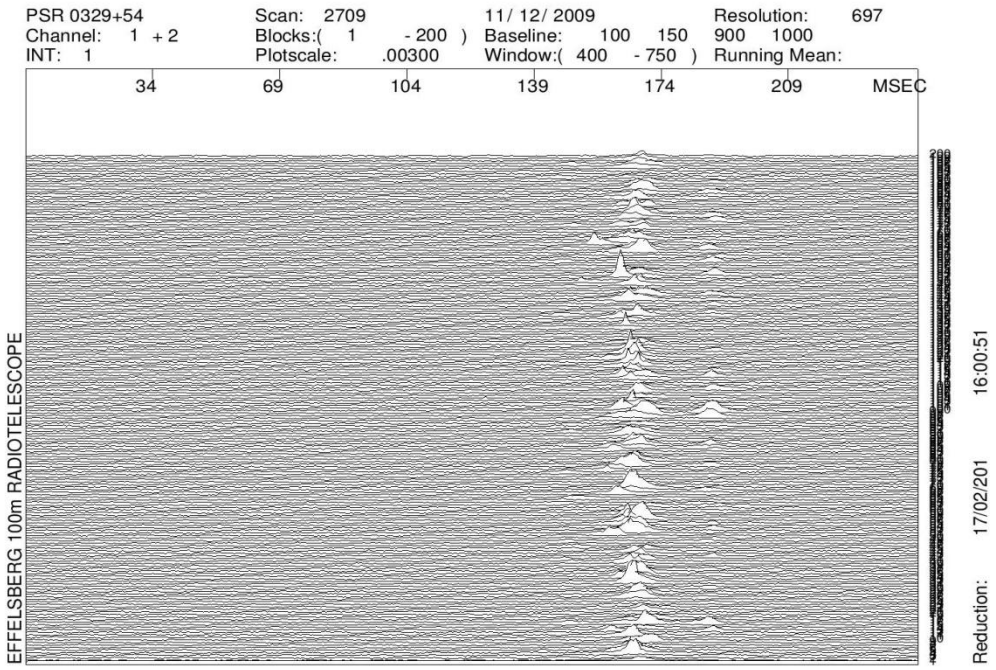
PSR 0329+54
Scan: 2709
11/ 12/ 2009
Resolution: 697
Channel: 1 + 2
Blocks:(1 - 200)
Baseline: 100 150
900 1000
INT: 1
Plotscale: .00300
Window:(400 - 750)
Running Mean:
34
69
104
139
174
209
MSEC
EFFELSBERG 100m RADIOTELESCOPE
Reduction: 17/02/201
16:00:51

Appendix B

B.1 Quality plots: distribution of single pulses in each quality class

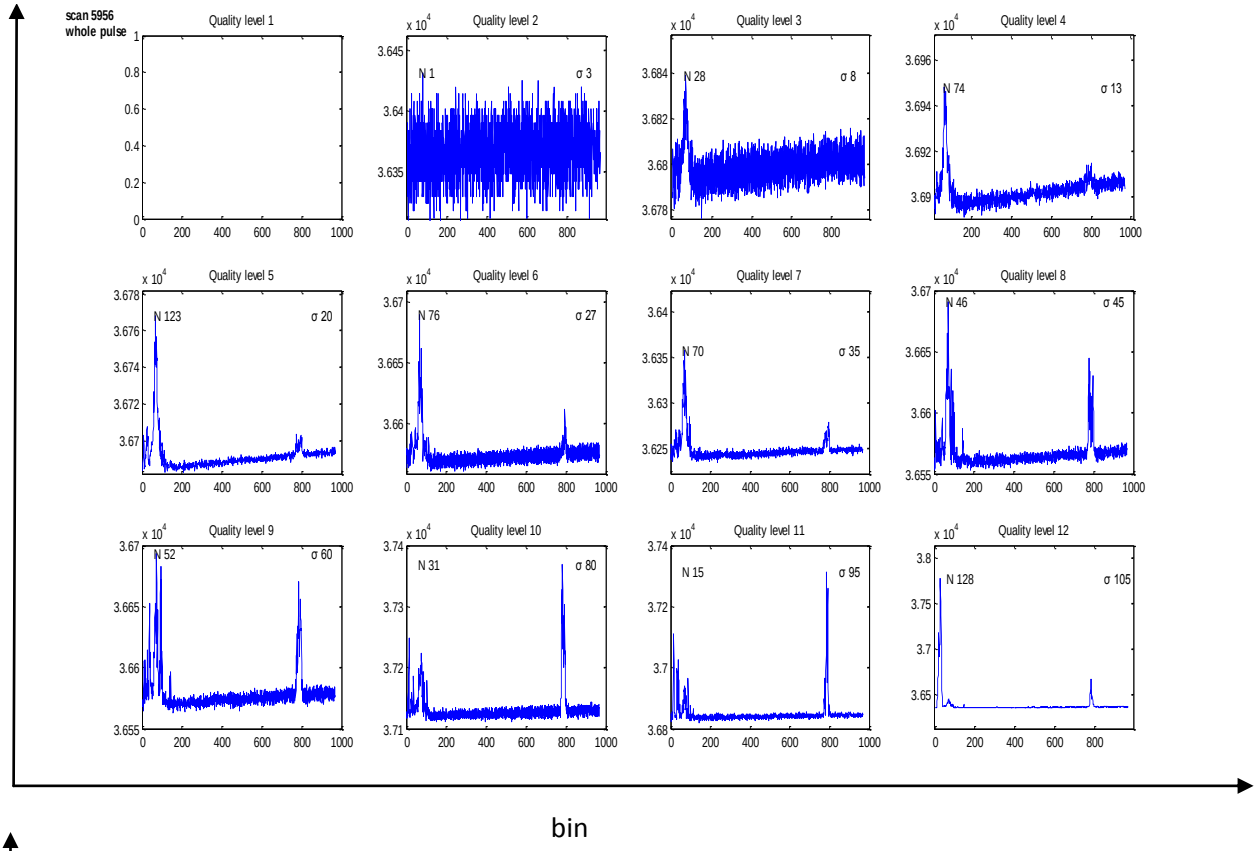

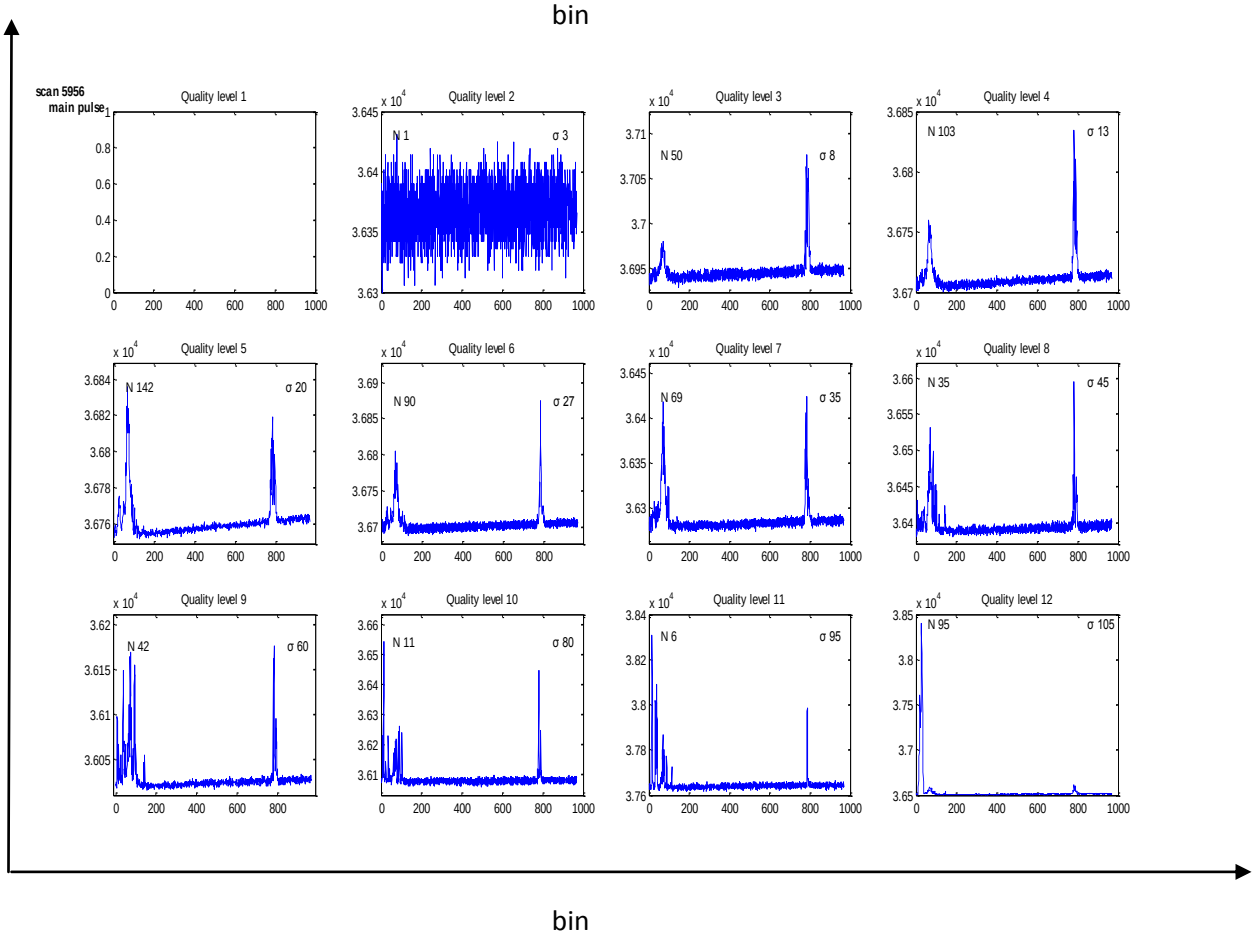

V/f counts

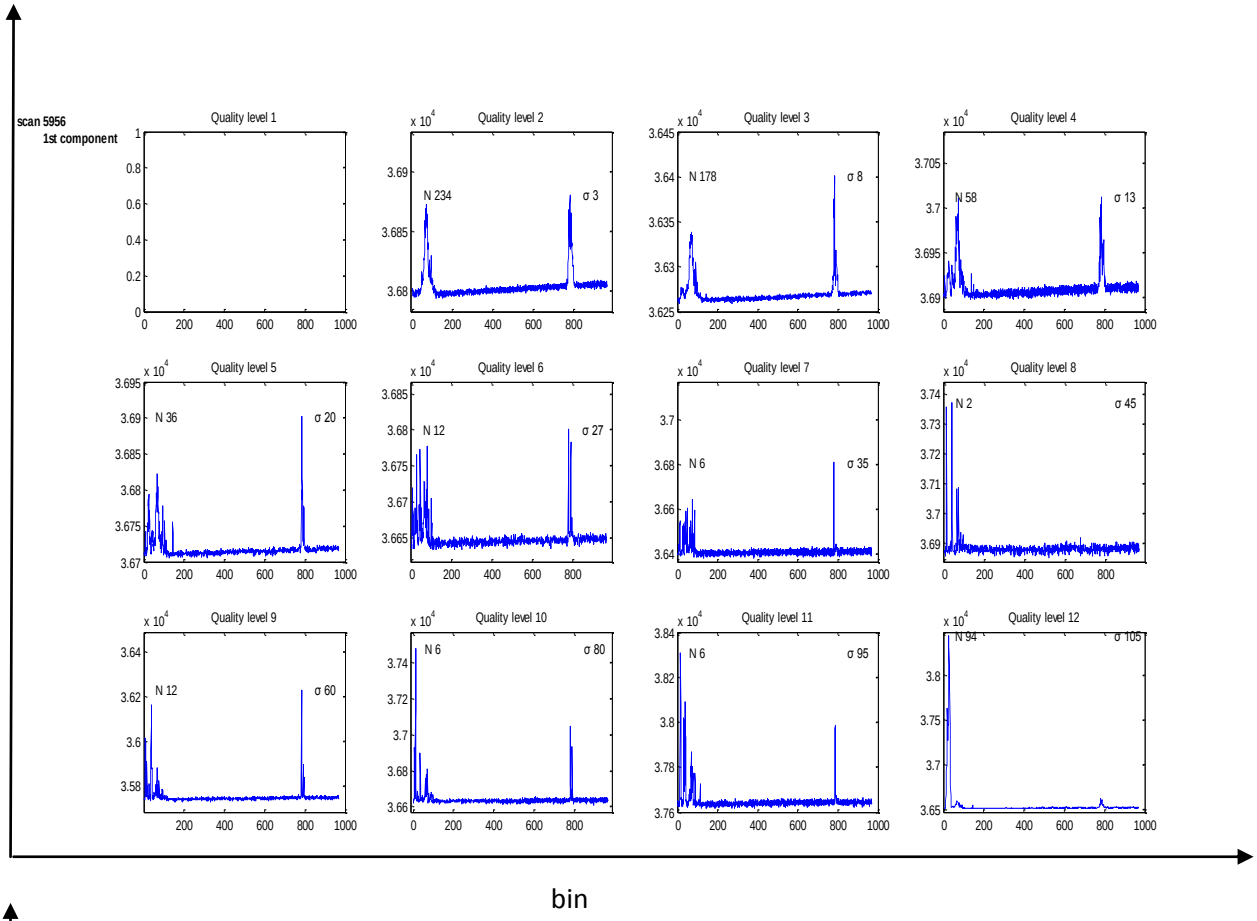

bin

V/f counts

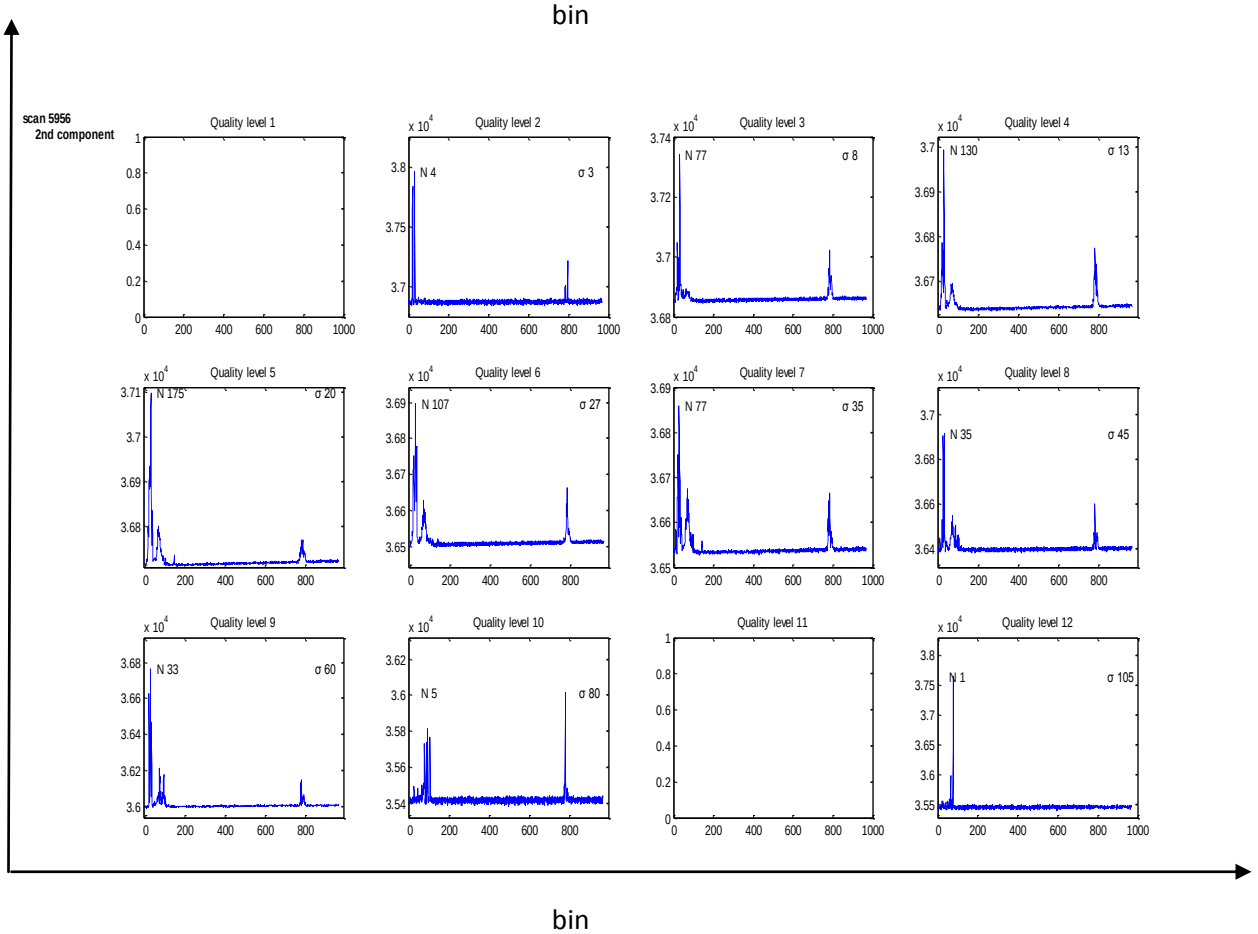

bin

V/f counts

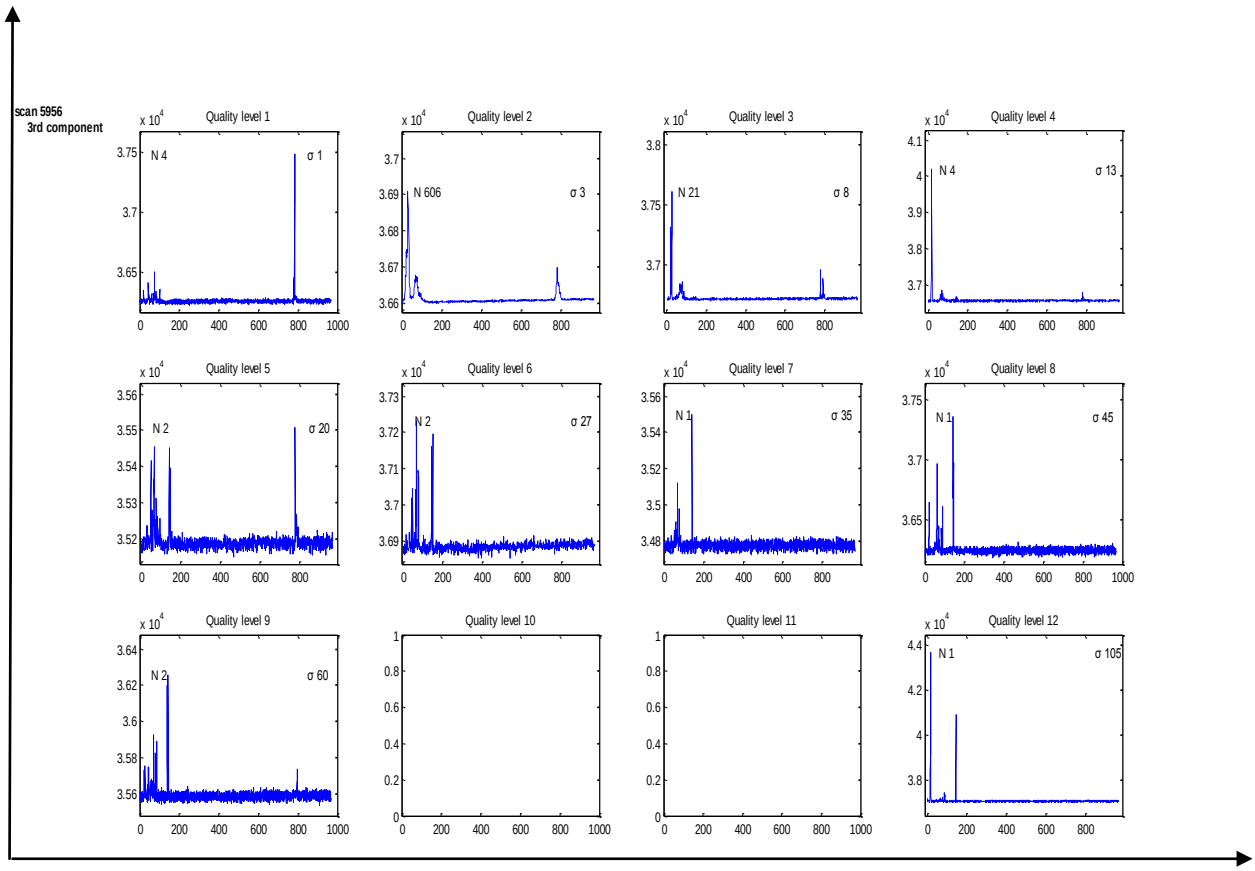

bin

V/f counts

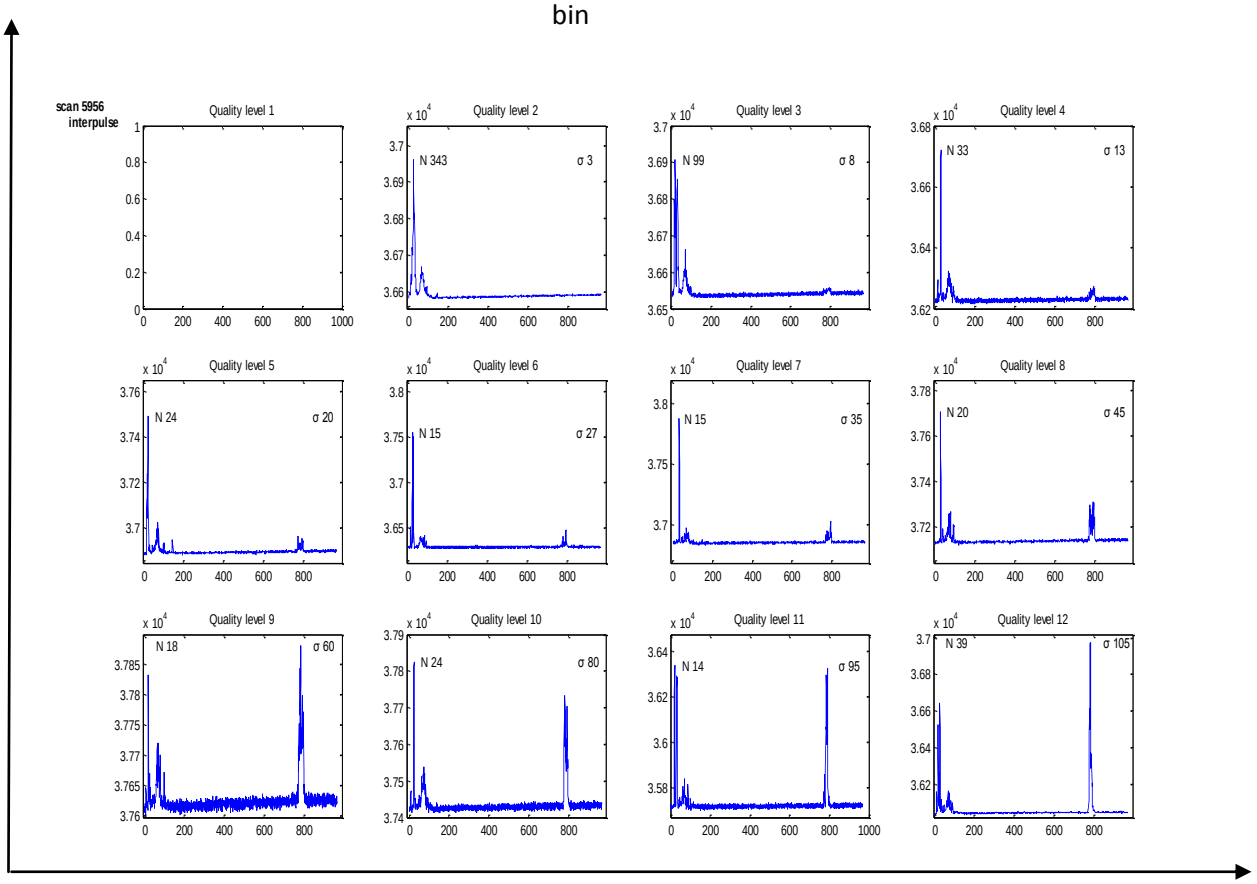

bin

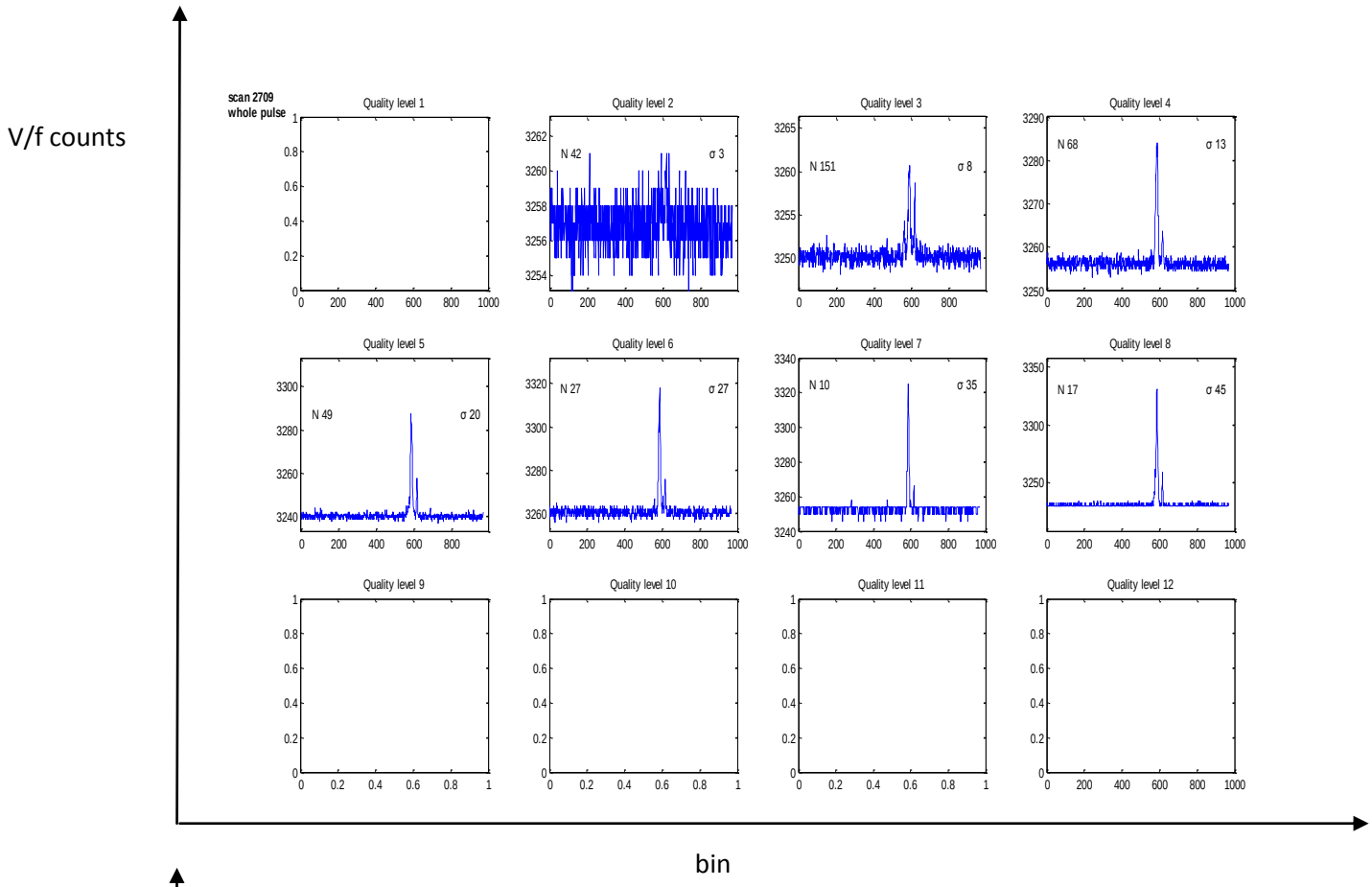
V/f counts
scan 2709
whole pulse
Quality level 1
Quality level 2
N 42
σ 3
Quality level 3
N 151
σ 8
Quality level 4
N 68
σ 13
Quality level 5
N 49
σ 20
Quality level 6
N 27
σ 27
Quality level 7
N 10
σ 35
Quality level 8
N 17
σ 45
Quality level 9
Quality level 10
Quality level 11
Quality level 12
bin

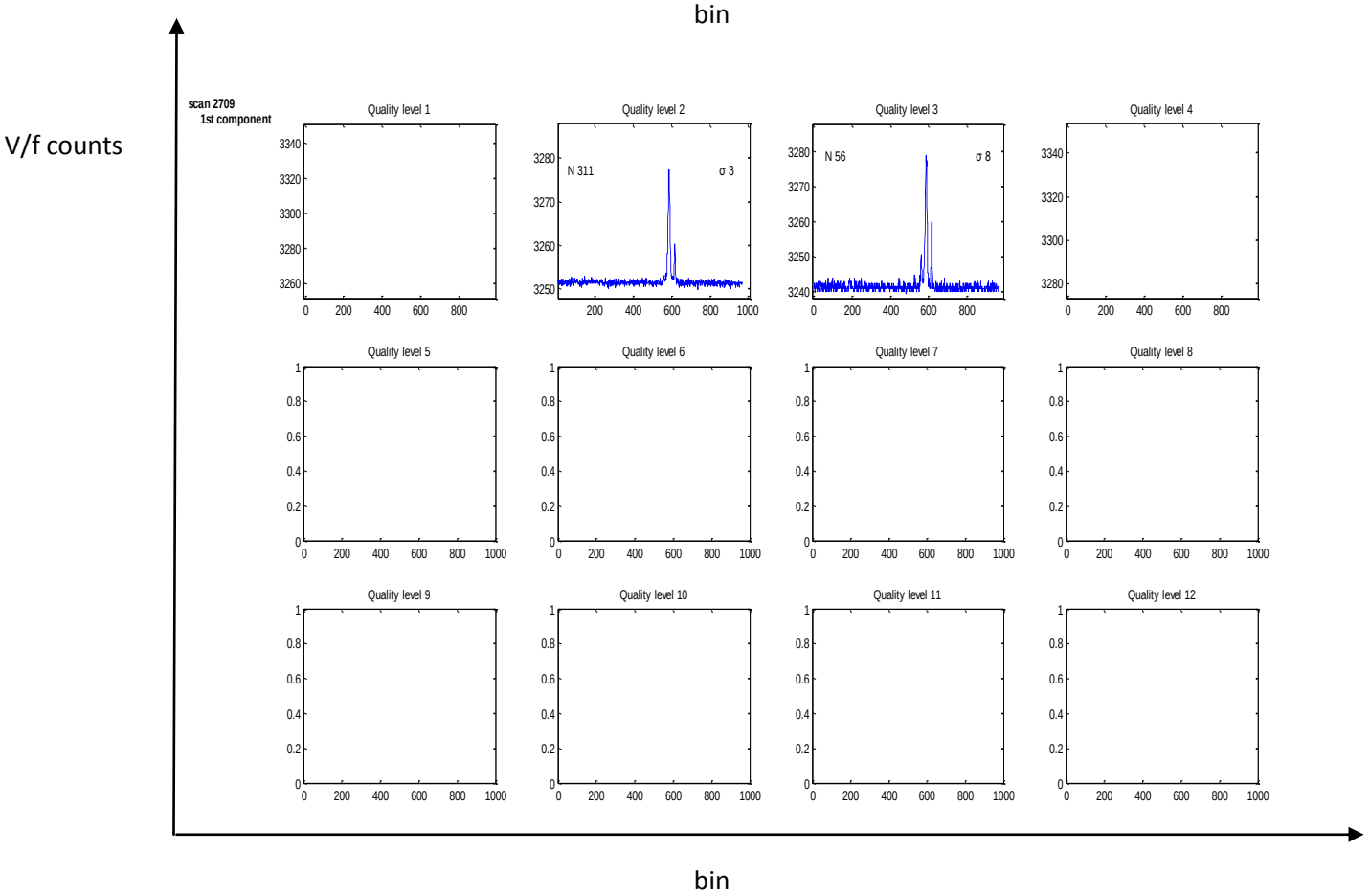
V/f counts
scan 2709
1st component
Quality level 1
Quality level 2
N 311
σ 3
Quality level 3
N 56
σ 8
Quality level 4
Quality level 5
Quality level 6
Quality level 7
Quality level 8
Quality level 9
Quality level 10
Quality level 11
Quality level 12
bin

V/f counts

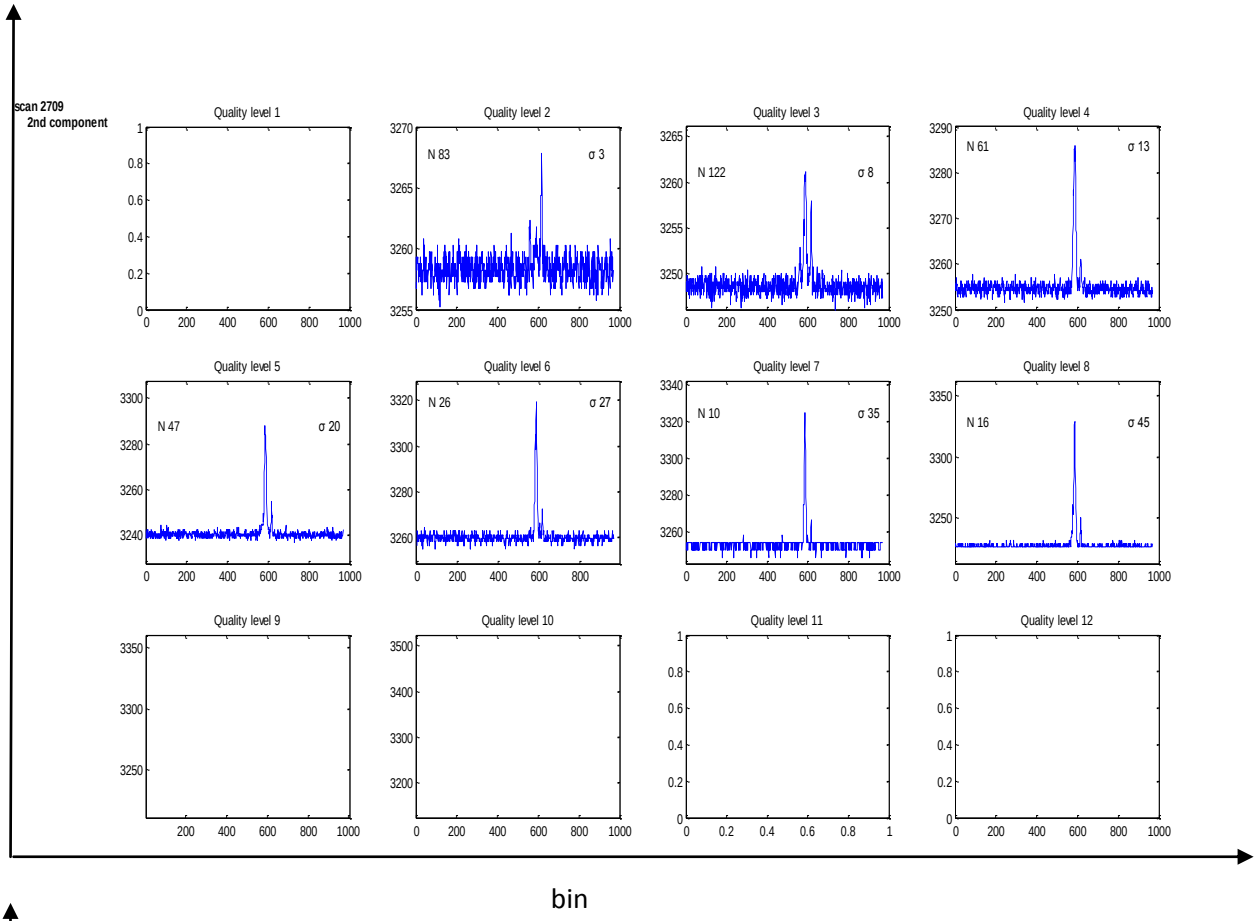

bin

V/f counts

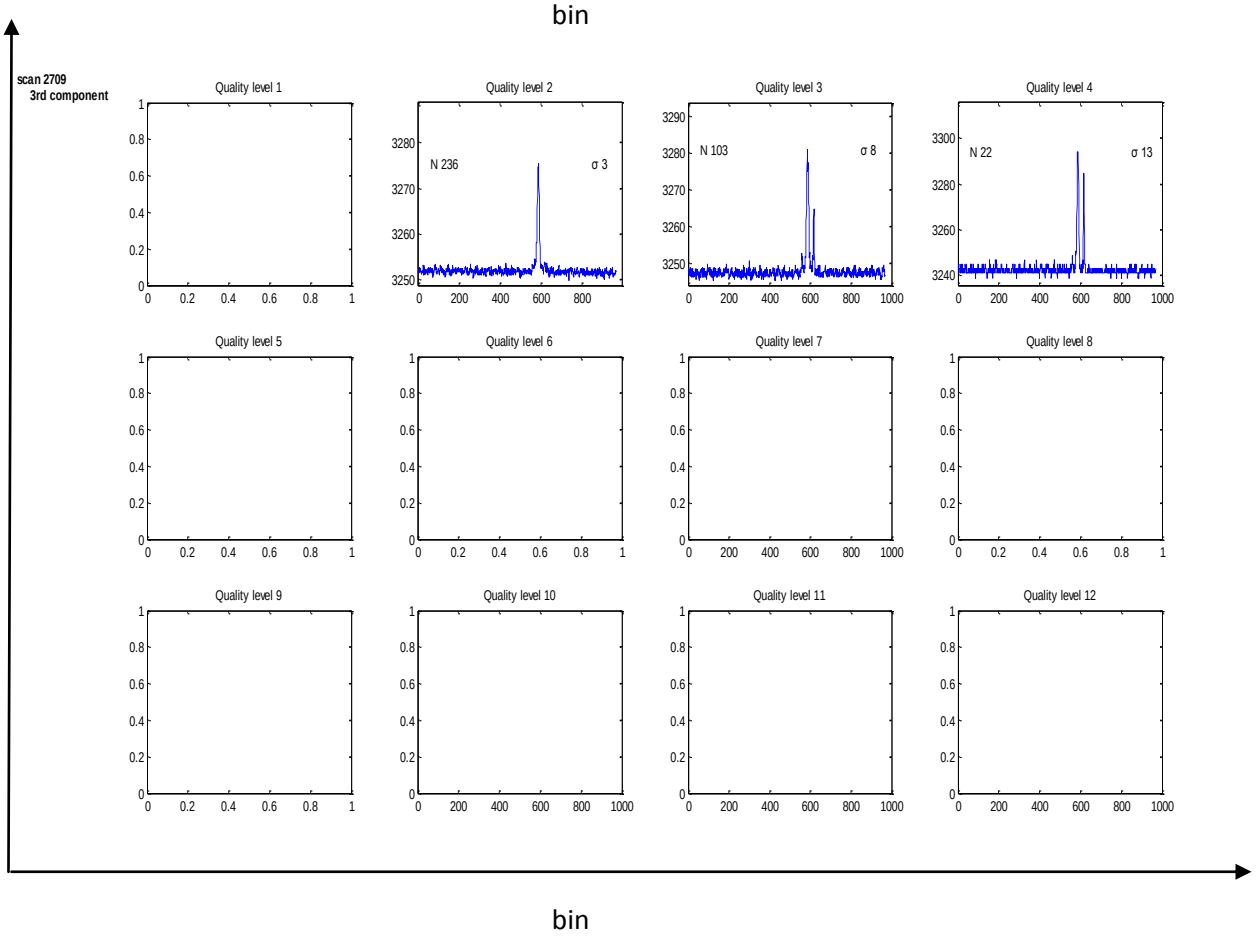

bin

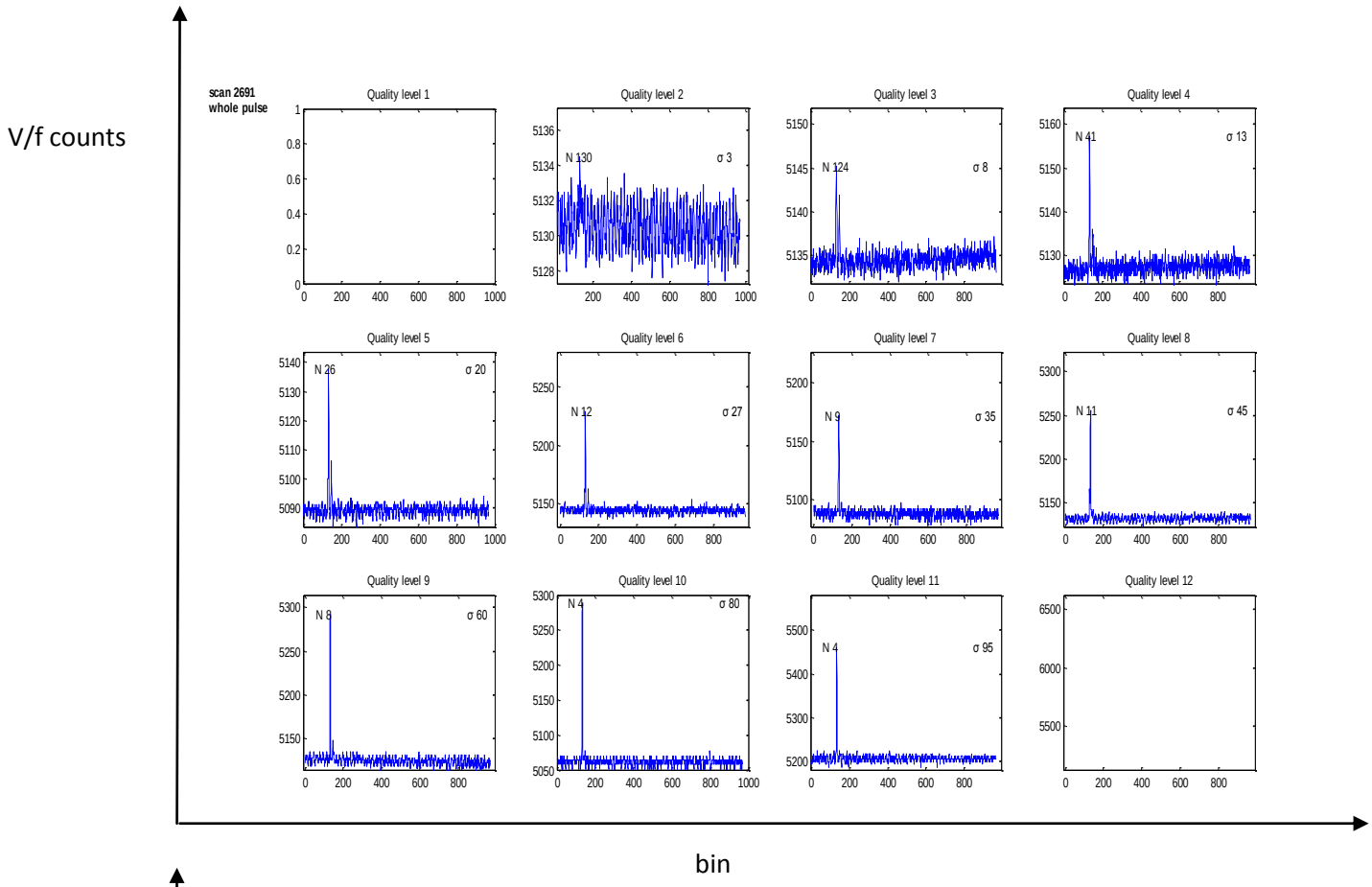
V/f counts
scan 2691
whole pulse
Quality level 1
Quality level 2
N 130
σ 3
Quality level 3
N 124
σ 8
Quality level 4
N 41
σ 13
Quality level 5
N 26
σ 20
Quality level 6
N 12
σ 27
Quality level 7
N 9
σ 35
Quality level 8
N 11
σ 45
Quality level 9
N 8
σ 60
Quality level 10
N 4
σ 80
Quality level 11
N 4
σ 95
Quality level 12
bin

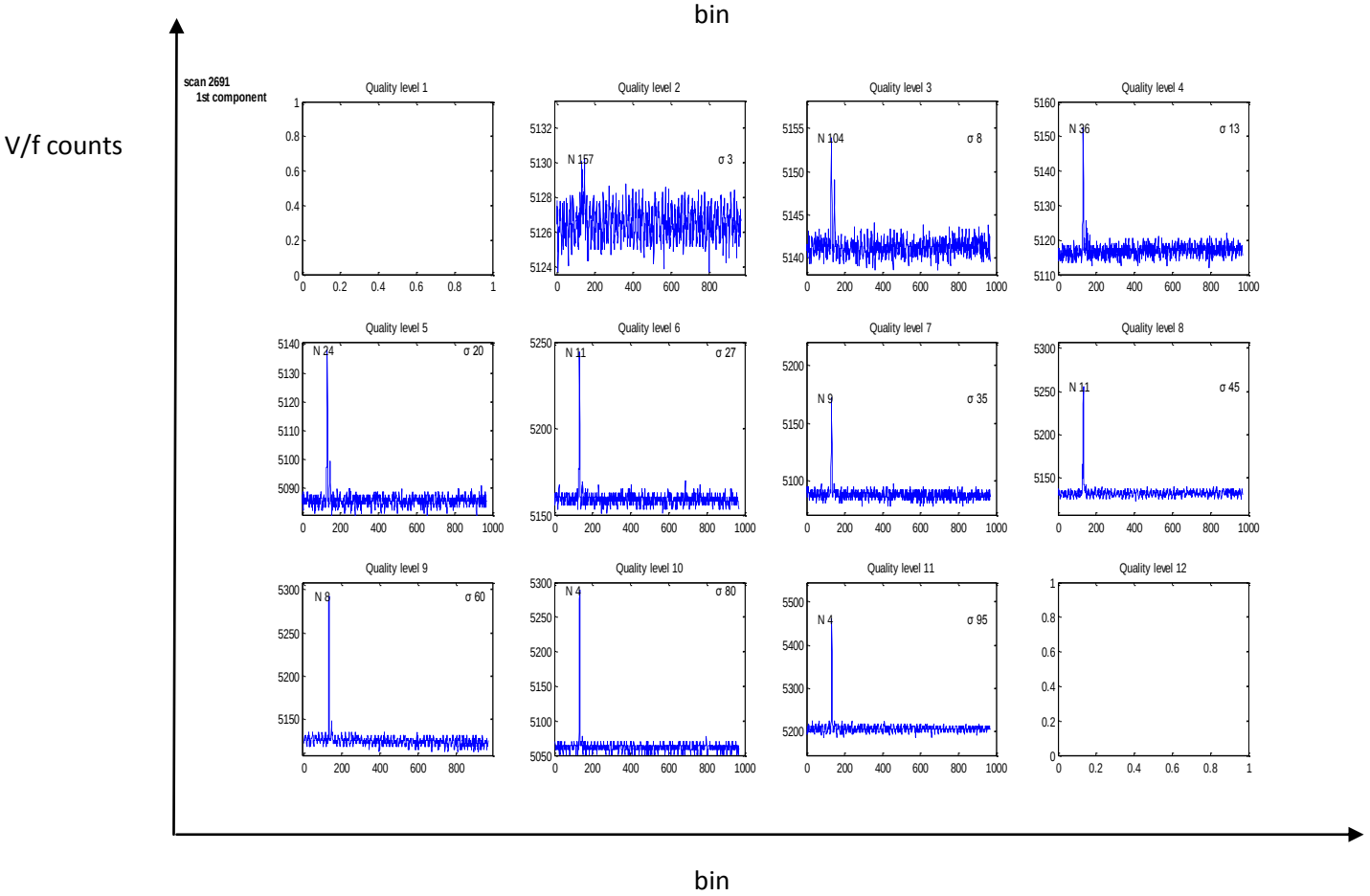
V/f counts
scan 2691
1st component
Quality level 1
Quality level 2
N 157
σ 3
Quality level 3
N 104
σ 8
Quality level 4
N 36
σ 13
Quality level 5
N 24
σ 20
Quality level 6
N 11
σ 27
Quality level 7
N 9
σ 35
Quality level 8
N 11
σ 45
Quality level 9
N 8
σ 60
Quality level 10
N 4
σ 80
Quality level 11
N 4
σ 95
Quality level 12
bin

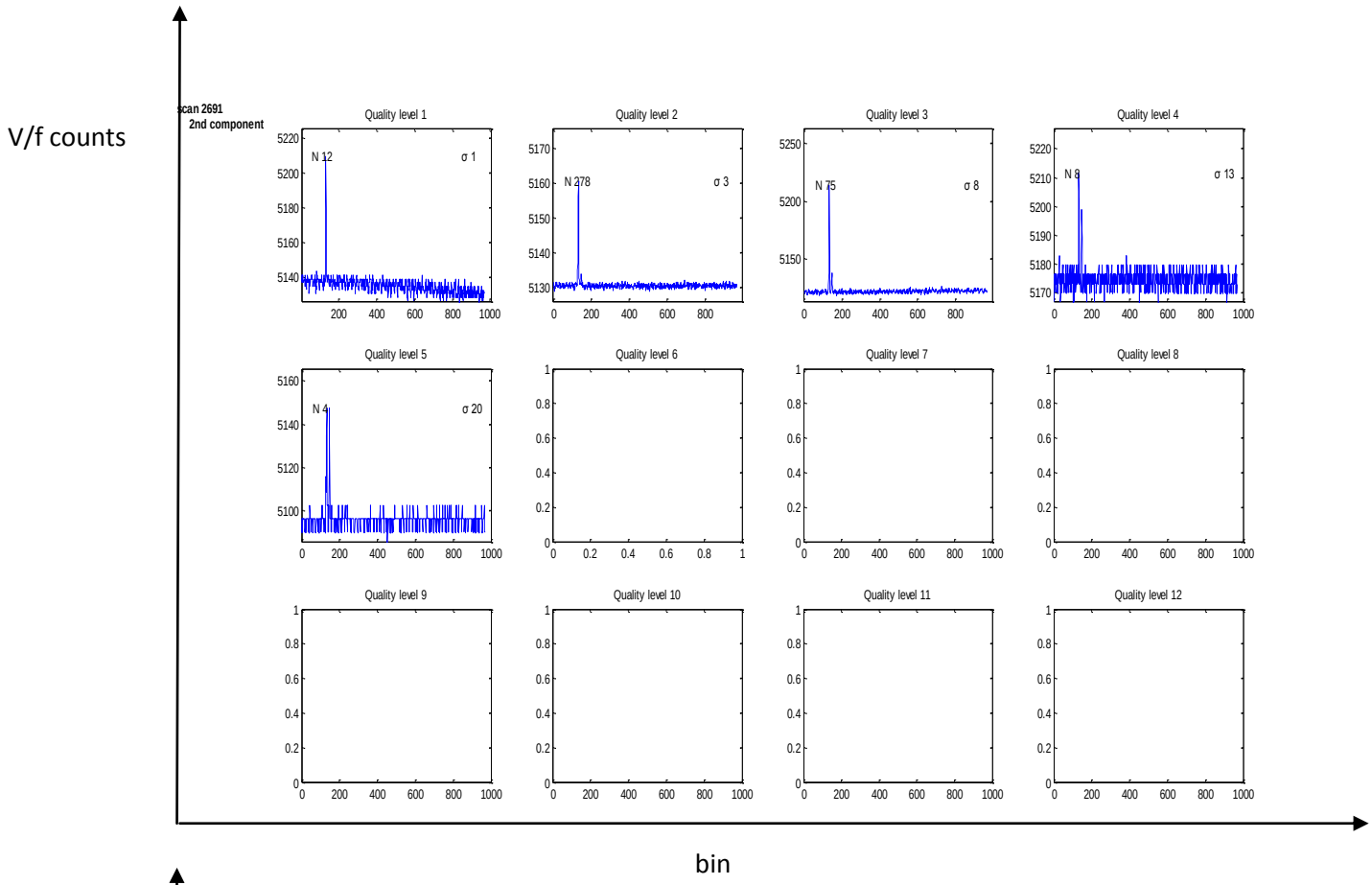
V/f counts
scan 2691
2nd component
Quality level 1
N 12
σ 1
Quality level 2
N 278
σ 3
Quality level 3
N 75
σ 8
Quality level 4
N 8
σ 13
Quality level 5
N 4
σ 20
Quality level 6
Quality level 7
Quality level 8
Quality level 9
Quality level 10
Quality level 11
Quality level 12
bin

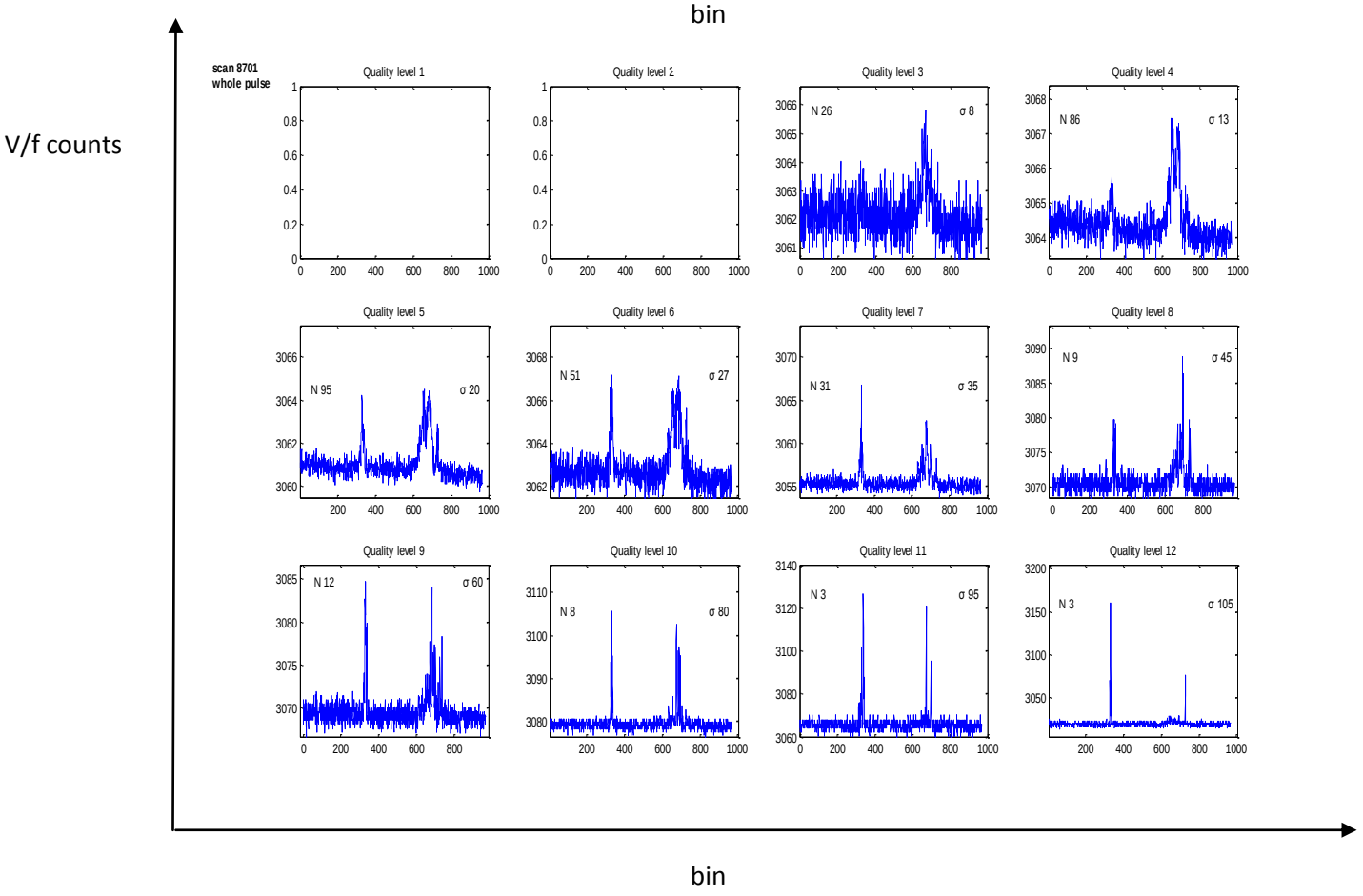
V/f counts
scan 8701
whole pulse
Quality level 1
Quality level 2
Quality level 3
N 26
σ 8
Quality level 4
N 86
σ 13
Quality level 5
N 95
σ 20
Quality level 6
N 51
σ 27
Quality level 7
N 31
σ 35
Quality level 8
N 9
σ 45
Quality level 9
N 12
σ 60
Quality level 10
N 8
σ 80
Quality level 11
N 3
σ 95
Quality level 12
N 3
σ 105
bin

V/f counts

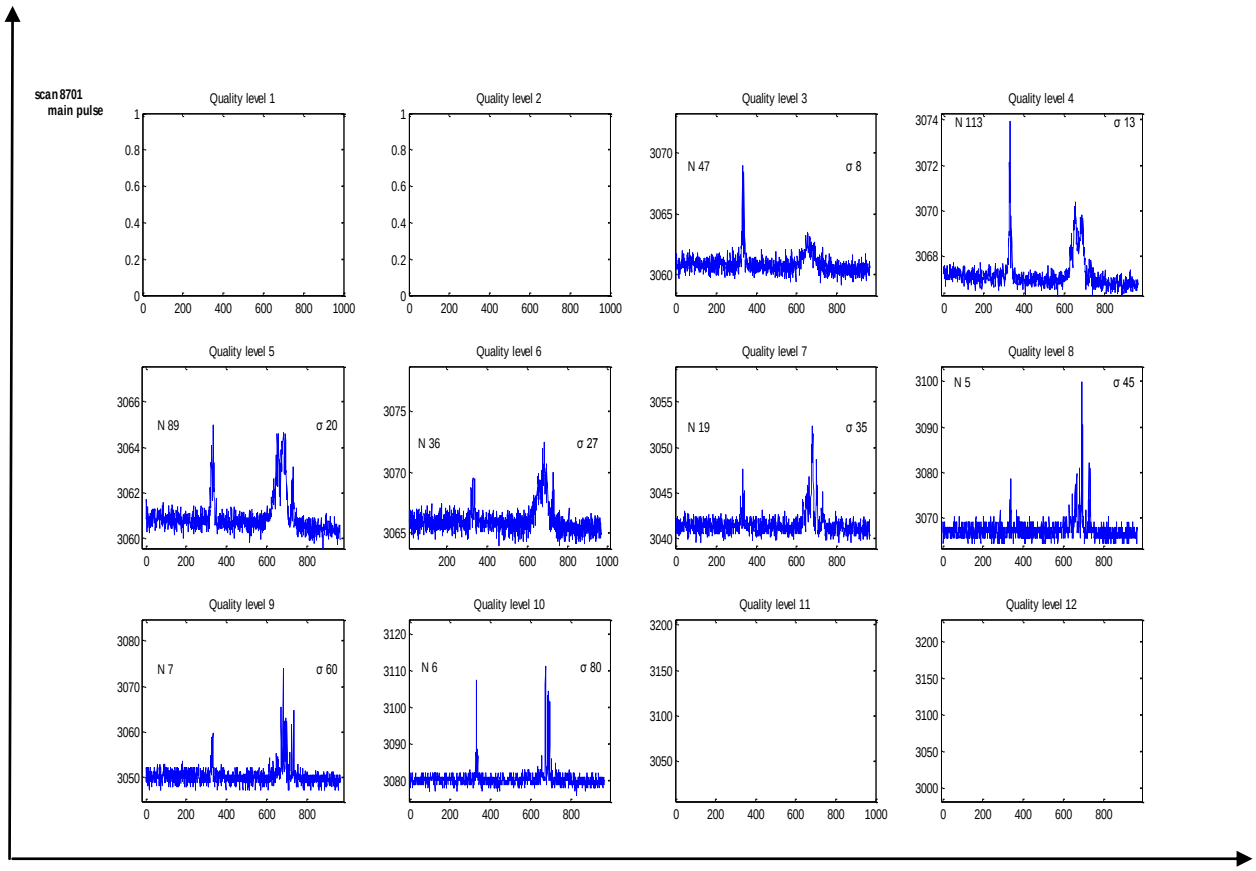

bin

V/f counts

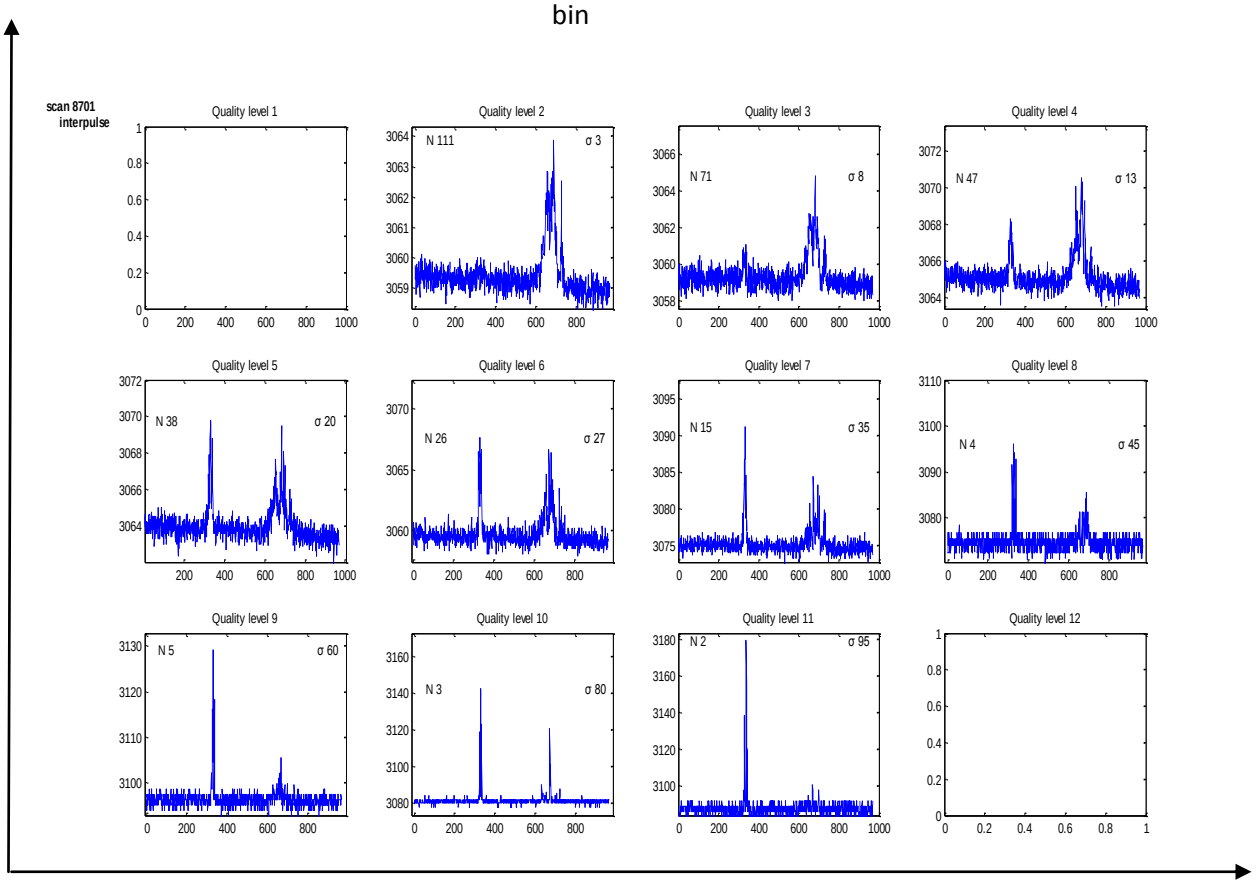

bin

V/f counts

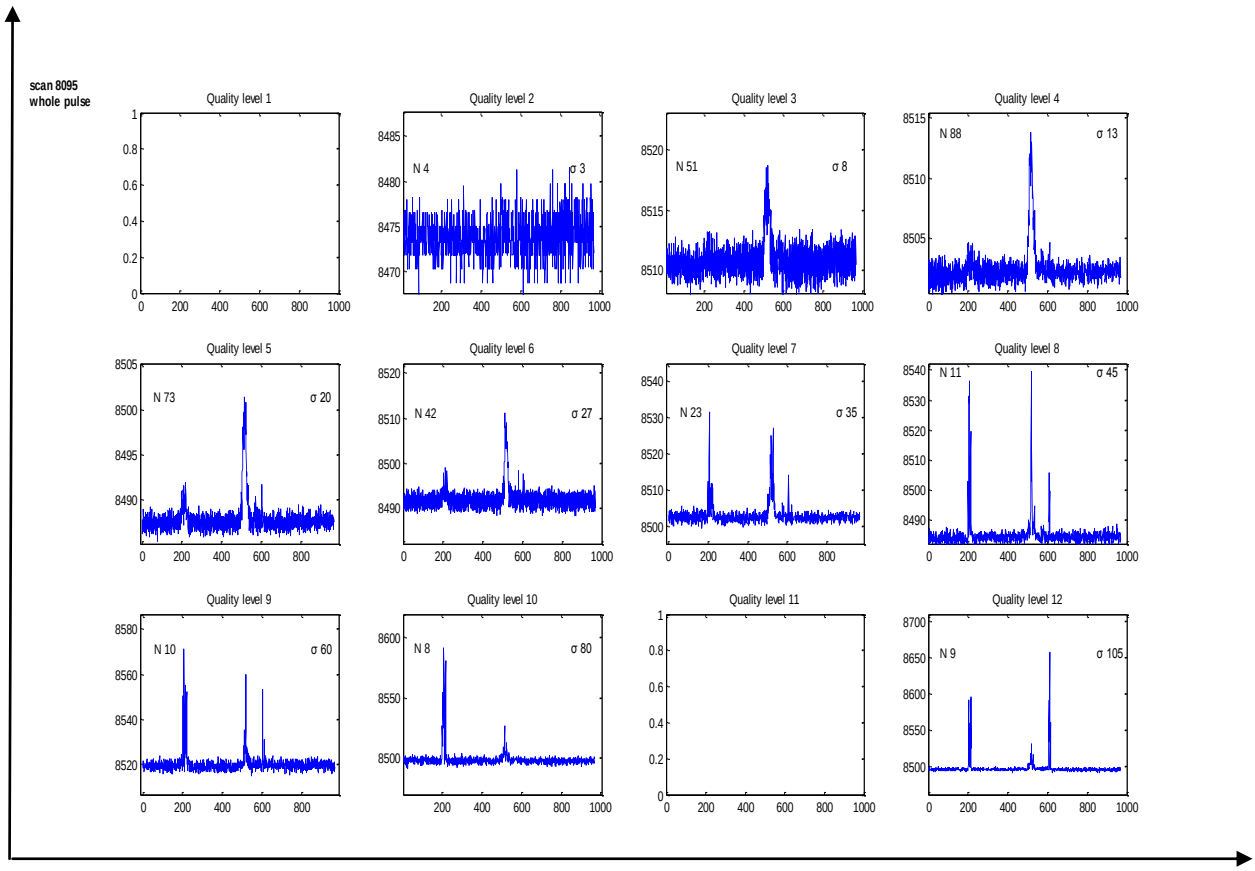

bin

V/f counts

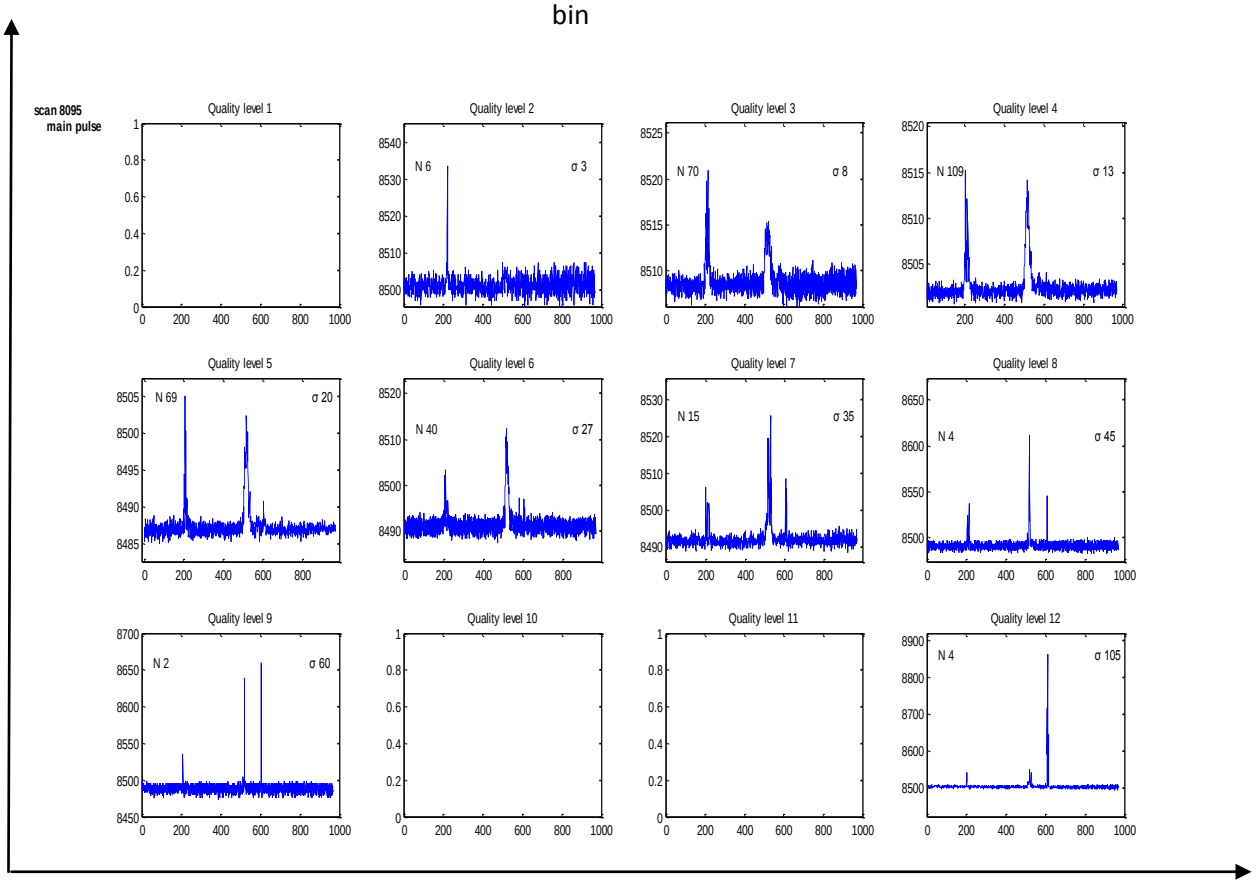

bin

V/f counts

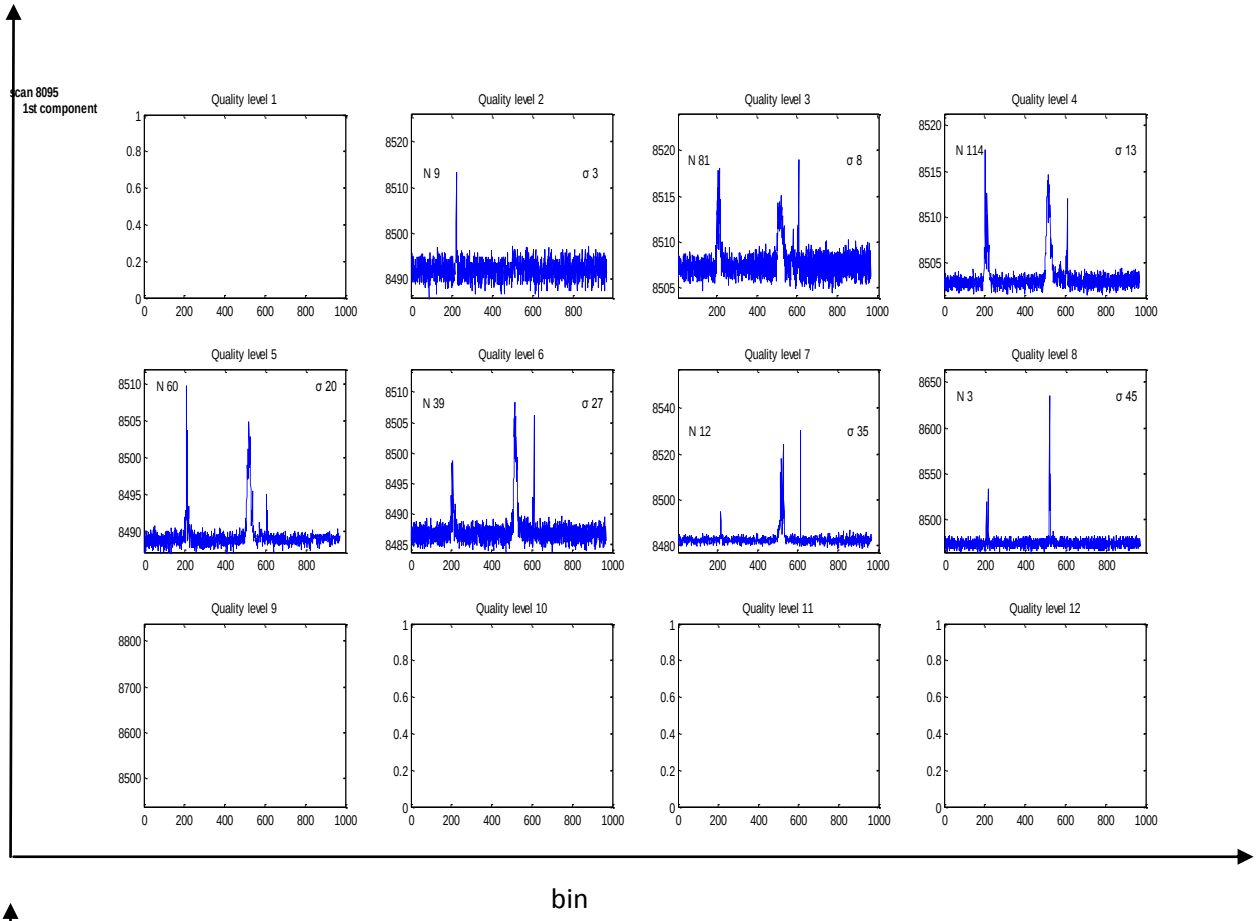

V/f counts

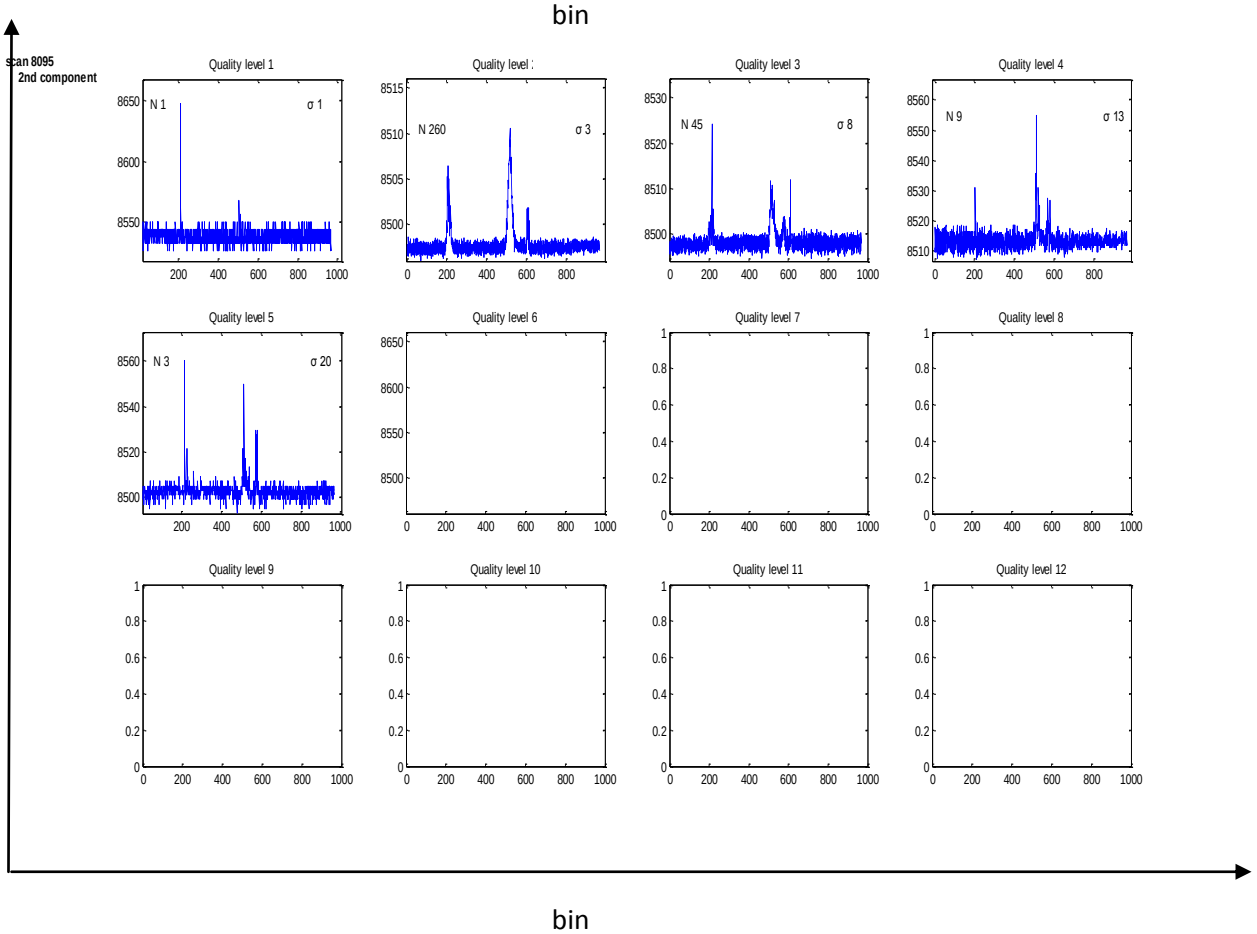

V/f counts

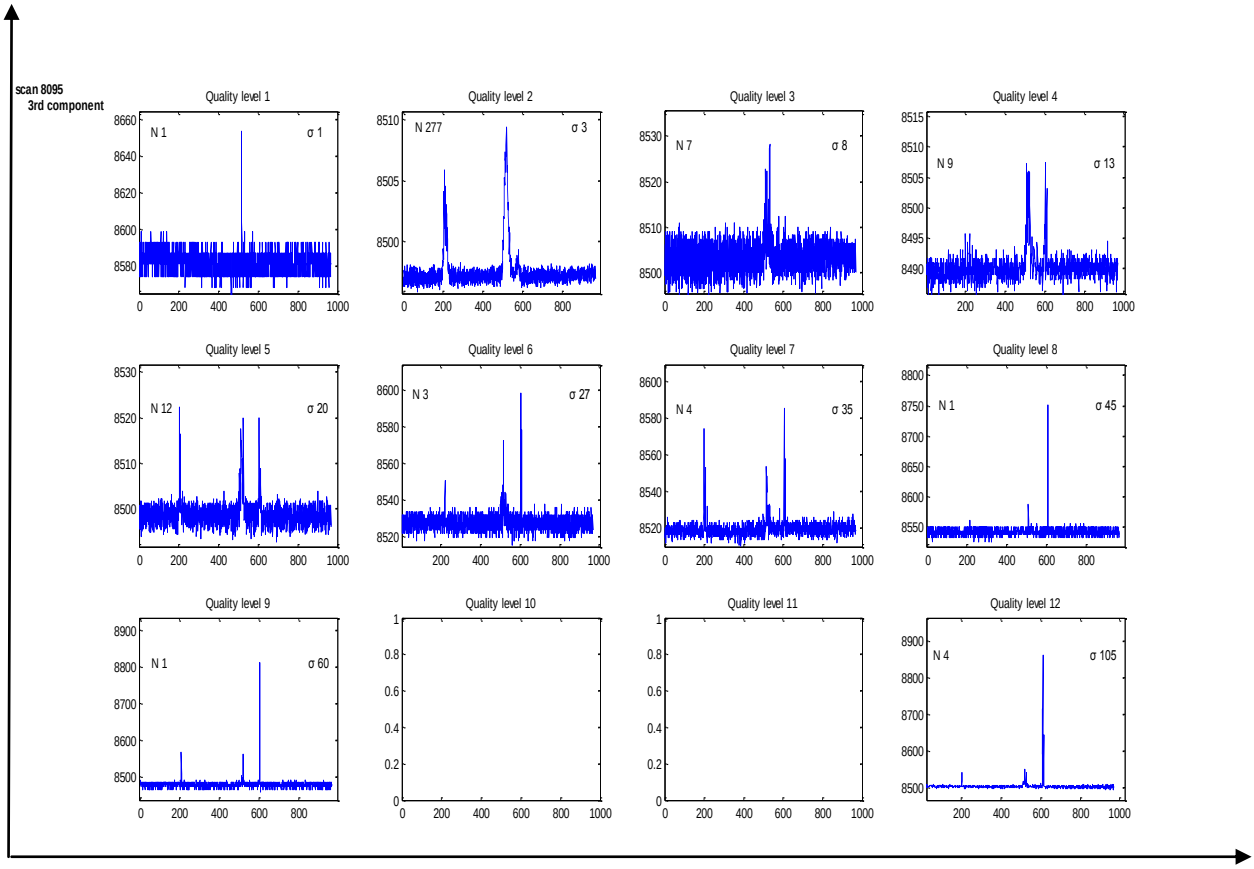

bin

V/f counts

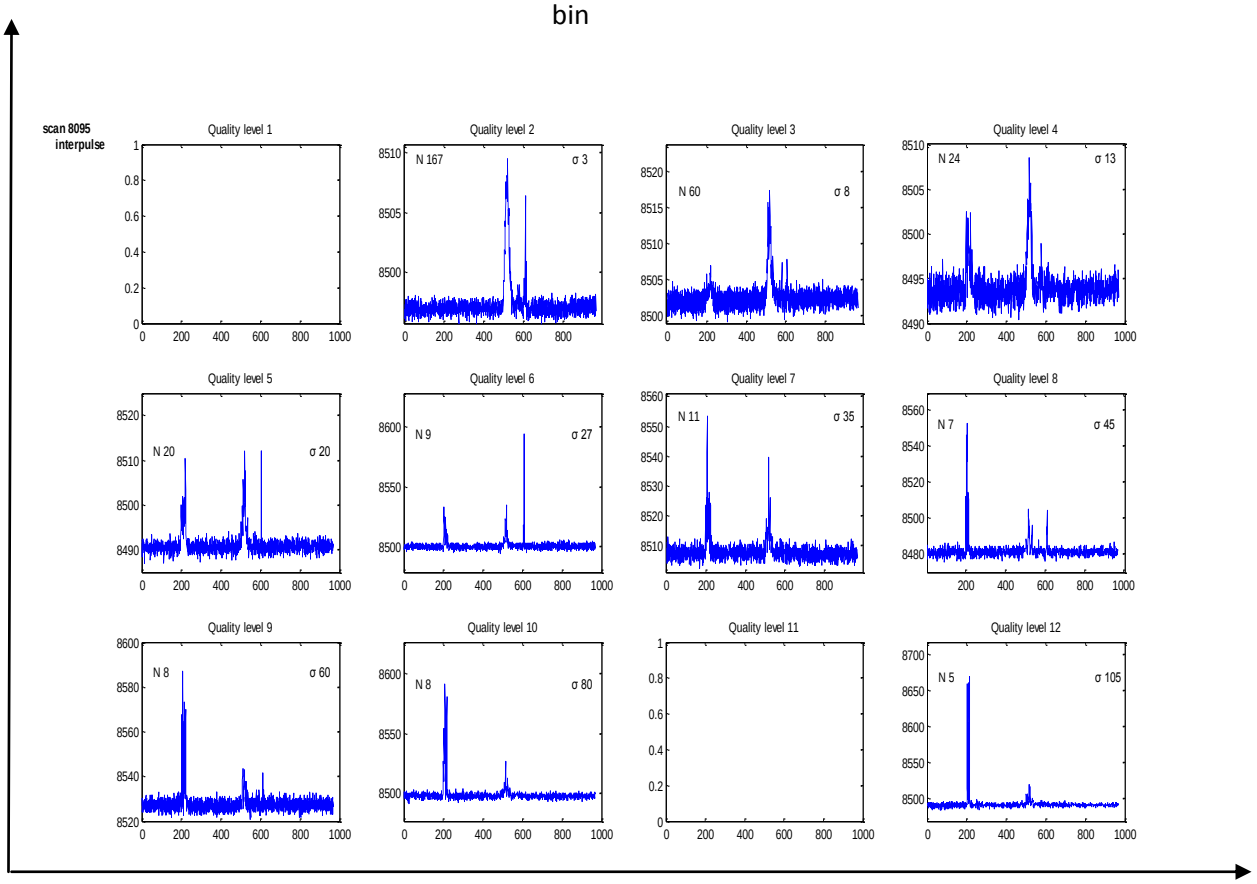

bin

V/f counts

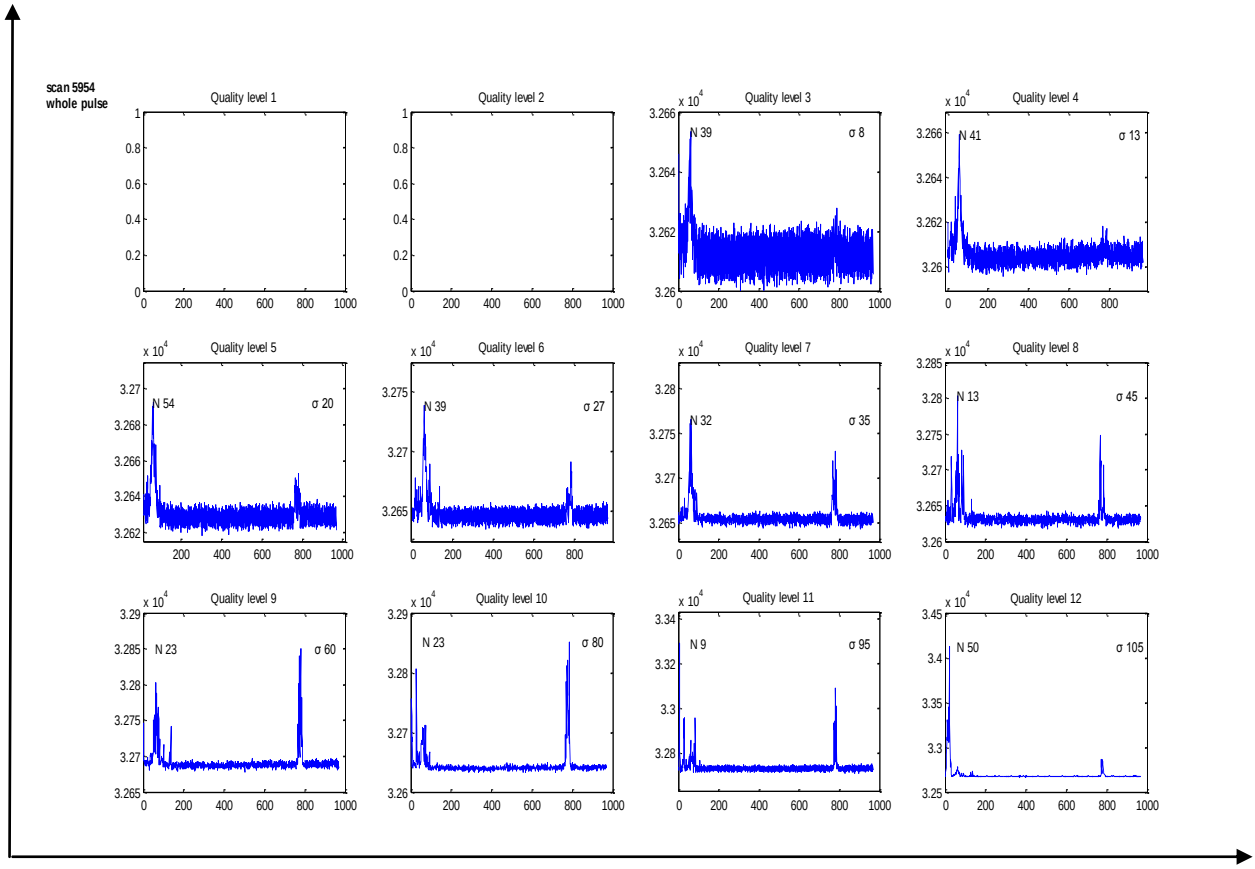

bin

V/f counts

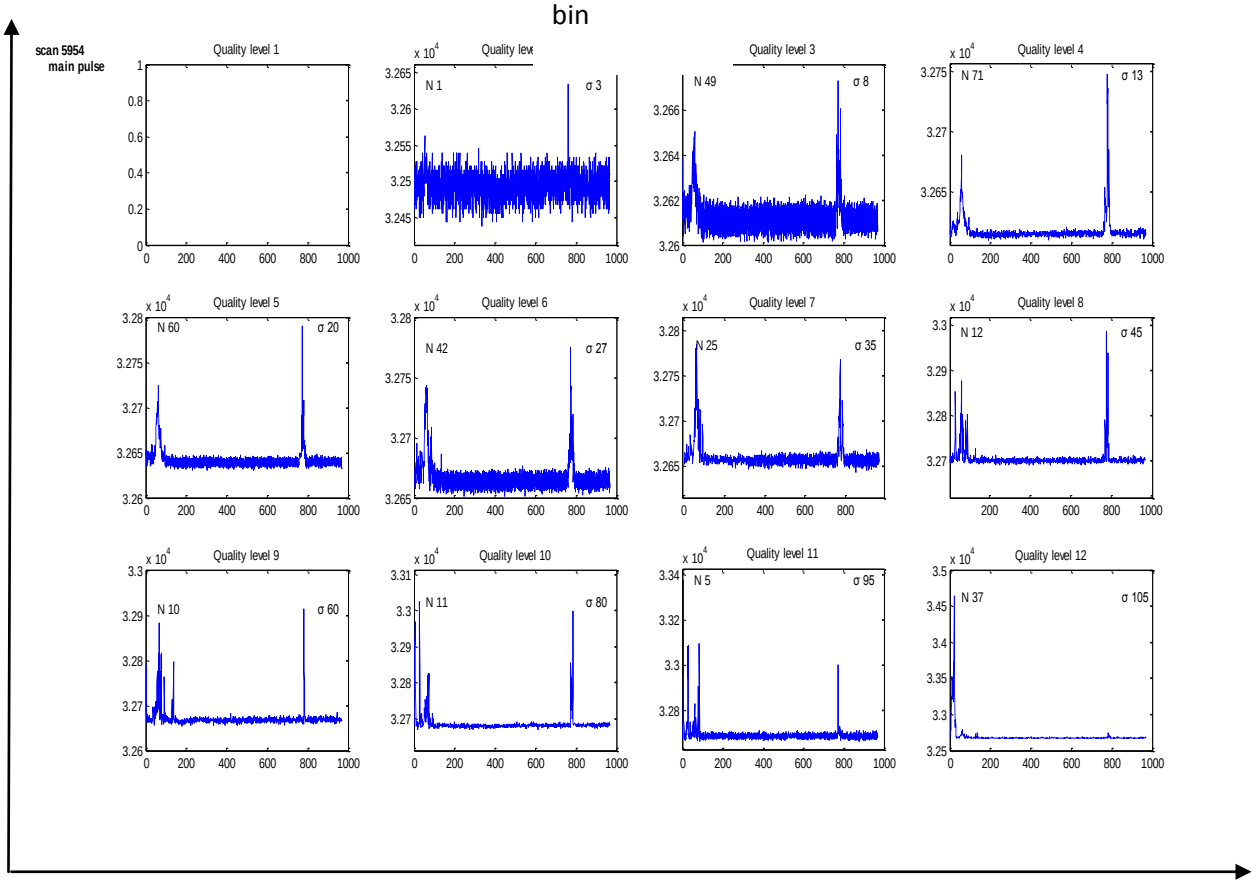

bin

V/f counts

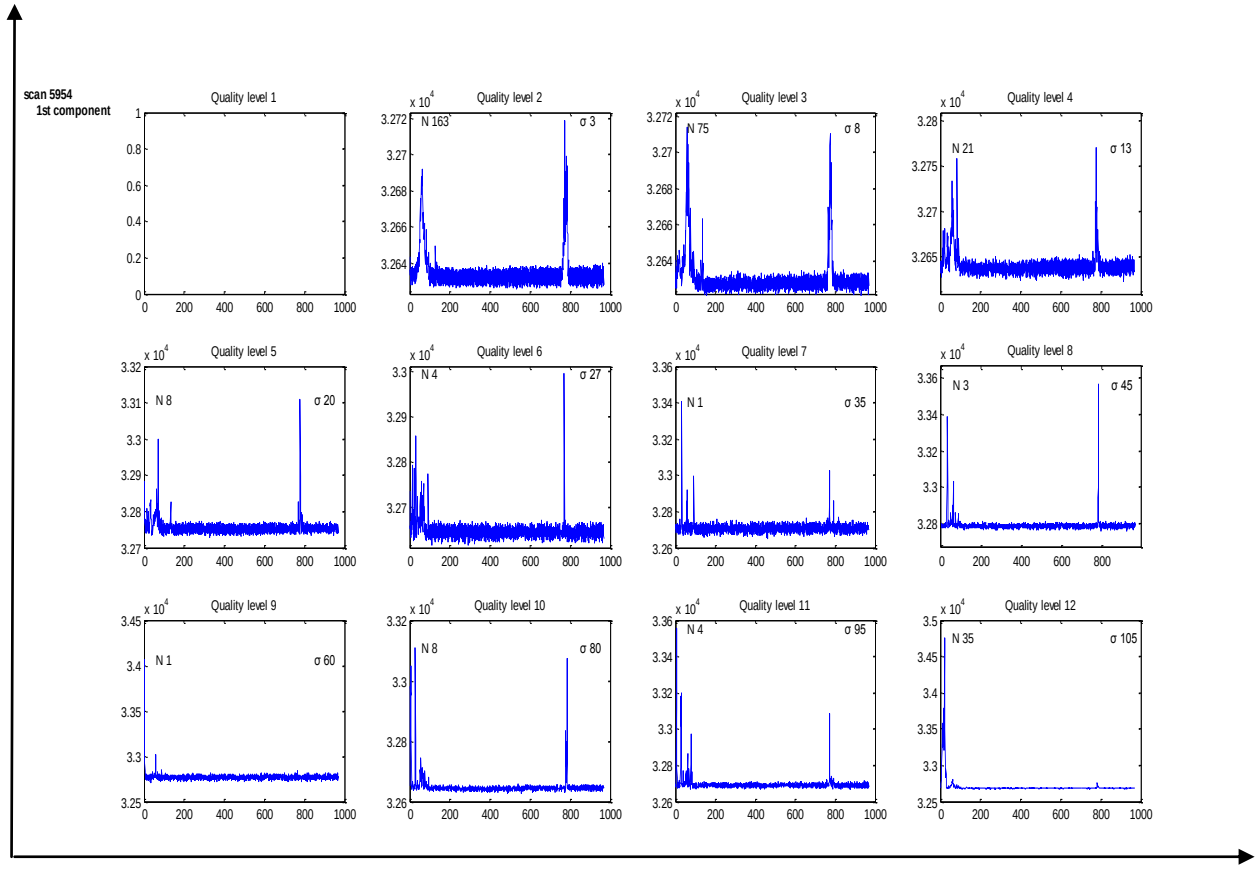

bin

V/f counts

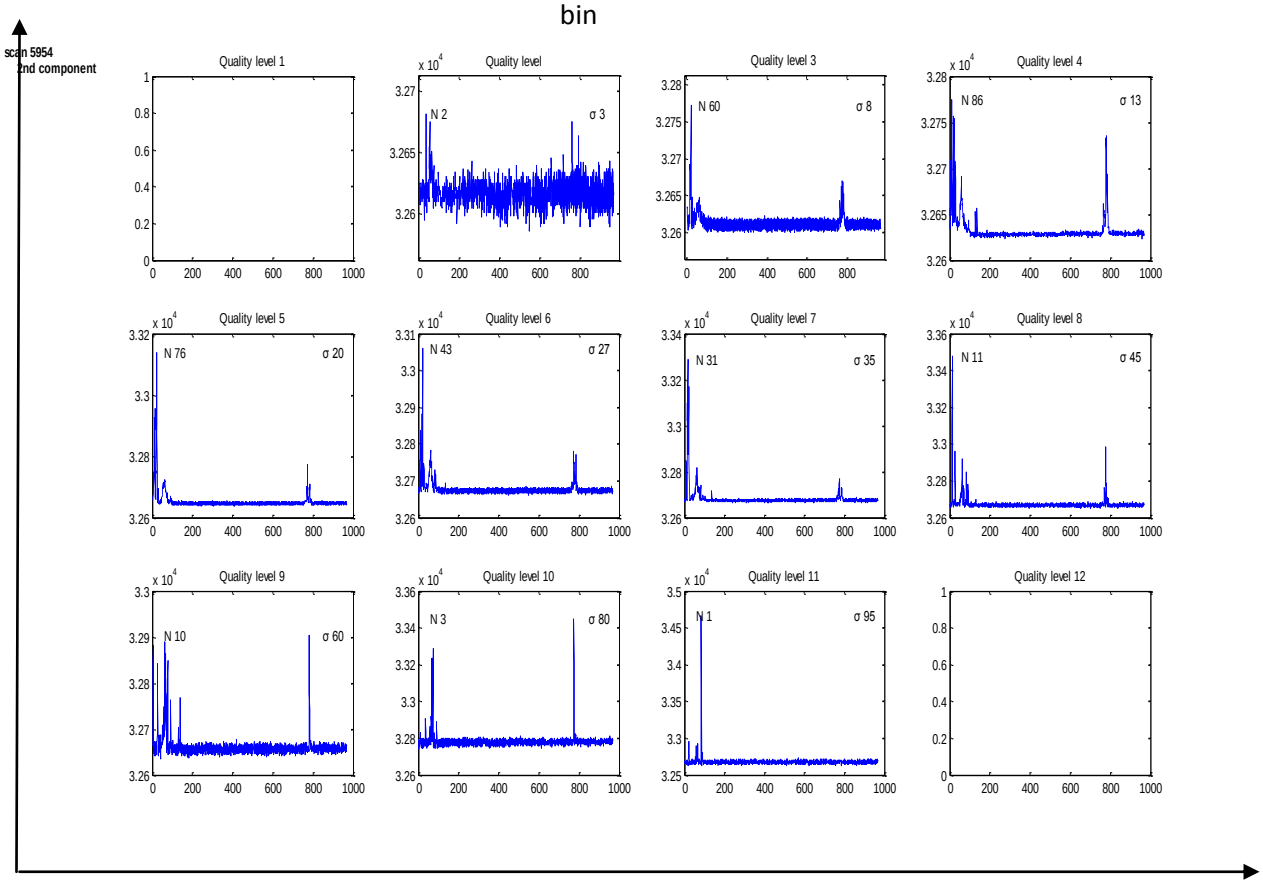

bin

V/f counts

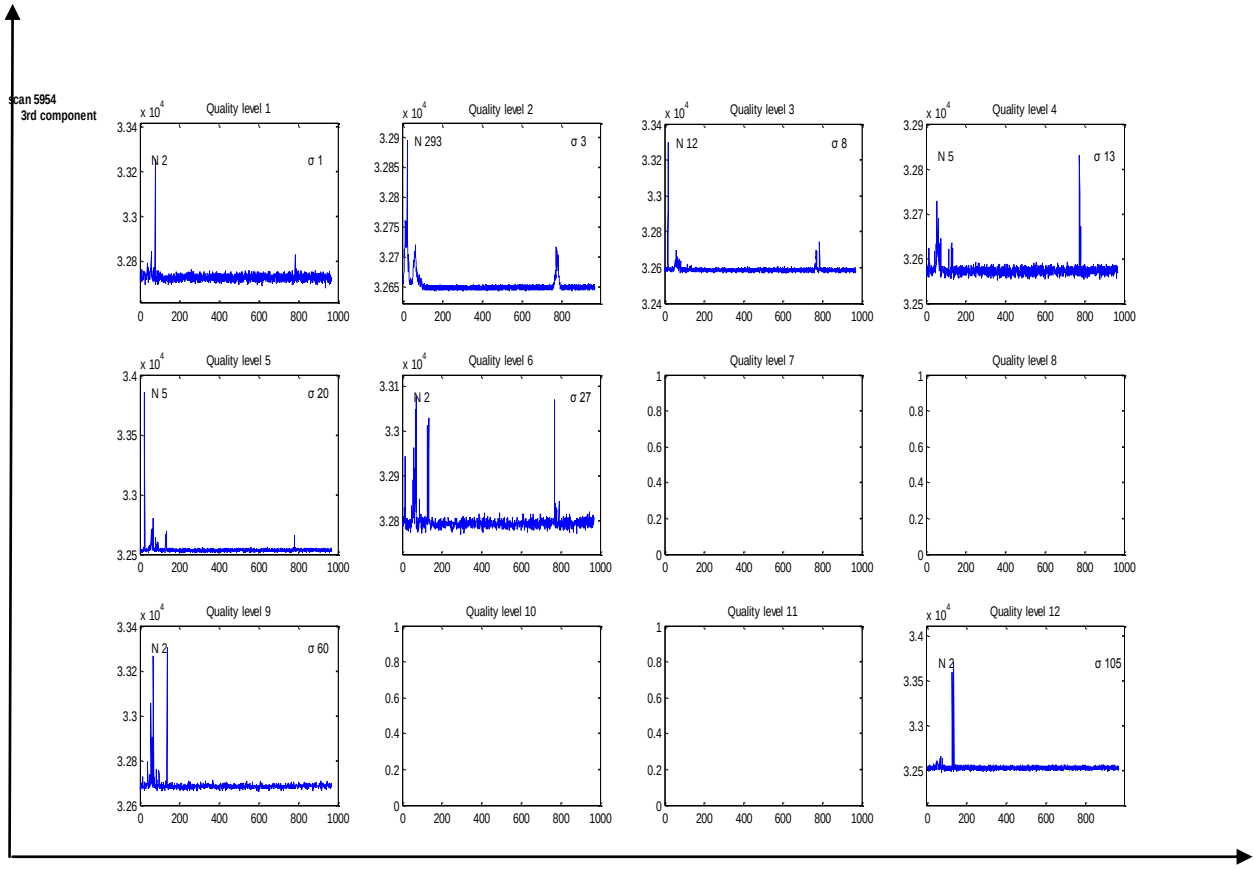

bin

V/f counts

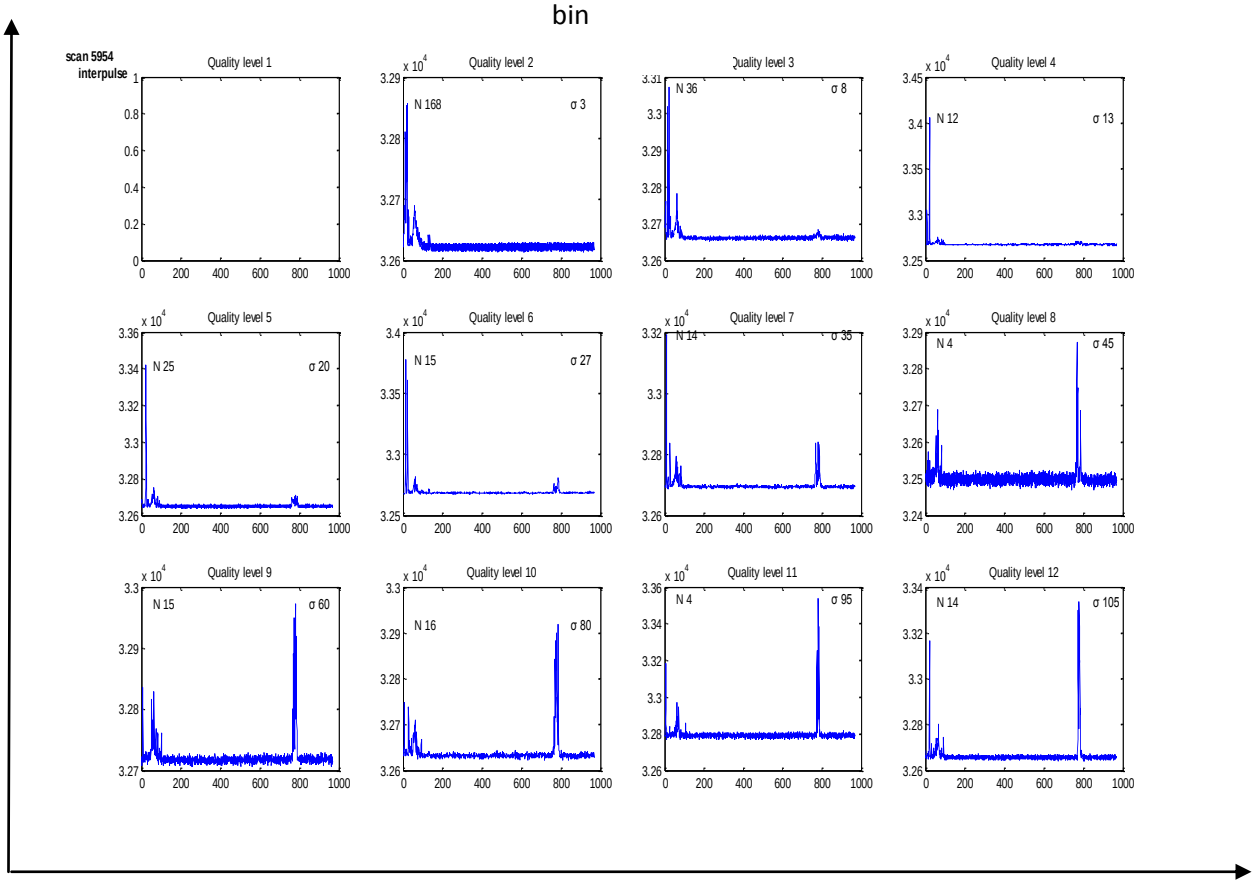

bin

V/f counts

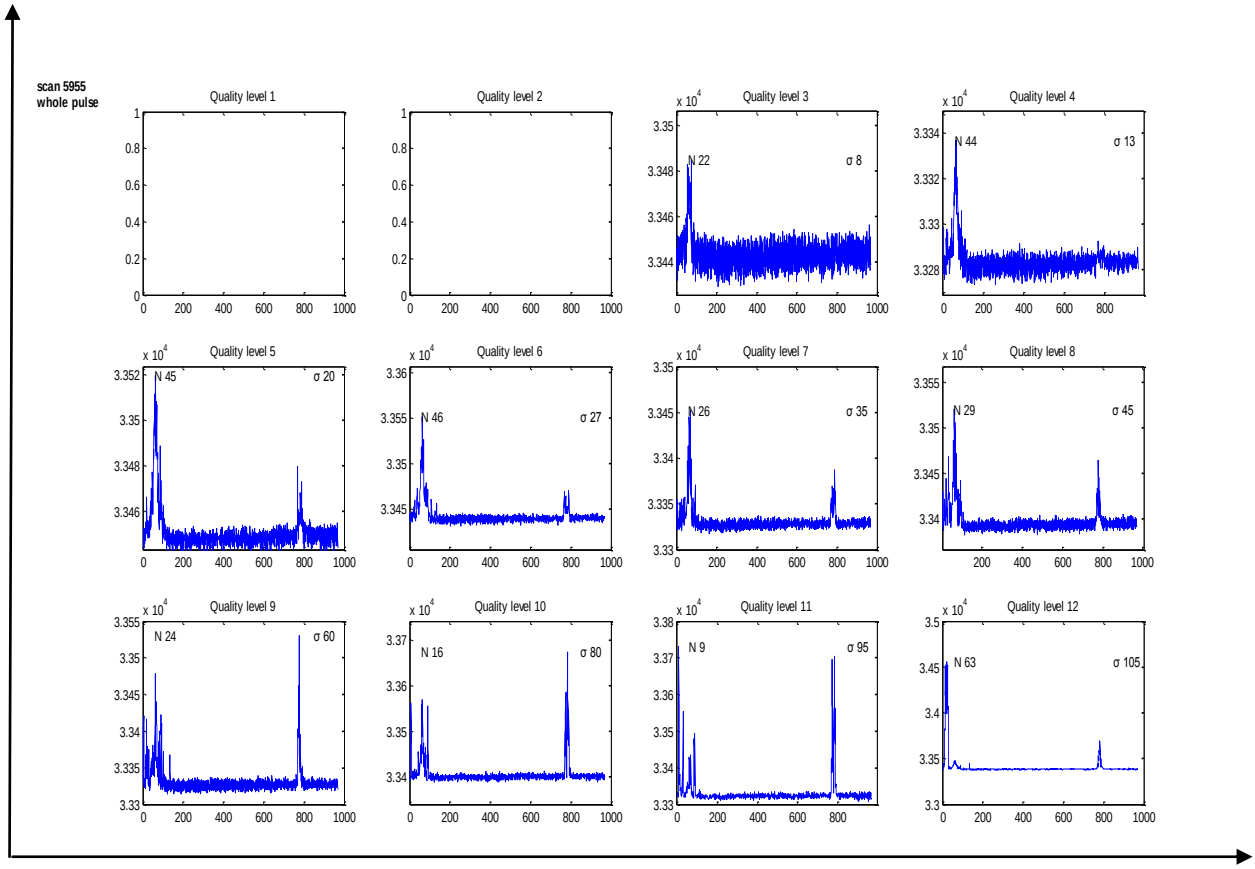

bin

V/f counts

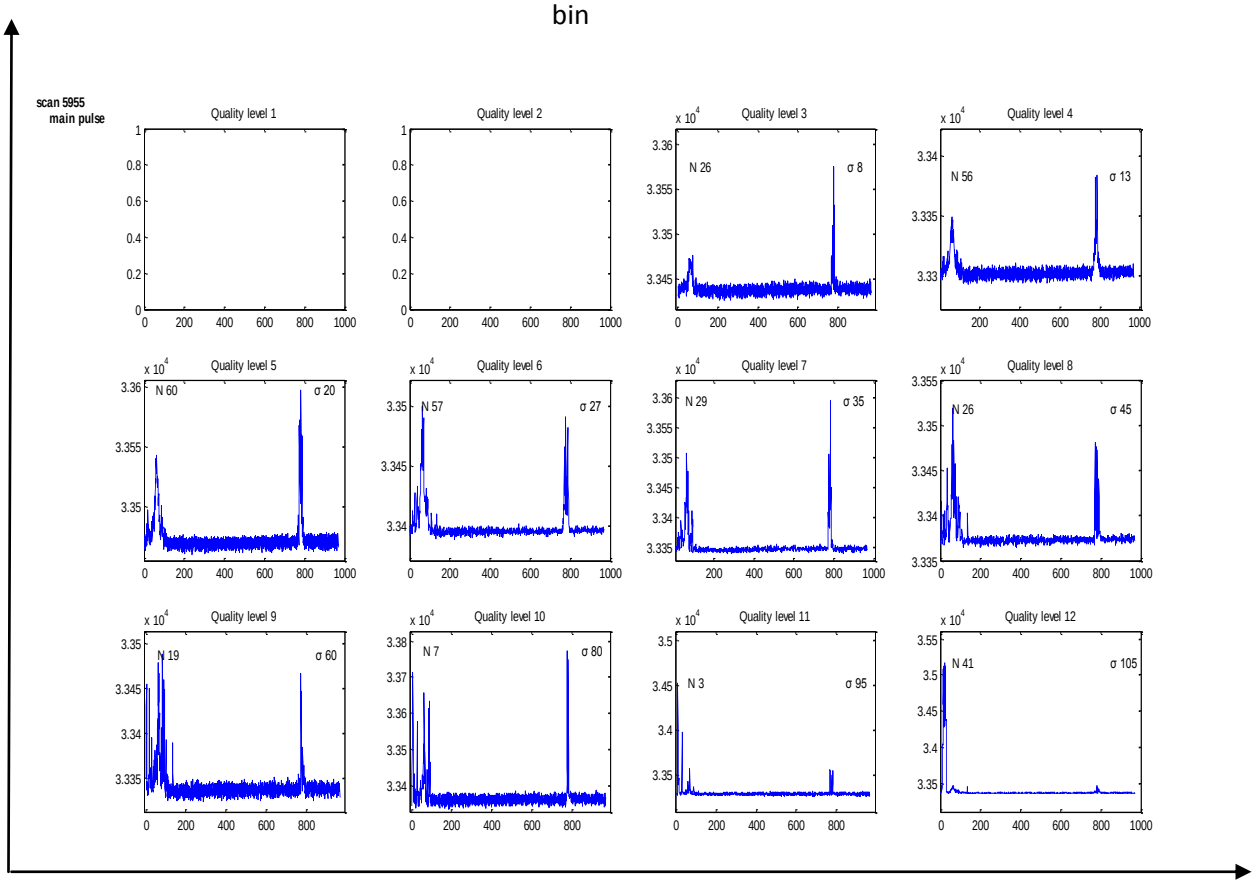

bin

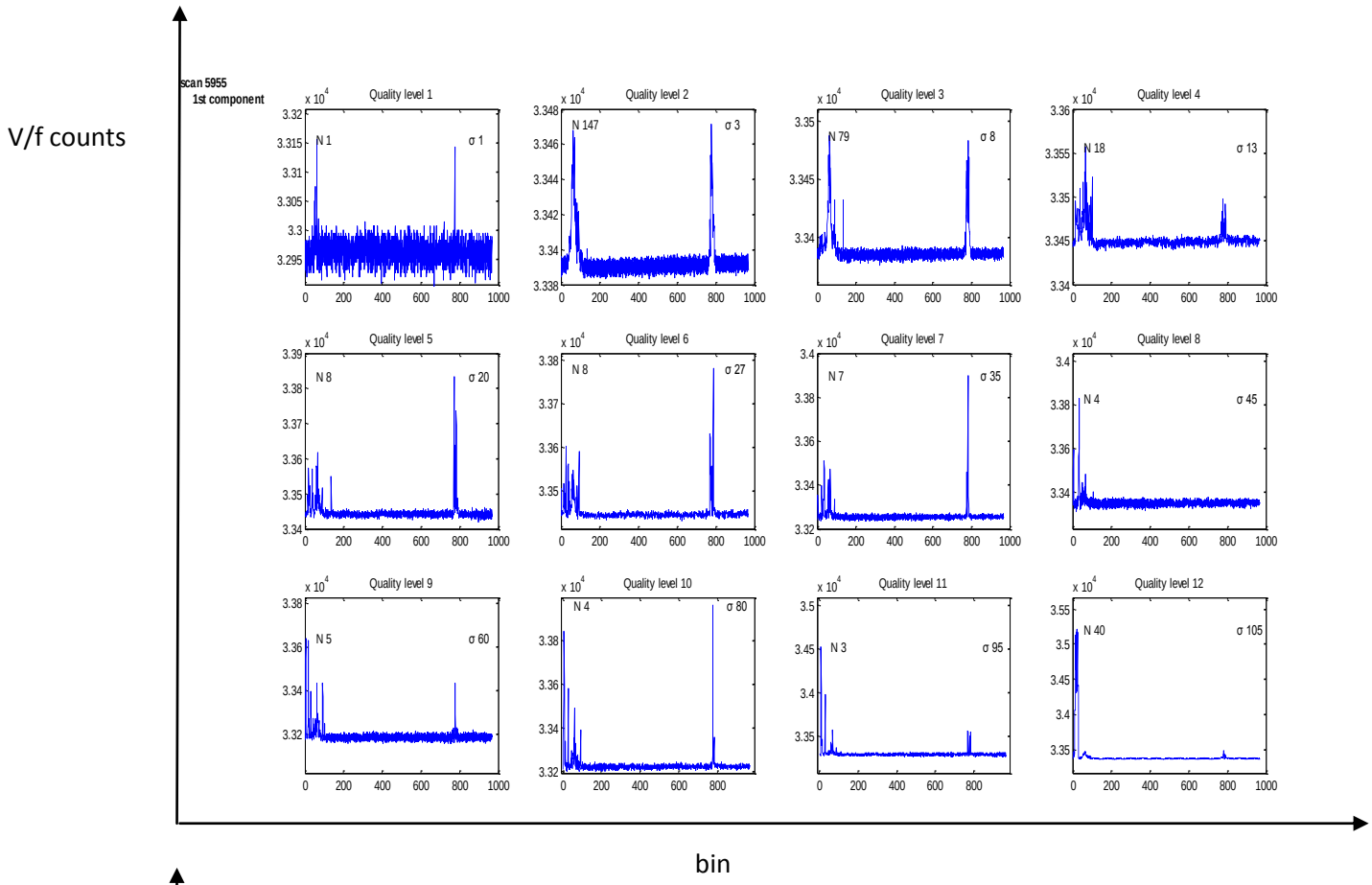
V/f counts
scan 5955
1st component
Quality level 1
N 1
σ 1
Quality level 2
N 147
σ 3
Quality level 3
N 79
σ 8
Quality level 4
N 18
σ 13
Quality level 5
N 8
σ 20
Quality level 6
N 8
σ 27
Quality level 7
N 7
σ 35
Quality level 8
N 4
σ 45
Quality level 9
N 5
σ 60
Quality level 10
N 4
σ 80
Quality level 11
N 3
σ 95
Quality level 12
N 40
σ 105
bin

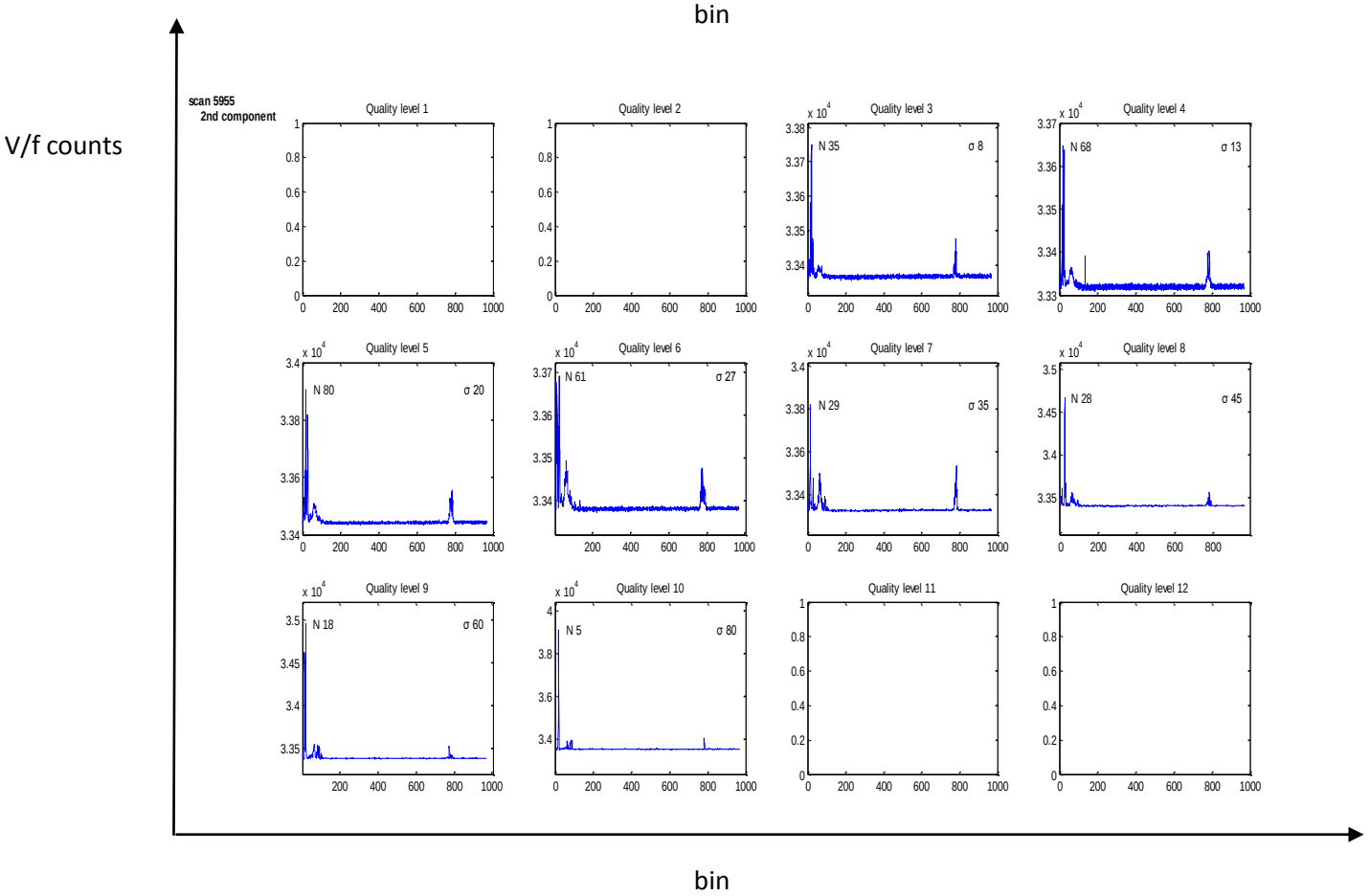
V/f counts
scan 5955
2nd component
Quality level 1
Quality level 2
Quality level 3
N 35
σ 8
Quality level 4
N 68
σ 13
Quality level 5
N 80
σ 20
Quality level 6
N 61
σ 27
Quality level 7
N 29
σ 35
Quality level 8
N 28
σ 45
Quality level 9
N 18
σ 60
Quality level 10
N 5
σ 80
Quality level 11
Quality level 12
bin

V/f counts

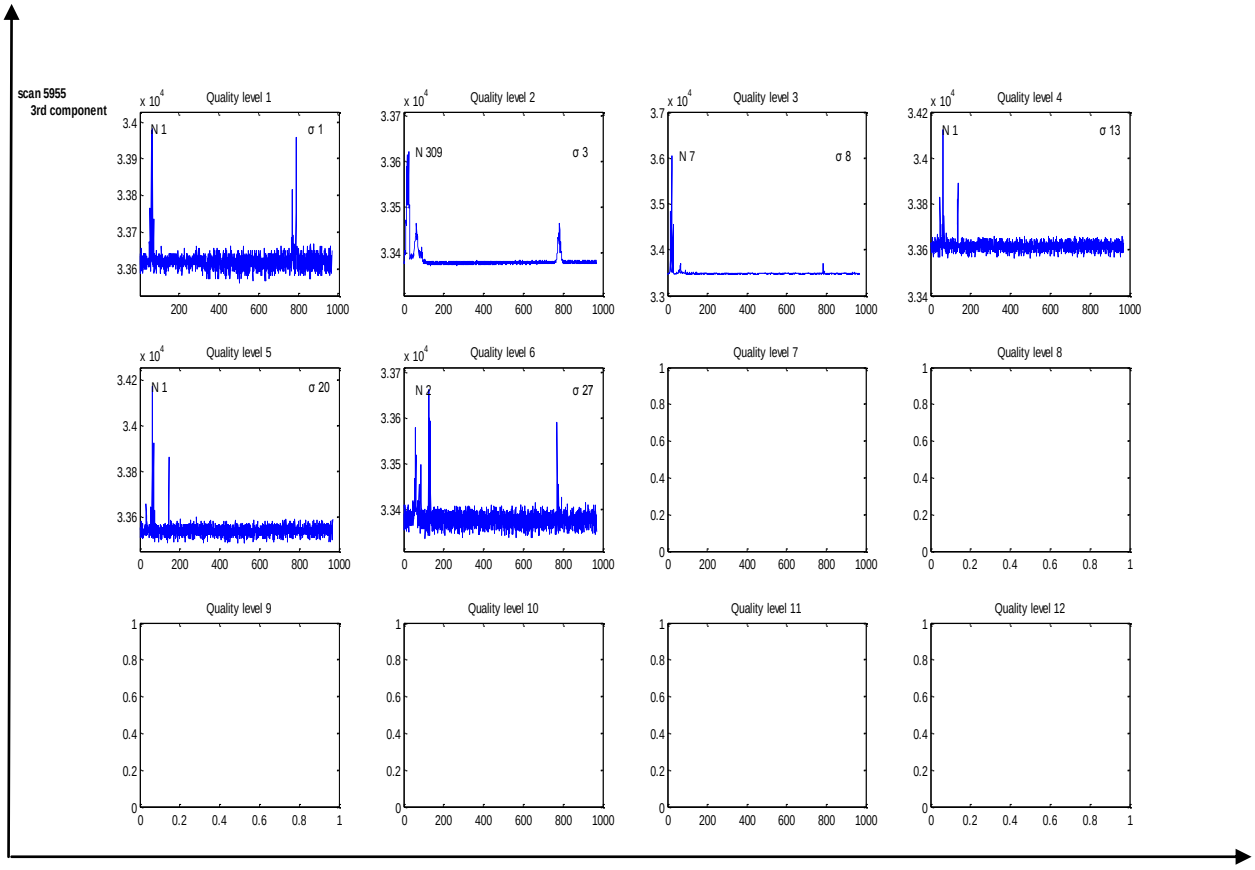

bin

V/f counts

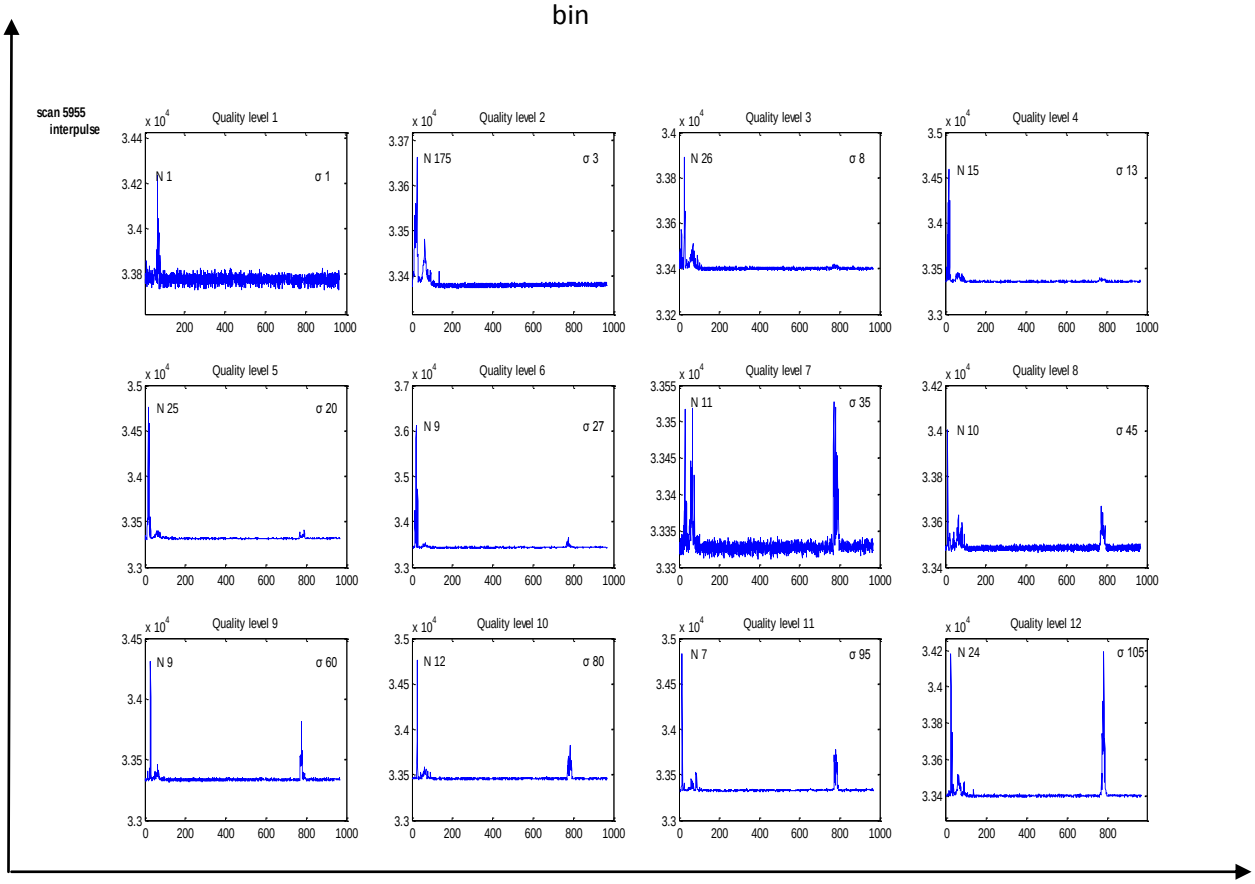

bin

V/f counts

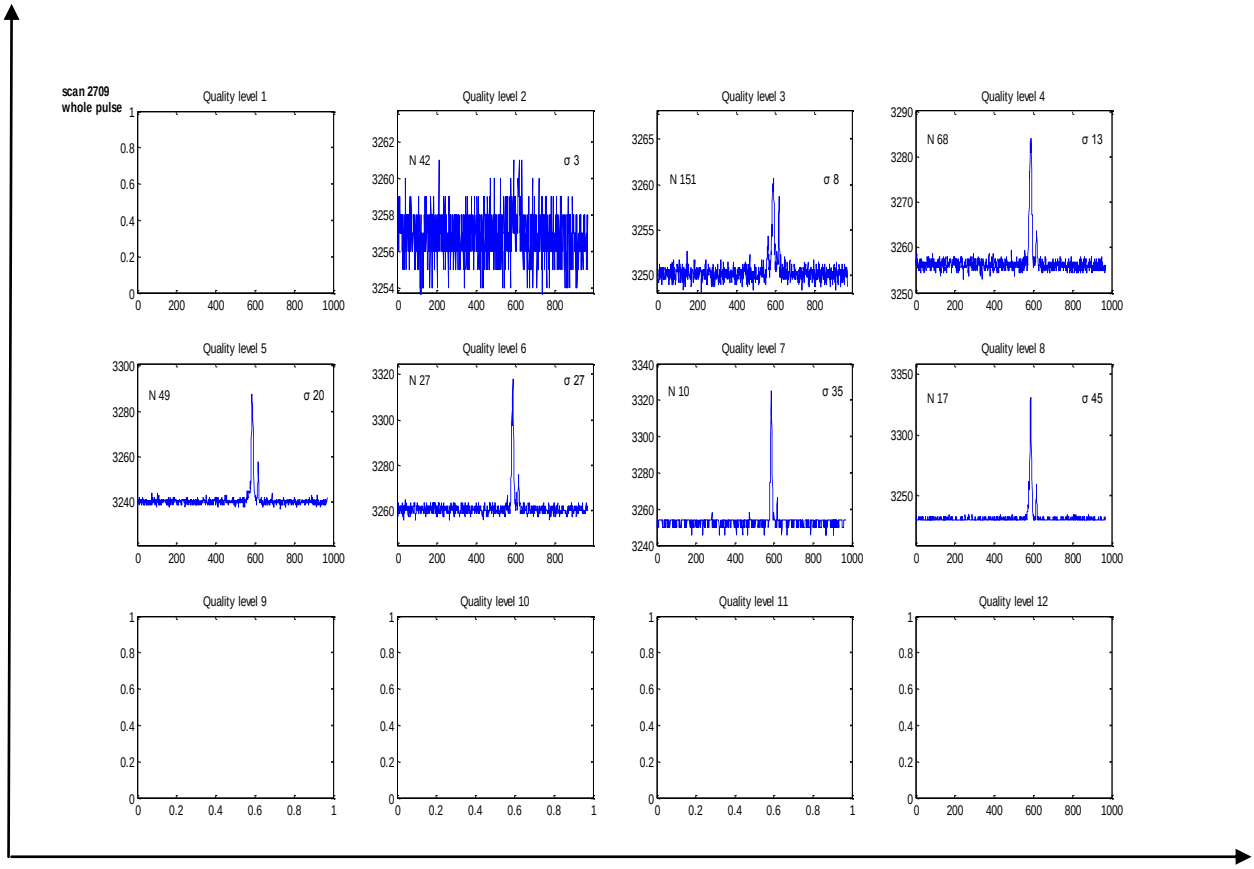

bin

V/f counts

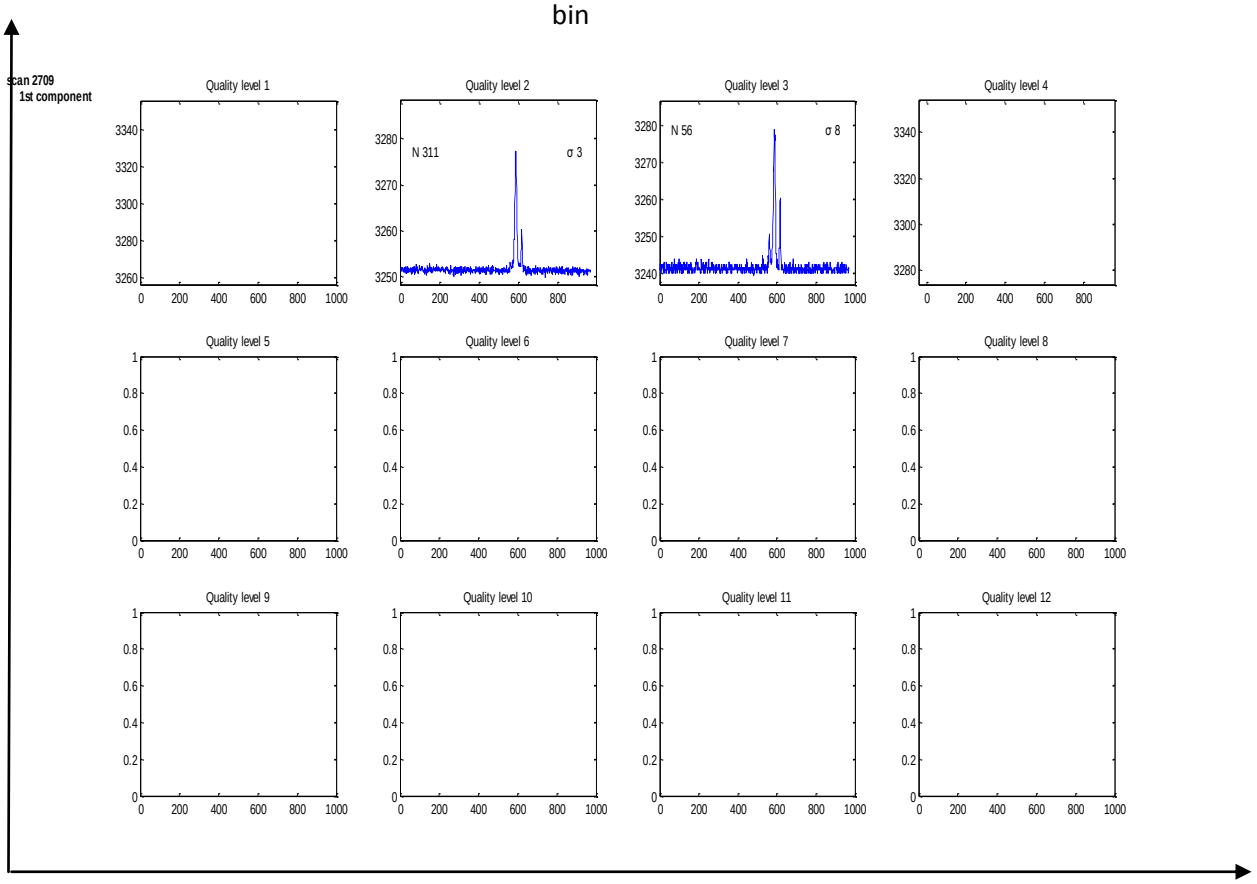

bin

V/f counts

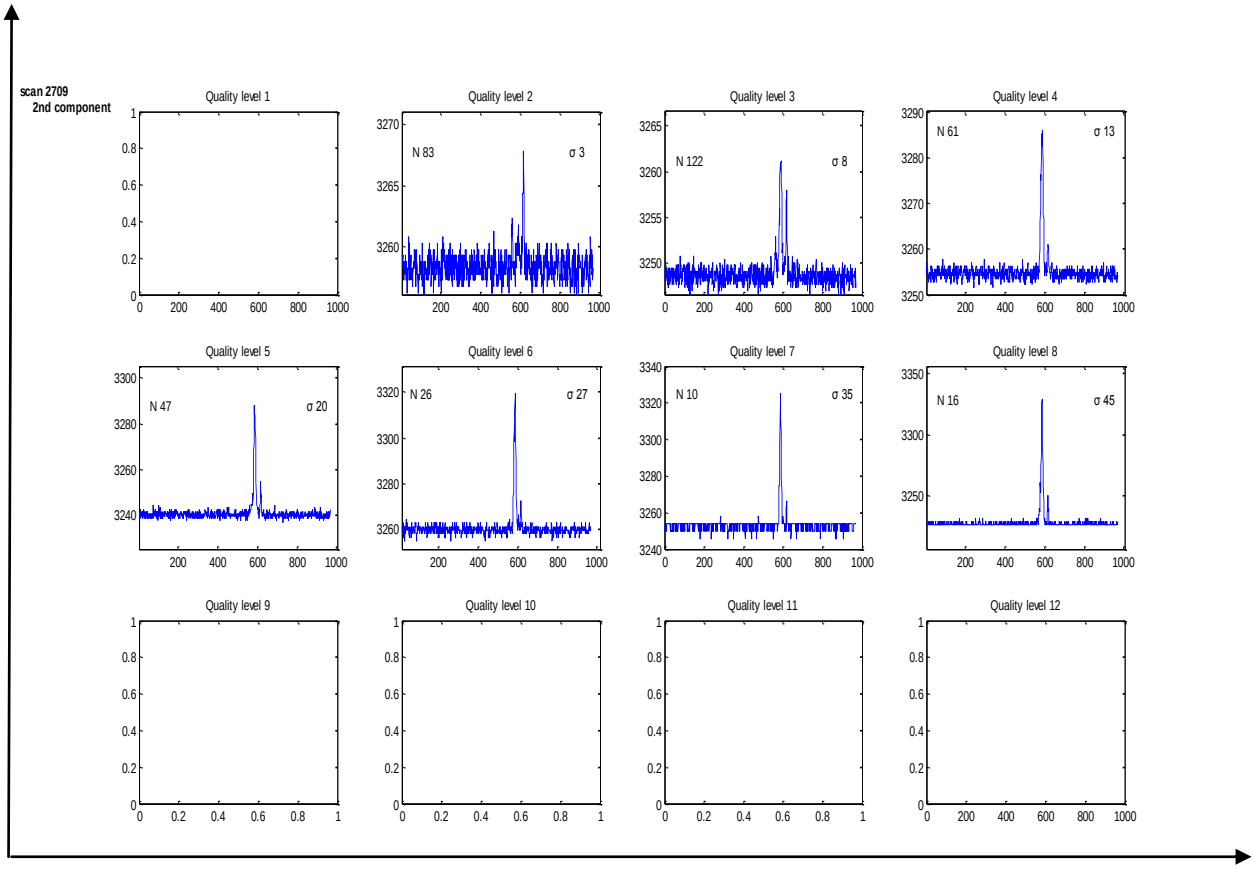

bin

V/f counts

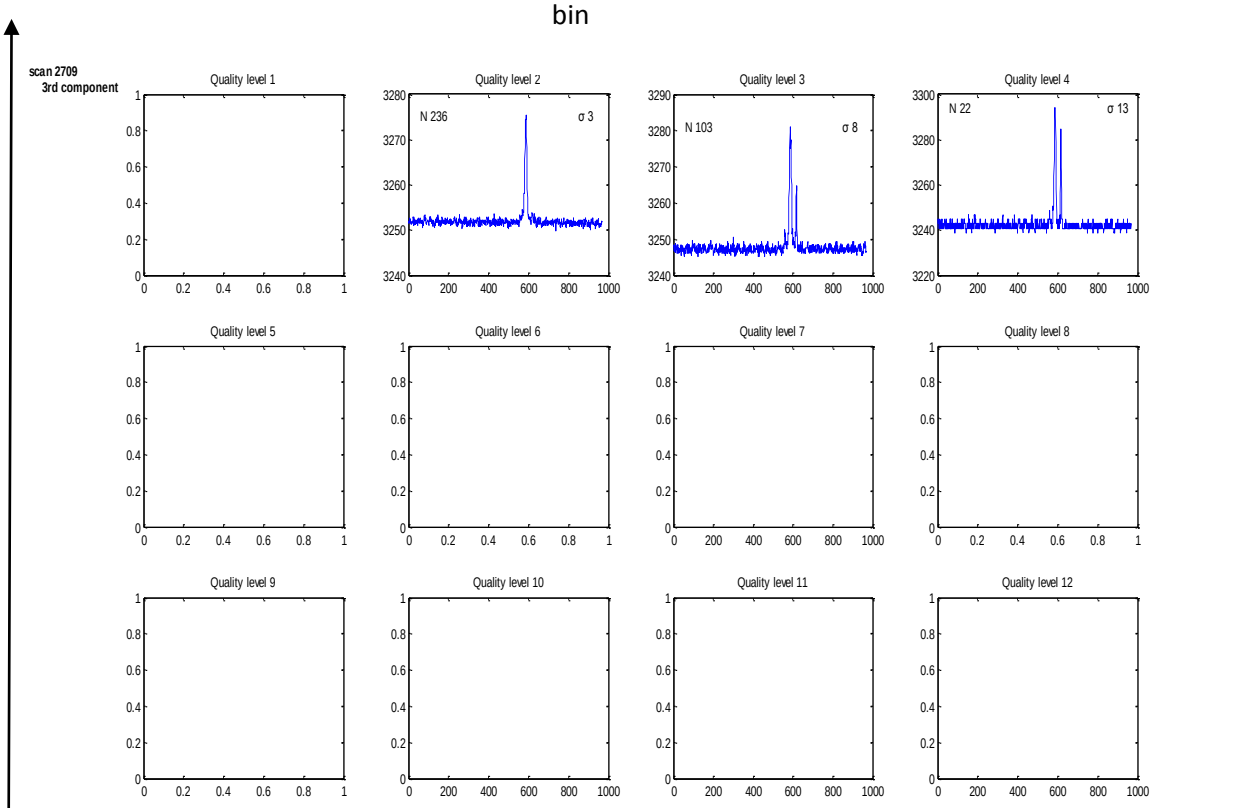

bin

V/f counts

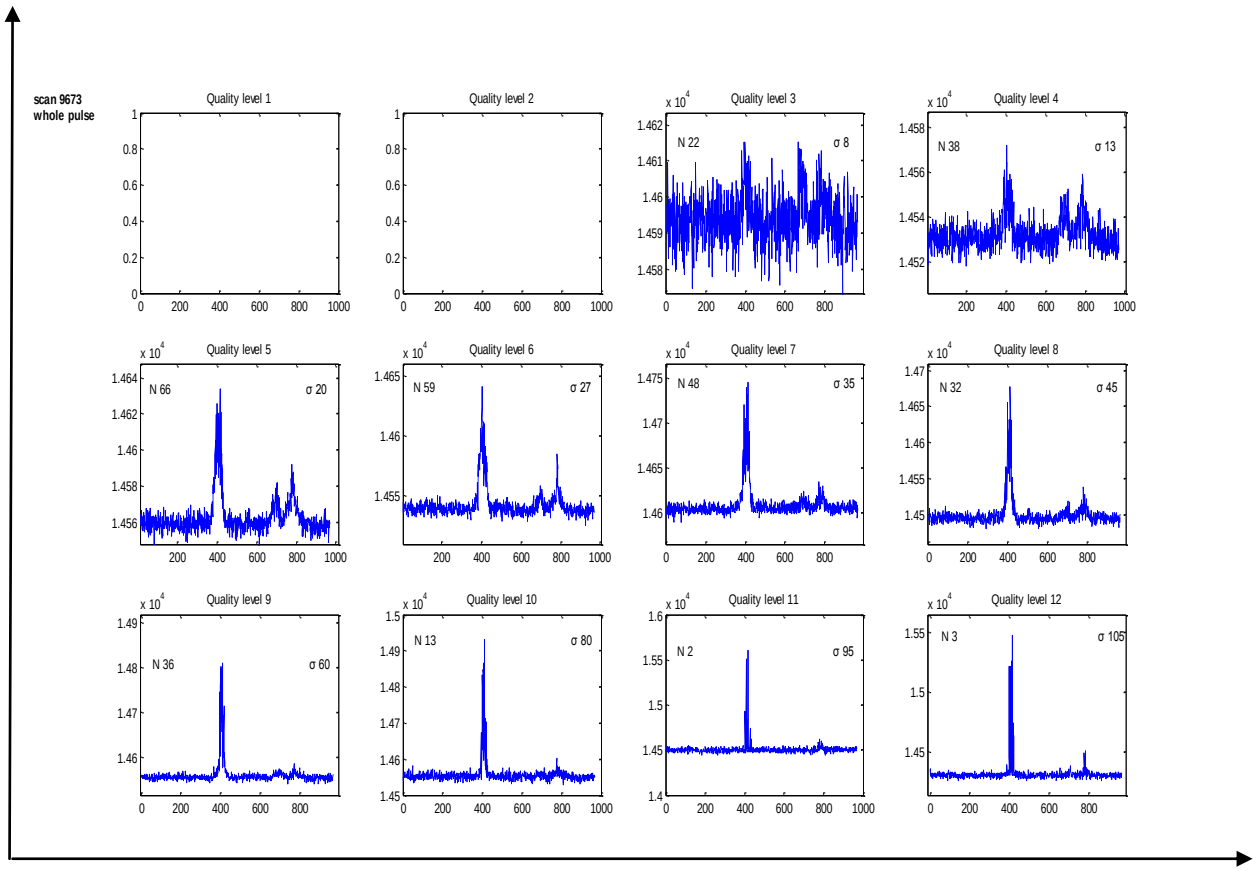

bin

V/f counts

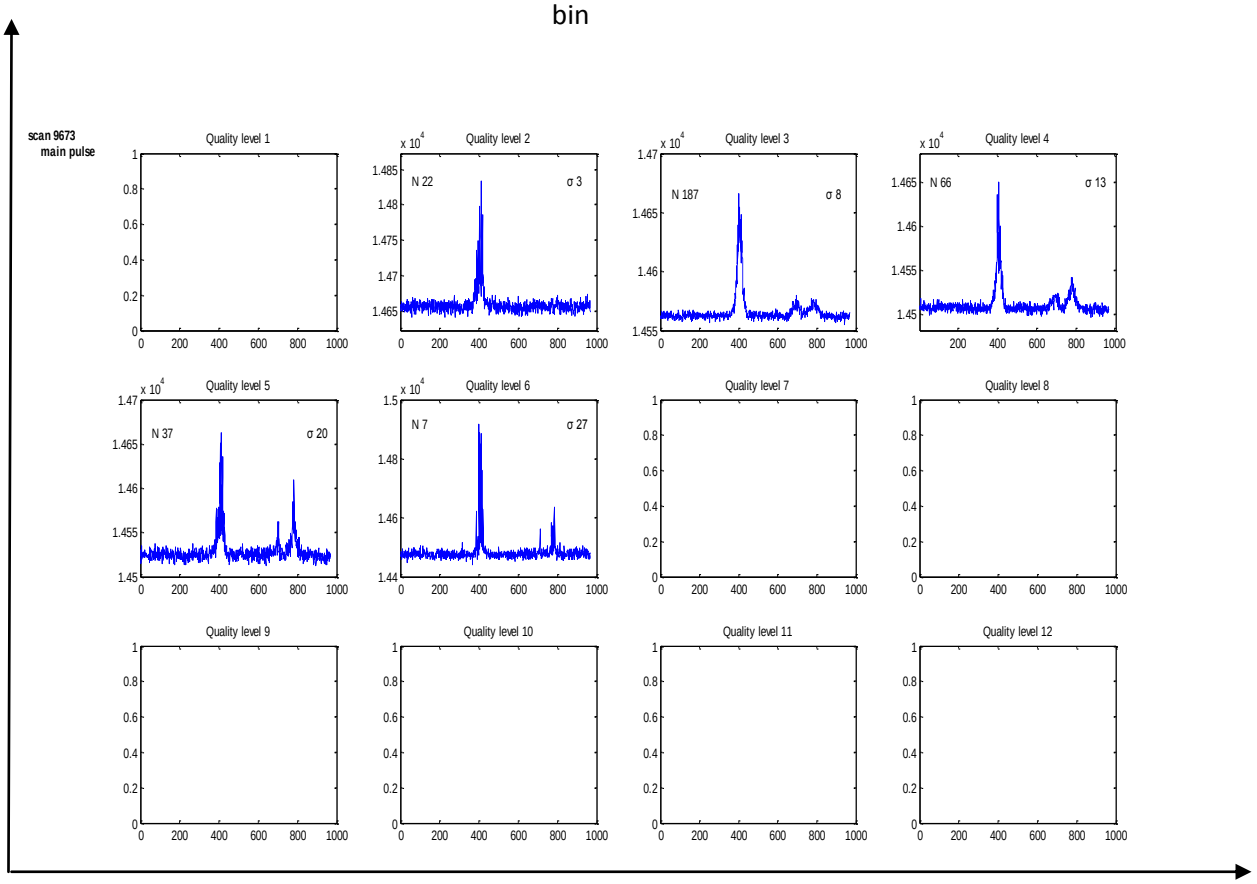

bin

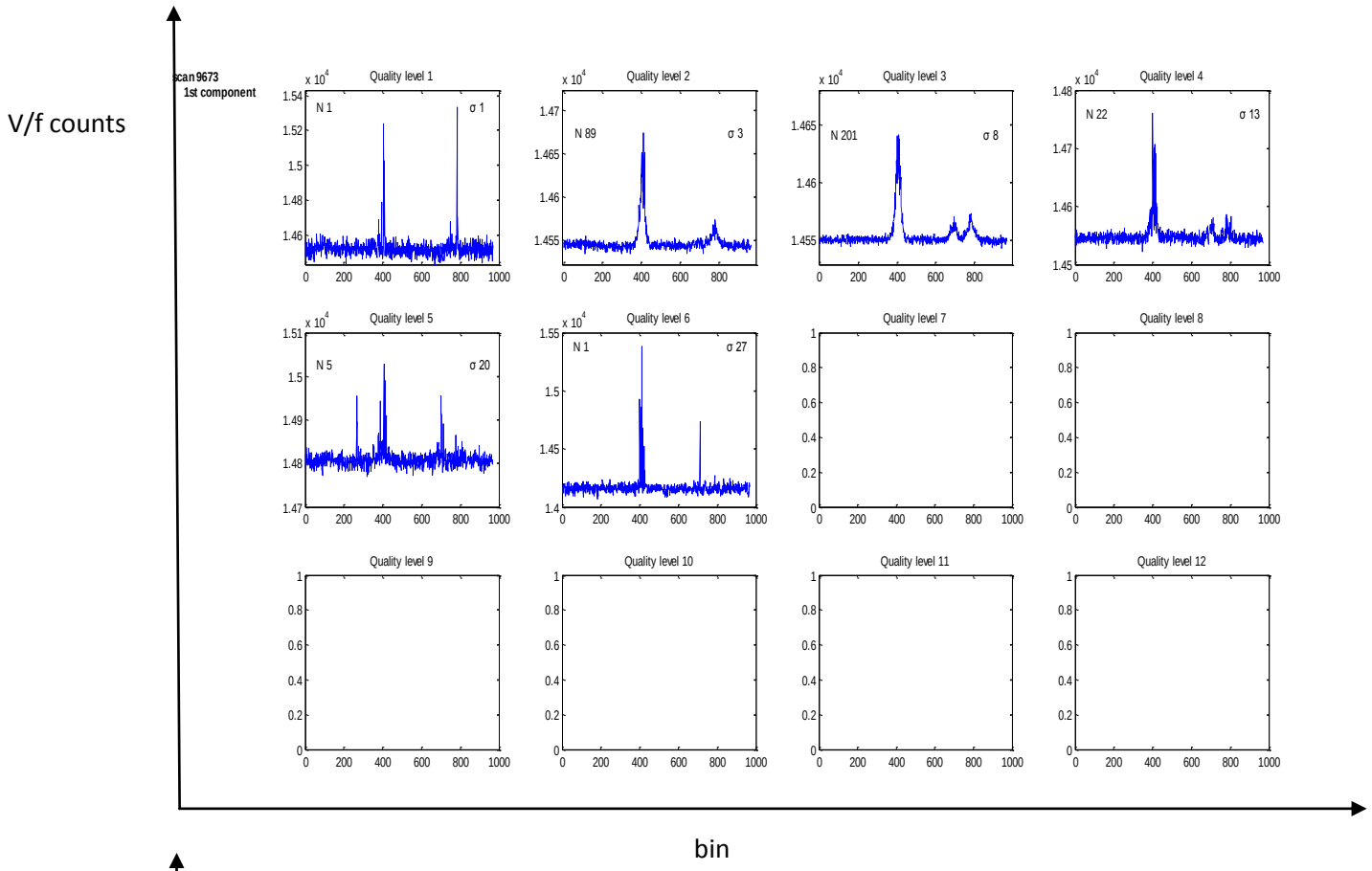
V/f counts
scan 9673
1st component
Quality level 1
N 1
σ 1
Quality level 2
N 89
σ 3
Quality level 3
N 201
σ 8
Quality level 4
N 22
σ 13
Quality level 5
N 5
σ 20
Quality level 6
N 1
σ 27
Quality level 7
Quality level 8
Quality level 9
Quality level 10
Quality level 11
Quality level 12
bin

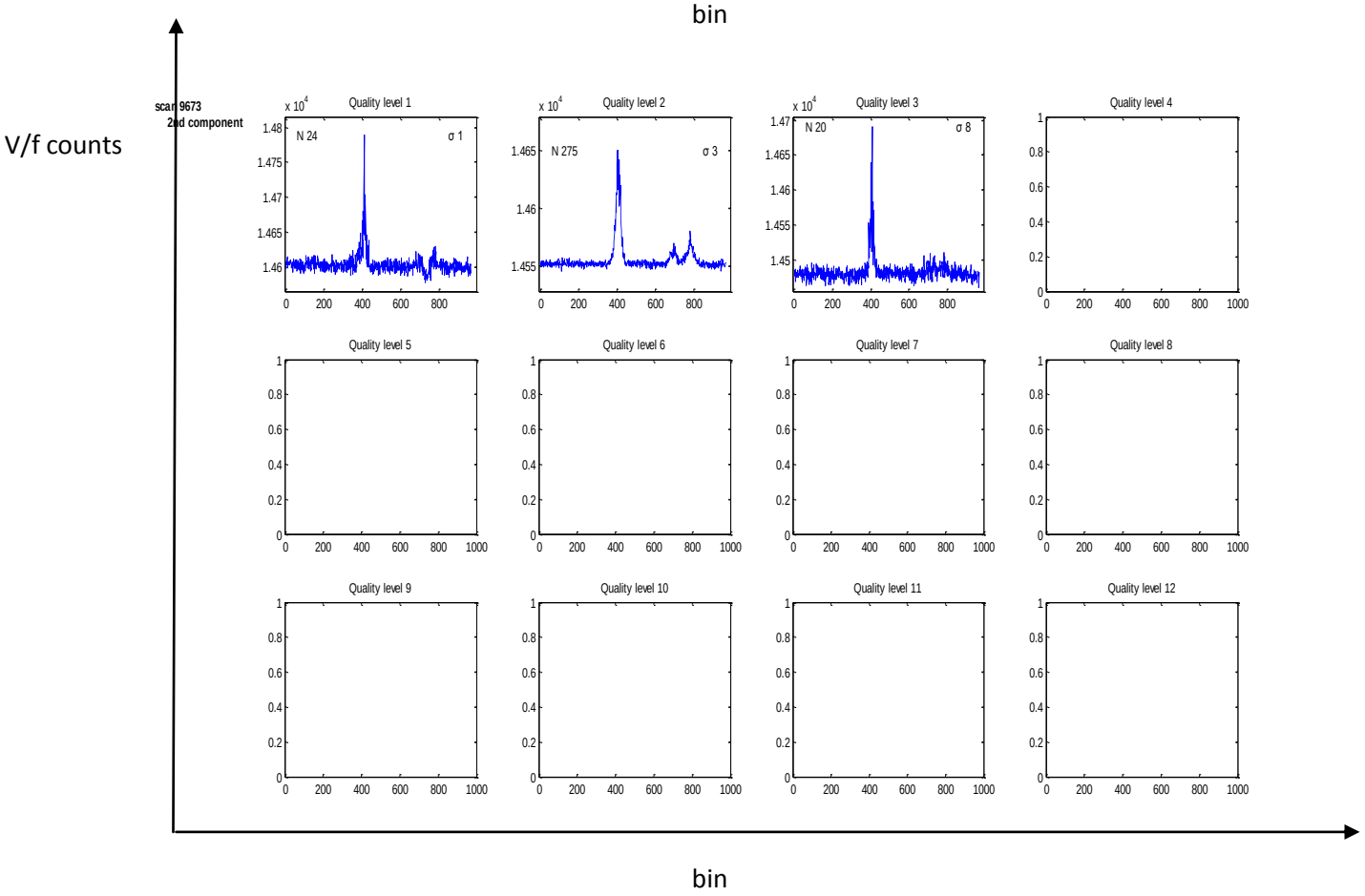
V/f counts
scan 9673
2nd component
Quality level 1
N 24
σ 1
Quality level 2
N 275
σ 3
Quality level 3
N 20
σ 8
Quality level 4
Quality level 5
Quality level 6
Quality level 7
Quality level 8
Quality level 9
Quality level 10
Quality level 11
Quality level 12
bin

V/f counts

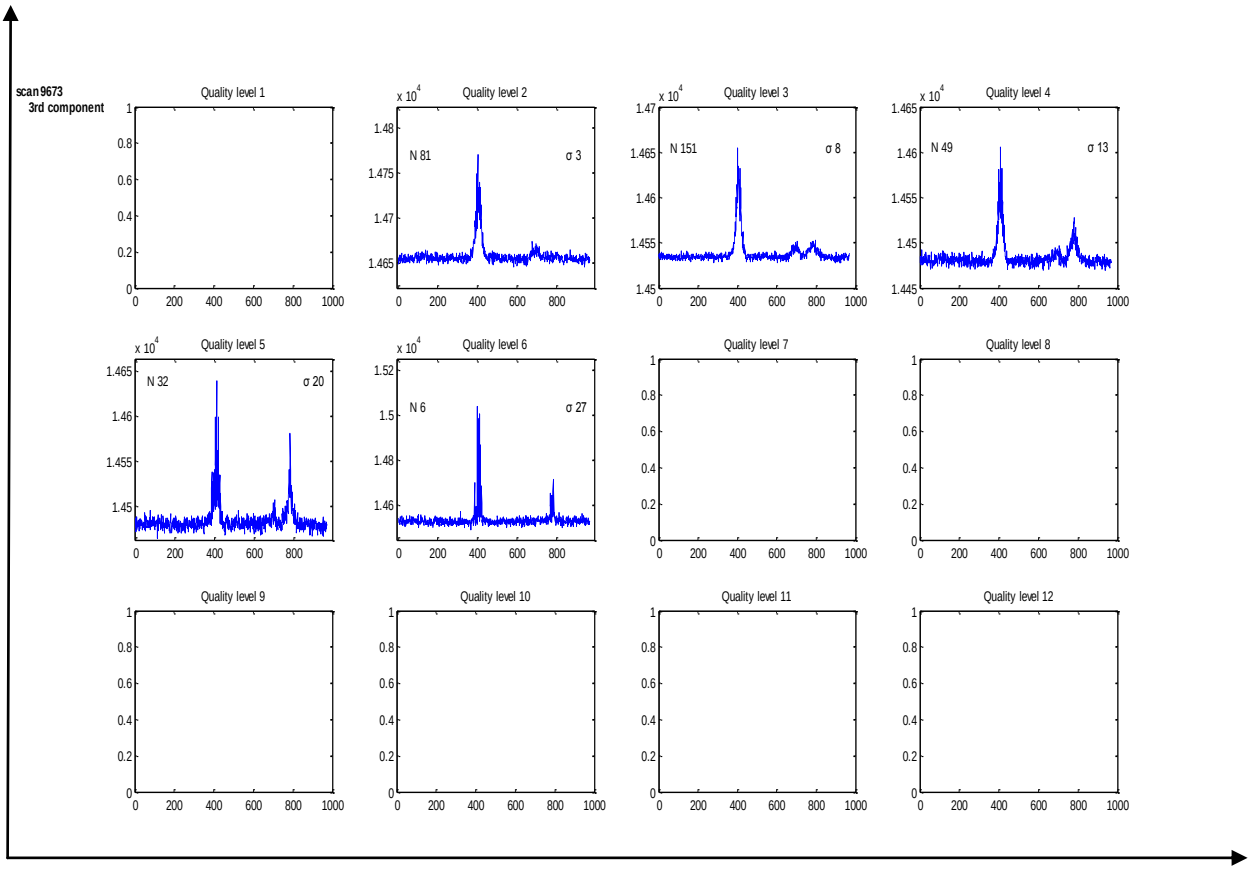

bin

V/f counts

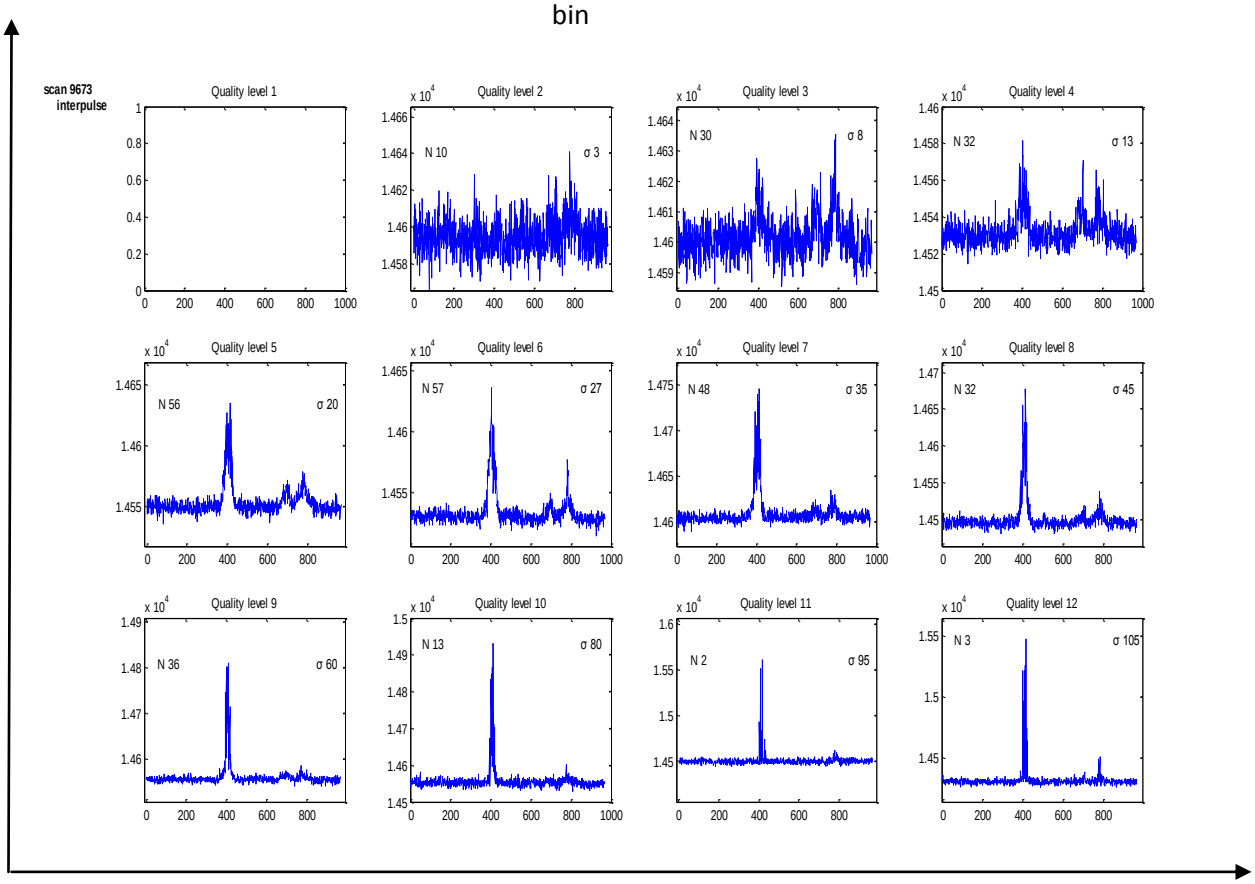

bin

V/f counts

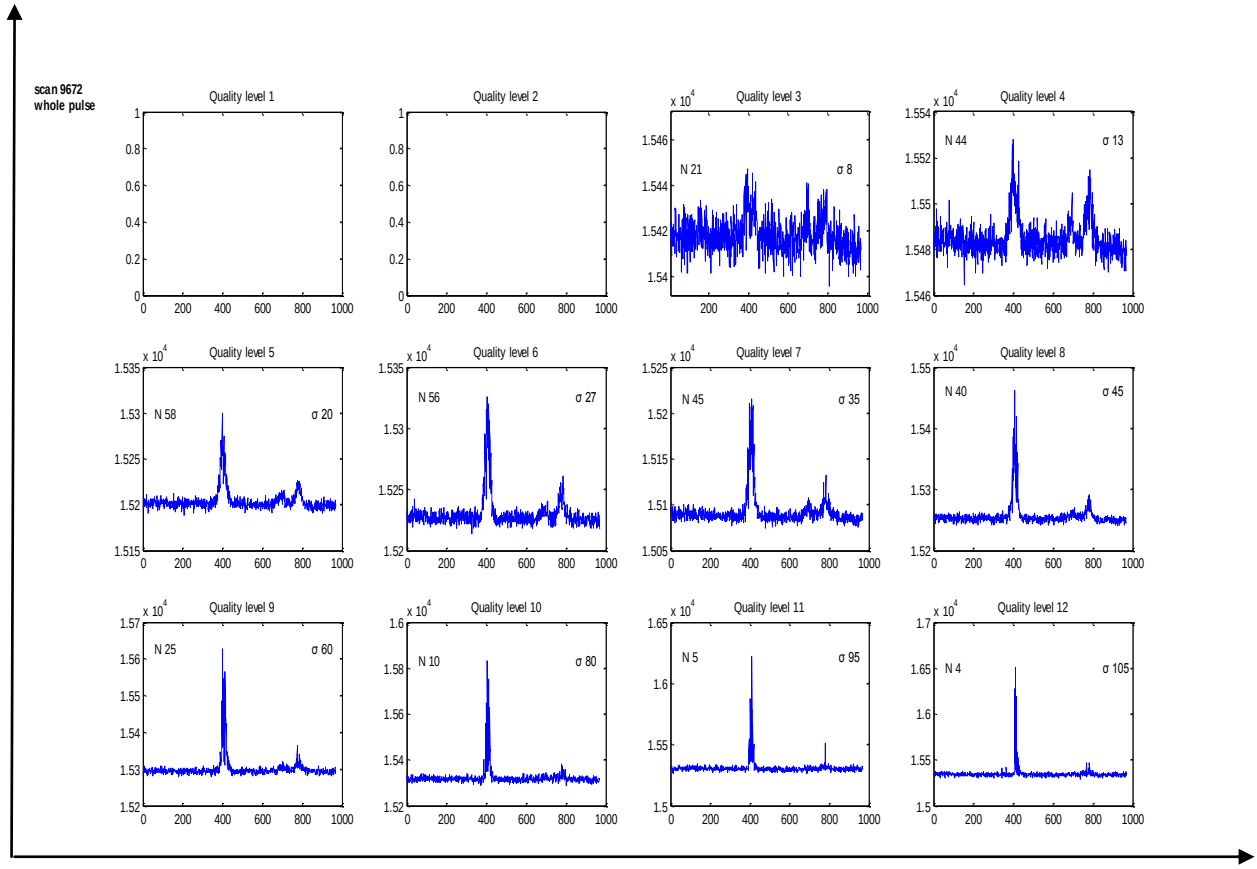

bin

V/f counts

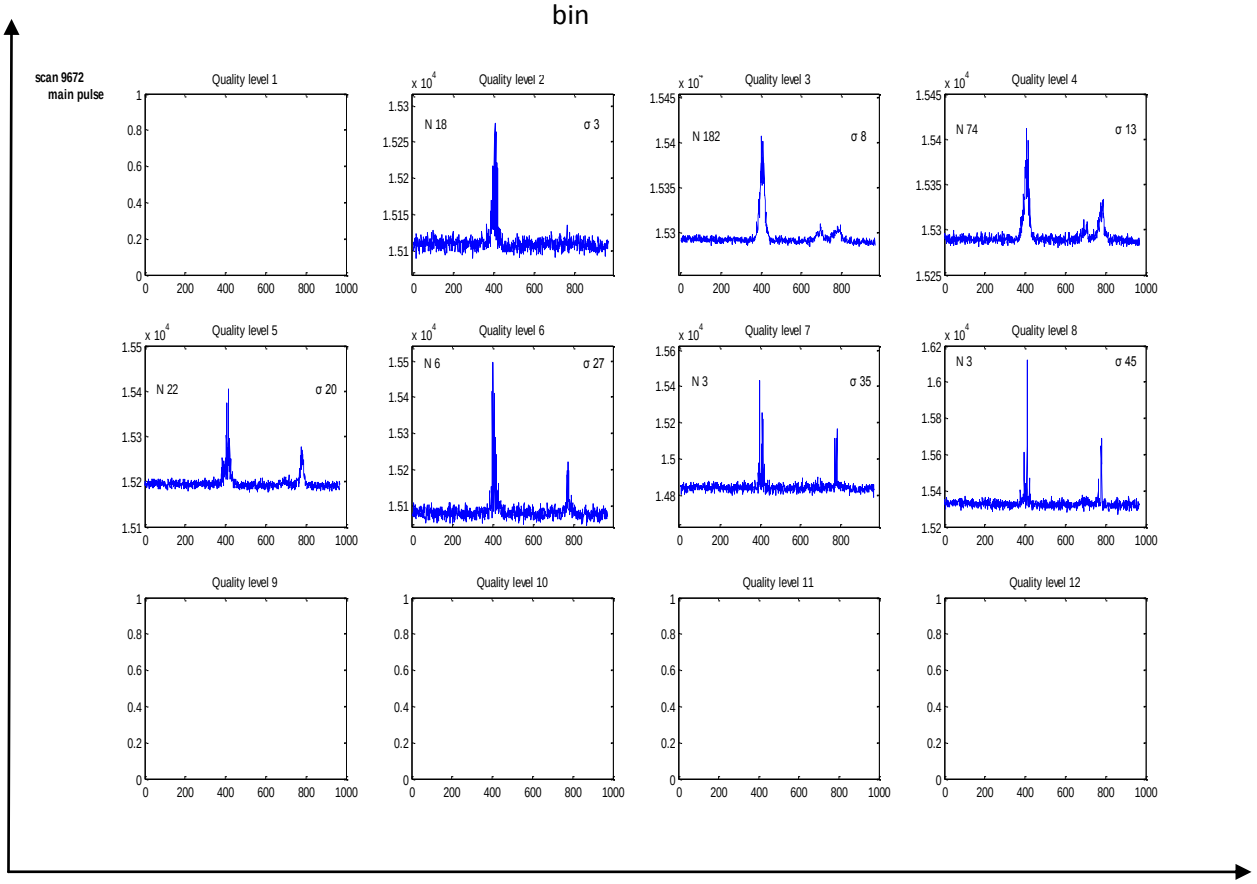

bin

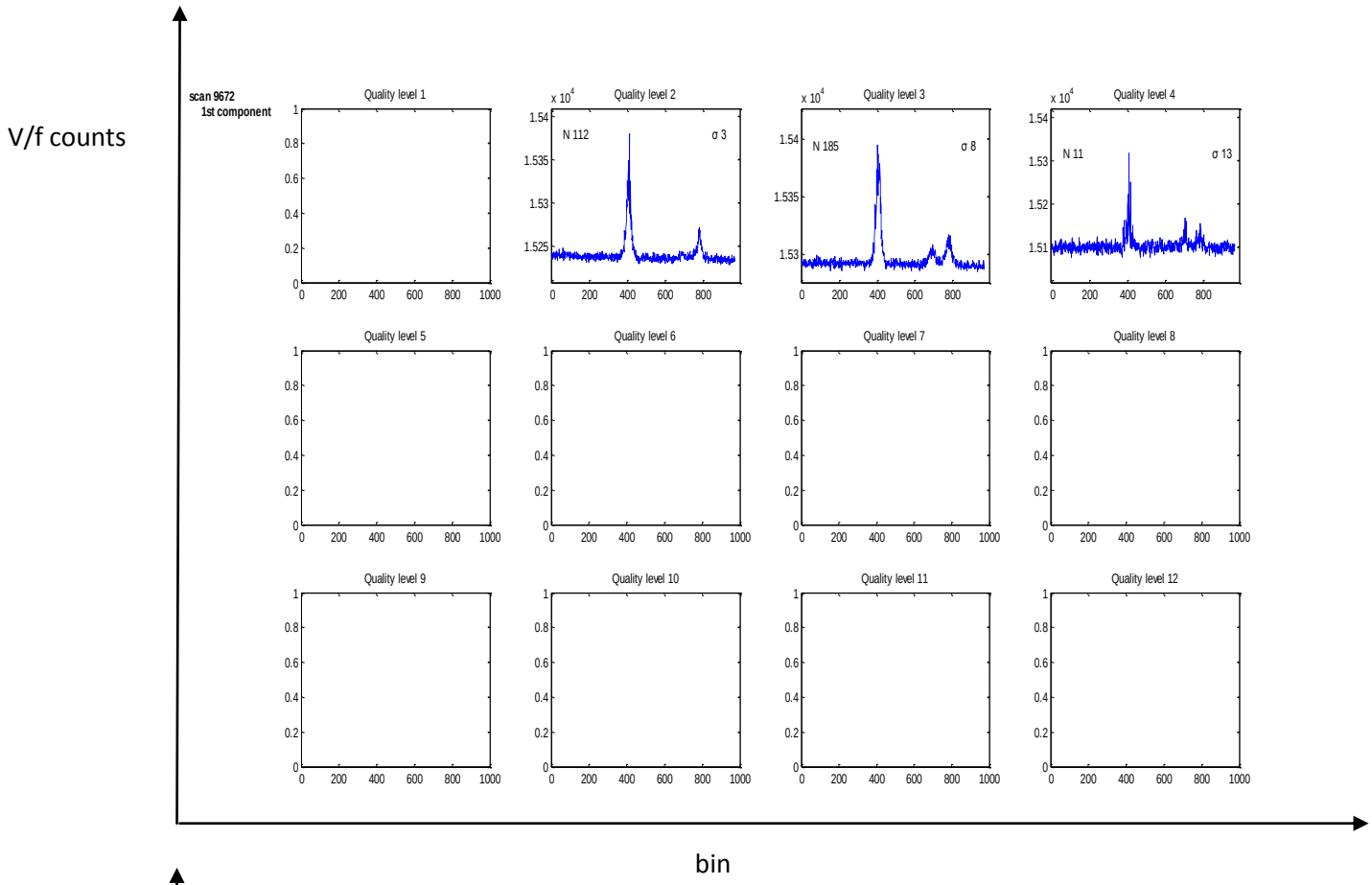
V/f counts
scan 9672
1st component
Quality level 1
Quality level 2
N 112
σ 3
Quality level 3
N 185
σ 8
Quality level 4
N 11
σ 13
Quality level 5
Quality level 6
Quality level 7
Quality level 8
Quality level 9
Quality level 10
Quality level 11
Quality level 12
bin

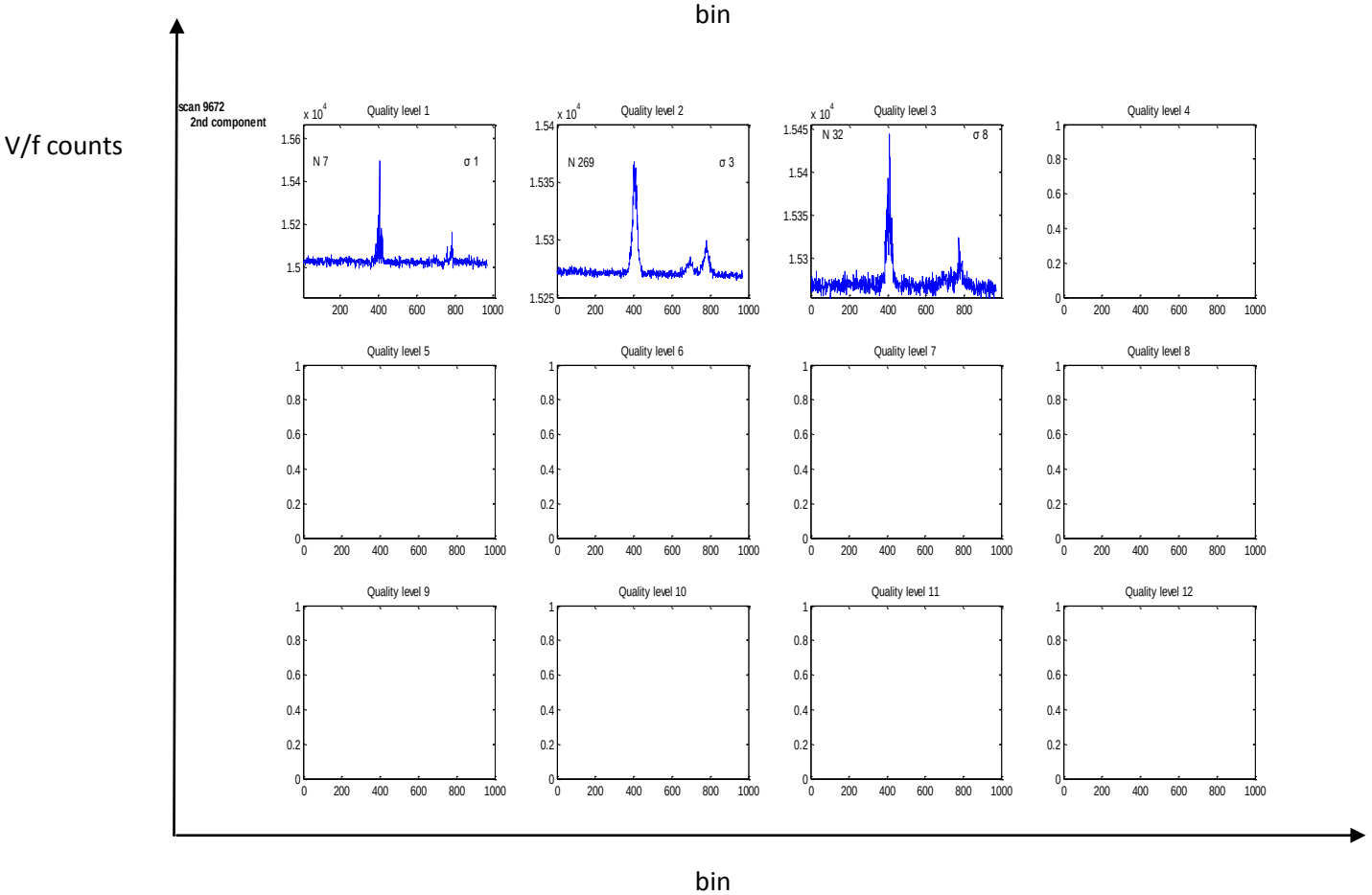
V/f counts
scan 9672
2nd component
Quality level 1
N 7
σ 1
Quality level 2
N 269
σ 3
Quality level 3
N 32
σ 8
Quality level 4
Quality level 5
Quality level 6
Quality level 7
Quality level 8
Quality level 9
Quality level 10
Quality level 11
Quality level 12
bin

V/f counts

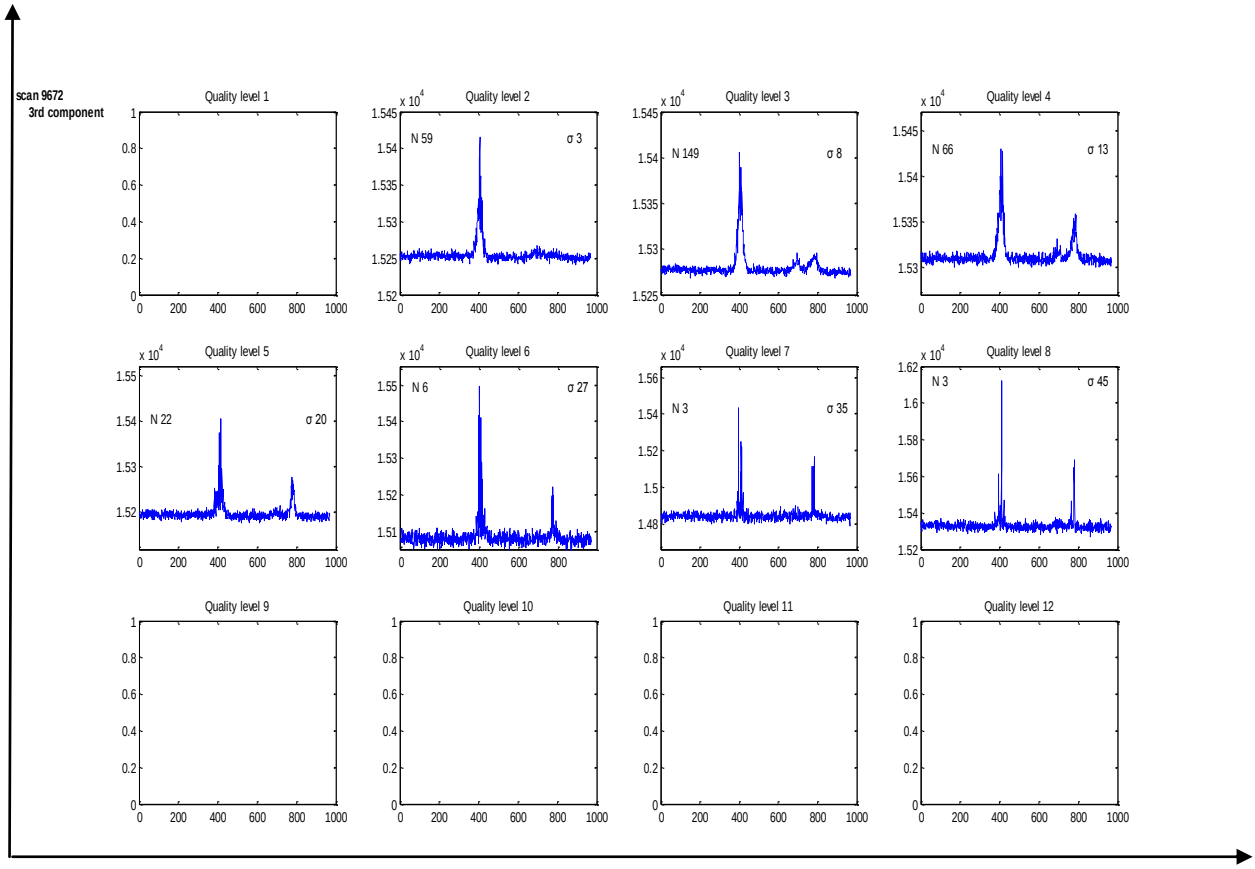

bin

V/f counts

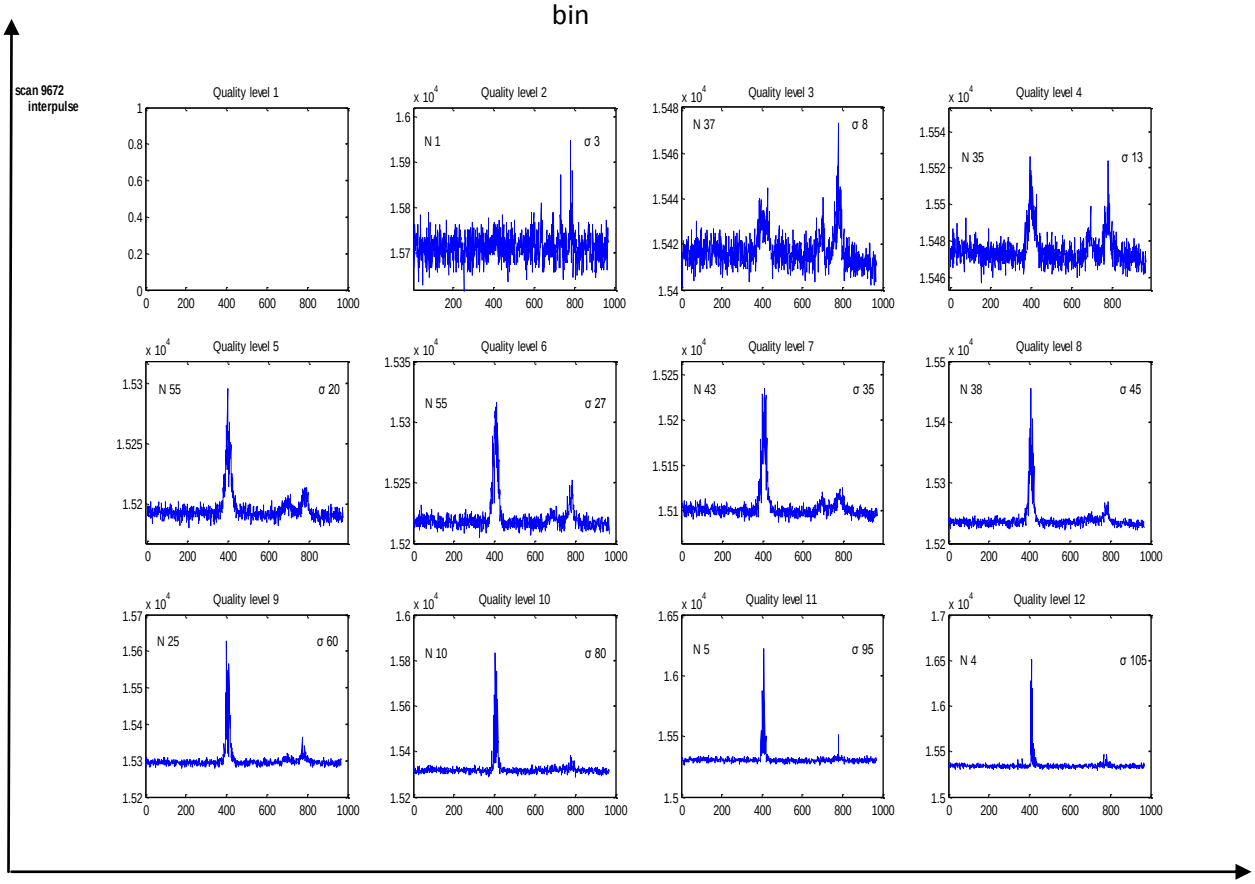

bin

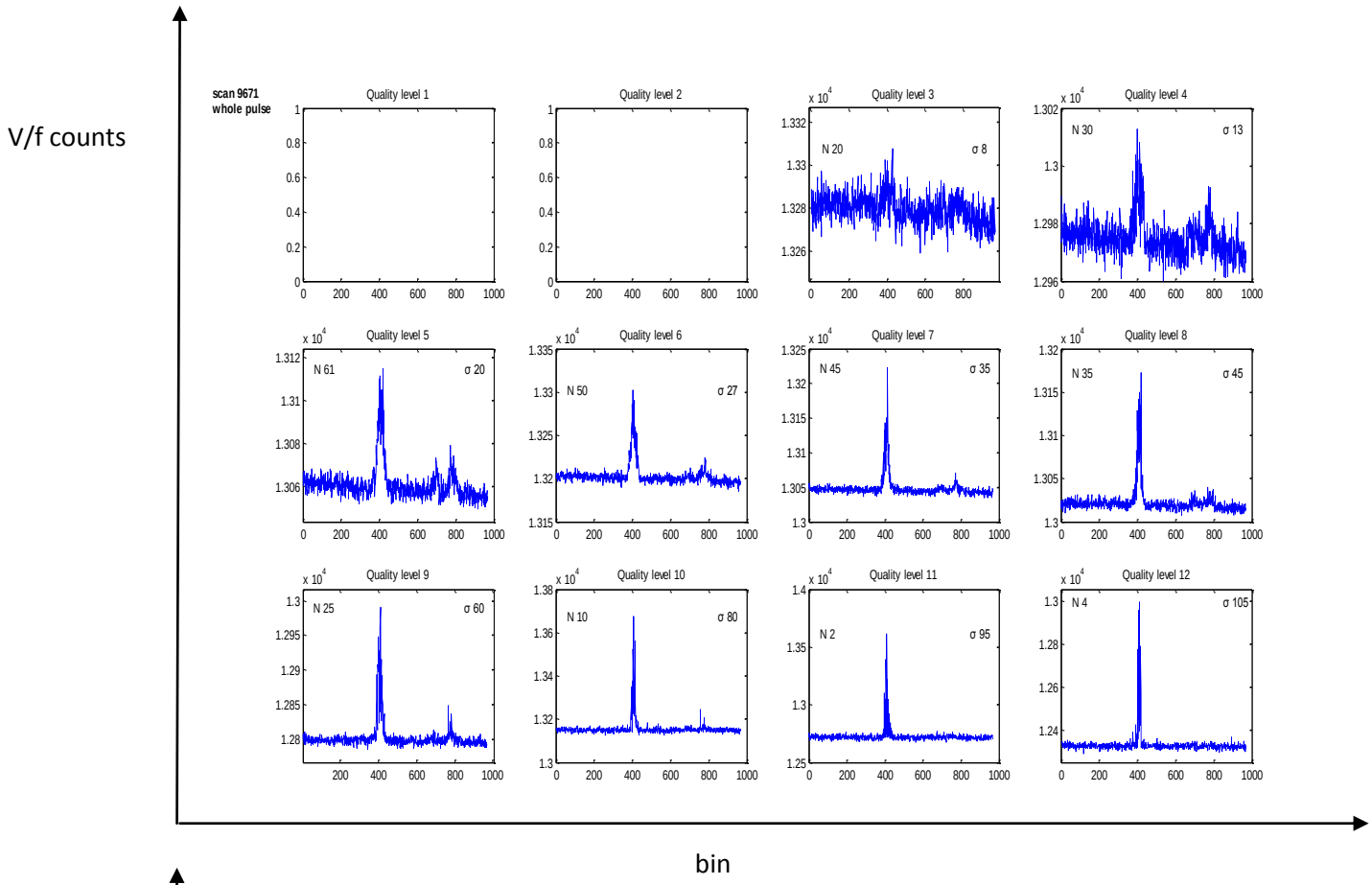
V/f counts
scan 9671
whole pulse
Quality level 1
Quality level 2
Quality level 3
N 20
σ 8
Quality level 4
N 30
σ 13
Quality level 5
N 61
σ 20
Quality level 6
N 50
σ 27
Quality level 7
N 45
σ 35
Quality level 8
N 35
σ 45
Quality level 9
N 25
σ 60
Quality level 10
N 10
σ 80
Quality level 11
N 2
σ 95
Quality level 12
N 4
σ 105
bin

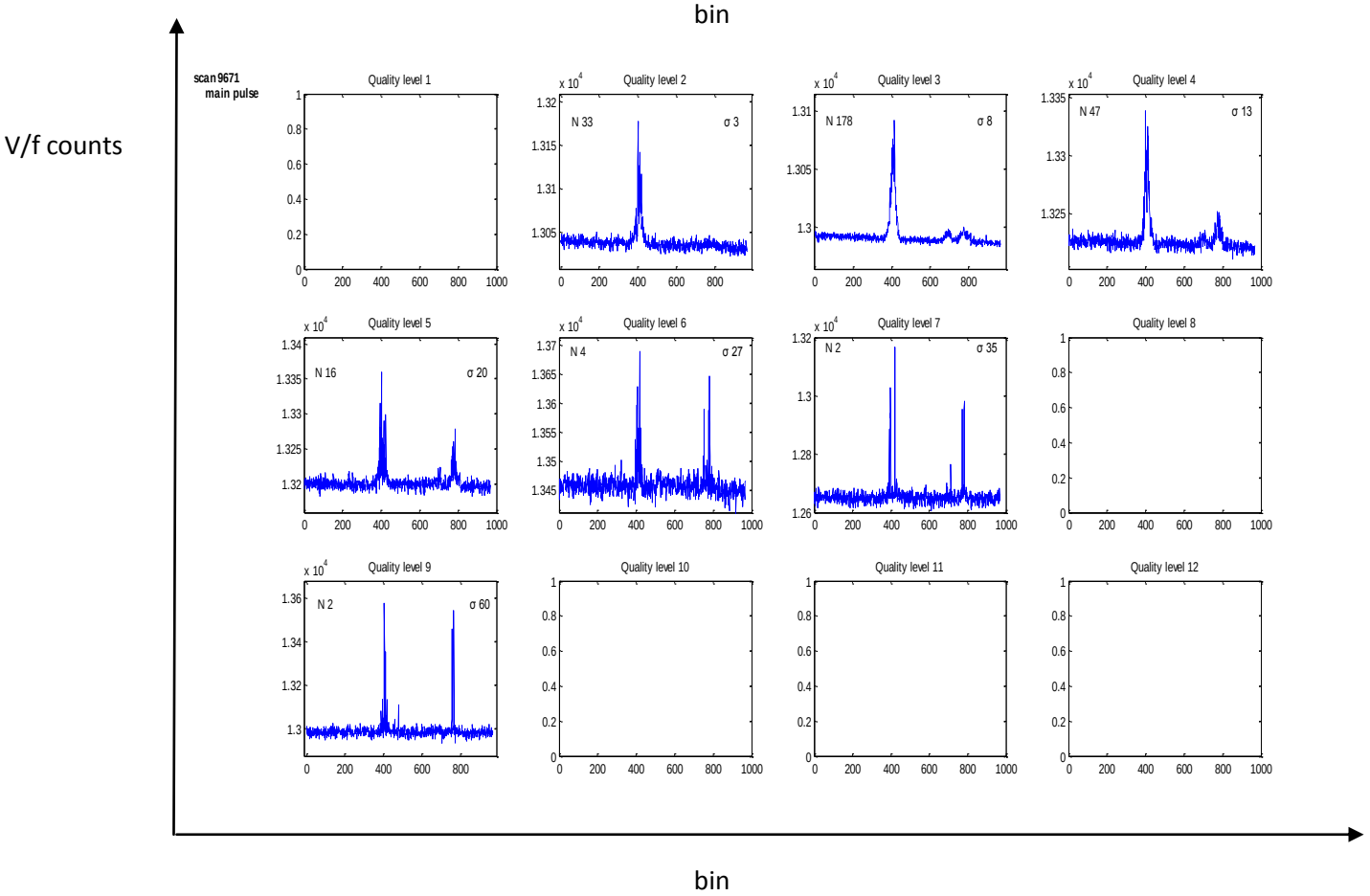
V/f counts
scan 9671
main pulse
Quality level 1
Quality level 2
N 33
σ 3
Quality level 3
N 178
σ 8
Quality level 4
N 47
σ 13
Quality level 5
N 16
σ 20
Quality level 6
N 4
σ 27
Quality level 7
N 2
σ 35
Quality level 8
Quality level 9
N 2
σ 60
Quality level 10
Quality level 11
Quality level 12
bin

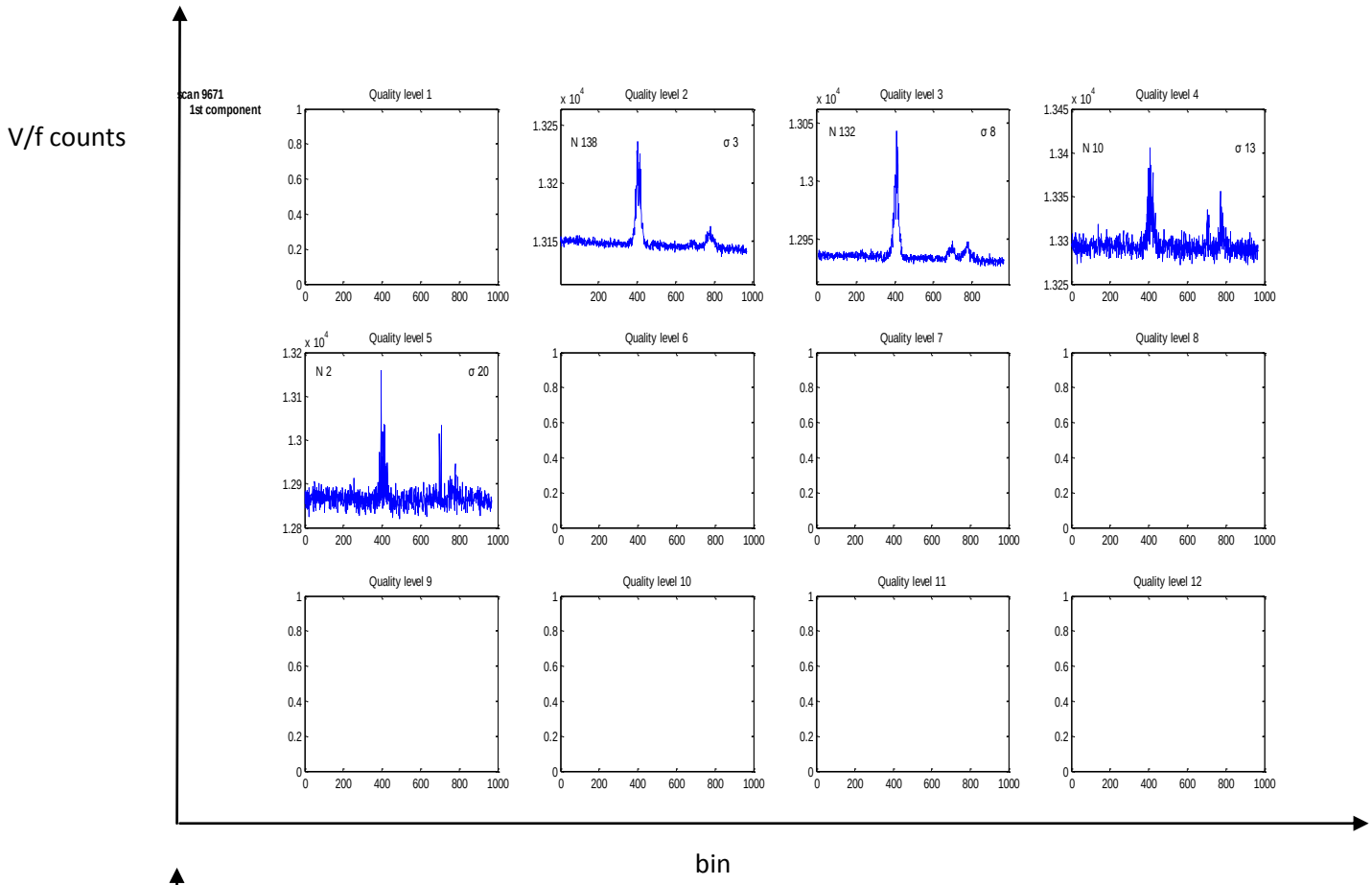
V/f counts
scan 9671
1st component
Quality level 1
Quality level 2
N 138
σ 3
Quality level 3
N 132
σ 8
Quality level 4
N 10
σ 13
Quality level 5
N 2
σ 20
Quality level 6
Quality level 7
Quality level 8
Quality level 9
Quality level 10
Quality level 11
Quality level 12
bin

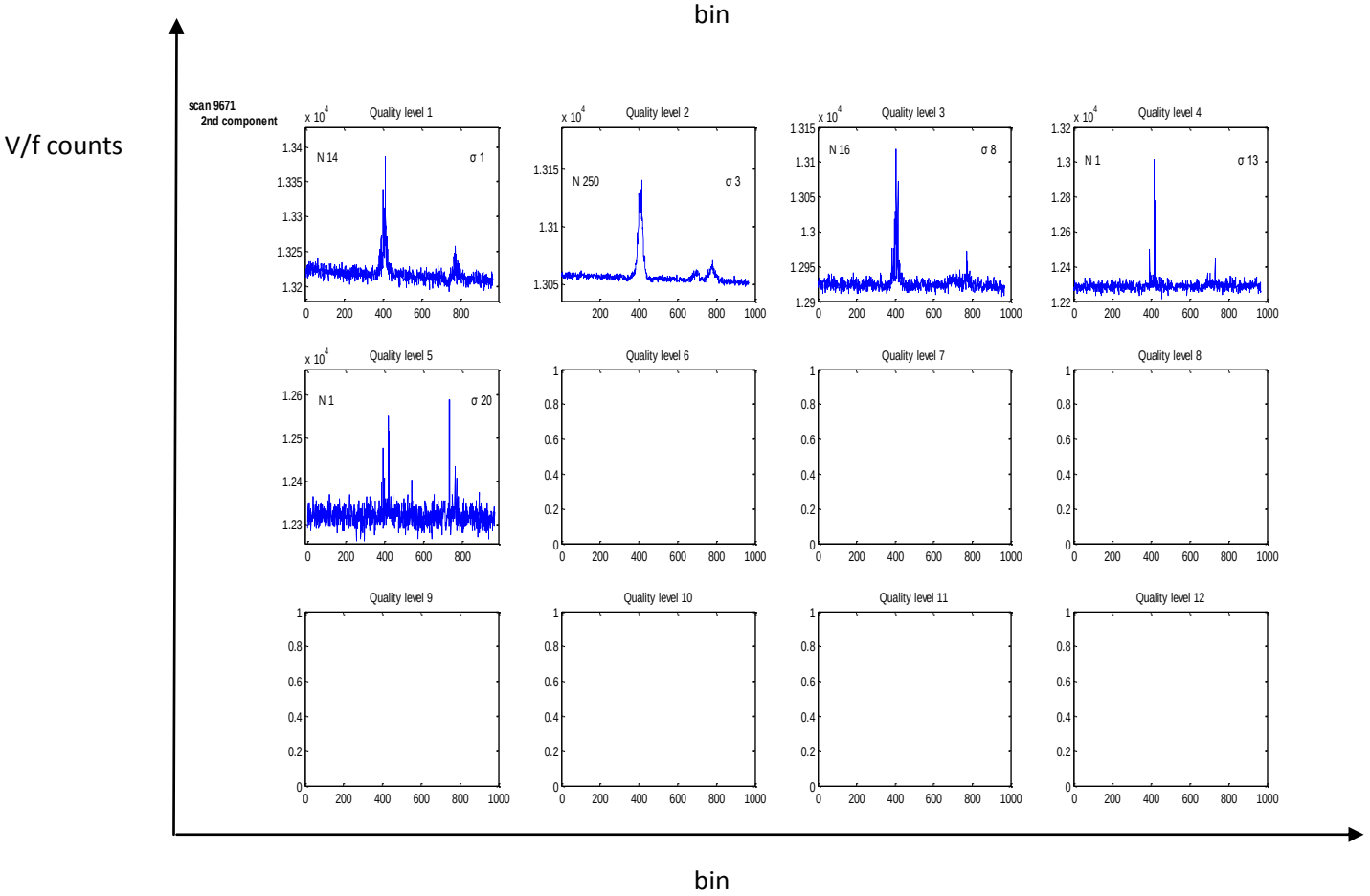
V/f counts
scan 9671
2nd component
Quality level 1
N 14
σ 1
Quality level 2
N 250
σ 3
Quality level 3
N 16
σ 8
Quality level 4
N 1
σ 13
Quality level 5
N 1
σ 20
Quality level 6
Quality level 7
Quality level 8
Quality level 9
Quality level 10
Quality level 11
Quality level 12
bin

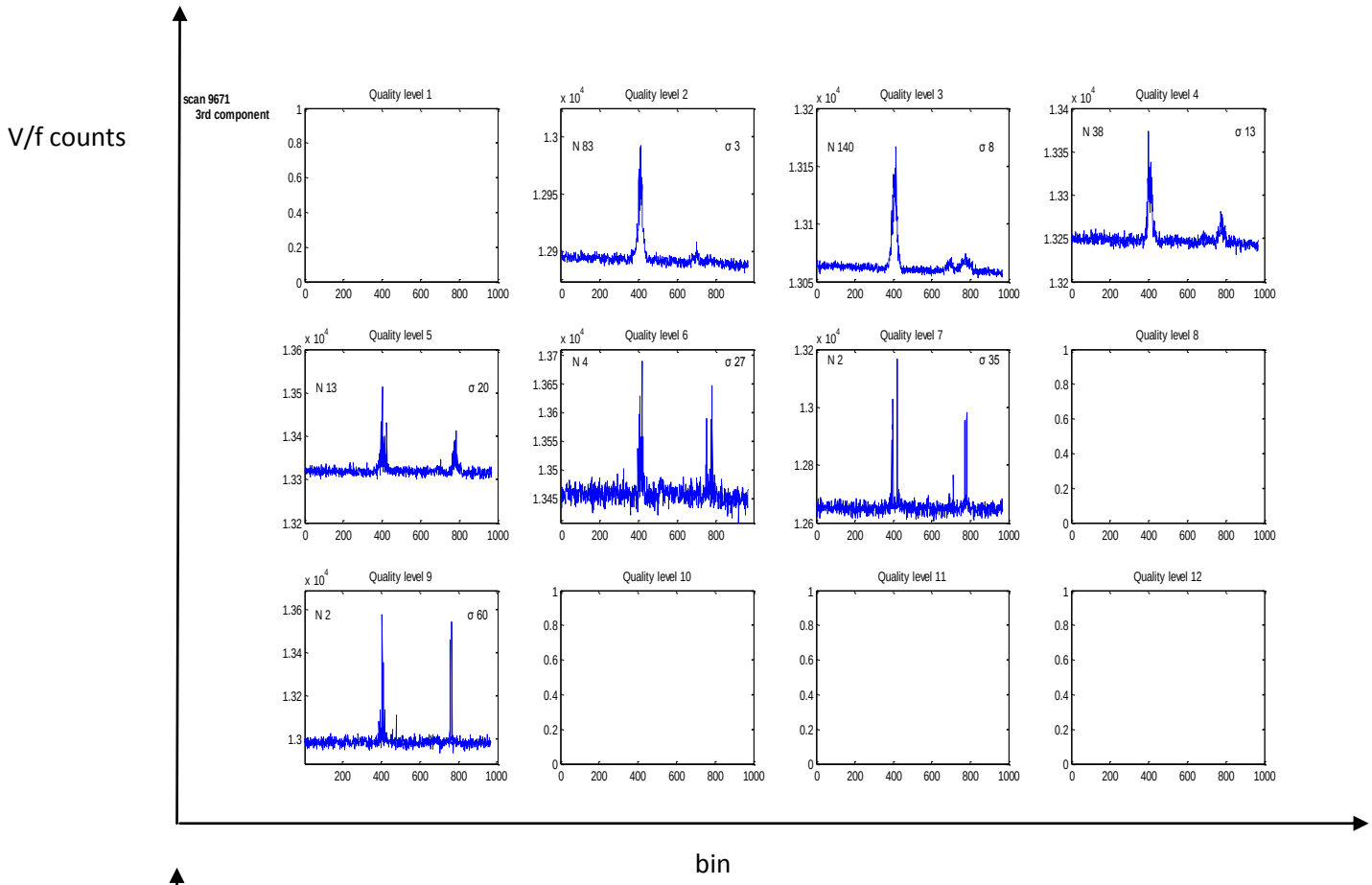
V/f counts
scan 9671
3rd component
Quality level 1
Quality level 2
N 83
σ 3
Quality level 3
N 140
σ 8
Quality level 4
N 38
σ 13
Quality level 5
N 13
σ 20
Quality level 6
N 4
σ 27
Quality level 7
N 2
σ 35
Quality level 8
Quality level 9
N 2
σ 60
Quality level 10
Quality level 11
Quality level 12
bin

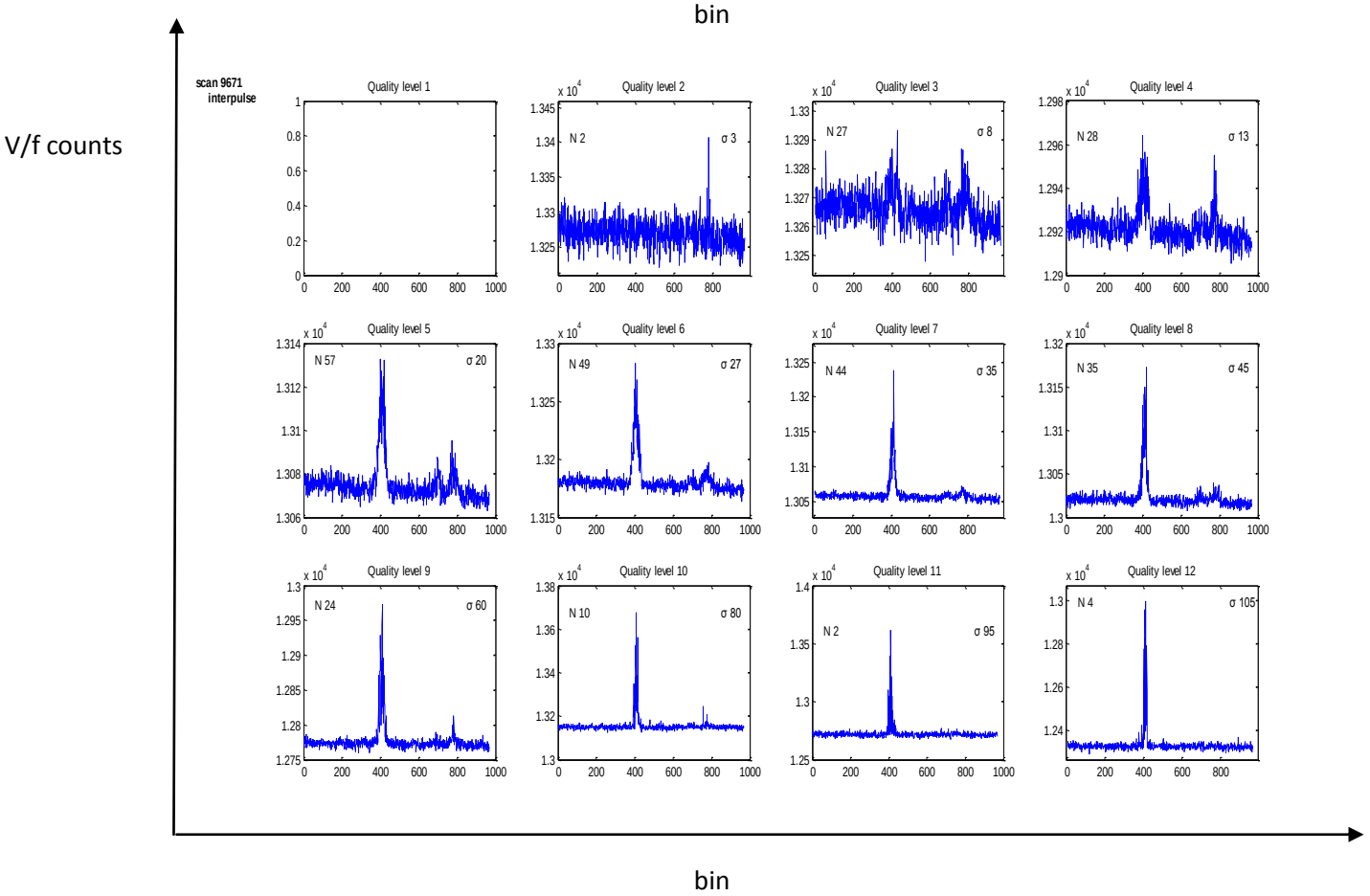
V/f counts
scan 9671
interpulse
Quality level 1
Quality level 2
N 2
σ 3
Quality level 3
N 27
σ 8
Quality level 4
N 28
σ 13
Quality level 5
N 57
σ 20
Quality level 6
N 49
σ 27
Quality level 7
N 44
σ 35
Quality level 8
N 35
σ 45
Quality level 9
N 24
σ 60
Quality level 10
N 10
σ 80
Quality level 11
N 2
σ 95
Quality level 12
N 4
σ 105
bin

V/f counts

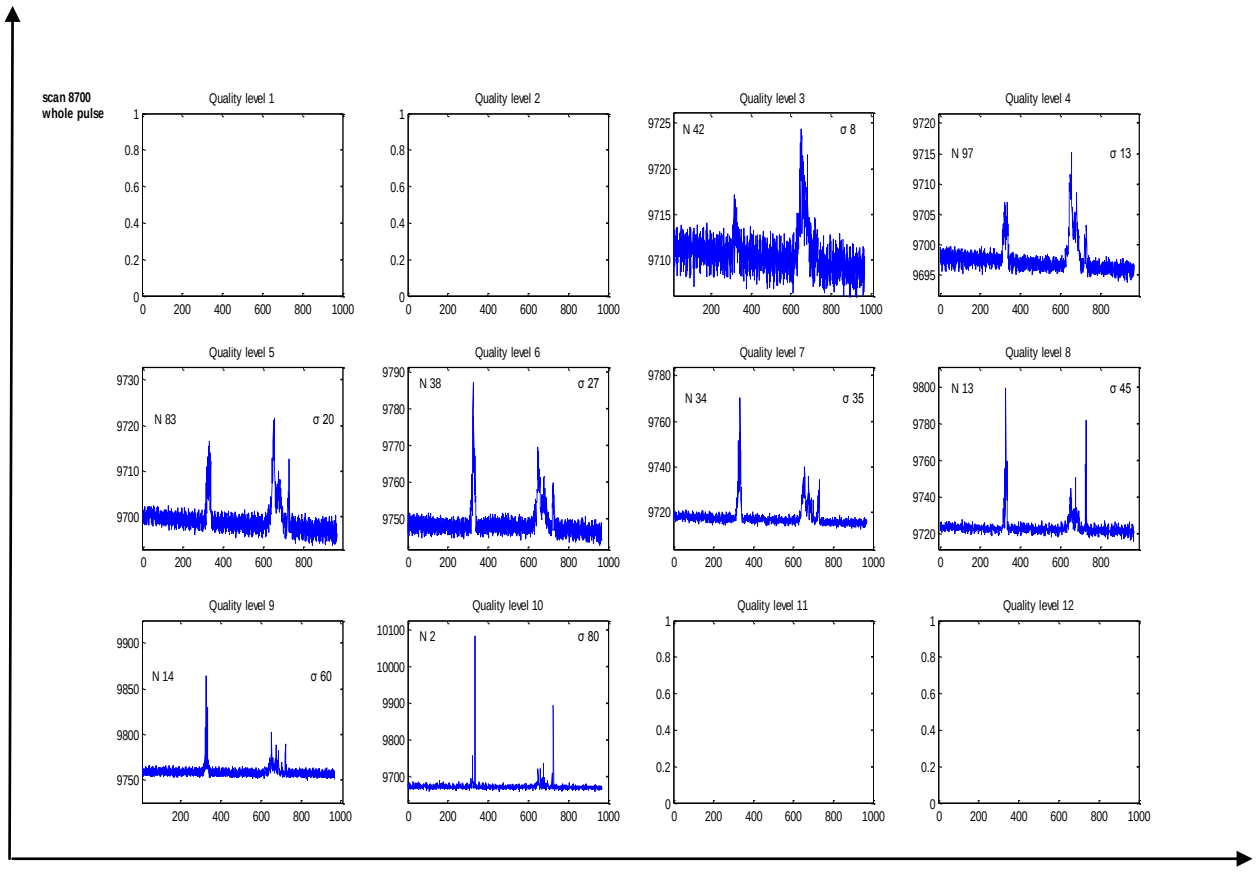

bin

V/f counts

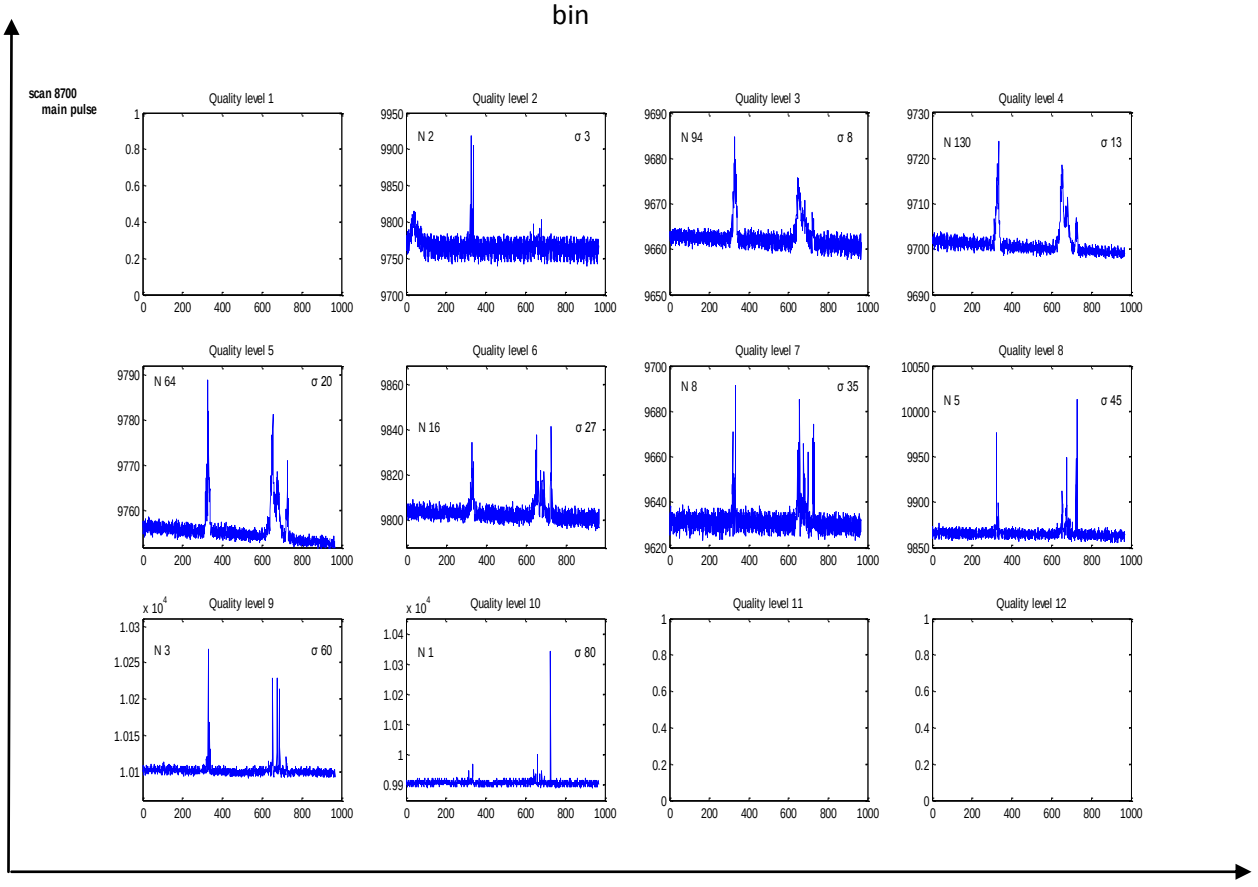

bin

V/f counts

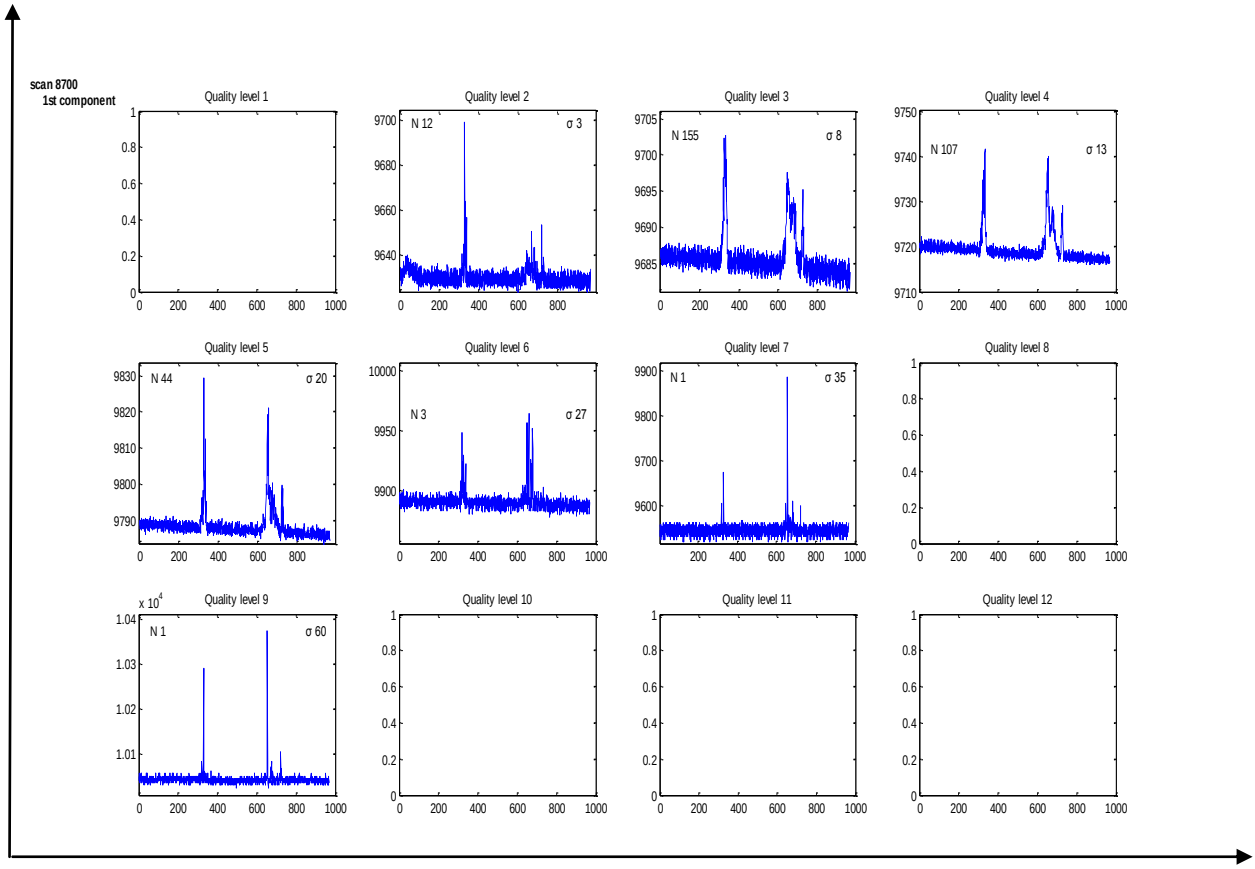

bin

V/f counts

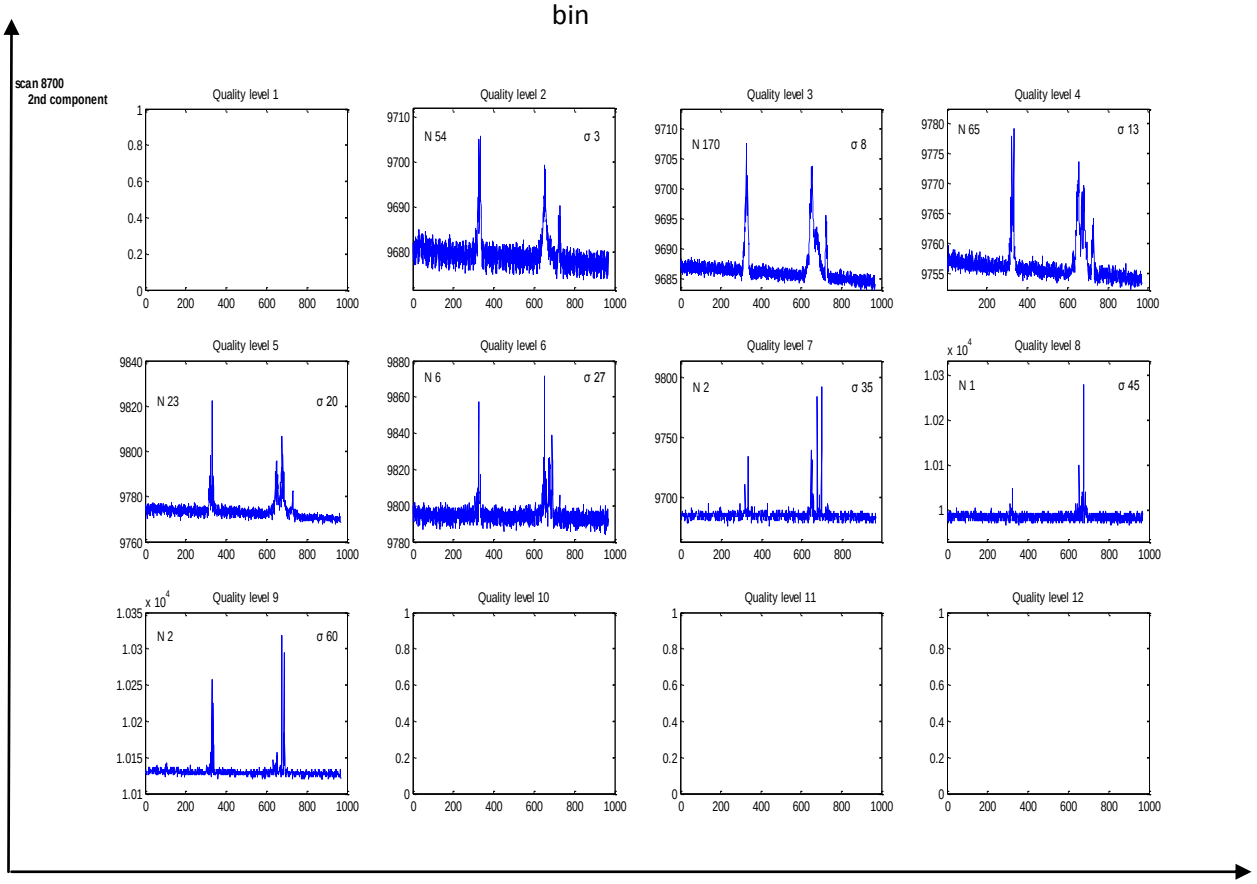

bin

V/f counts

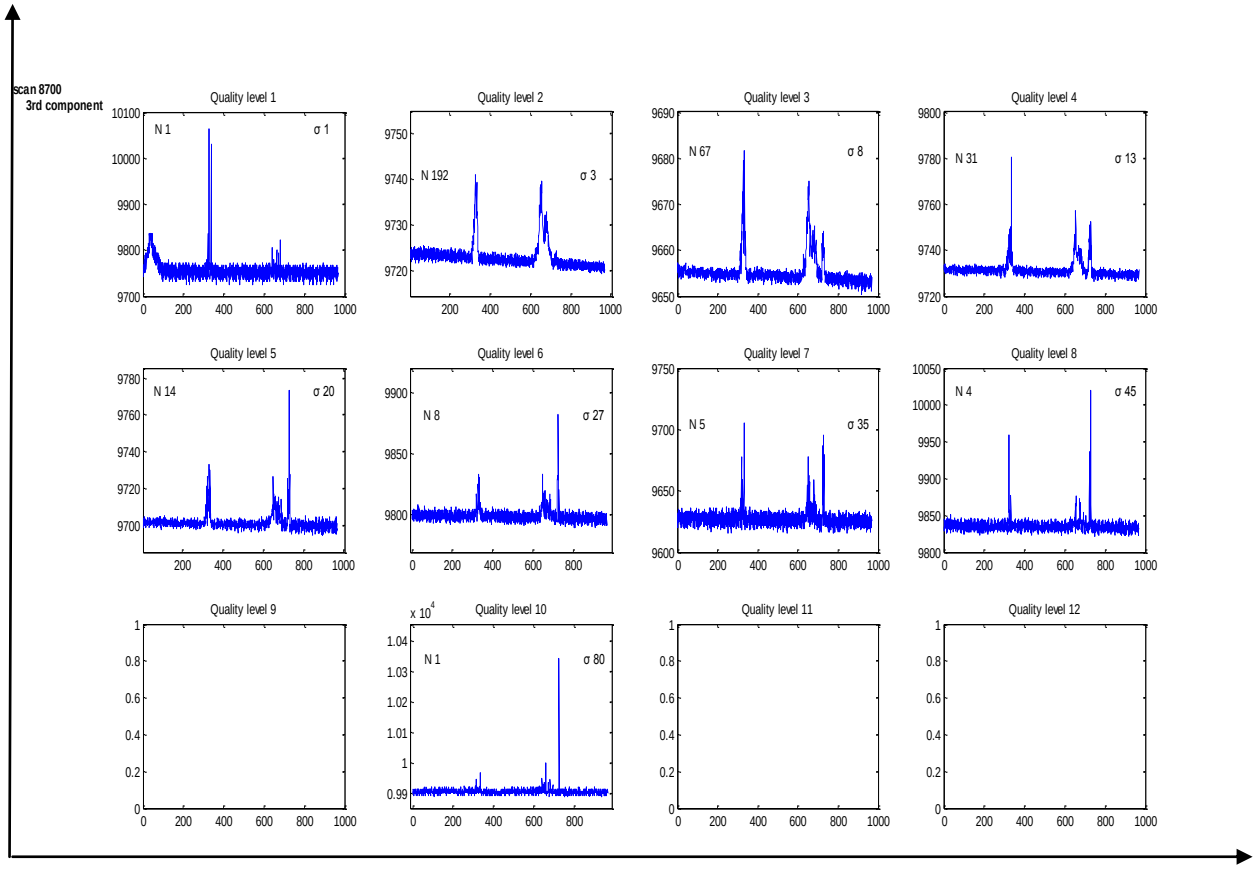

bin

V/f counts

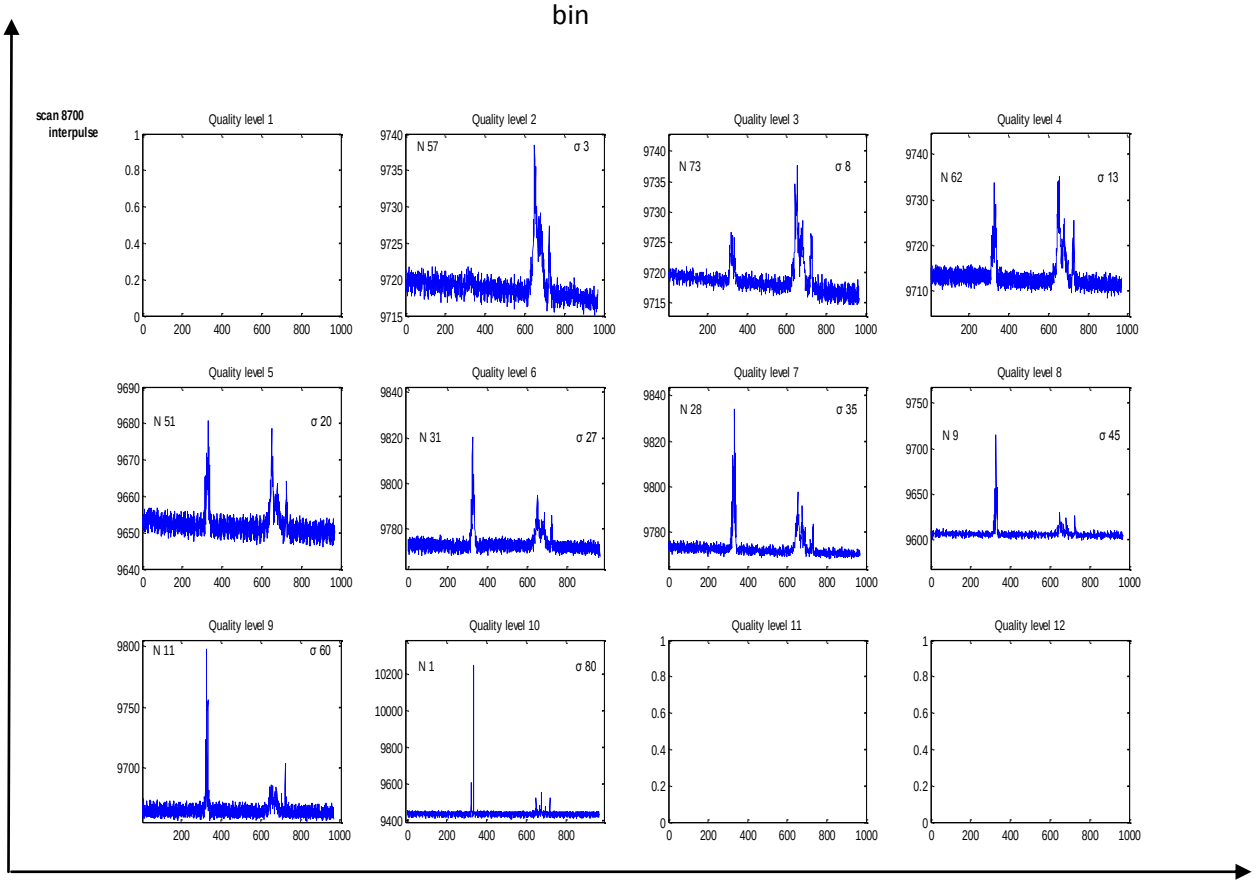

bin

V/f counts

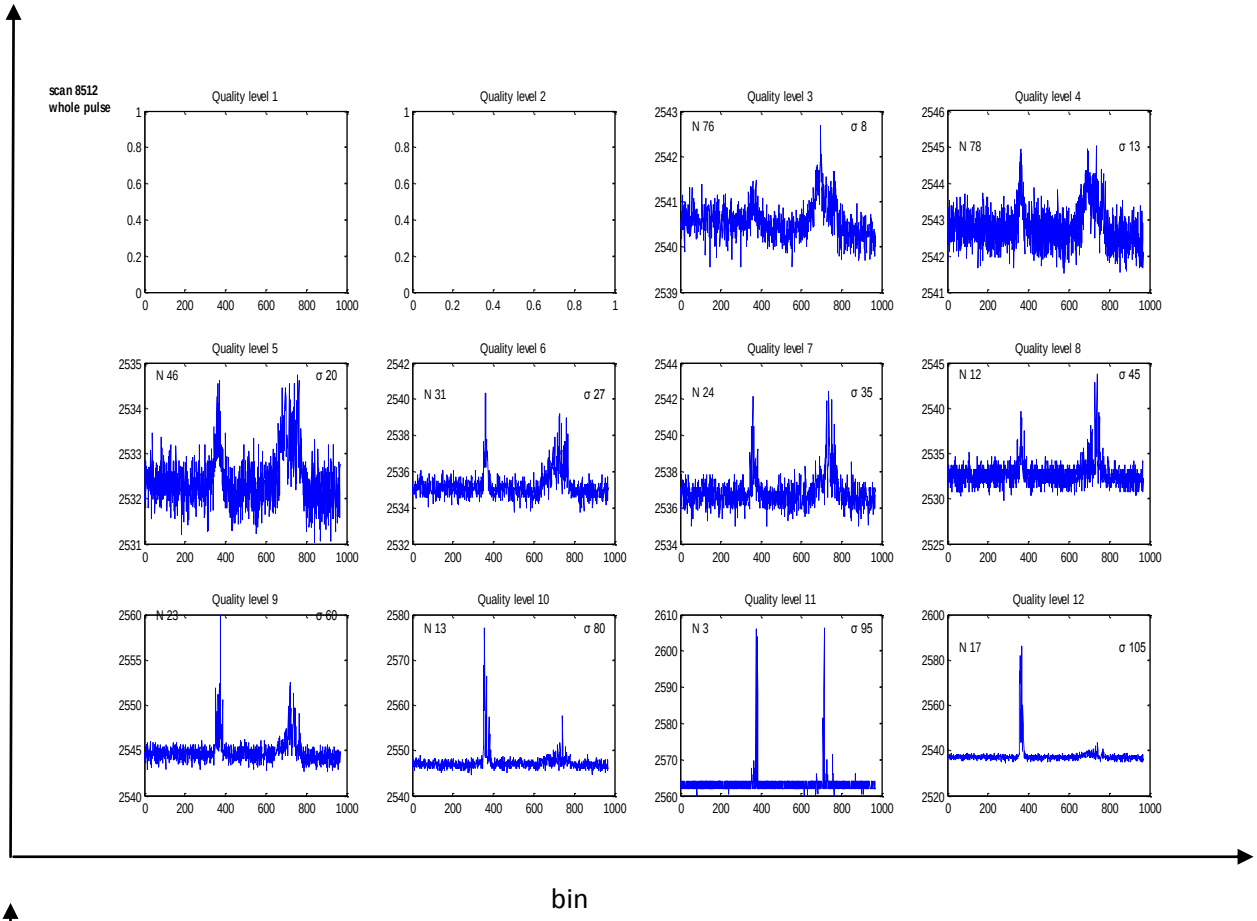

bin

V/f counts

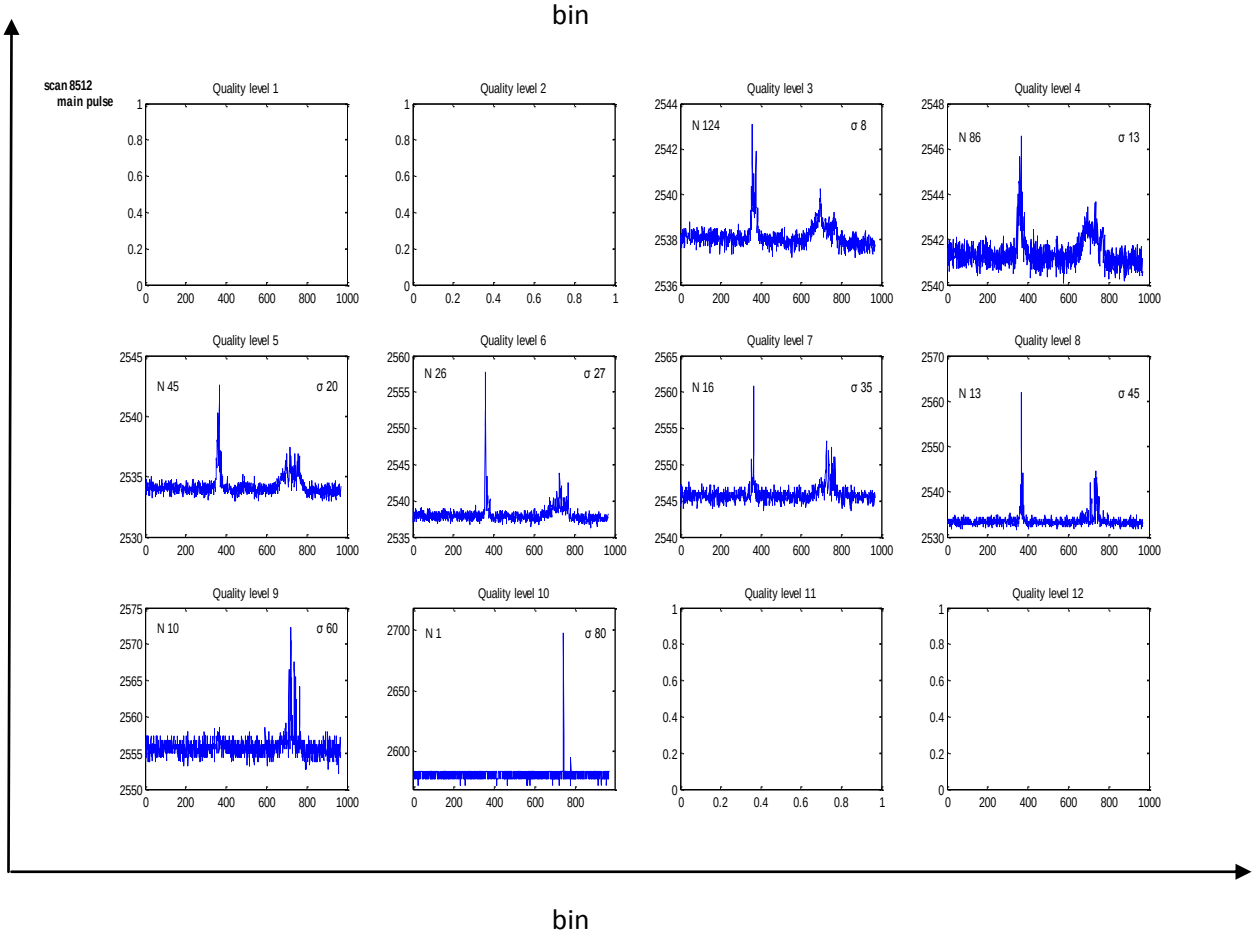

bin

V/f counts

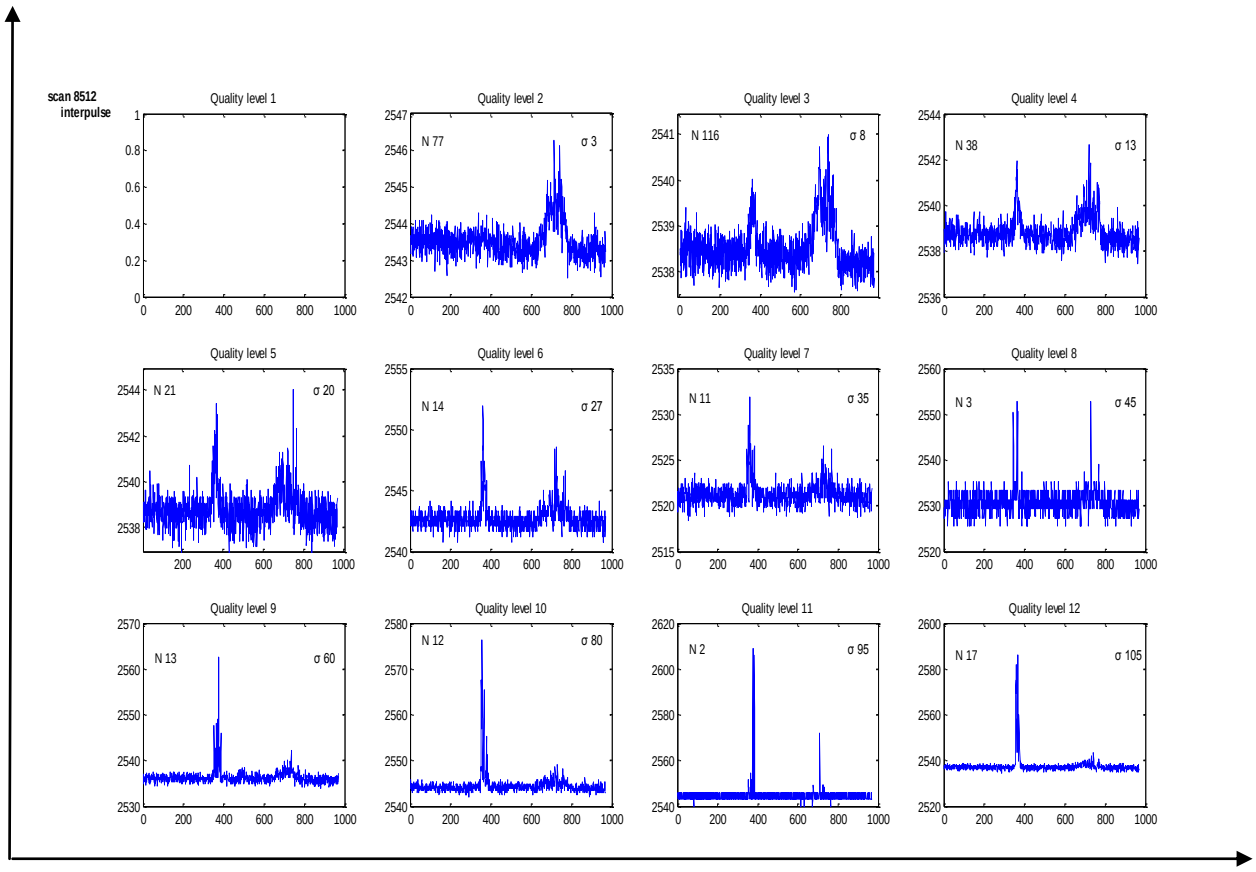

bin

V/f counts

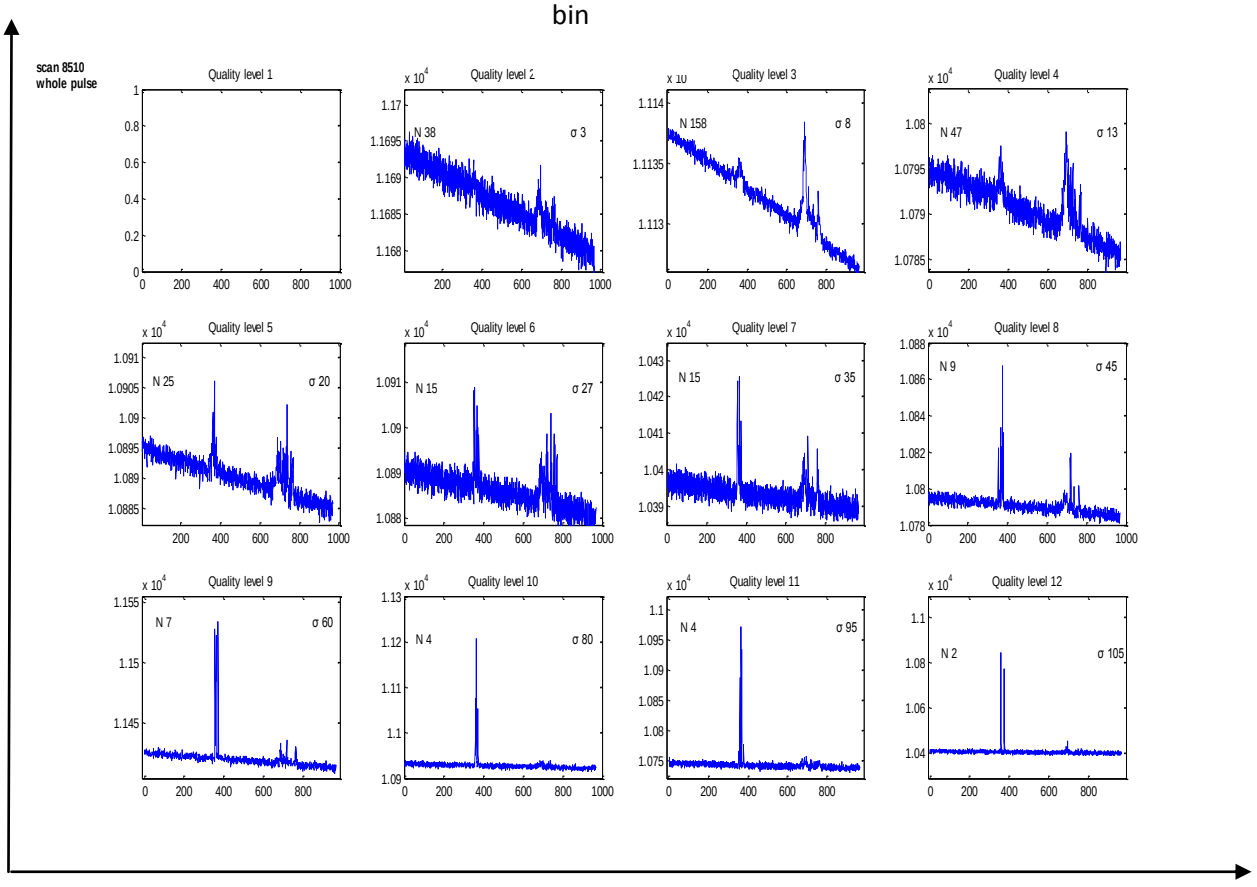

bin

V/f counts

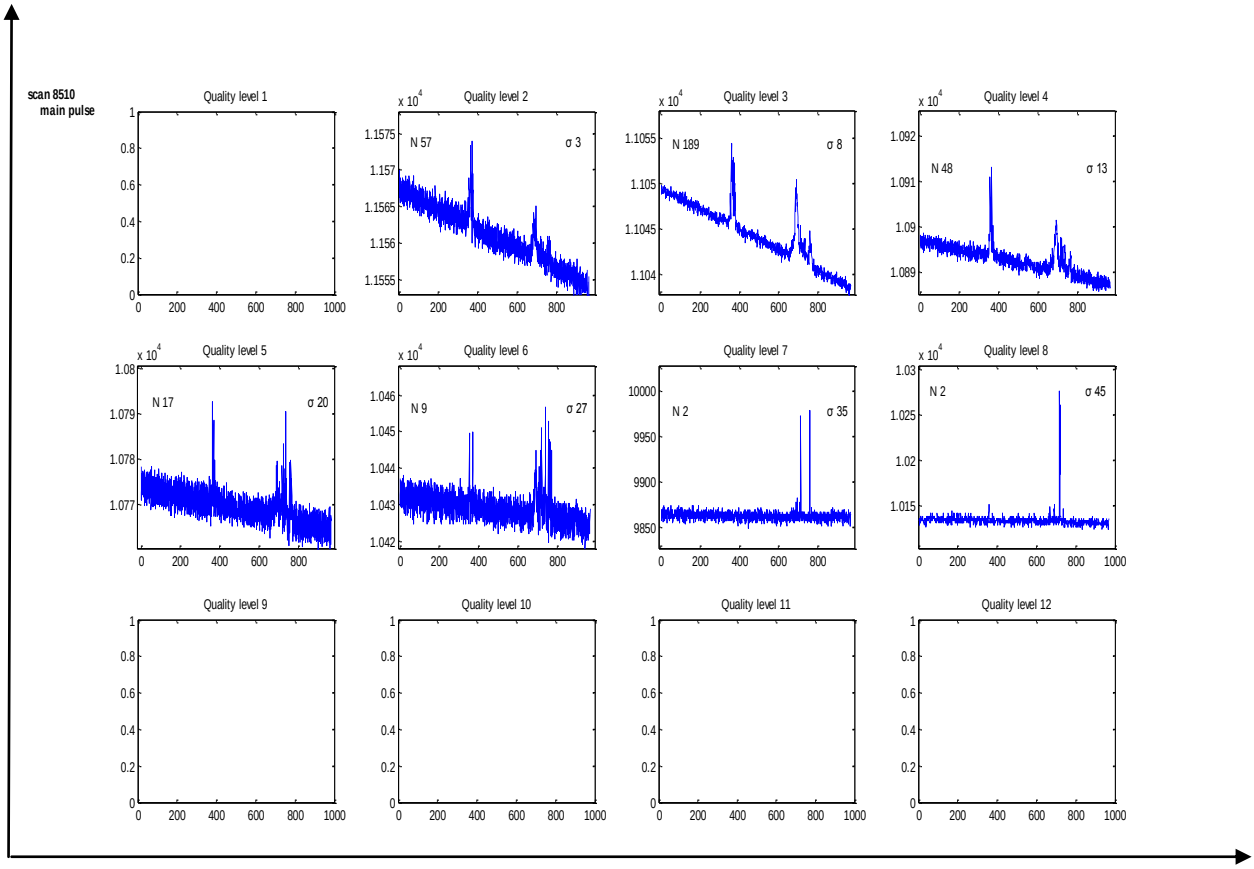

bin

V/f counts

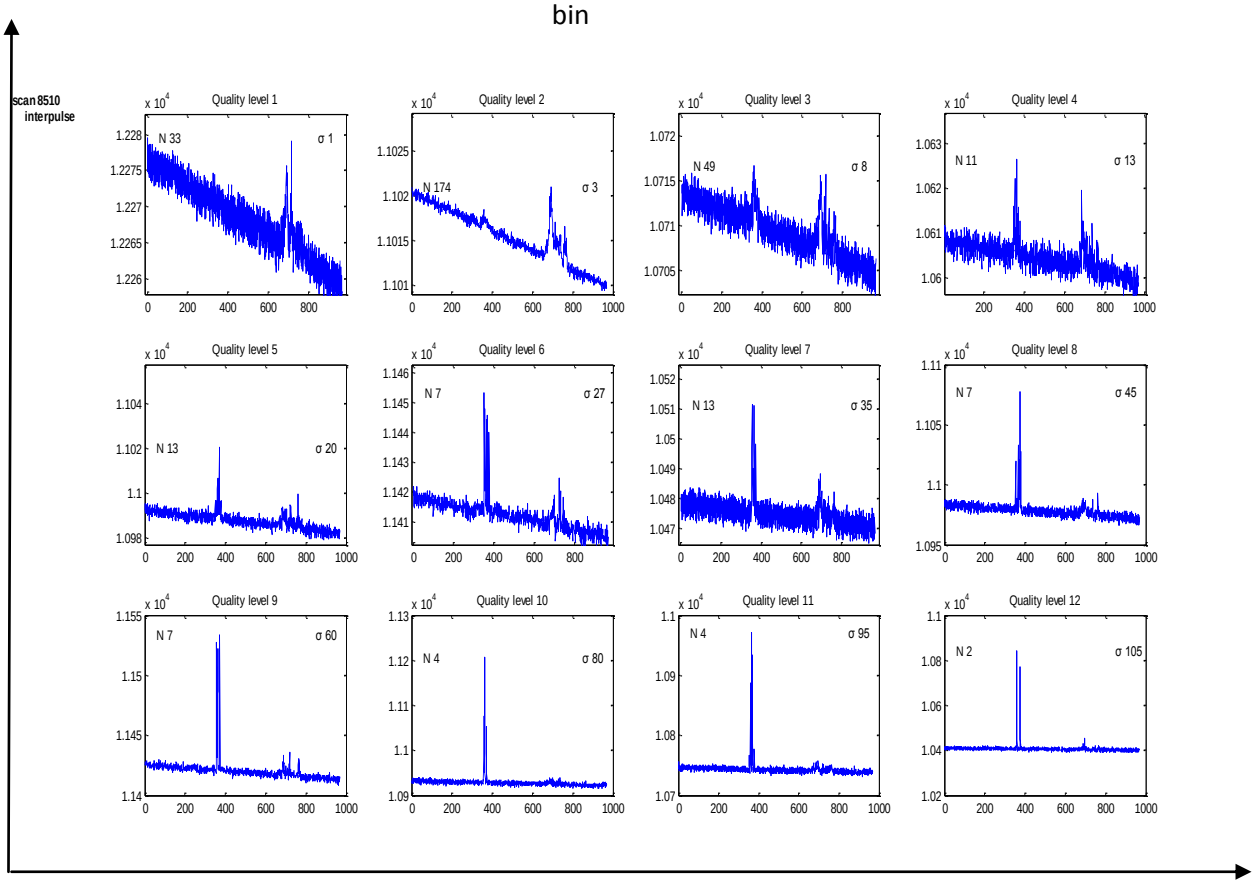

bin

V/f counts

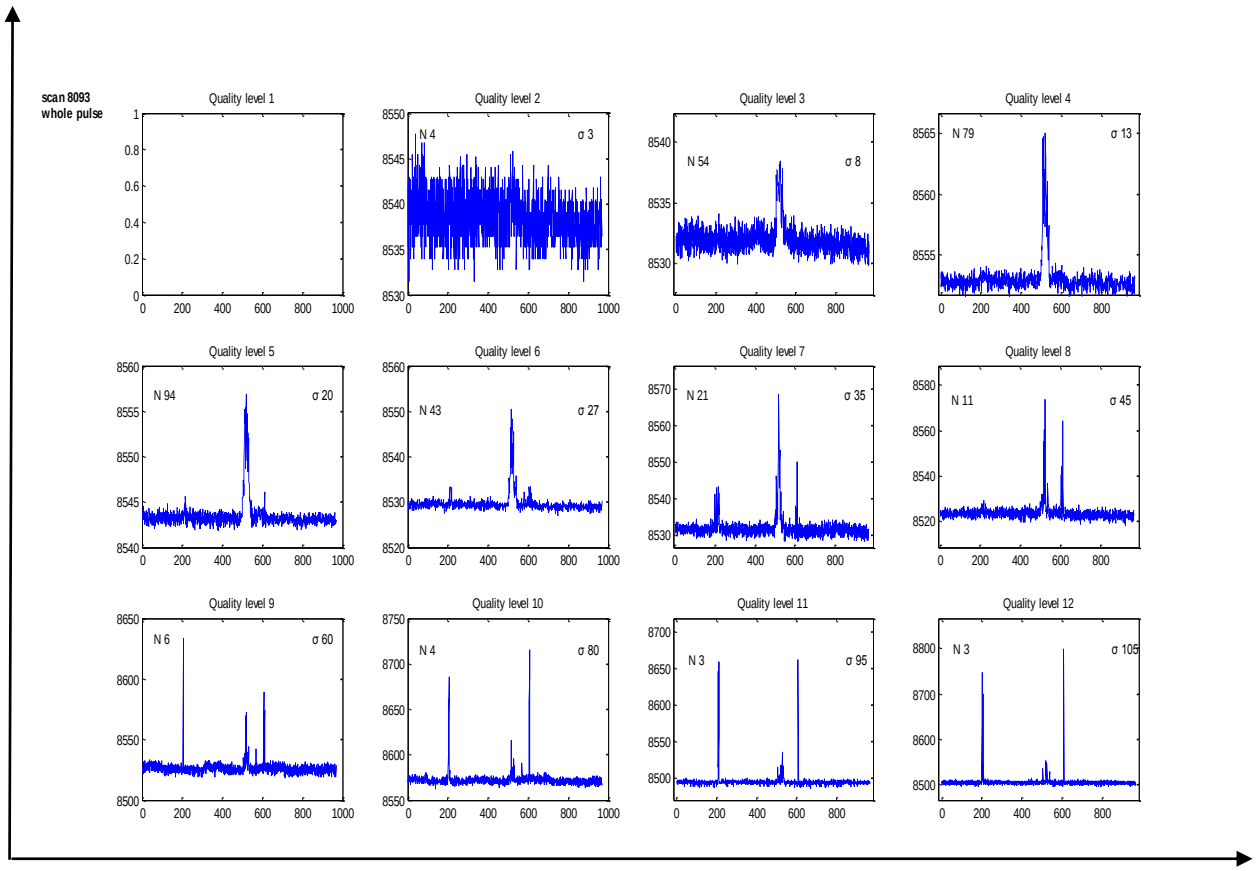

bin

V/f counts

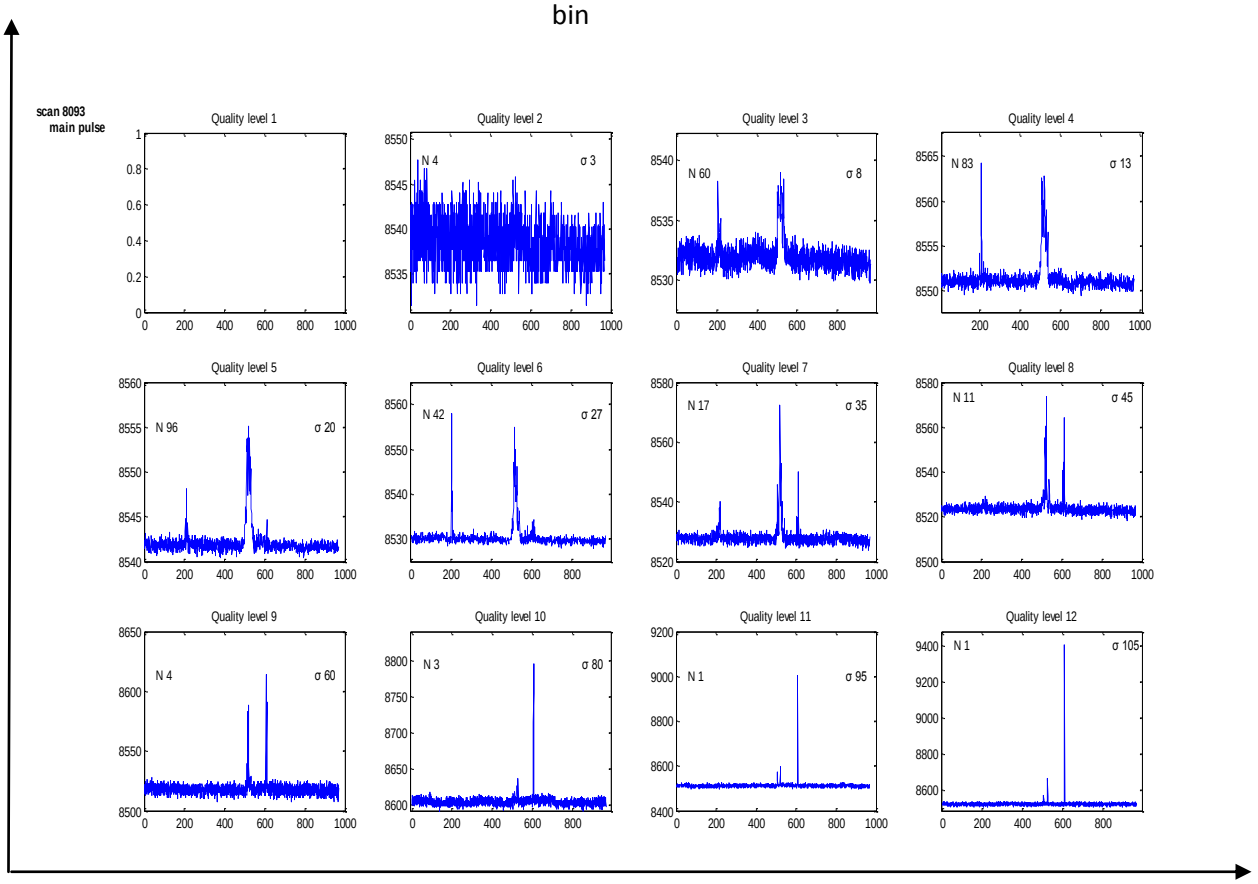

bin

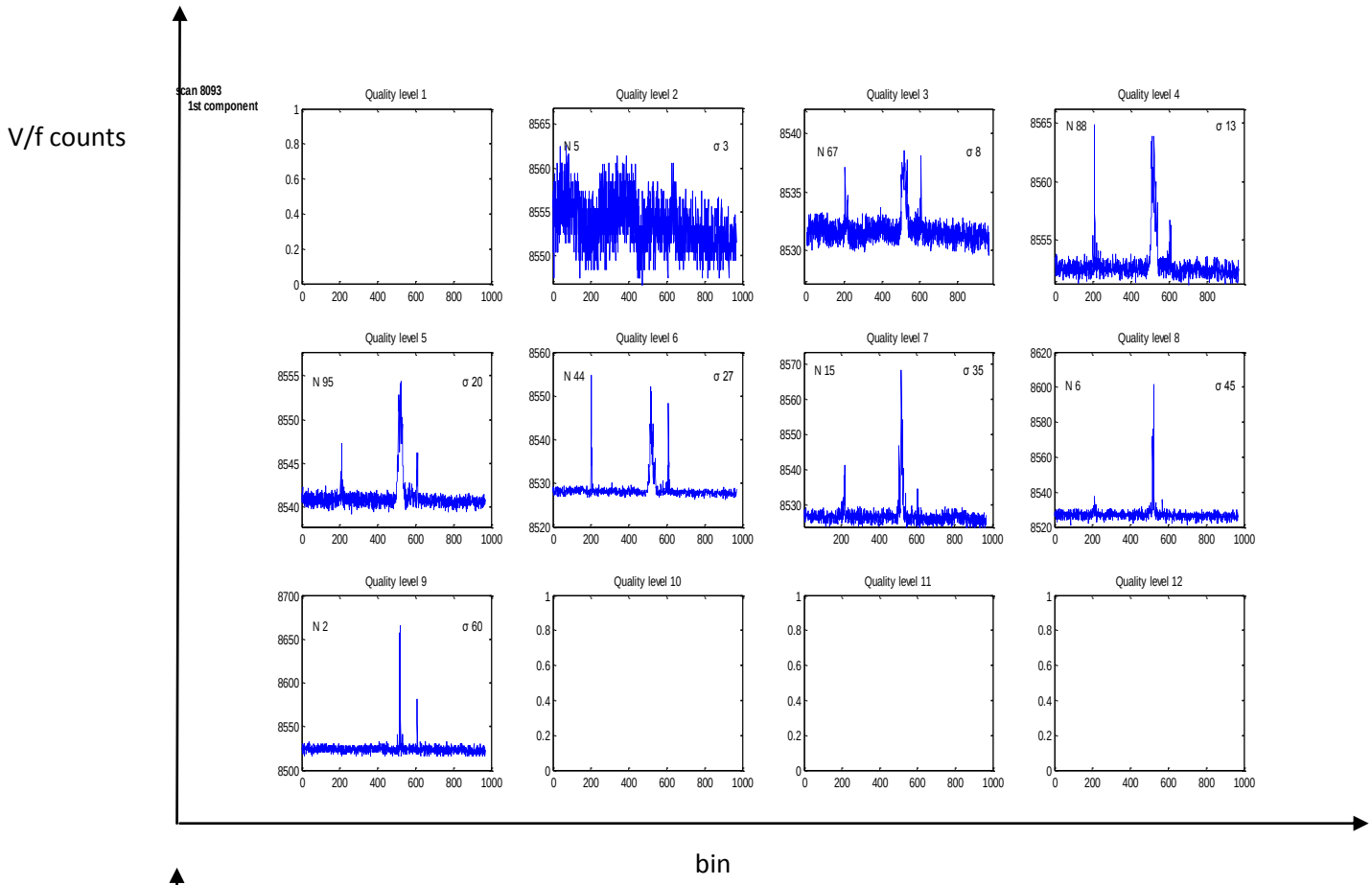
V/f counts
scan 8093
1st component
Quality level 1
Quality level 2
N 5
σ 3
Quality level 3
N 67
σ 8
Quality level 4
N 88
σ 13
Quality level 5
N 95
σ 20
Quality level 6
N 44
σ 27
Quality level 7
N 15
σ 35
Quality level 8
N 6
σ 45
Quality level 9
N 2
σ 60
Quality level 10
Quality level 11
Quality level 12
bin

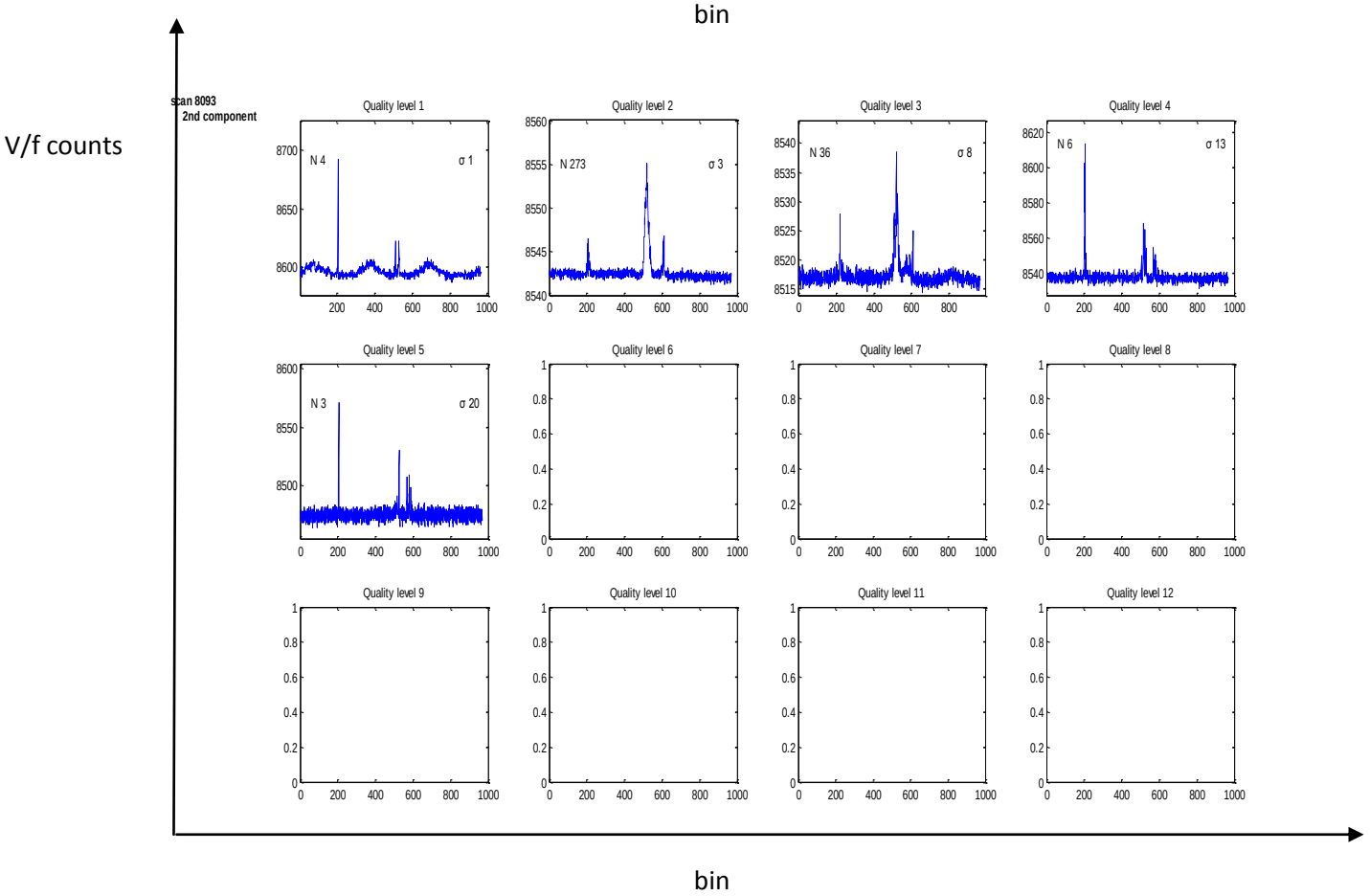
V/f counts
scan 8093
2nd component
Quality level 1
N 4
σ 1
Quality level 2
N 273
σ 3
Quality level 3
N 36
σ 8
Quality level 4
N 6
σ 13
Quality level 5
N 3
σ 20
Quality level 6
Quality level 7
Quality level 8
Quality level 9
Quality level 10
Quality level 11
Quality level 12
bin

V/f counts

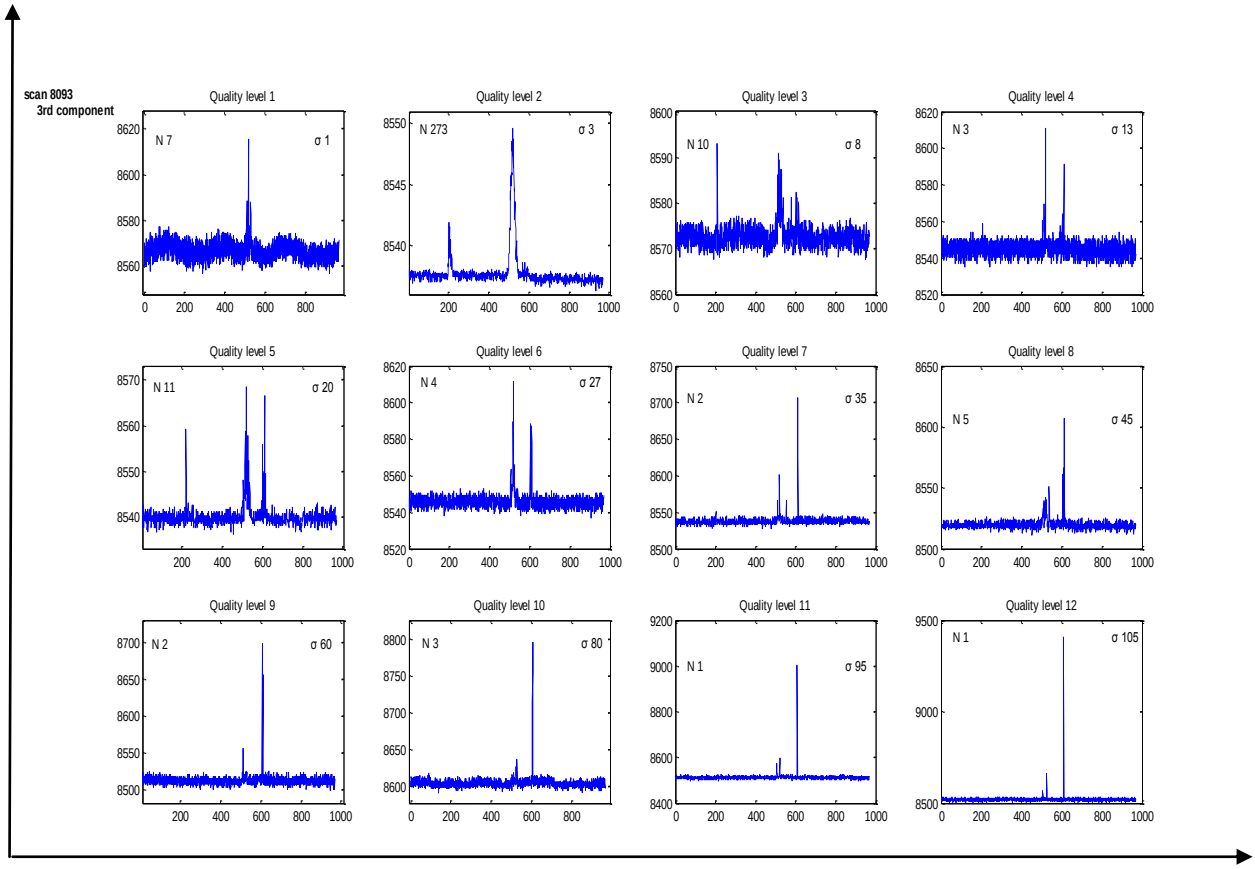

bin

V/f counts

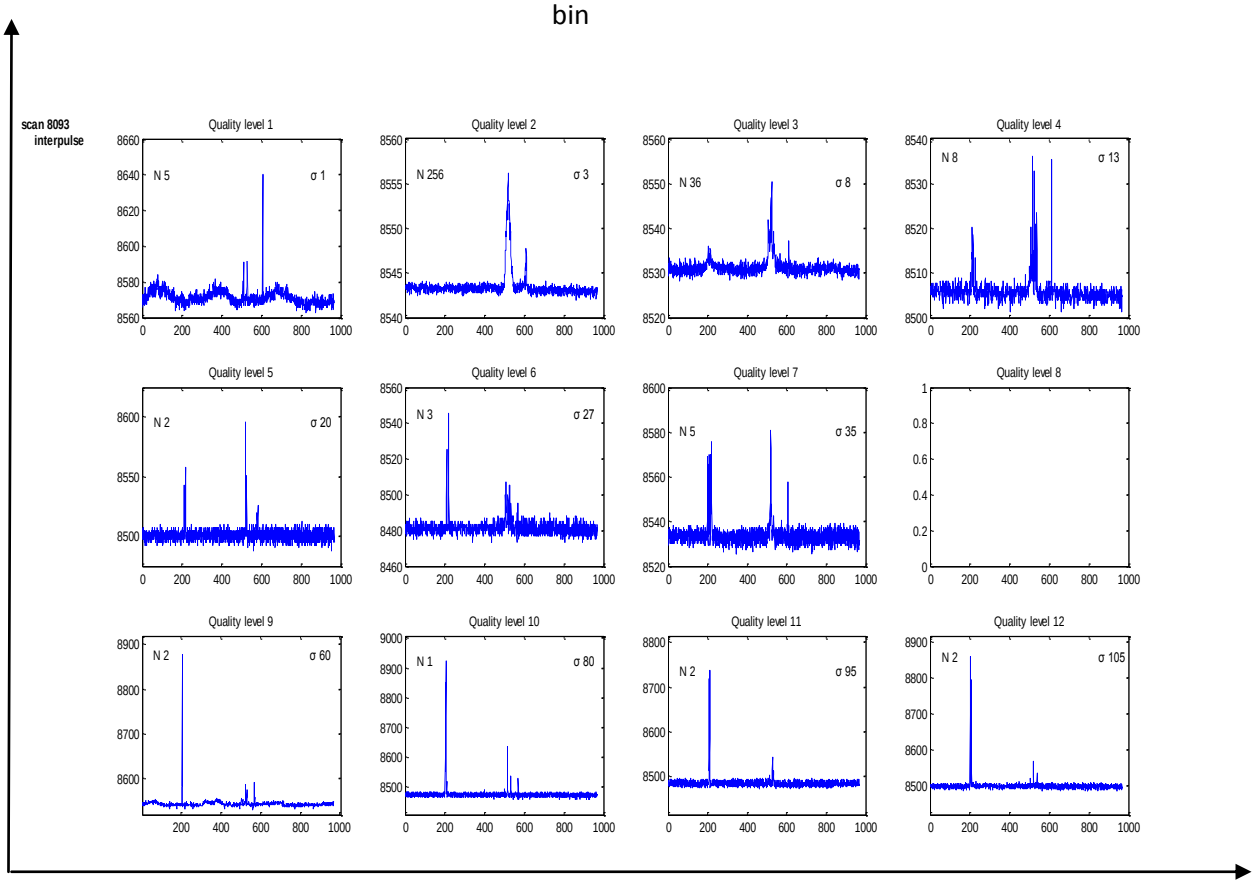

bin

V/f counts

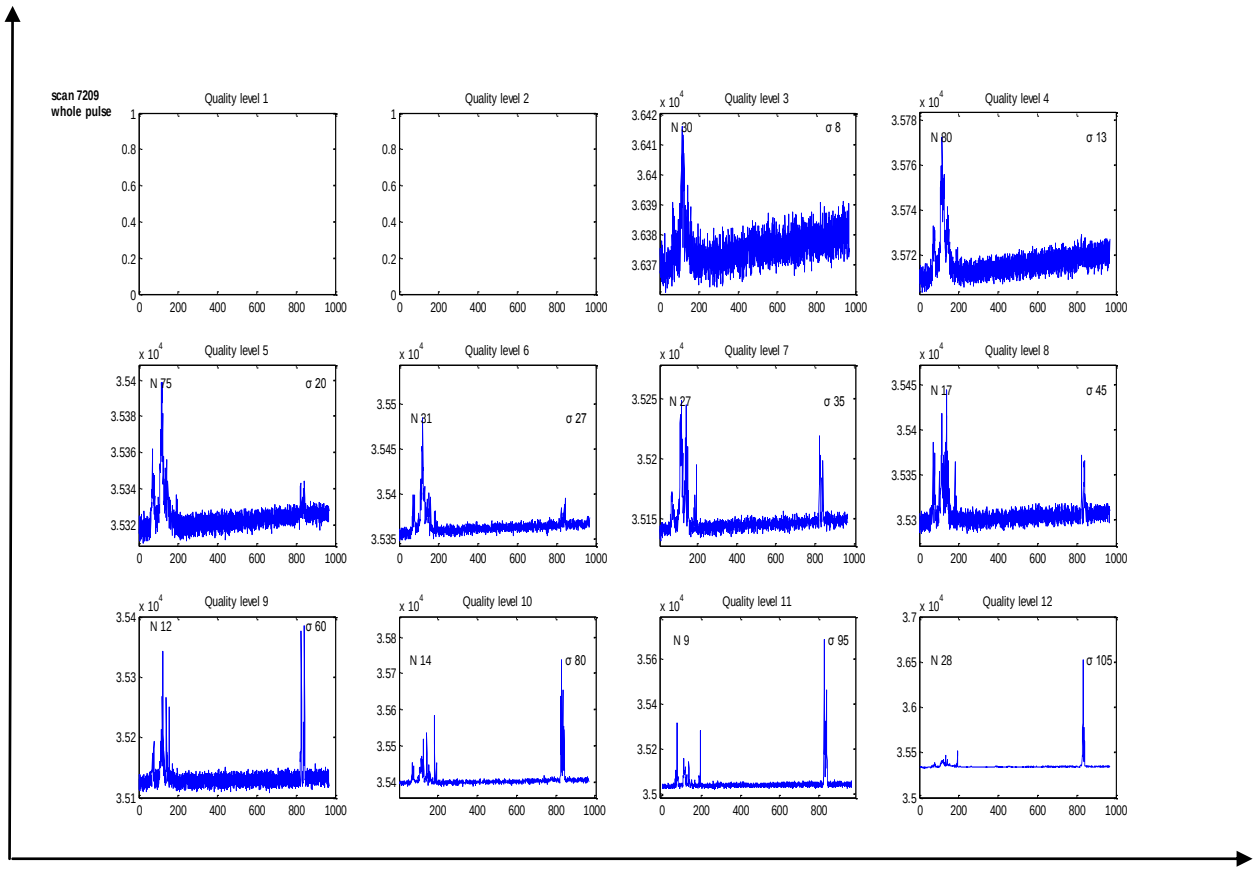

bin

V/f counts

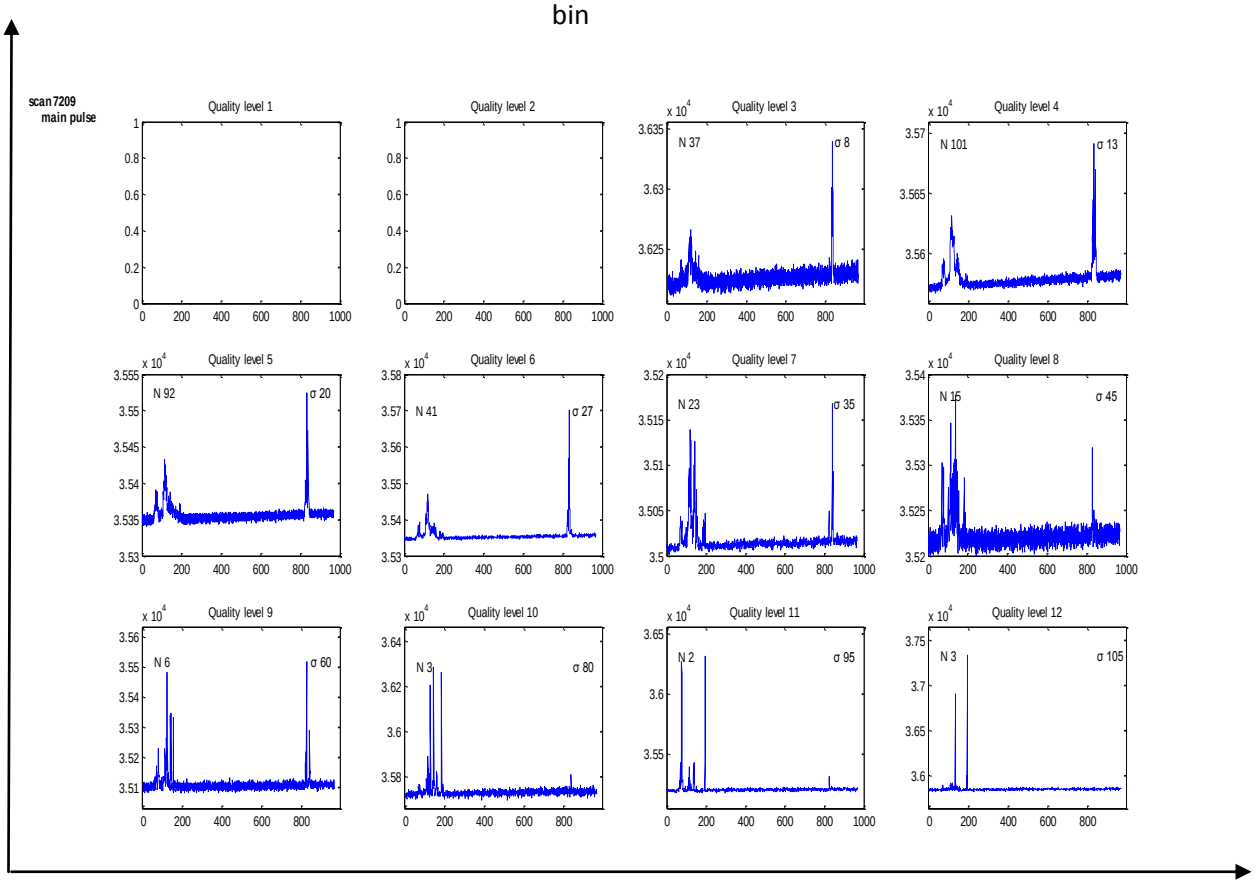

bin

V/f counts

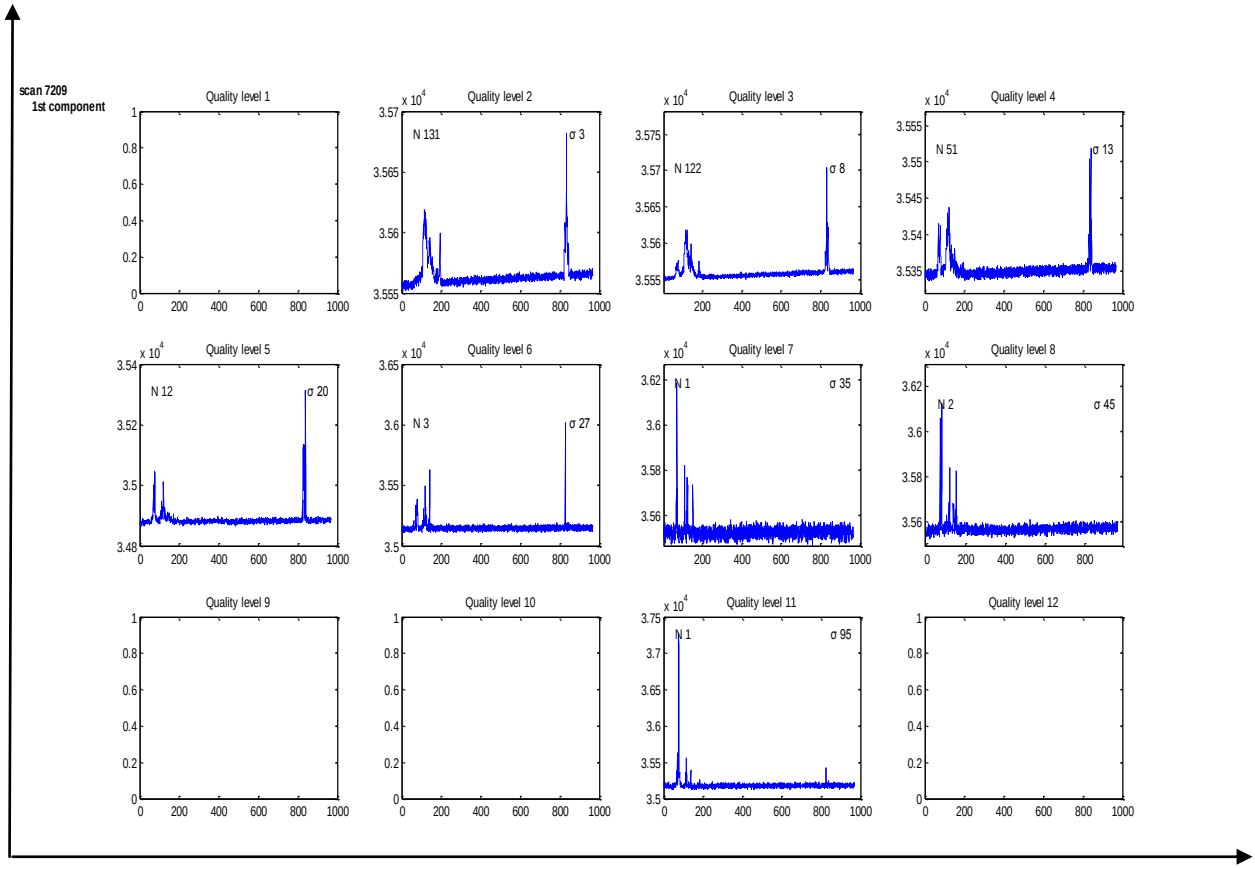

bin

V/f counts

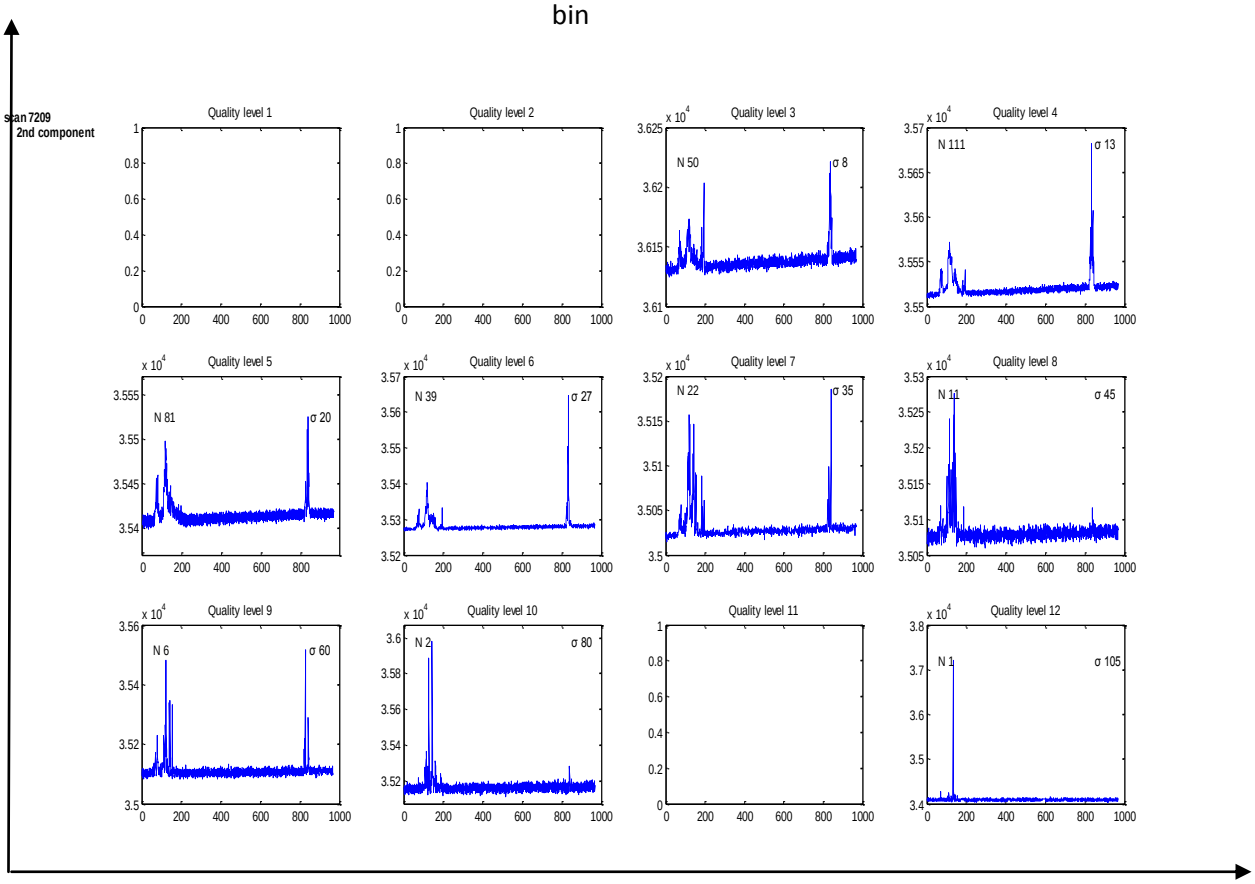

bin

V/f counts

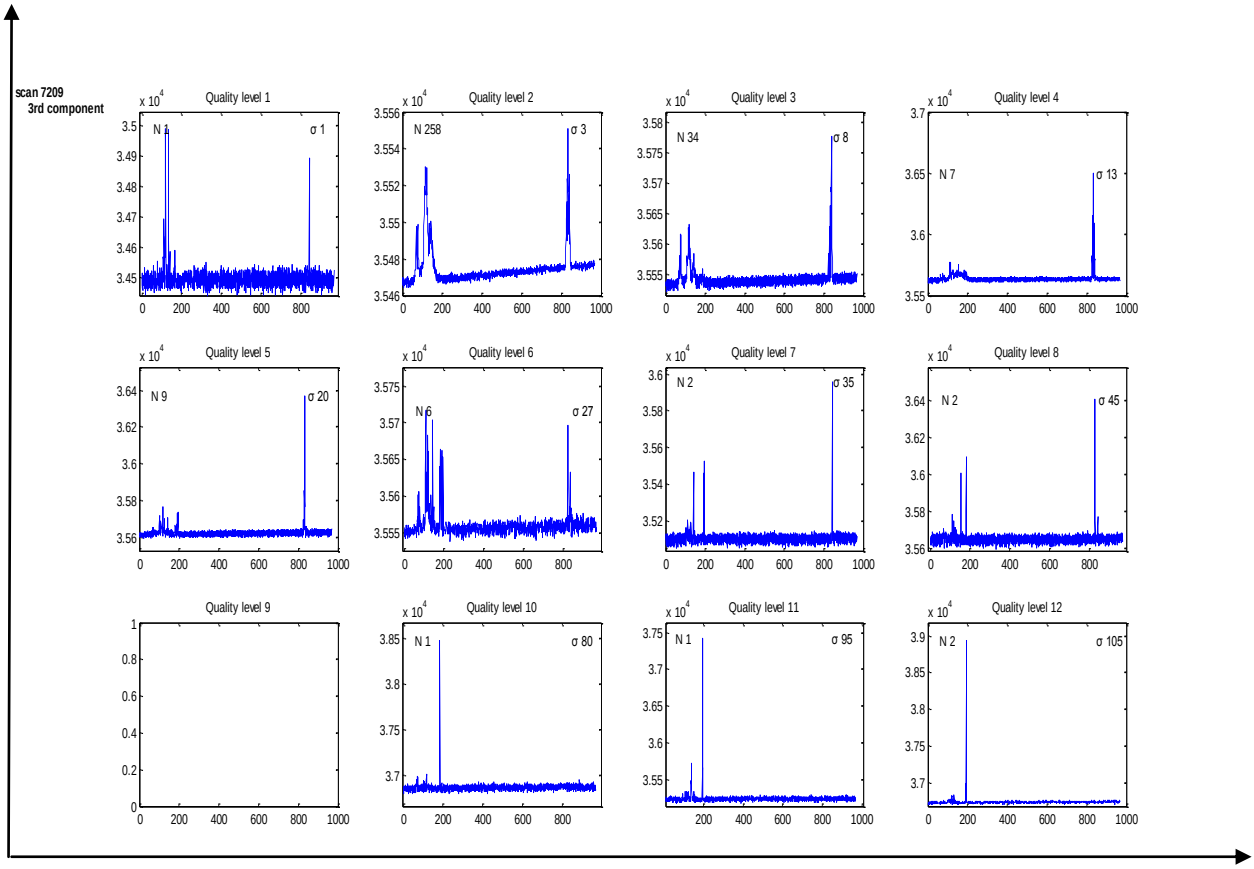

bin

V/f counts

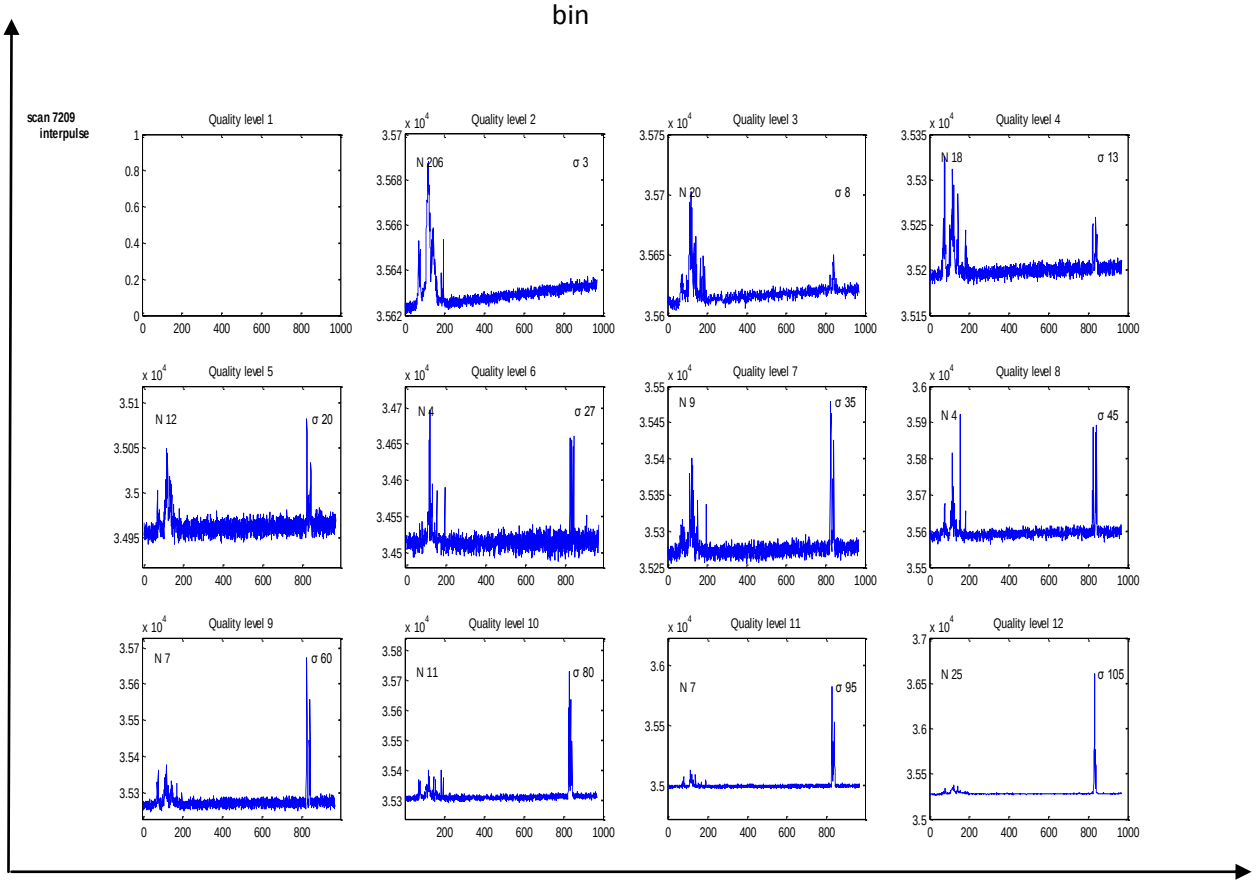

bin

V/f counts

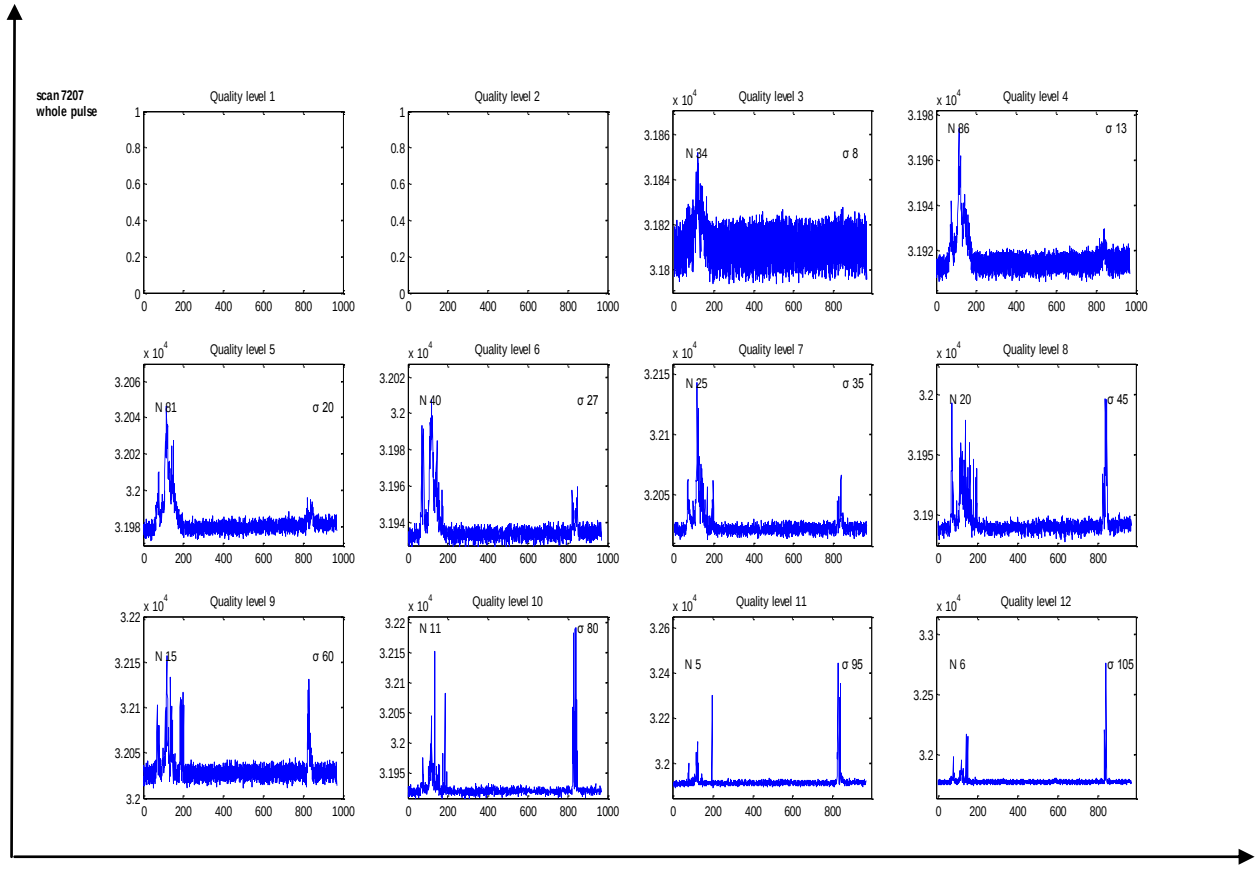

bin

V/f counts

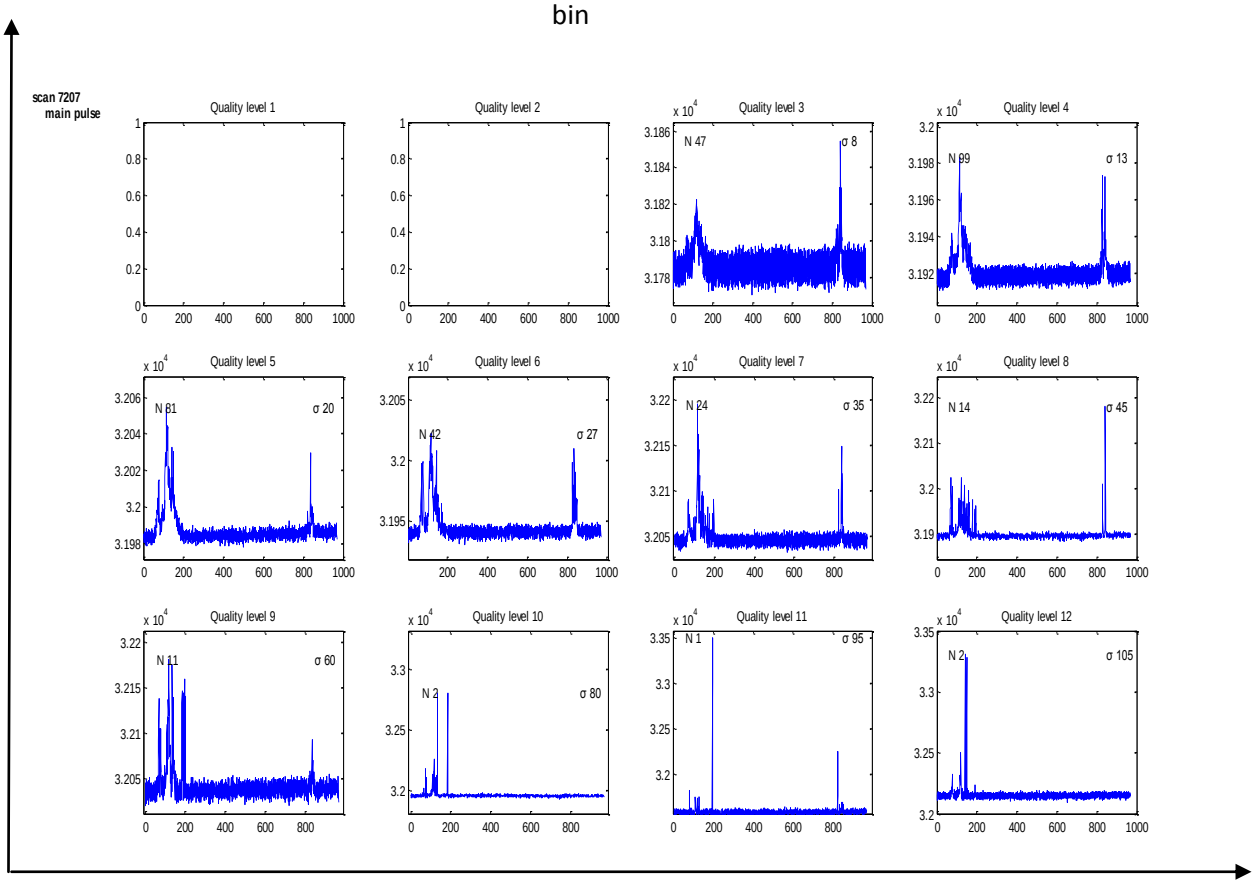

bin

V/f counts

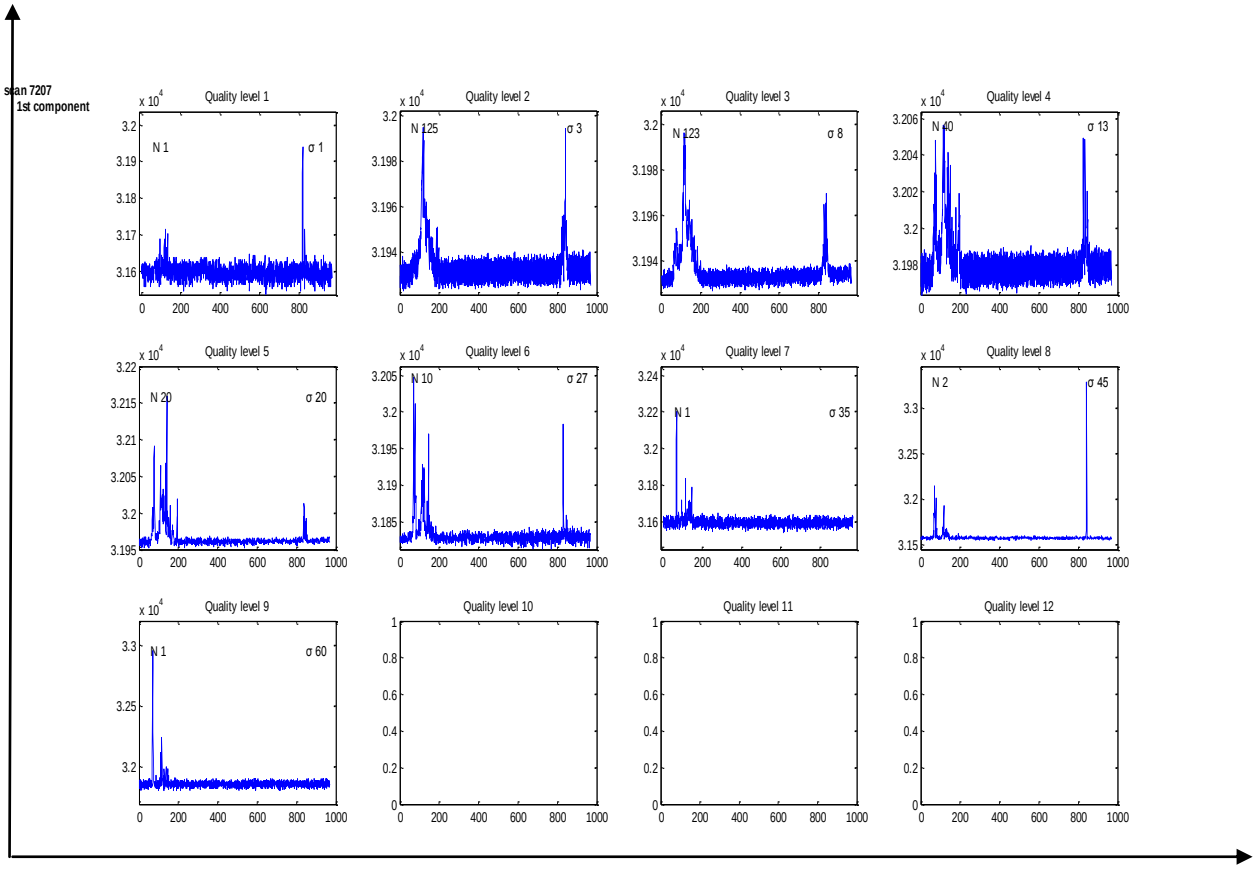

bin

V/f counts

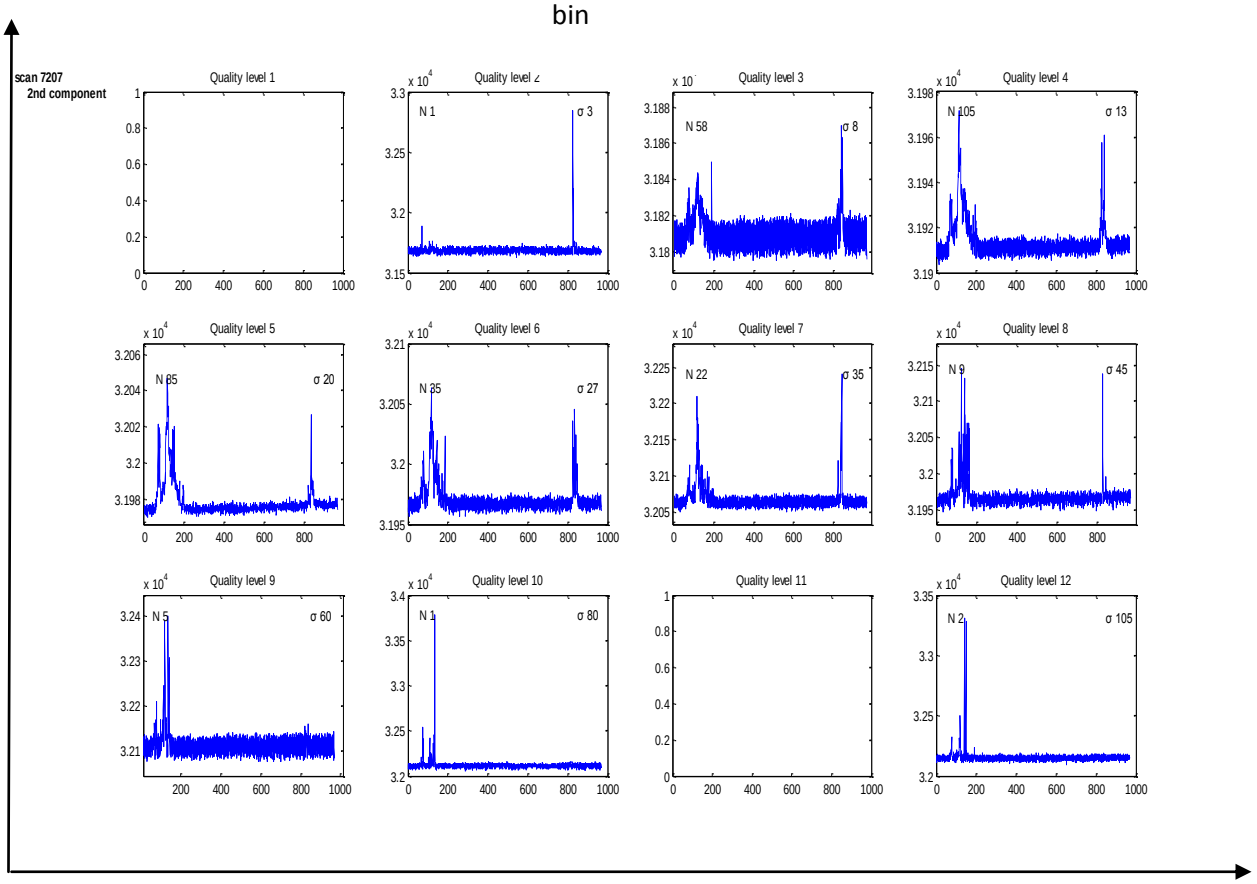

bin

V/f counts

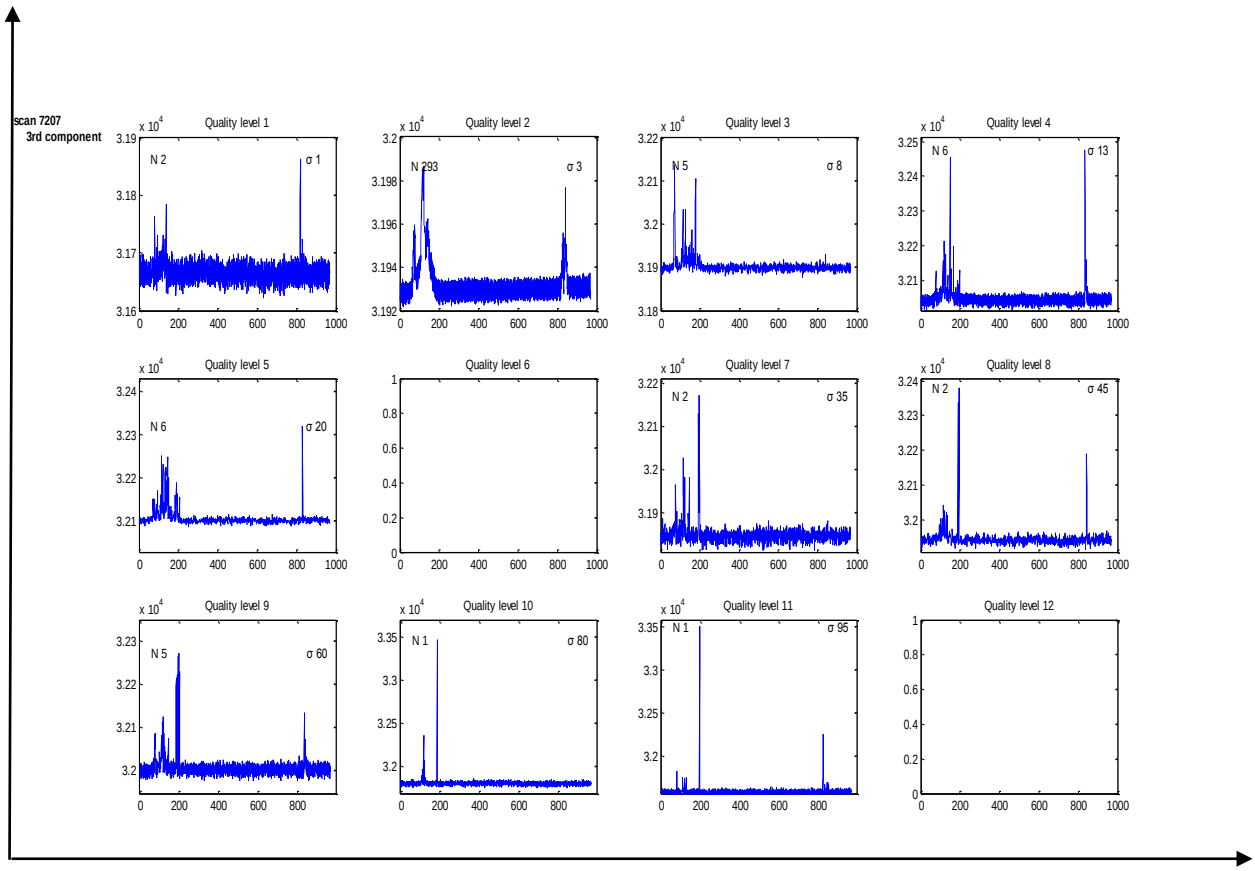

bin

V/f counts

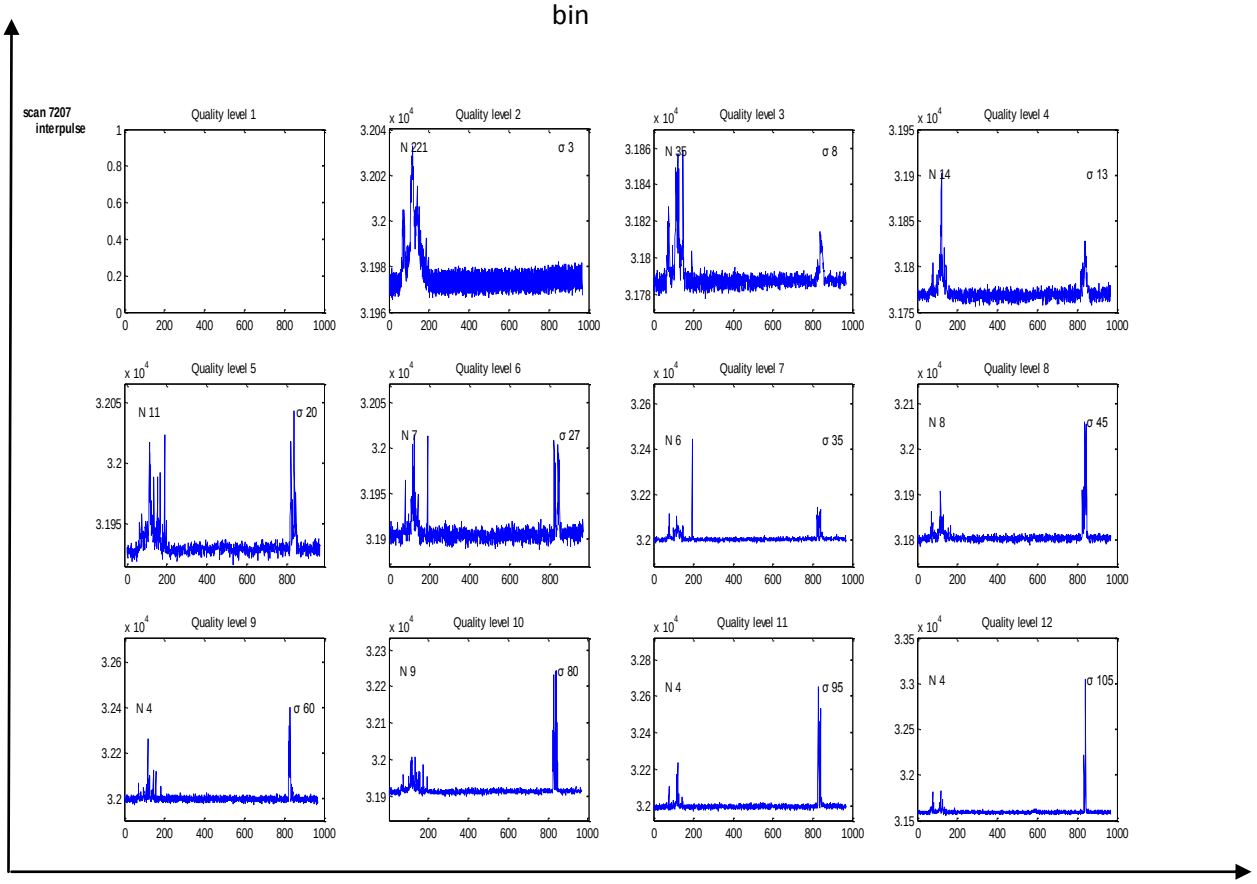

bin

V/f counts

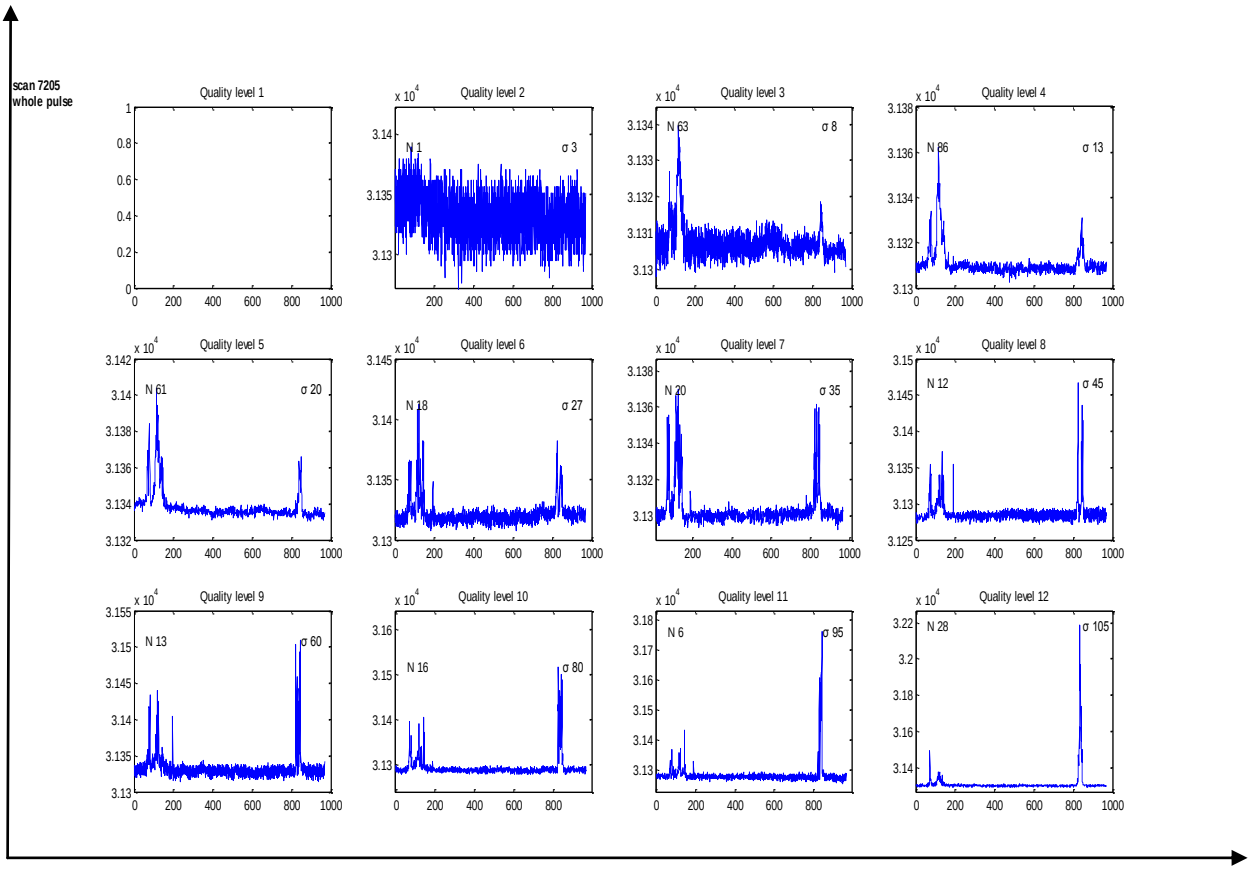

bin

V/f counts

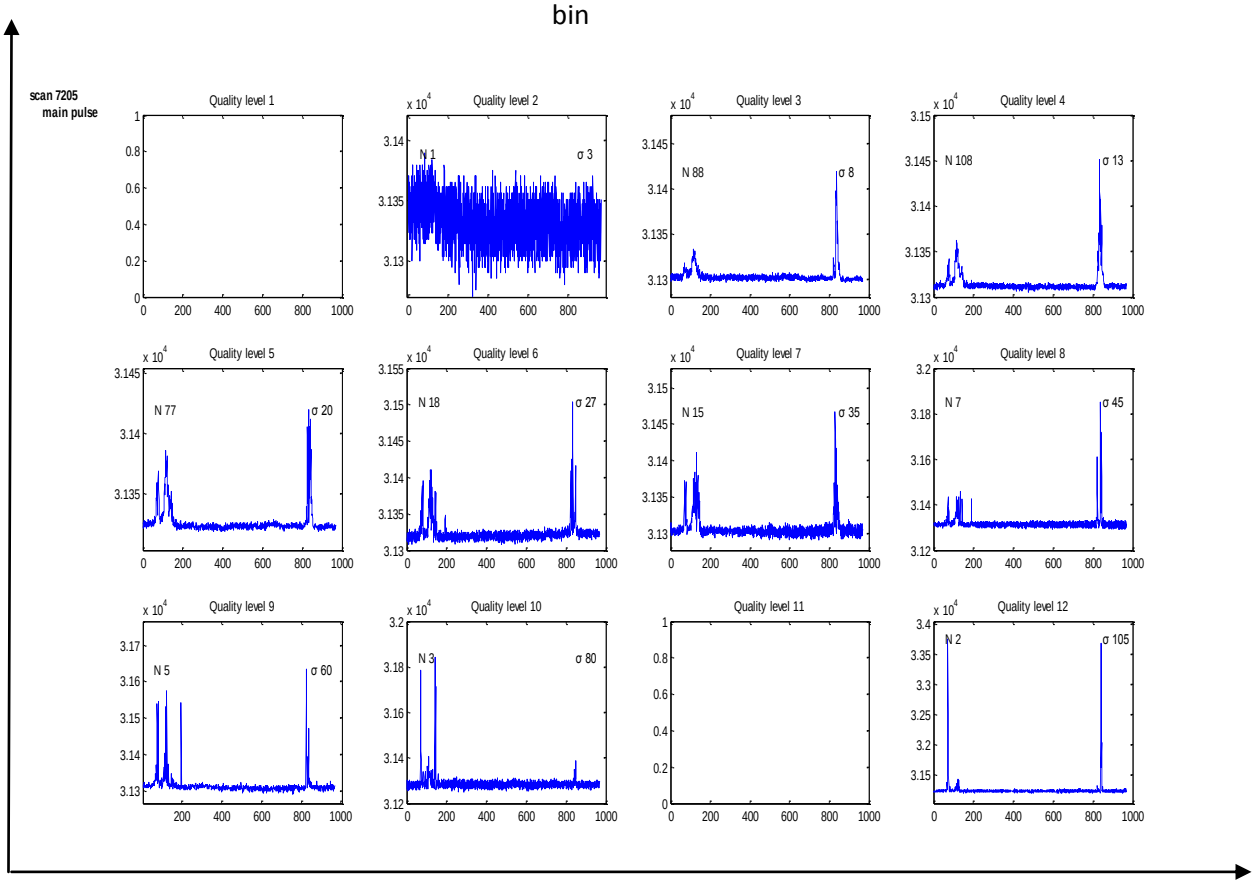

bin

V/f counts

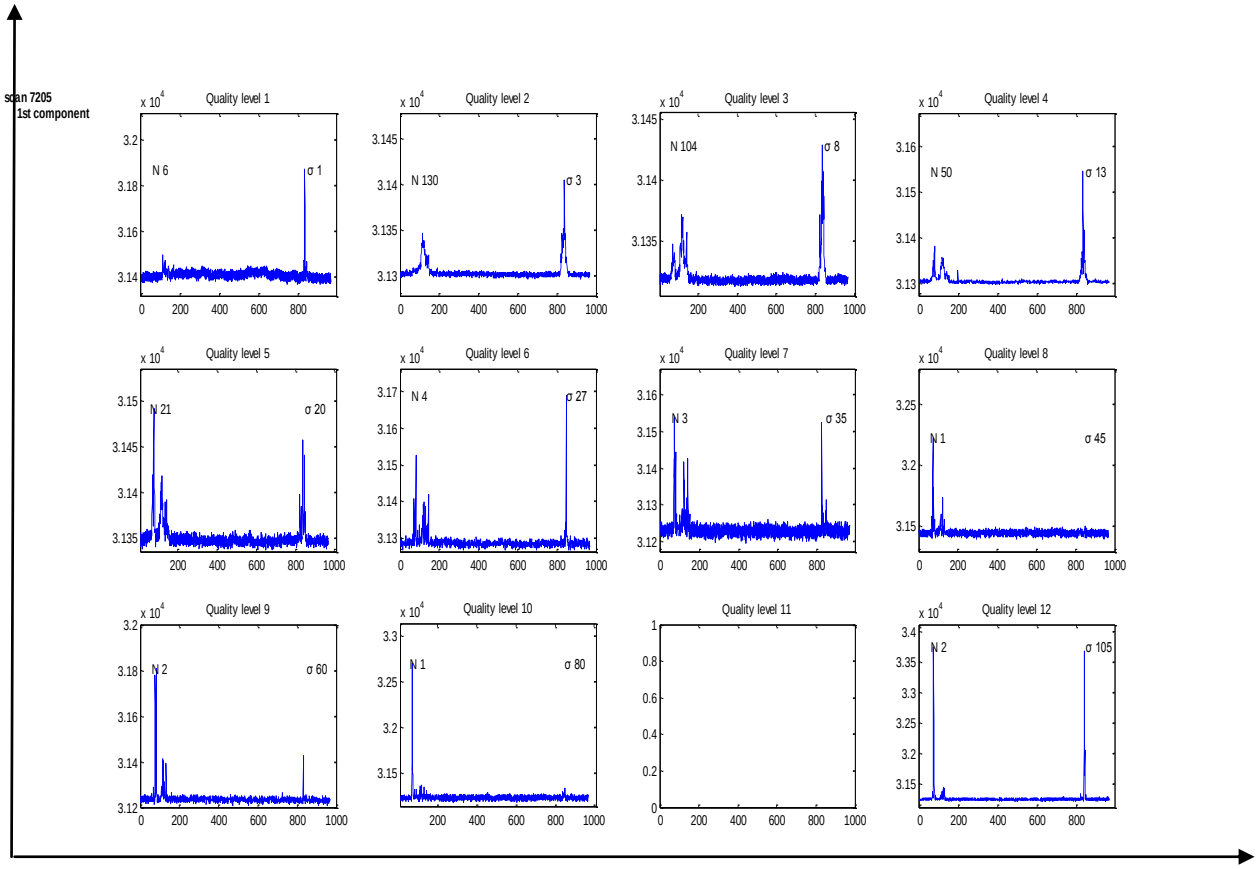

bin

V/f counts

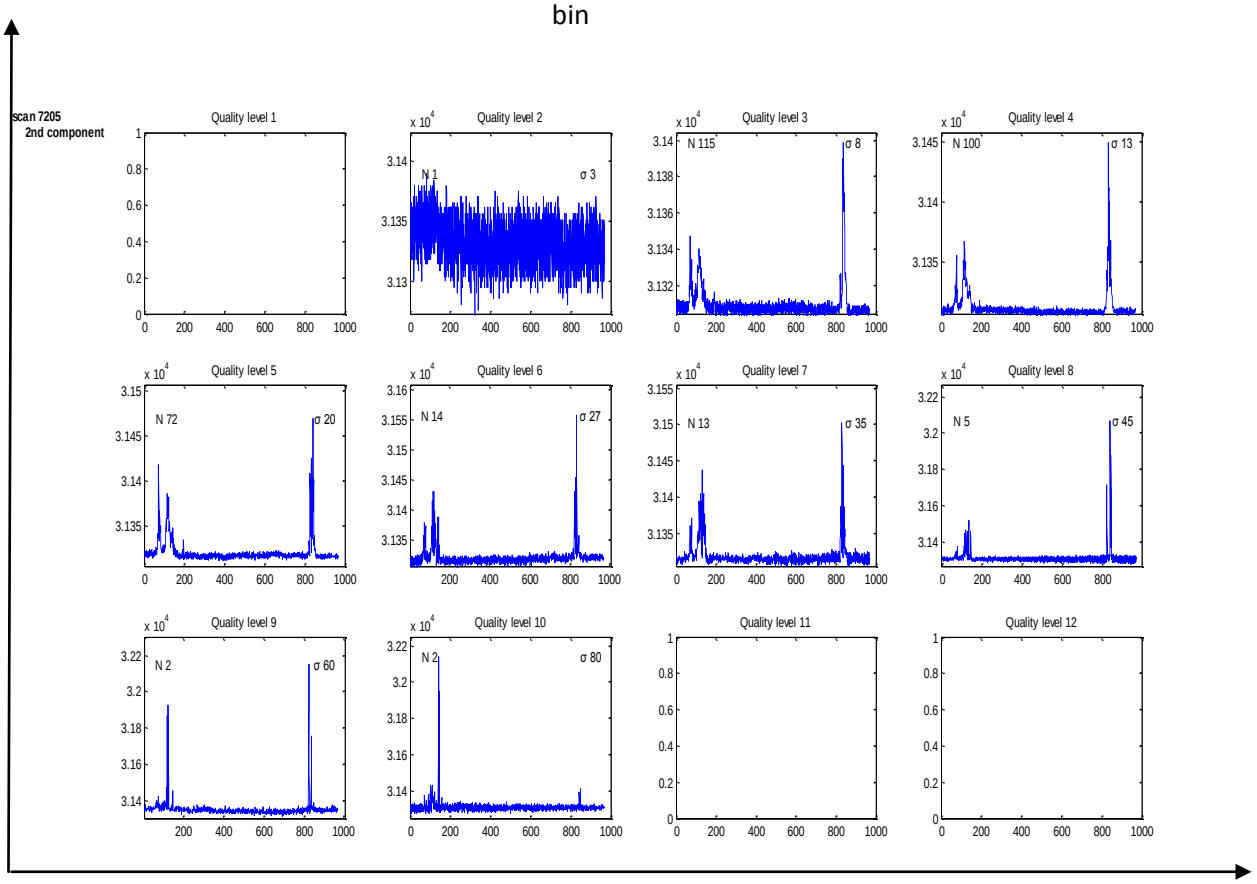

bin

V/f counts

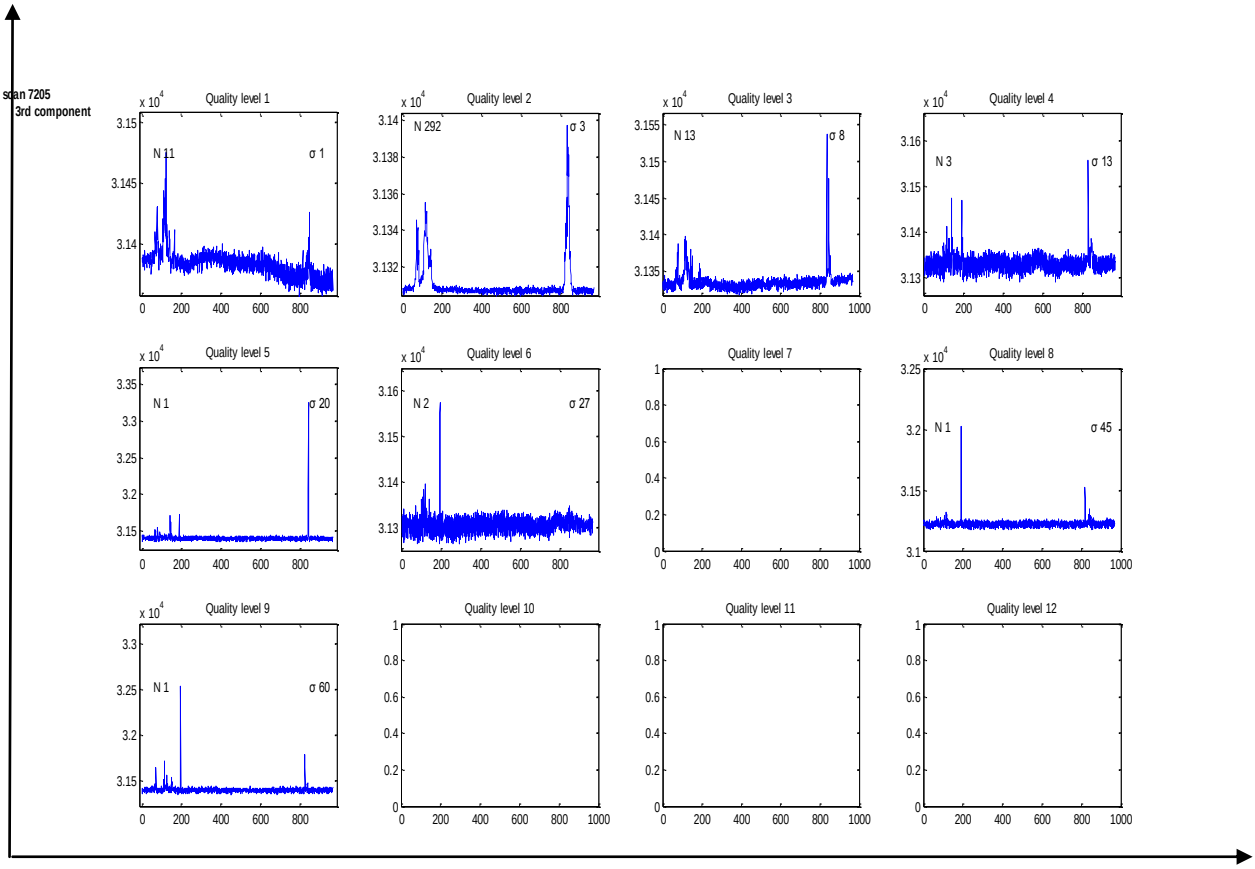

bin

V/f counts

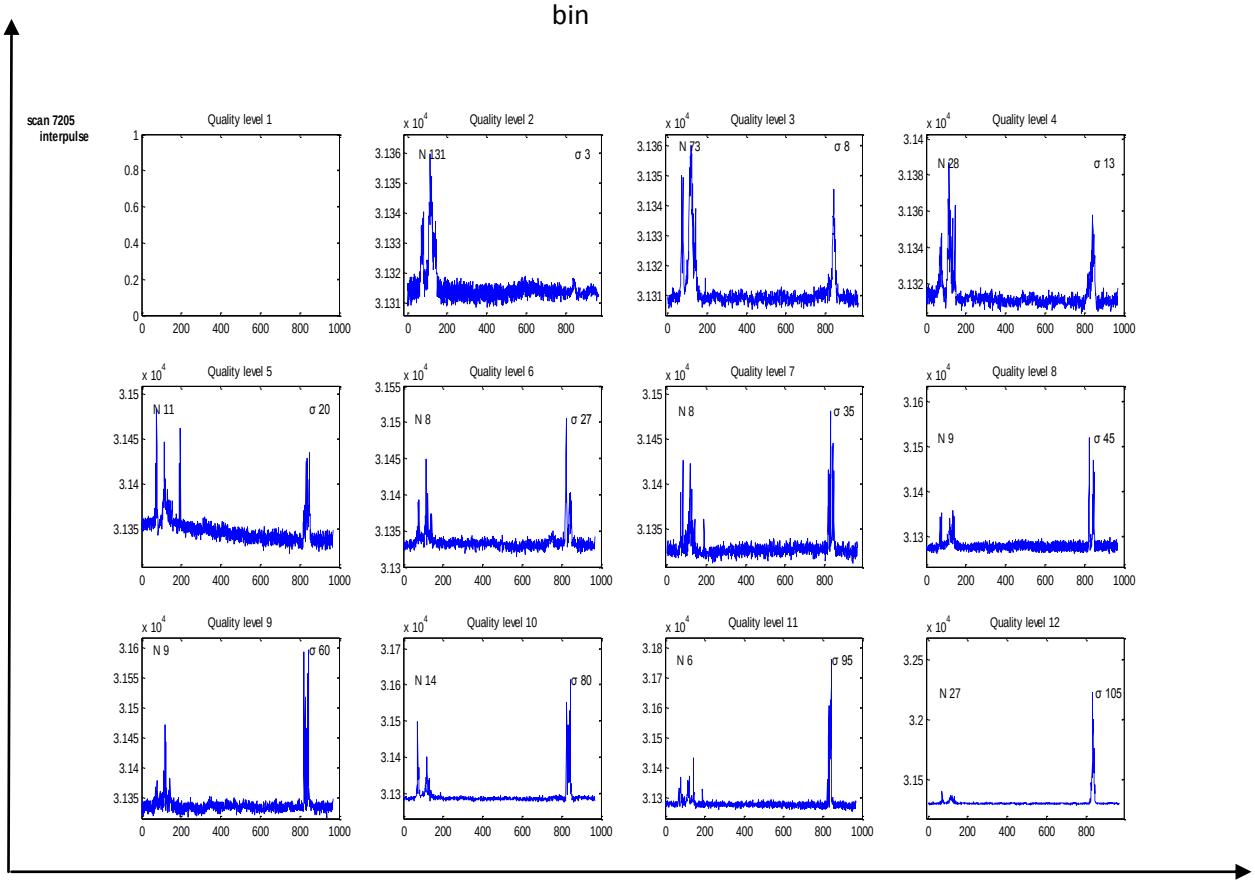

bin

V/f counts

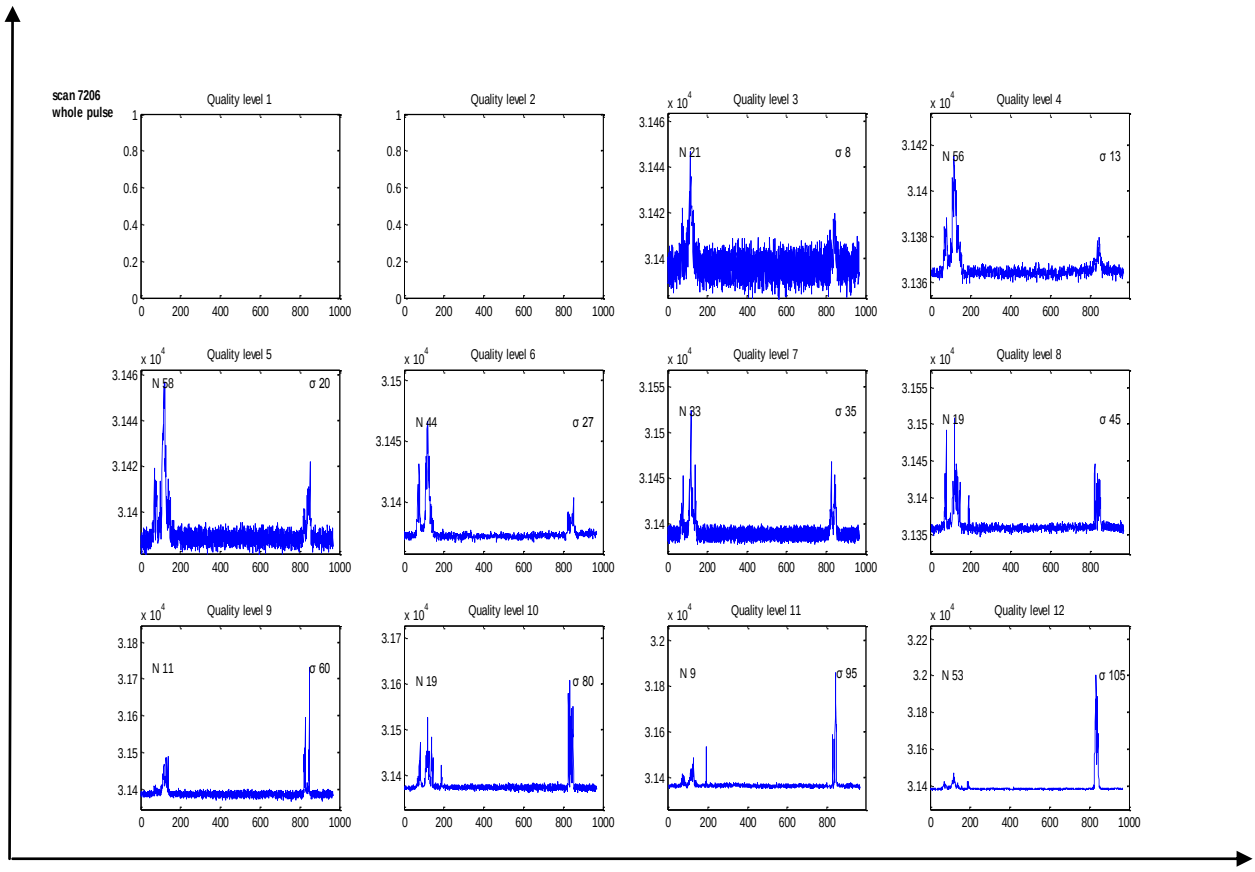

bin

V/f counts

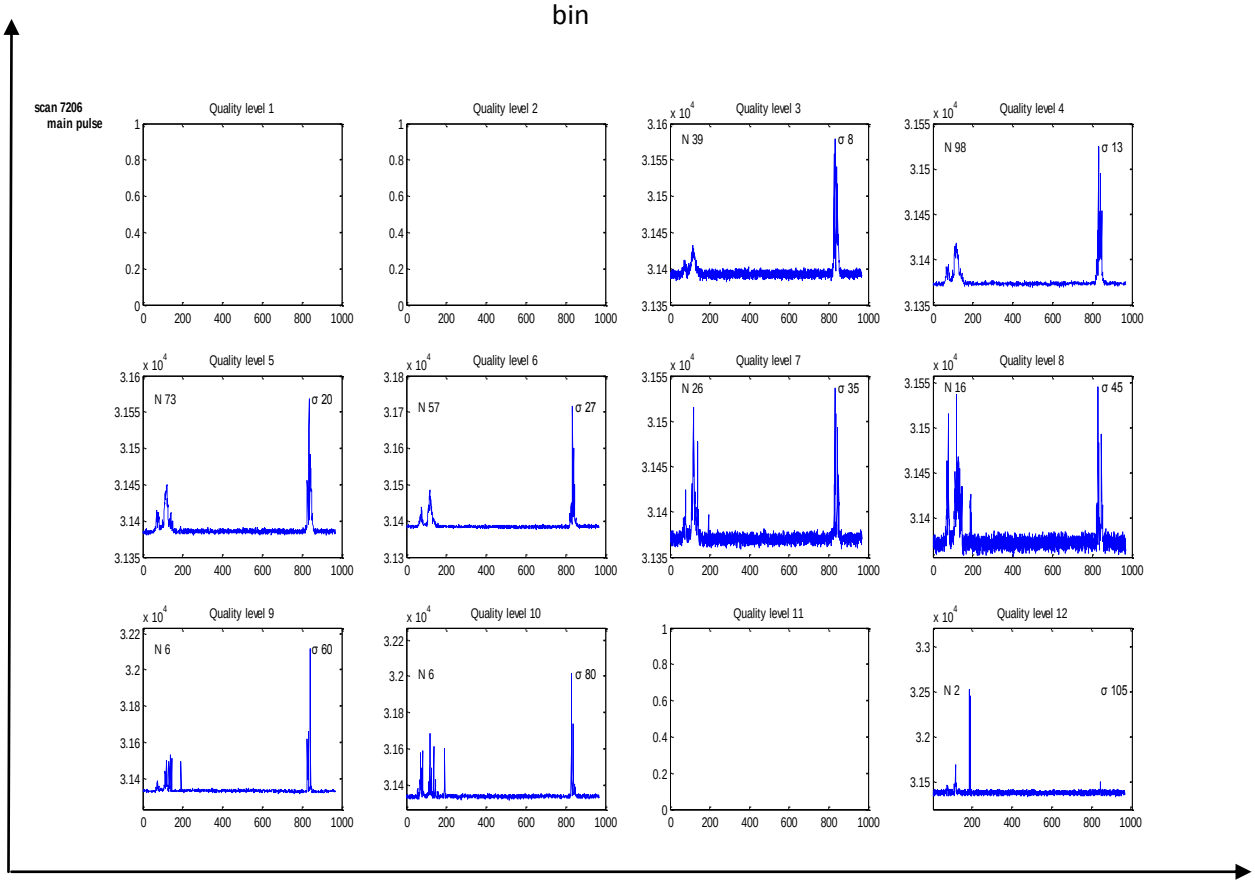

bin

V/f counts

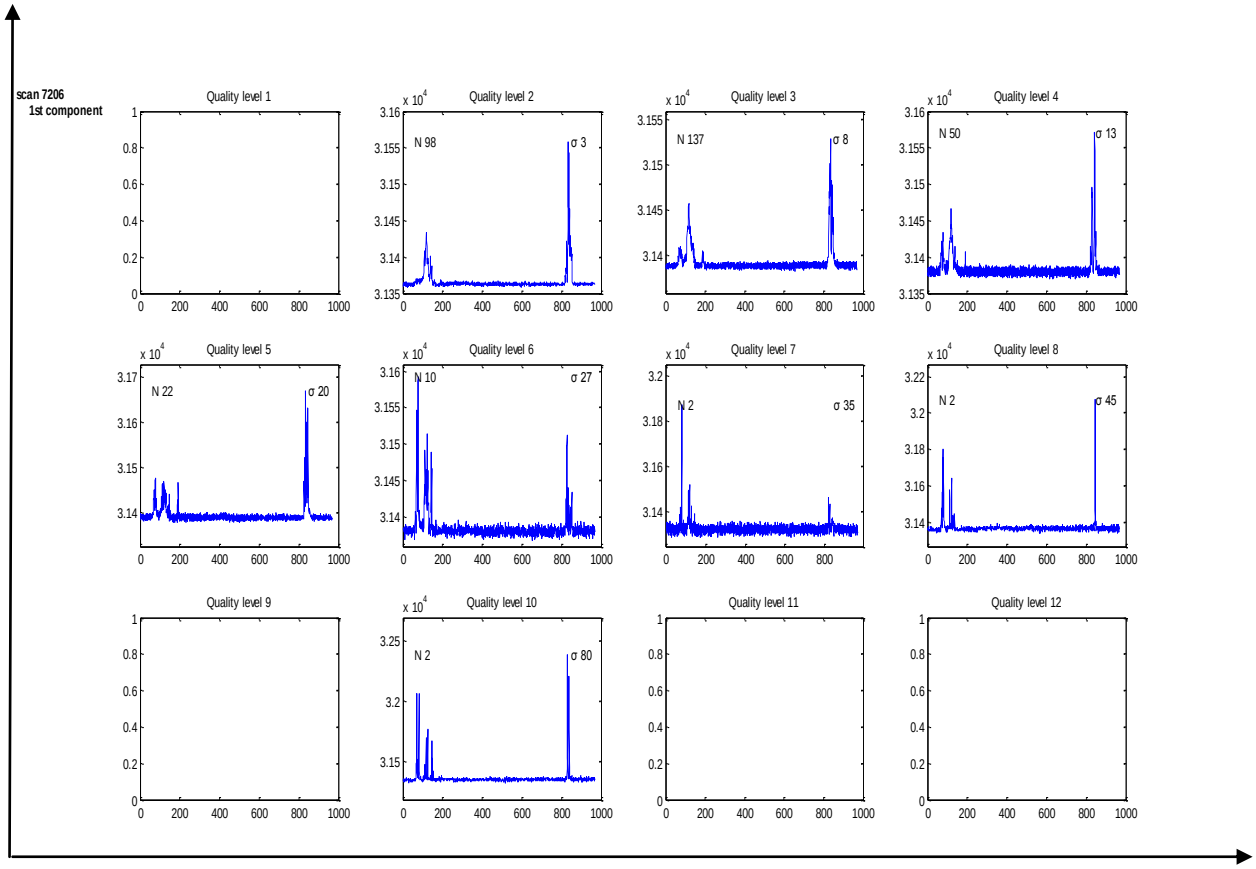

bin

V/f counts

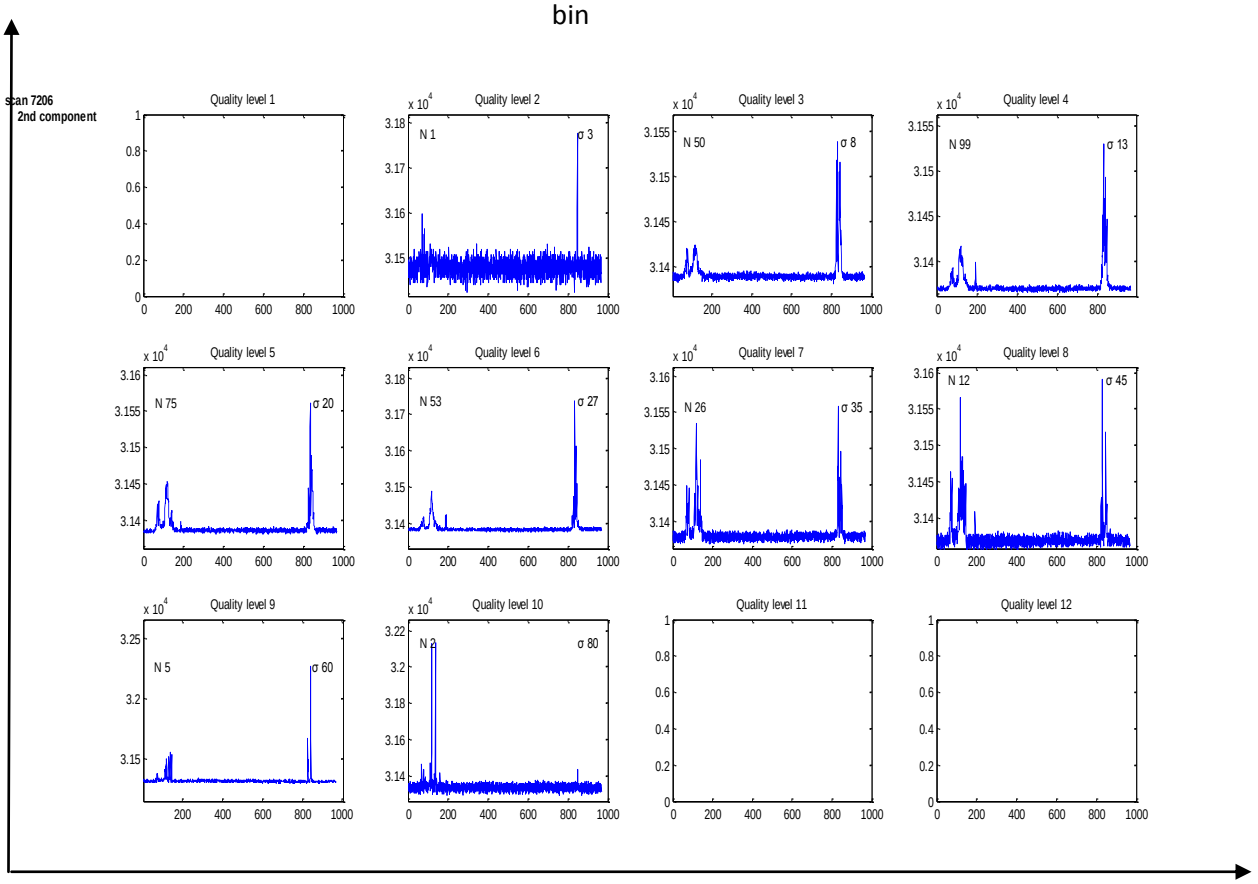

bin

V/f counts

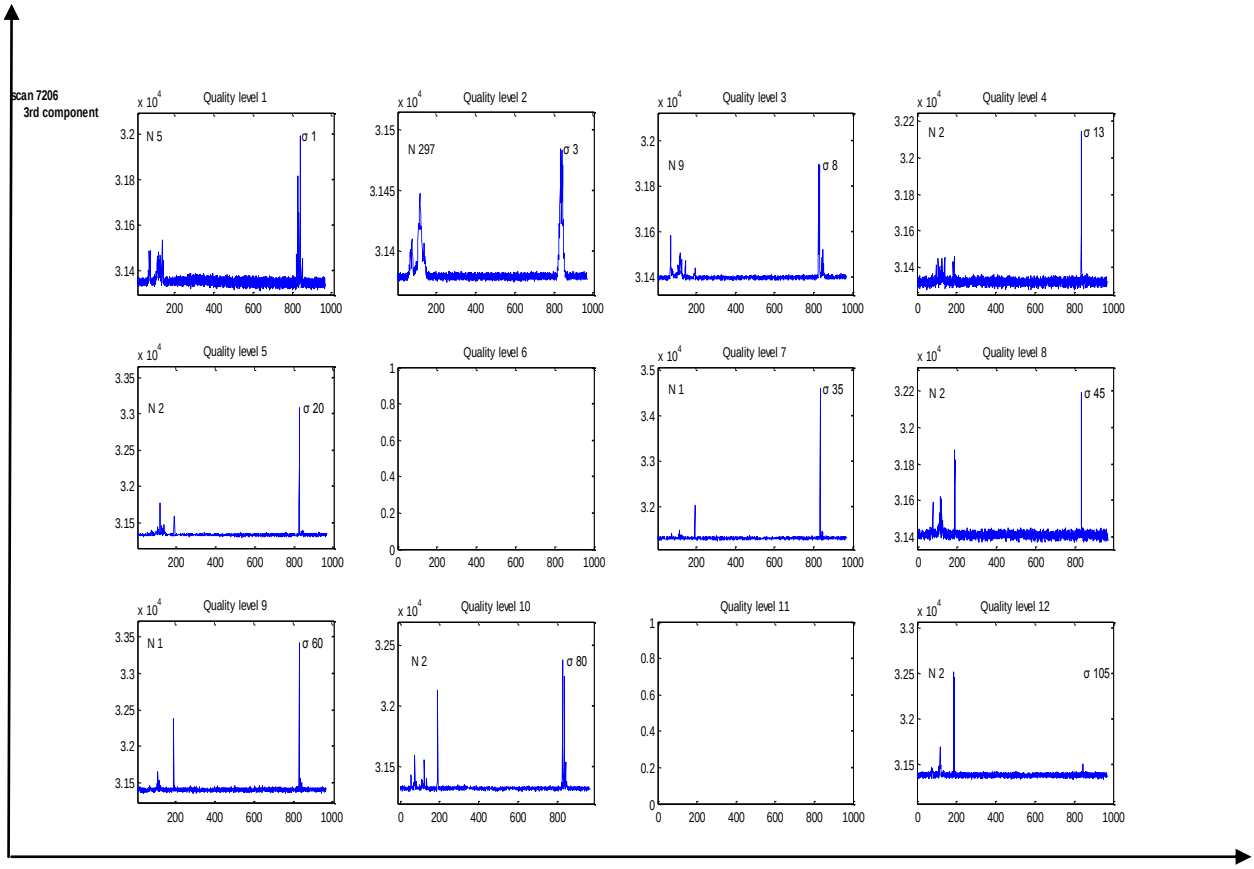

bin

V/f counts

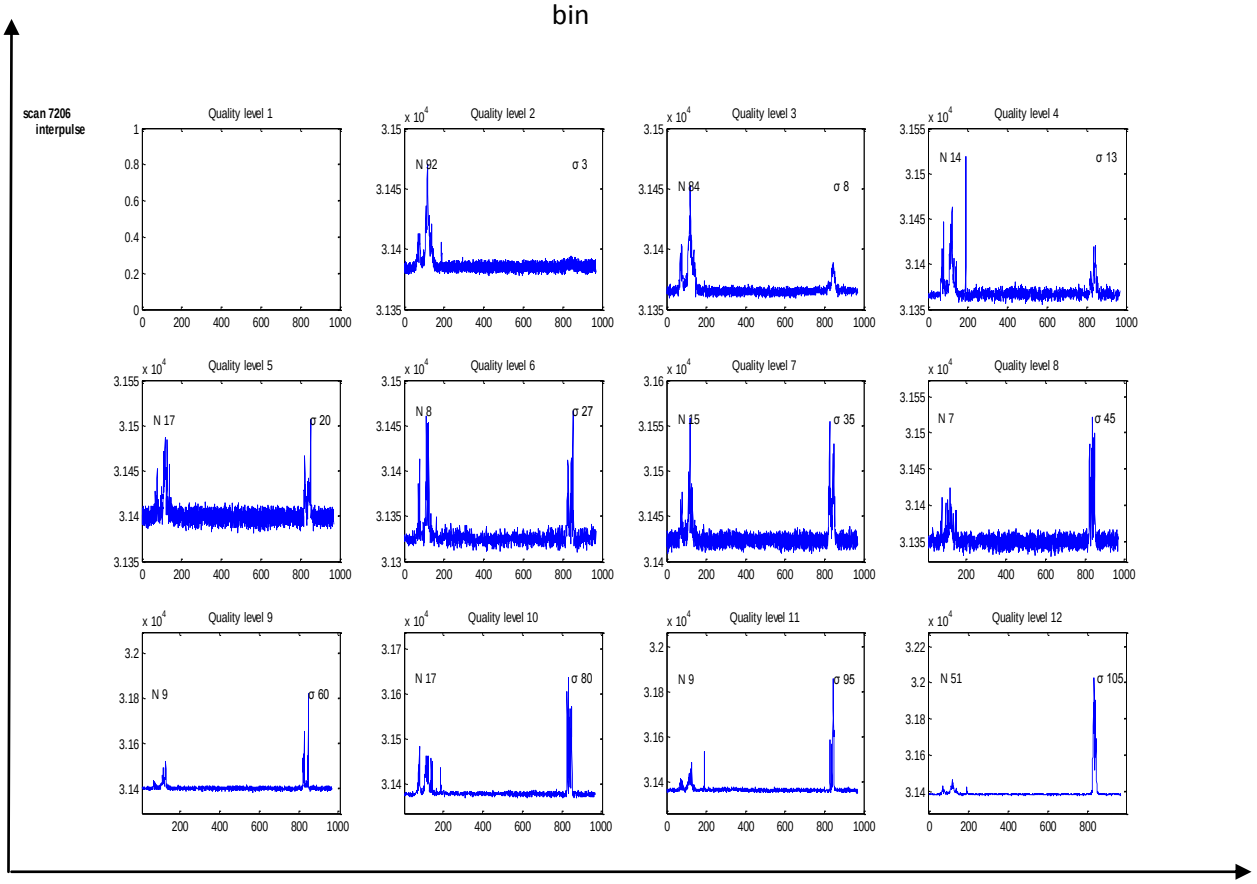

bin

V/f counts

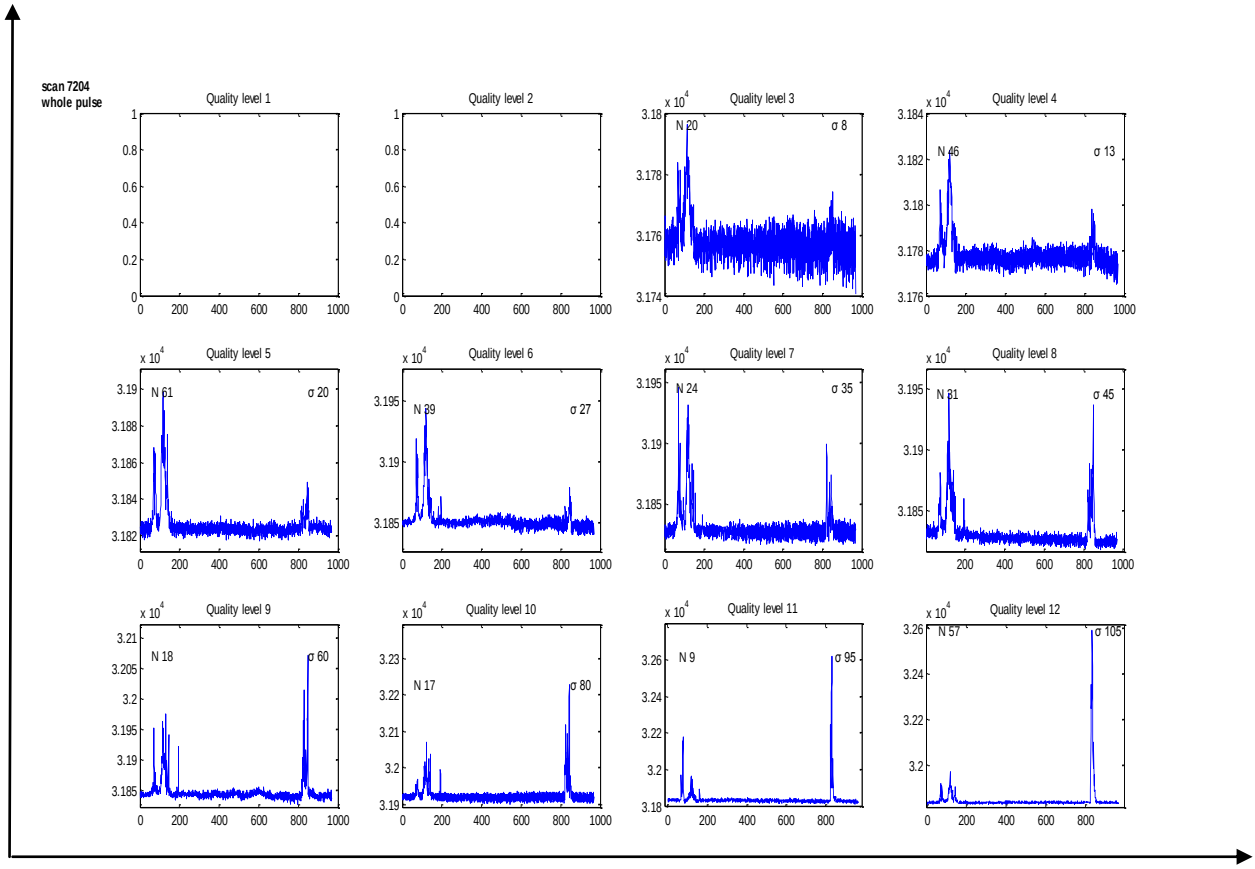

bin

V/f counts

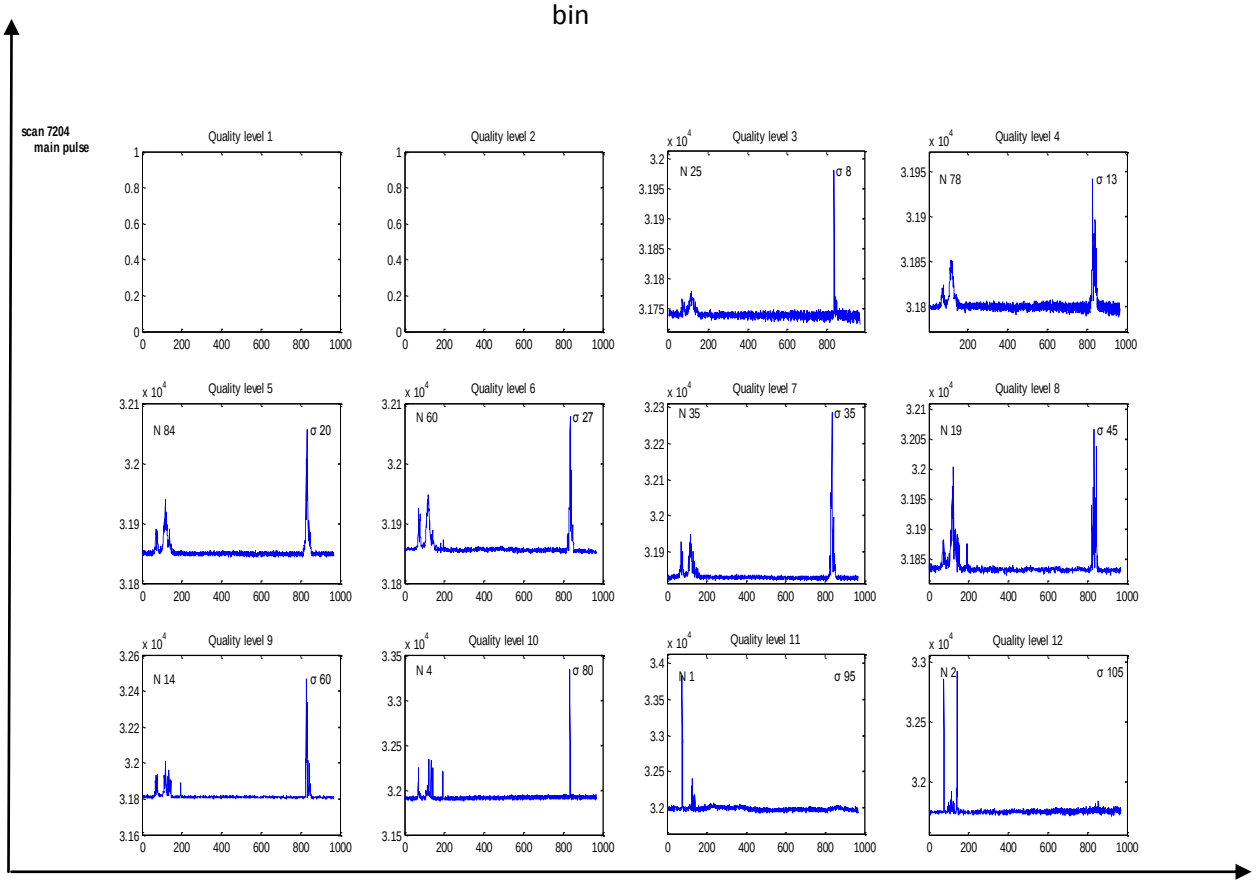

bin

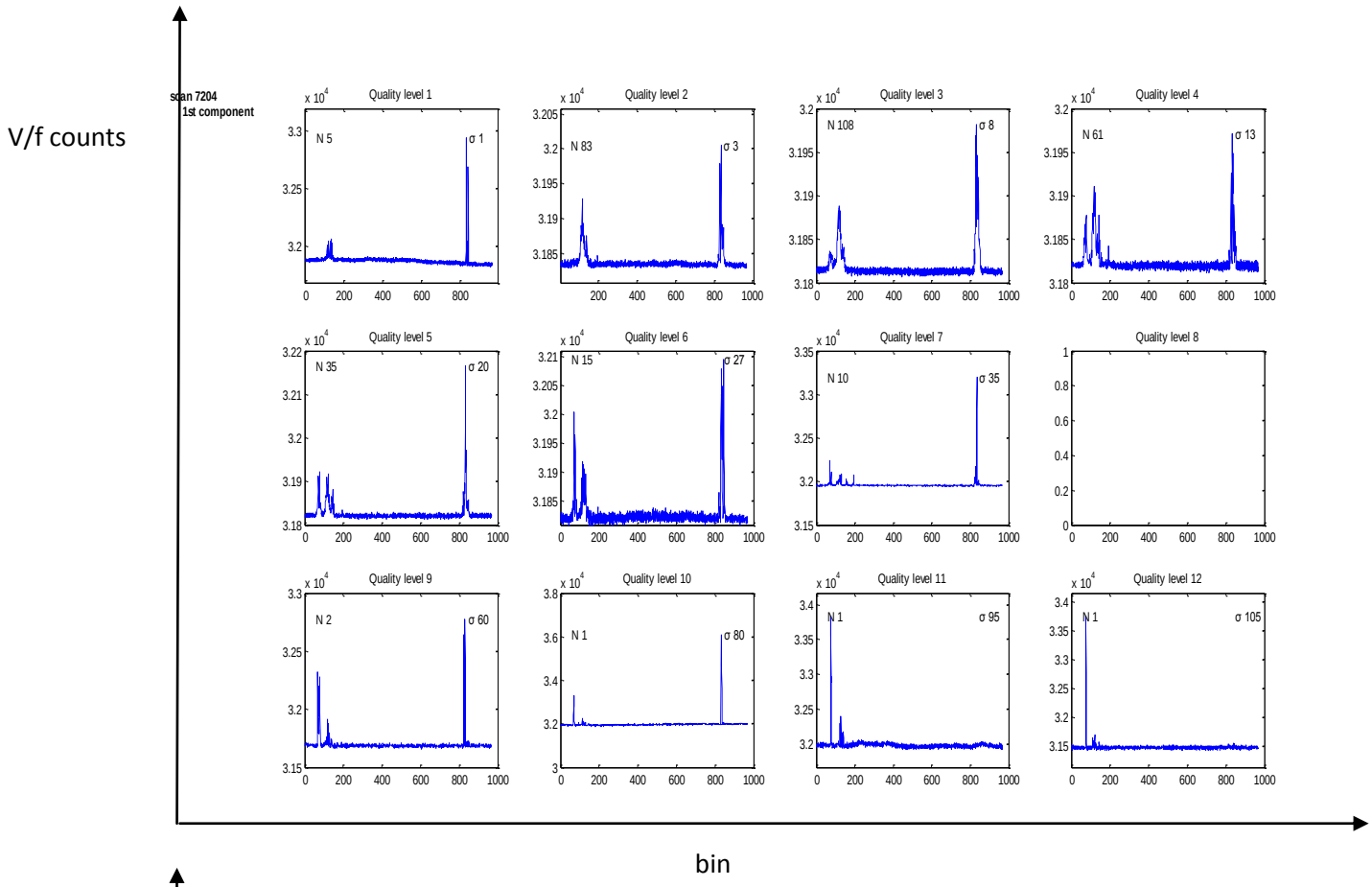
V/f counts
scan 7204
1st component
Quality level 1
N 5
σ 1
Quality level 2
N 83
σ 3
Quality level 3
N 108
σ 8
Quality level 4
N 61
σ 13
Quality level 5
N 35
σ 20
Quality level 6
N 15
σ 27
Quality level 7
N 10
σ 35
Quality level 8
Quality level 9
N 2
σ 60
Quality level 10
N 1
σ 80
Quality level 11
N 1
σ 95
Quality level 12
N 1
σ 105
bin

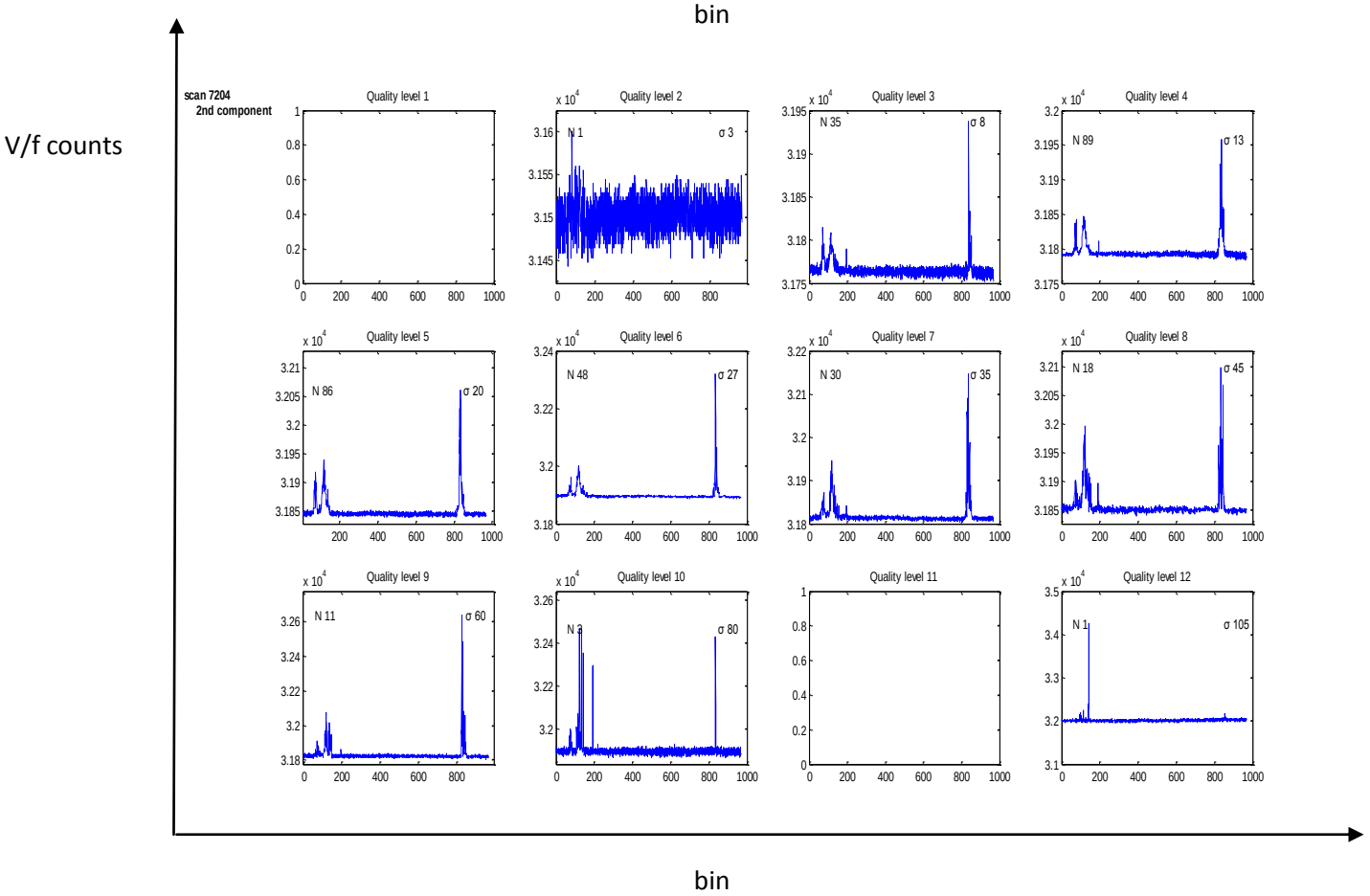
V/f counts
scan 7204
2nd component
Quality level 1
Quality level 2
N 1
σ 3
Quality level 3
N 35
σ 8
Quality level 4
N 89
σ 13
Quality level 5
N 86
σ 20
Quality level 6
N 48
σ 27
Quality level 7
N 30
σ 35
Quality level 8
N 18
σ 45
Quality level 9
N 11
σ 60
Quality level 10
N 2
σ 80
Quality level 11
Quality level 12
N 1
σ 105
bin

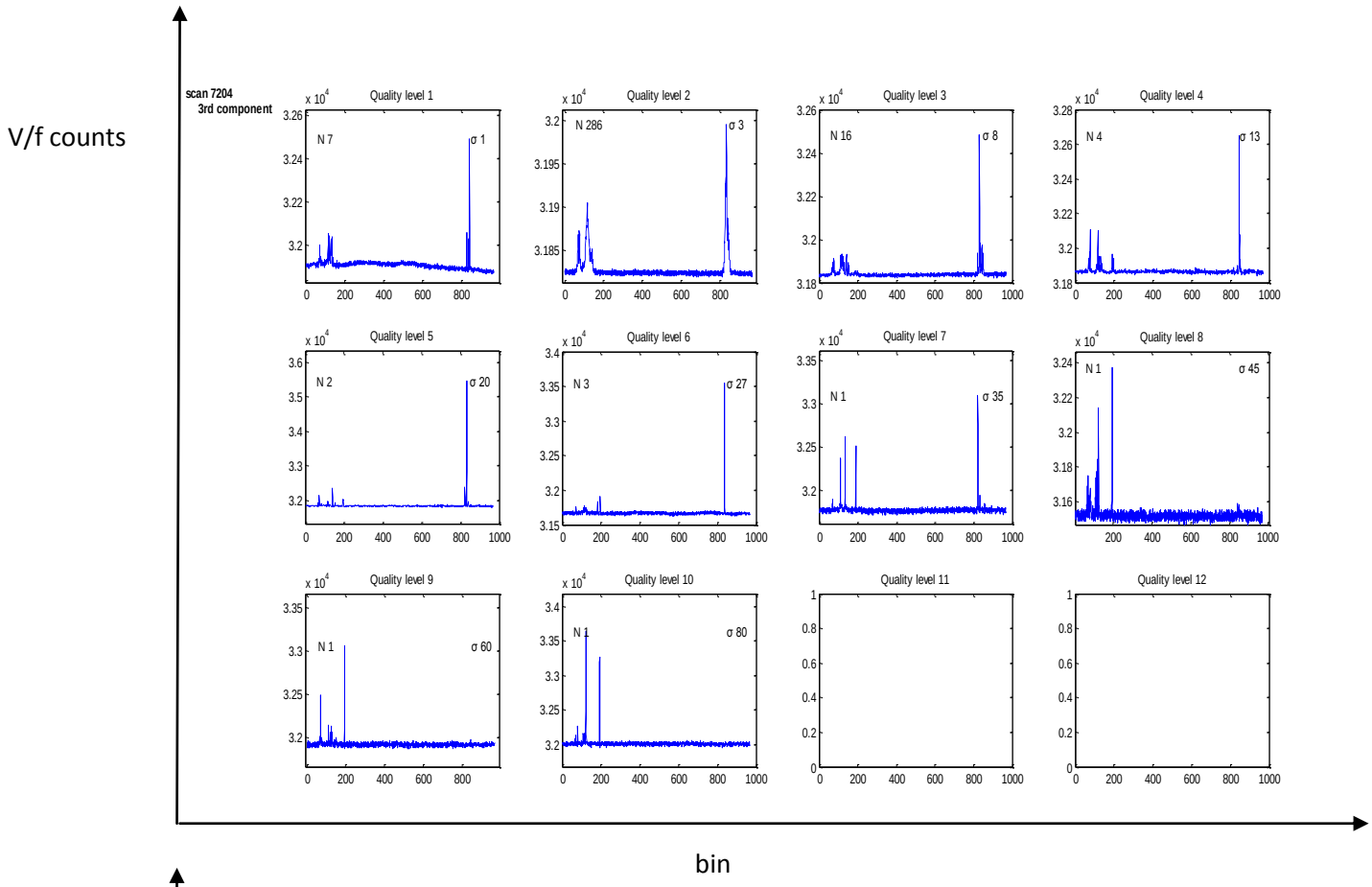
V/f counts
scan 7204
3rd component
Quality level 1
N 7
σ 1
Quality level 2
N 286
σ 3
Quality level 3
N 16
σ 8
Quality level 4
N 4
σ 13
Quality level 5
N 2
σ 20
Quality level 6
N 3
σ 27
Quality level 7
N 1
σ 35
Quality level 8
N 1
σ 45
Quality level 9
N 1
σ 60
Quality level 10
N 1
σ 80
Quality level 11
Quality level 12
bin

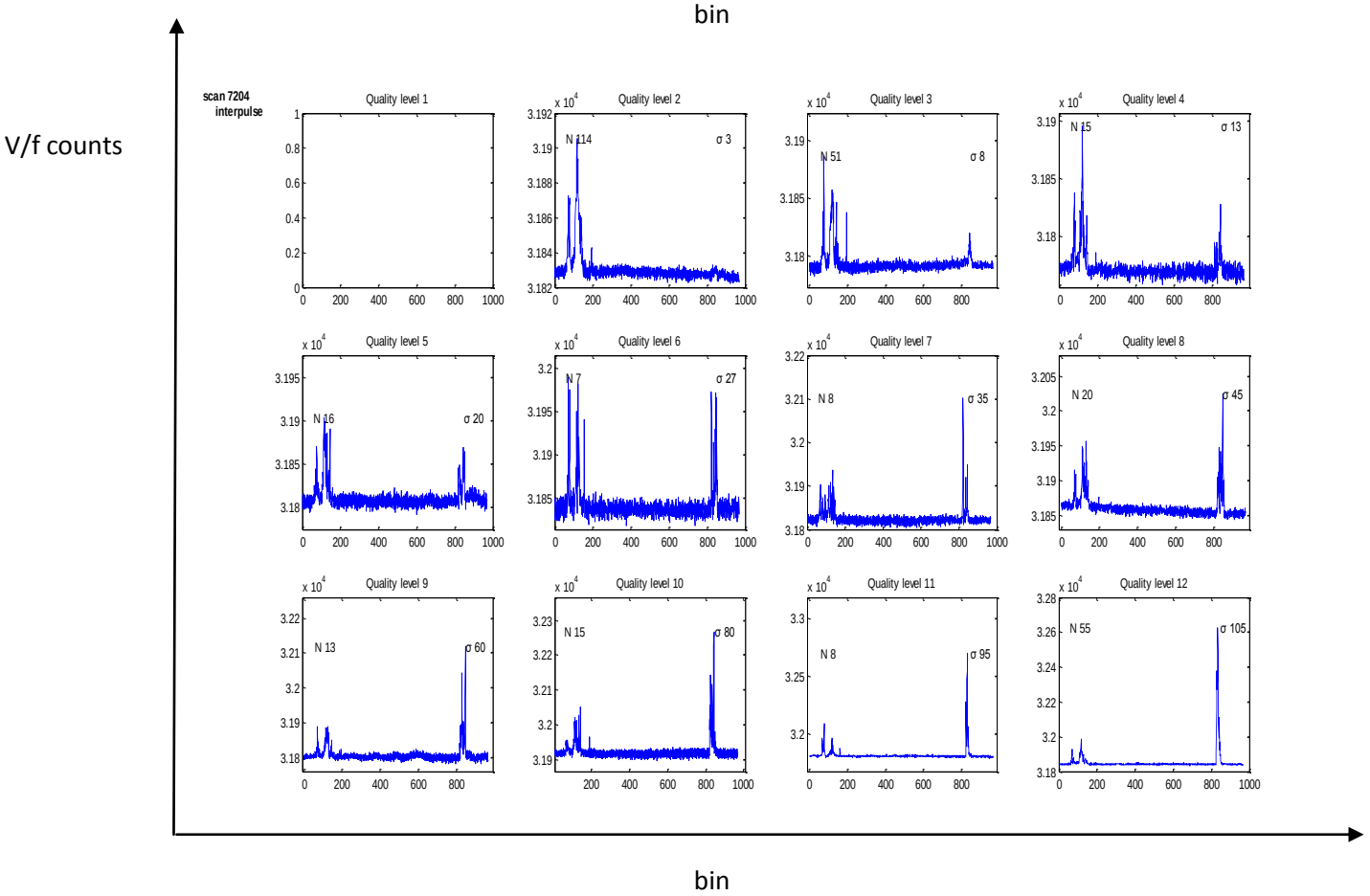
V/f counts
scan 7204
interpulse
Quality level 1
Quality level 2
N 114
σ 3
Quality level 3
N 51
σ 8
Quality level 4
N 15
σ 13
Quality level 5
N 16
σ 20
Quality level 6
N 7
σ 27
Quality level 7
N 8
σ 35
Quality level 8
N 20
σ 45
Quality level 9
N 13
σ 60
Quality level 10
N 15
σ 80
Quality level 11
N 8
σ 95
Quality level 12
N 55
σ 105
bin

V/f counts

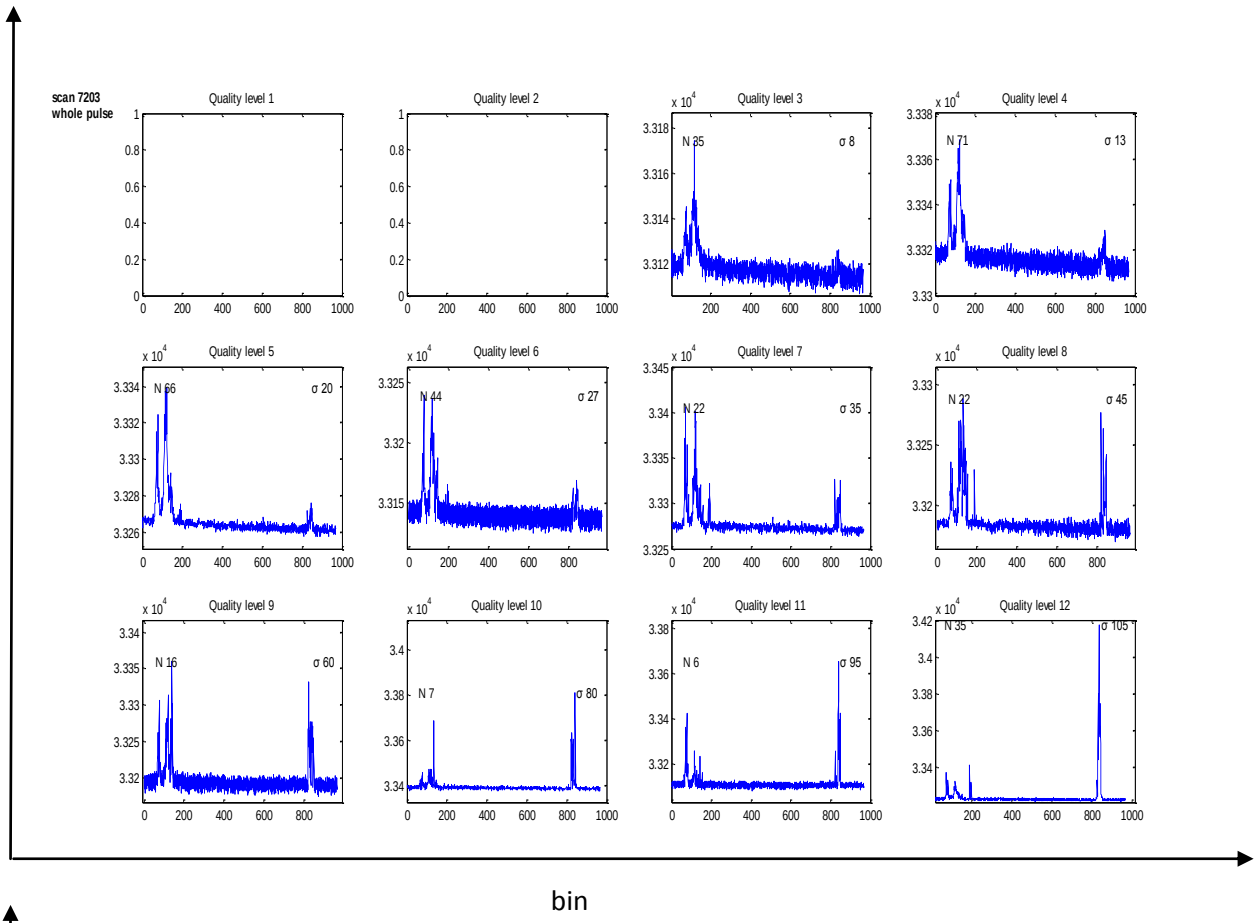

bin

V/f counts

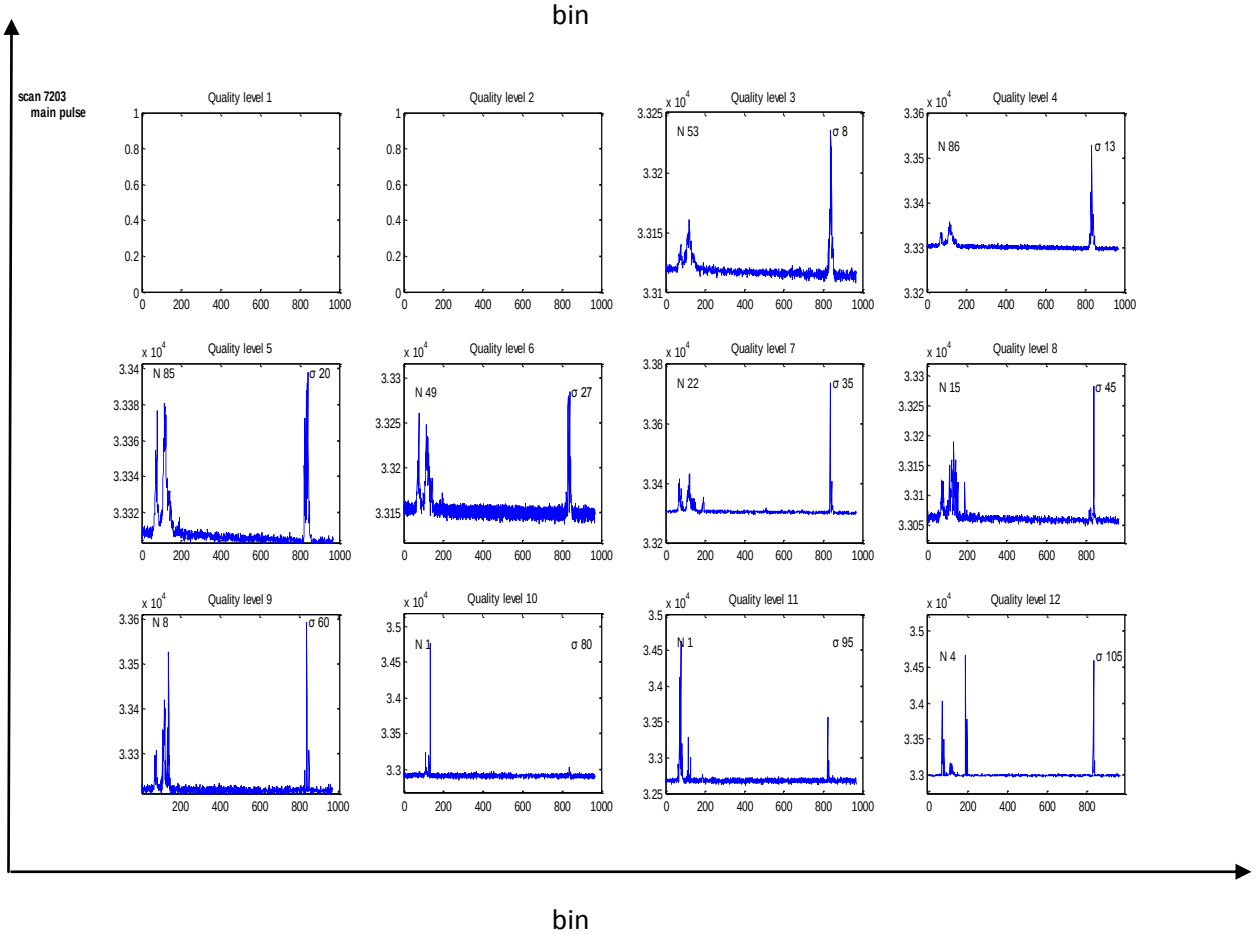

bin

V/f counts

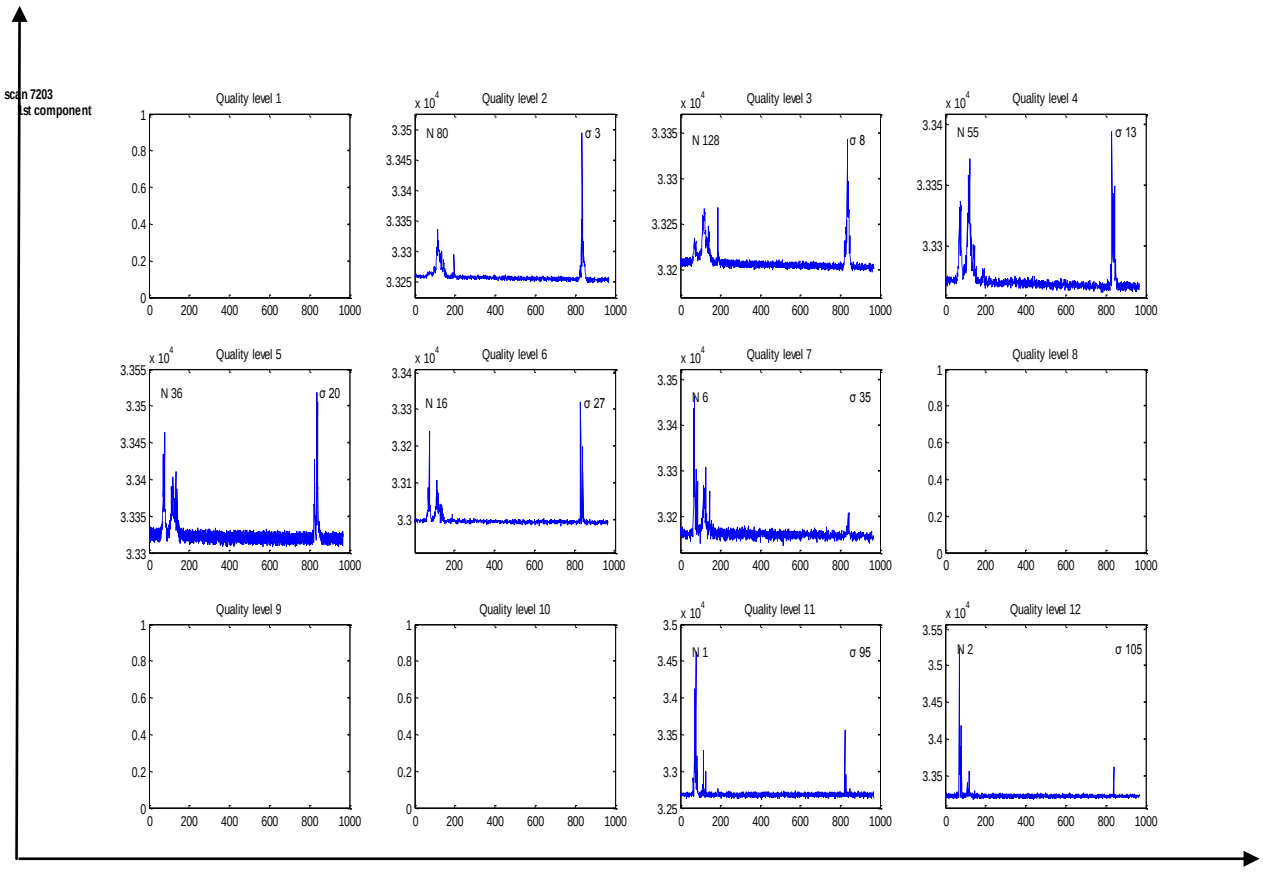

bin

V/f counts

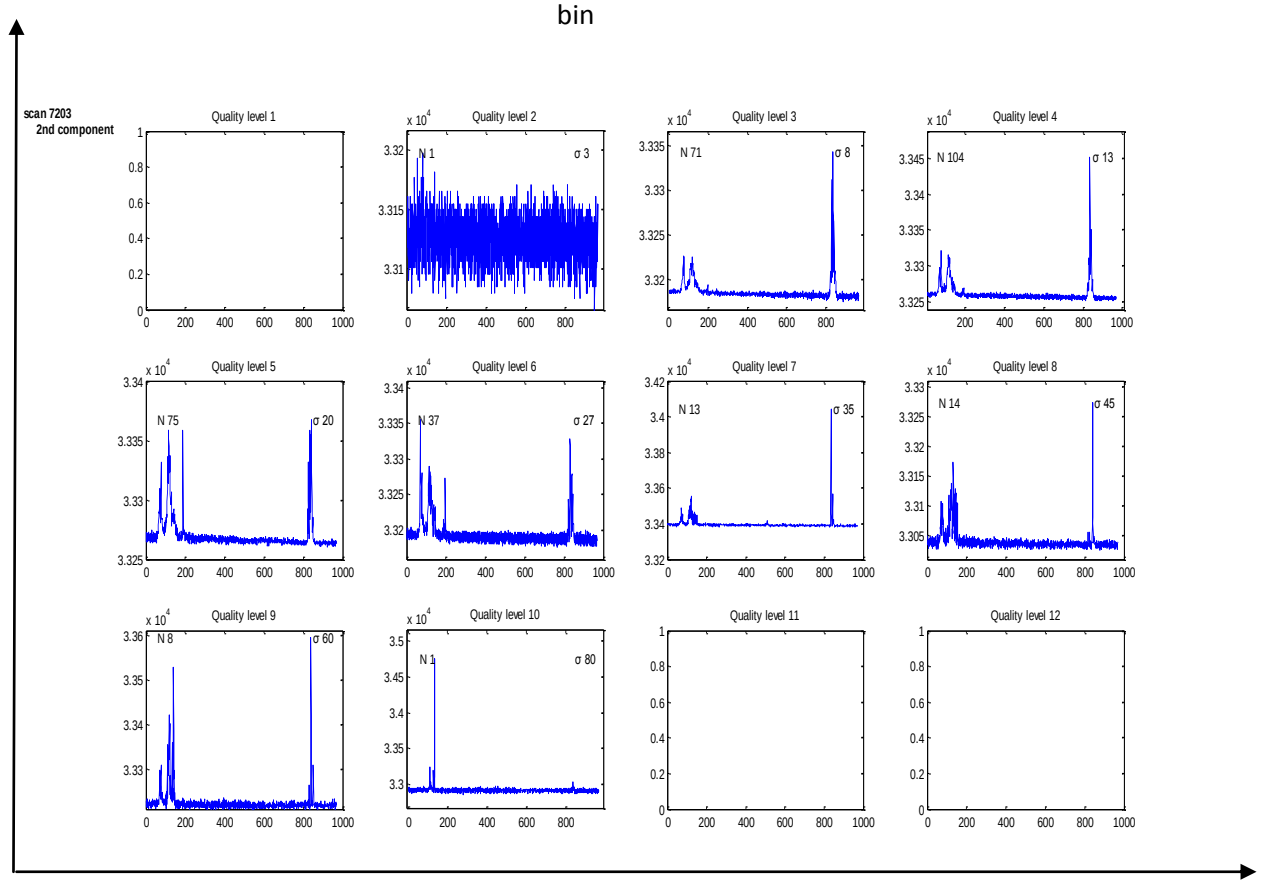

bin

V/f counts

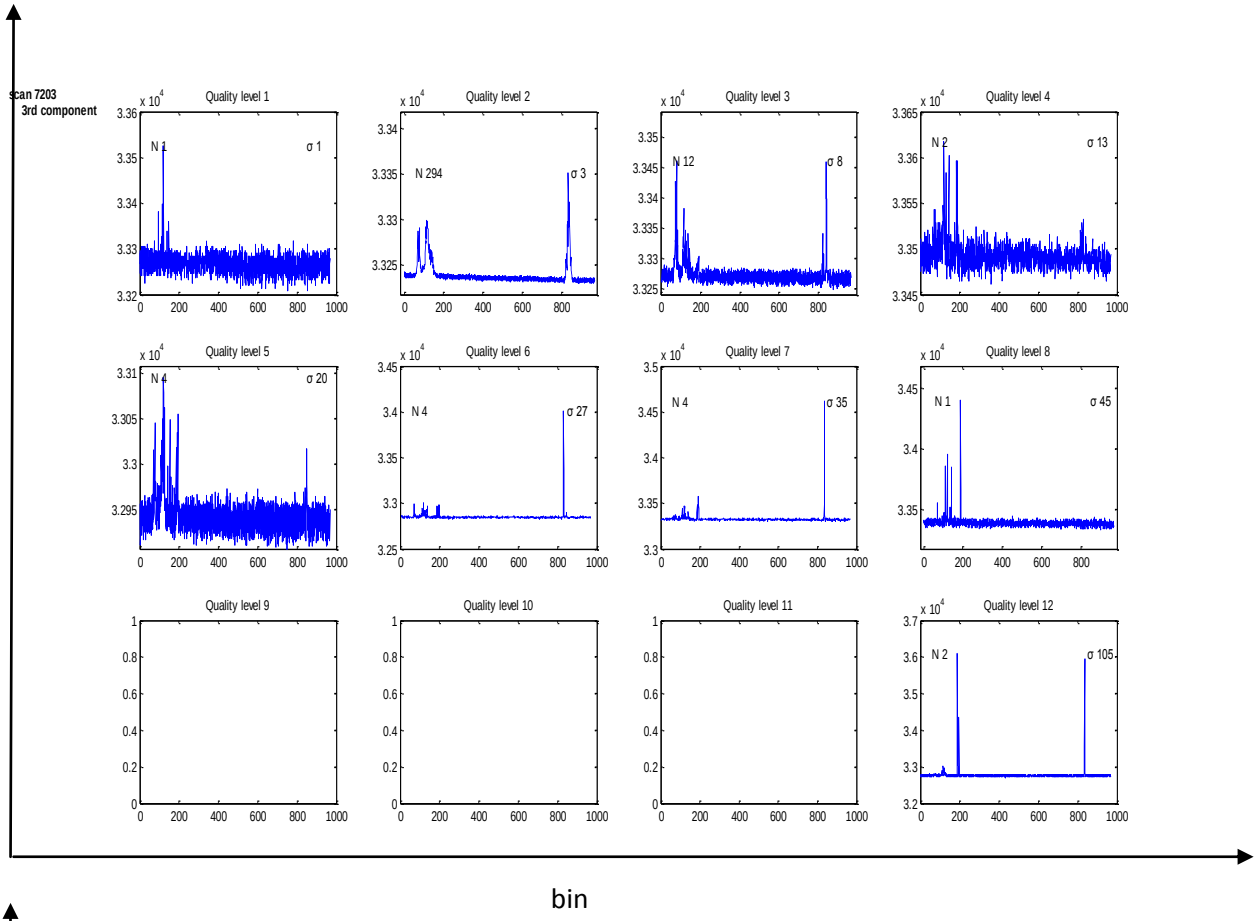

V/f counts

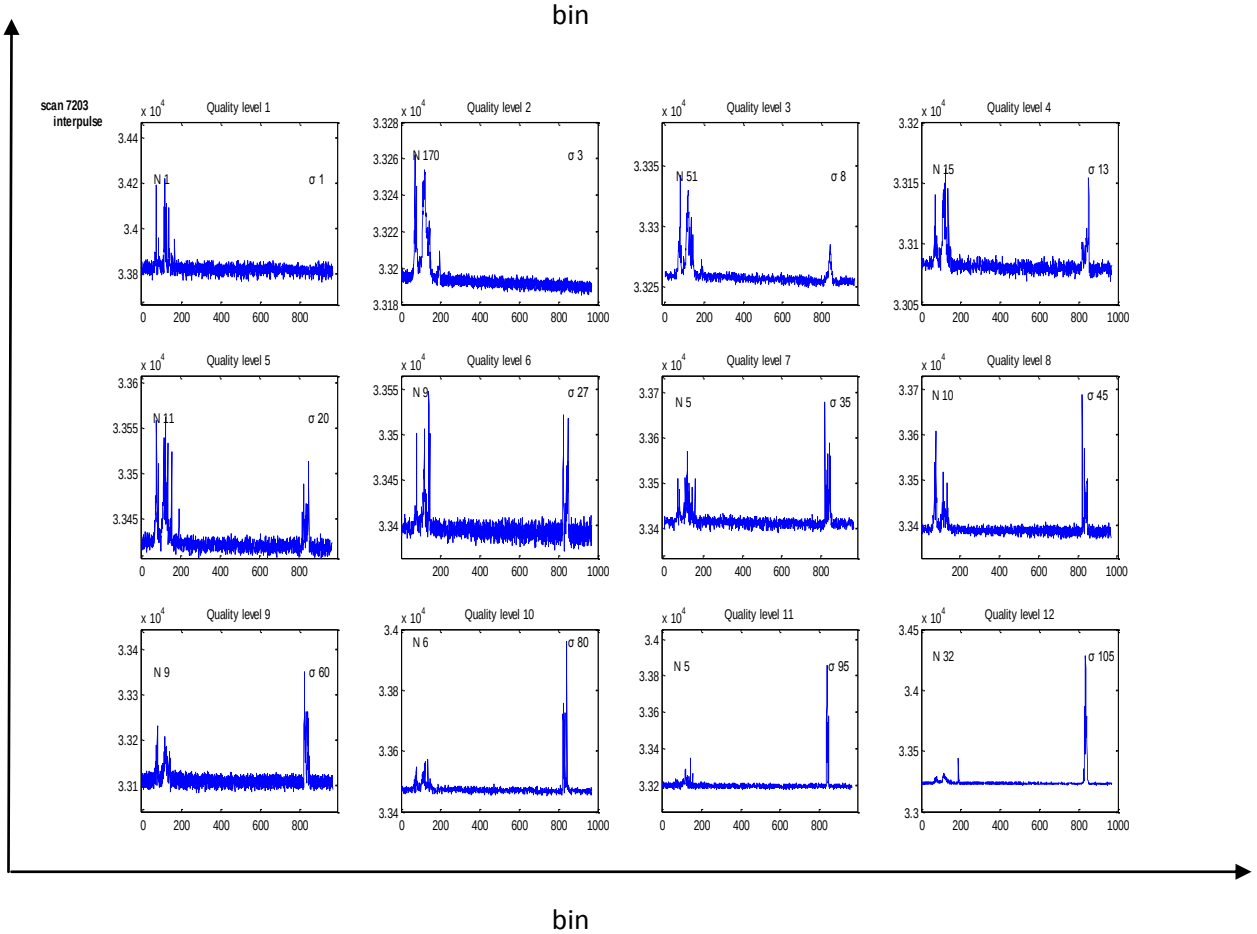

V/f counts

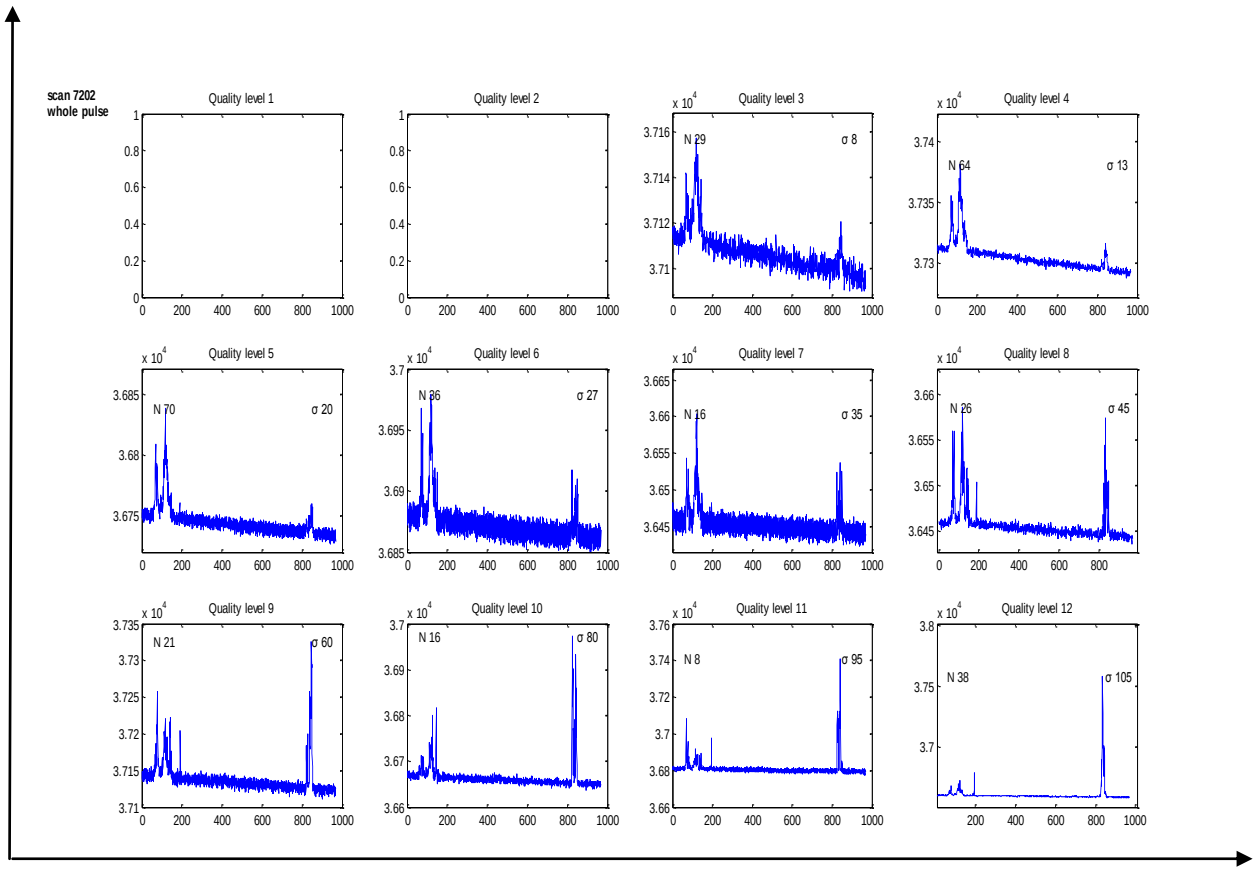

bin

V/f counts

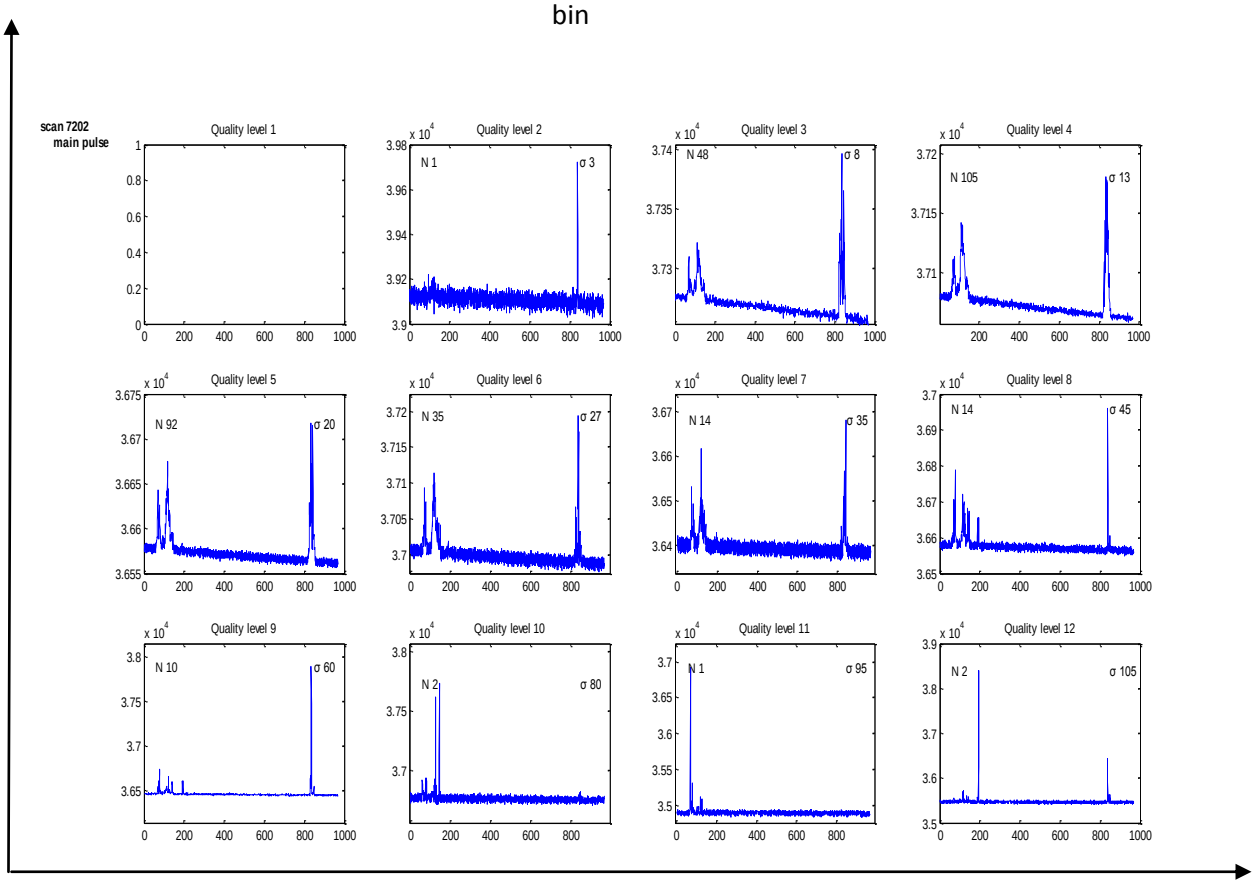

bin

V/f counts

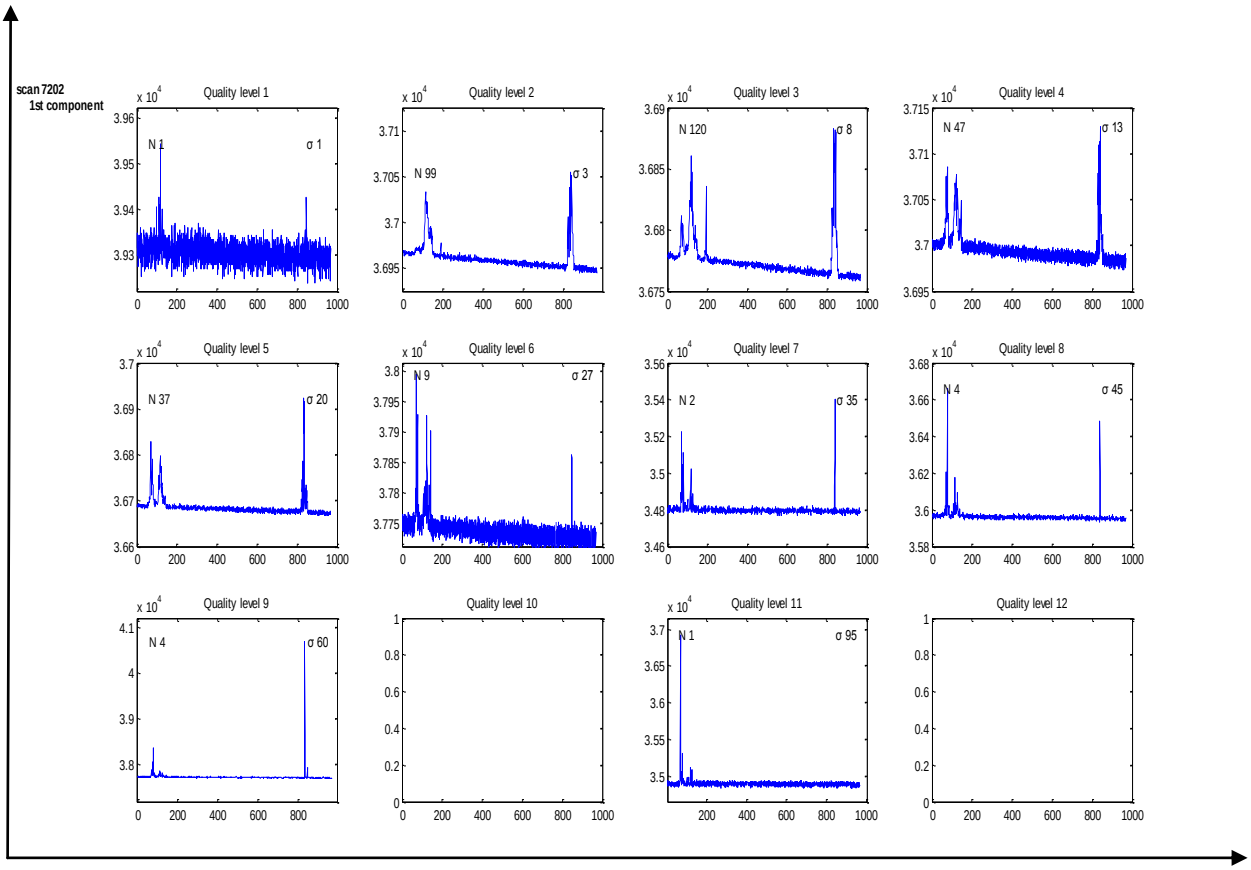

bin

V/f counts

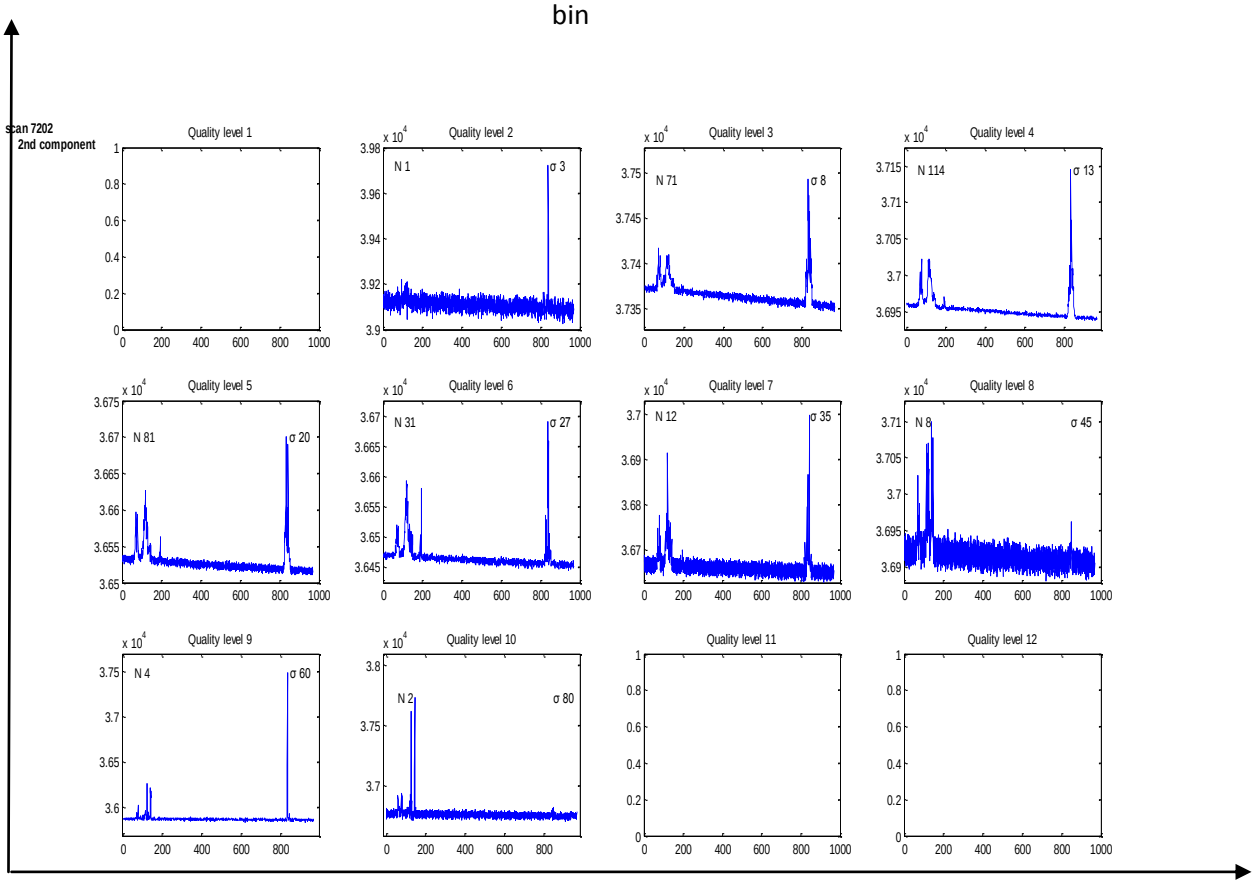

bin

V/f counts

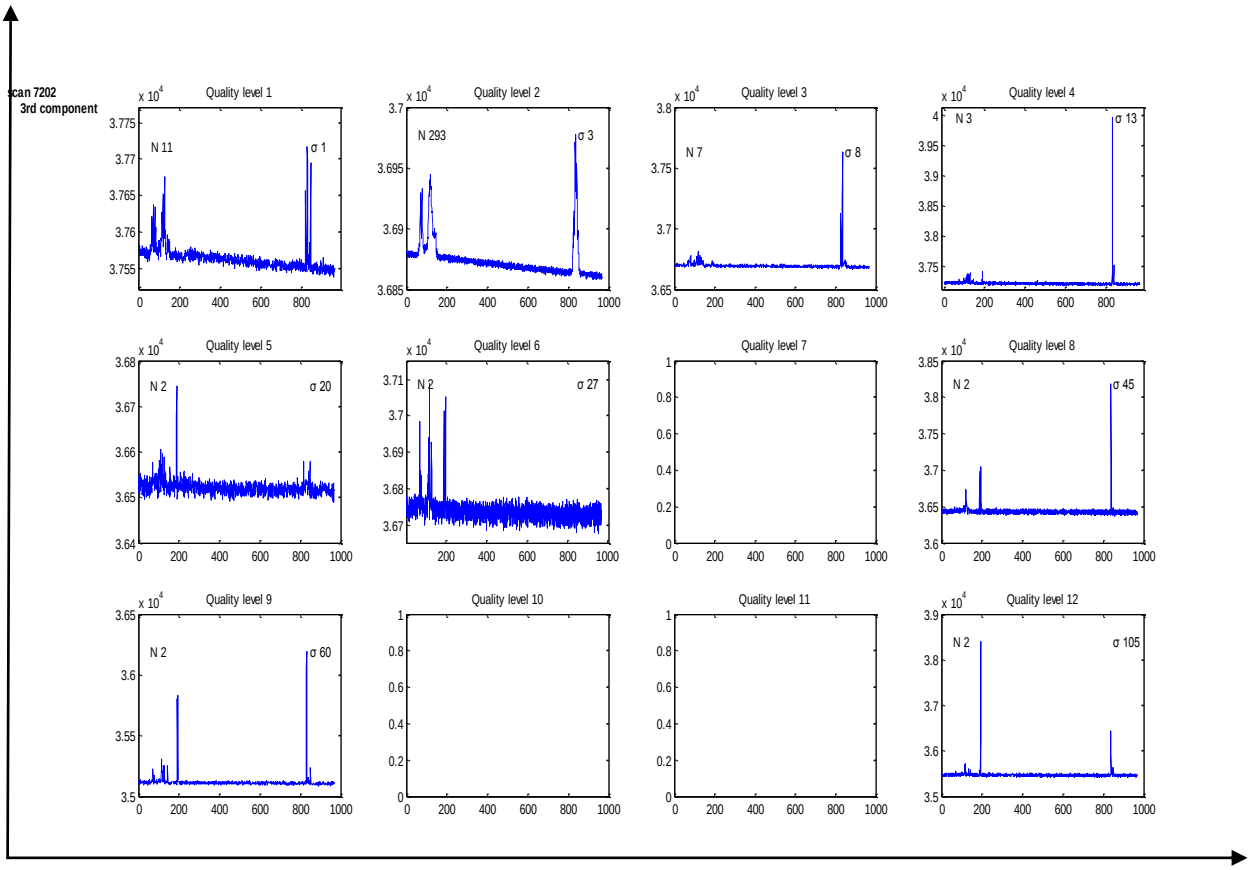

bin

V/f counts

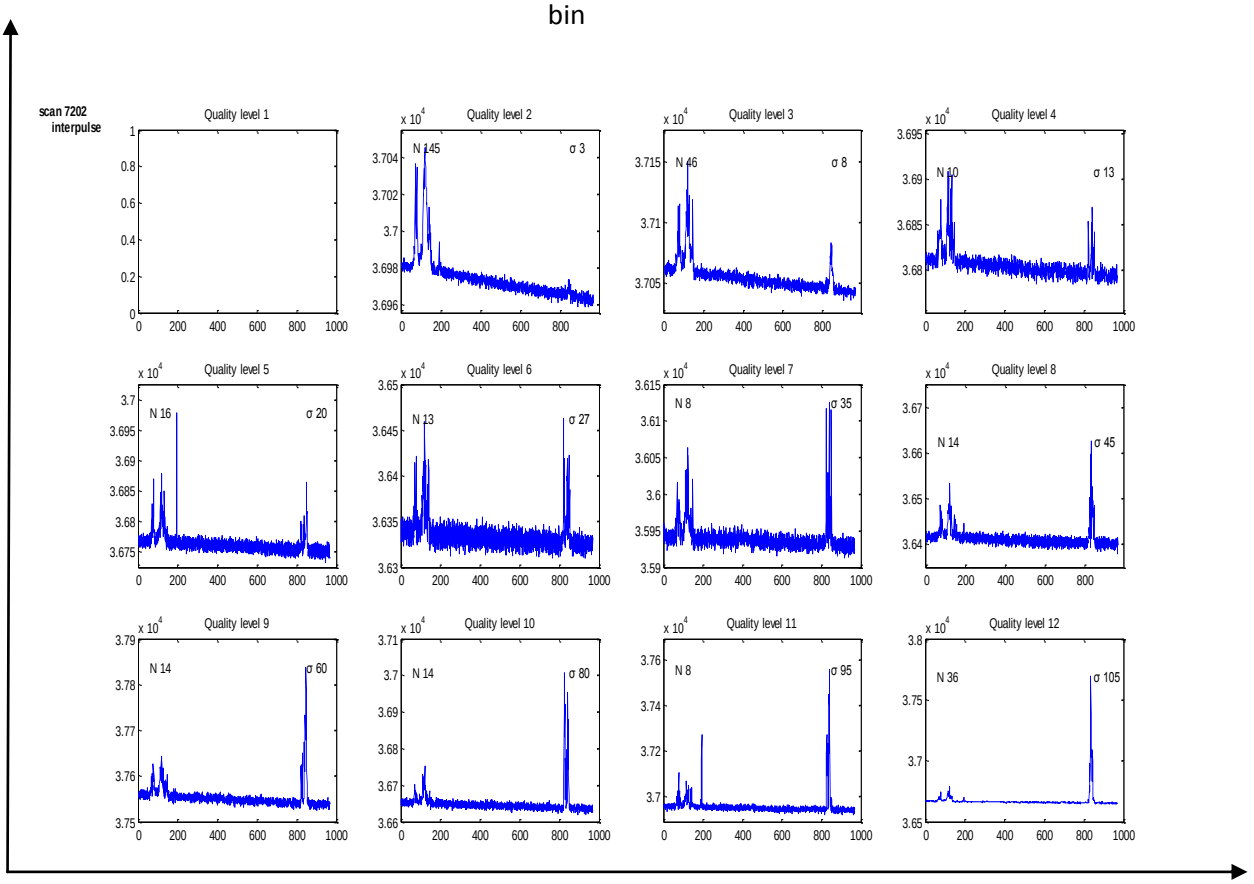

bin

Bibliography

Backer, D. C. (1970). Peculiar Pulse Burst in Psr 1237+25. *Nature* .

Beskin, V. (2010). "Hollow Cone" Model. In V. Beskin, *MHD Flows in Compact Astrophysical Objects Accretion, Winds and Jets* (p. 116). Berlin: Springer.

Carroll, B. W., & Ostlie, D. A. (2006). *An Introduction to Modern Astrophysics.* Addison Wesley Publishing Company.

Discovered: A New Kind Of Pulsar. (2008, October 17).

Manchester, R. N., & Taylor, J. H. (1977). *Pulsars.* San Francisco: W. H. Freeman and Company.

Melrose, D. B. (Oct.15,1992). Coherent radio emission from pulsars. *Philosophical Transactions: Physical Sciences and Engineering* , 105-115.

Mereghetti, S. (2012). Pulsars ans Magnetars. *26th Texas Symposium on Relativistic Astrophysics*, (pp. 1-14). Sao Paolo.

Michel, F. C. (1991). Extentions of the Standard Model: Pair Production Cascade. In F. C. Michel, *Theory of Neutron Star Magnetospheres* (pp. 278-280). Chicago: The University of Chicago Press.

NASA. (n.d.). Glossary.

Ritchings, R. T. (1976). Pulsar single pulse intensity measurements and pulse nulling. *Monthly Notices of the Royal Astronomical Society* , p. 249-263.

Sieber, W. (1996). Geometrical effects on radio pulsar profiles and spectra. *ASP Conference Series* , 167.

Spyrou, N. K. (2008). *Principles of Stellar Evolution - White Dwarfs, Neutron stars, Black Holes.* Thessaloniki: A. S. Gartaganis.

The ATNF Pulsar Database. (n.d.).

Acknowledgements

At first I would like to thank Prof. Dr. John H. Seiradakis who as my thesis supervisor led me to face and surmount challenges unprecedented to me. I would also like to thank him for his guidance and precious advice, without them I could not write this paper. I would also like to thank my co-supervisor Dr. Kosmas Lazaridis who was always there willing to help me and to contribute to this work.

Part of this work is based on observations with the 100-m telescope of the Max-Plank-Institute für Radioastronomie (MPIfR) at Effelsberg. Also I would like to thank Prof. Dr. Emmanouil Plionis and Prof. Dr. Nikolaos Stergioulas for being in the examination committee.

I would like to thank my parents for their support and for their approach on life that is an example and an inspiration to me, my sisters and my brother for their help when I needed it. Last but not least I would like to thank my friends for making my life more beautiful.